The Function of Pigmentation Genes in the Development and Evolution of *Drosophila* Mating Behavior

by

Jonathan H. Massey

A dissertation submitted in partial fulfillment
of the requirements for the degree of
Doctor of Philosophy
(Ecology and Evolutionary Biology)
in the University of Michigan
2019

Doctoral Committee:

Professor Patricia J. Wittkopp, Chair
Assistant Professor E. Josie Clowney
Assistant Professor Alison Davis Rabosky
David Stern, Group Leader, Janelia Research Campus
Professor George Zhang

Jonathan H. Massey

jhmassey@umich.edu

ORCID iD: 0000-0001-6182-2604

To Anneka, for all your encouragement, love, and support

To Mom, for getting me hooked on books

Acknowledgements

I would like to thank Trisha Wittkopp for being an incredible advisor. She is endlessly encouraging and supportive. She repeatedly builds a lab group with colleagues that look forward to working with each other every day. And, she makes science fun. I have learned so much from her, not just about science, but also writing and being an effective leader. I would like to thank David Stern for believing in me, for keeping the bar set high, and for reigniting my love of insects. David is a fantastic scientist and inspires me to always work hard at the bench. His bioinformatic expertise made Chapter 4 possible. I would also like to thank: Abby Lamb for teaching me everything in lab, from PCR to CRISPR; Daayun Chung for pioneering Chapter 2; Jun Li for fearlessly injecting hundreds of embryos to make the first *D. elegans ebony* mutant; members of the Wittkopp lab, past and present, for their endless support, feedback, and encouragement; Shu-Dan Yeh for inspiring the work in Chapter 4, for laying the groundwork to study *D. elegans* and *D. gunungcola* in the wild, and for hosting me in Taiwan and Indonesia; Joanne Yew for hosting me in Hawaii, teaching me about CHCs, and being a fantastic collaborator; my talented and supportive Ph.D. cohort, especially Joe Walker who was always willing to help; members of the Stern lab for welcoming me when I moved to Janelia, especially Yun Ding for her mentorship; Igor Siwanowicz for imaging support and sharing my love of insects; my thesis committee, Josie Clowney, Alison Davis Rabosky, Orie Shafer, and George Zhang who all provided important insights and advice to improve this thesis; the Buttitta Lab, especially Shyama Nandakumar and Ajai Pulianmackal for walking me through IHC for the first time; the Genetics Training Program and Howard Hughes Medical Institute for professional and financial support; my family and friends for believing in me and giving me a home full of love and support; and Anneka, for brightening every day, for friendship, encouragement, and giving feedback on every talk, paper, and idea in this thesis.

Table of Contents

List of Figures

List of Tables

List of Appendices

Abstract

Phenotypic evolution within and between species involves correlated changes in traits that facilitate survival and reproduction. Mating behaviors, in particular, and their correlated anatomical structures enable animals to court and reproduce with mates using a mixture of visual, chemical, and mechanical cues. How genes and genomes evolve to generate correlated differences in these traits is unclear. In this thesis, I investigate how genes and genomes contribute to correlated differences in mating behavior and pigmentation in *Drosophila*. Using tissue-specific genetic manipulations, I illustrate how the *yellow* gene influences male mating success through its function in melanizing a secondary sexual character; using CRISPR/Cas9 genome editing, I demonstrate a role of the *ebony* and *tan* genes in cuticular hydrocarbon synthesis and natural variation; and using multiplexed shotgun genotyping, I map the genomic location of species differences in wing pigmentation and mating display, identifying new genes involved in pigmentation evolution and new evidence explaining how behavior and anatomy evolve together. Together, these data show 1) that behavioral development and evolution involves correlated changes in structures that animals use to interact with their environment, 2) that changes in these structures correlate with the behaviors that use them, 3) that changes in individual genes can generate these differences, and 4) that complex evolution of sex chromosomes can explain species correlated differences in sex-specific behavior and anatomy.

Chapter 1

Introduction

One cannot intelligently discuss behavior and structure separately. Behavior is what an animal does with its structure; structure is what an animal uses to behave

–Howard Evans, 1966

The problem

Animal species often interact with their environments using specialized structures that are adapted for specific activities. Correlations between behavior and anatomy exist as a consequence of both development and evolution: Males often grow bigger and more aggressive due to higher levels of testosterone, and females tend to select males with more stunning courtship rituals. How do correlations between behavior and anatomy originate and why might they persist (or not) during evolution? How does heritable variation shape these interactions? This thesis dissects the genetic and molecular basis of correlations between mating behavior and pigmentation in *Drosophila* to better understand how genes and genomes shape the development and coevolution of behavior and anatomy.

Mechanisms linking behavior with anatomy during development and evolution

In numerous cases, patterns of animal behavior correlate with the anatomical structures used during specific social and sexual activities (reviewed in West-Eberhard, 2003): Birds with crests display their crests (Mayr, 1963); lizards with dewlaps bob their

dewlaps (Jenssen, 1977); fishes with spots shake their spots (Endler, 1983). These patterns are observable on both macro- and microevolutionary time scales. Between species, animals show correlated gains or losses of behavior and structure that evolve repeatedly (reviewed in Brooks and McLennan, 1991). Gregariousness in caterpillars, for example, is phylogenetically correlated with aposematic coloration: more colorful species tend to be more social (Sillén-Tullberg, 1988). Within species, individuals show correlated changes in behavior and anatomy that often scale with growth or differentiate sexes. Changes in horn size in dung beetles, for example, are correlated with reproductive behavior: large horned males tend to guard females, hornless males tend to sneak, and hornless females tend to engage in brood care (Cook, 1990; Emlen, 1997; Moczek and Emlen, 2000). How do correlated differences in behavior and anatomy within species lead to correlated divergence between?

The ultimate source of biological variation is mutation. Correlated variation, whether segregating within or diverging between species, originates from mutational changes in gene regulation, gene function, and genome organization. Disentangling when, where, and how these mutations give rise to correlational change is the focus of developmental biology as much as it is evolution.

Pleiotropy

Some mutations are highly disruptive, causing changes in multiple traits throughout development. Mutations that alter multiple traits during development are said to be pleiotropic (Zhang and Wagner, 2013). Depending on where mutations arise in the genome, pleiotropy can manifest as a consequence of changes in gene regulation, protein function, or genome rearrangement. Mutations disrupting the function of transcription factors (TFs), for example, are often highly pleiotropic, because TFs regulate numerous genetic pathways (Wagner and Zhang, 2011). In butterflies, the *optix* gene encodes a homeobox containing TF (Seimiya and Gehring, 2000) that when disrupted alters multiple correlated components of wing scale structure and pigmentation (Zhang *et al.*, 2017). Ectopic expression of the same gene in *Drosophila* induces ectopic eye

development (Seimiya and Gehring, 2000). The degree to which a mutation behaves pleiotropically, therefore, often depends on the pleiotropic nature of the affected gene.

How does pleiotropy link behavior with anatomy? Several TFs and cell-cell signaling molecules patterning the development of the nervous system in vertebrates and invertebrates also regulate the development of morphological structures (Lewis, 1998; Louvi and Artavanis-Tsakonas, 2006; Wittkopp and Beldade, 2009; Rideout *et al.*, 2010; Robinett *et al*., 2010; Wagner and Zhang, 2011). The *Ectodysplasin* (*Eda*) gene, for example, encodes a tumor necrosis factor (TNF) transmembrane protein (Mikkola and Thesleff, 2003) that controls the development of armor plates, neuromasts, and schooling behavior in the three-spine stickleback (*Gasterosteus aculeatus*) (Colosimo *et al.*, 2005; Mills *et al*., 2014; Greenwood *et al.*, 2016). Pleiotropy at *Eda* is also associated with disease in humans that likely stems from its broad expression pattern in the skin, heart, nervous system, lung, liver, small intestine, and kidneys (Kere *et al*., 1996; Bayes *et al*., 1998; Montonen *et al*., 1998). But in sticklebacks, *Eda* expression specifically in neuromast cells is associated with both armor plate development (Mills *et al*., 2014) and schooling behavior (Greenwood *et al*., 2016), suggesting that developmental differences in TNF-mediated cell signaling within the same tissue underlies correlated variation in behavior and anatomy.

Pleiotropic mutations disrupting hormone synthesis and reception also contribute to correlated differences in behavior and anatomy during development. Hormones take many forms. In vertebrates, amines, peptides, proteins, and steroids can all behave as hormones (Nussey, 2001). One of the clearest examples illustrating how hormone signaling pairs behavior with anatomy involves the melanocortin system, including the five melanocortin receptors (MC1–5R) and the proopiomelanocortin (*POMC*) gene, which produces the peptide hormones adrenocorticotropin hormone (ACTH) and melanin-stimulating hormones (MSHs) (Ducrest *et al*., 2008). Knockout alleles of *POMC* in mice causes obesity and light coat color; knockout alleles of MC4R causes obesity and increased anxiety; and knockout alleles of MC5R causes higher hair lipid content and

decreased aggression (reviewed in Butler and Cone, 2002). Similar effects have been described in POMC-deficient humans (Kühnen *et al*., 2016). Pleiotropy in the melanocortin system is likely the consequence of multiple complimentary mechanisms: First, *POMC* post-transcriptional regulation is complex, leading to multiple peptide products with distinct functions (Ducrest *et al*., 2008); second, these peptide products are capable of binding different MCRs, each with their own unique expression profiles in the skin, brain, and endocrine glands (Butler and Cone, 2002); and third, POMC and MCR expression in the brain regulates feeding (Zhan *et al*., 2013) and stress response (Liu *et al*., 2013) each of which leads to changes in metabolism and growth. Mutations affecting POMC function, therefore, have the potential to echo throughout a cascade of hormone-mediated regulatory pathways controlling both behavioral and anatomical development.

Although mutations at *Eda* and *MCRs* are highly pleiotropic, causing disease malformations in humans and widespread phenotypic changes in model organisms, both *Eda* and *MCRs* have repeatedly contributed to anatomical evolution within and between species (reviewed in Martin and Orgogozo, 2013). In sticklebacks, natural variation at *Eda* has repeatedly caused armor plates to evolve in freshwater lake populations (Colosimo *et al*., 2005; Barrett *et al.*, 2008). In bananaquits, bears, cows, chickens, dogs, foxes, humans, and lizards, natural variation at *MC1R* is strongly associated with changes in pigmentation (reviewed in Martin and Orgogozo, 2013). It remains unclear to what extent natural alleles at *Eda* and *MC1R* contribute to behavioral evolution. Changes in armor plate number and pigmentation intensity in natural populations, however, repeatedly covary with behavioral traits that take advantage of these anatomical differences (Ducrest *et al.* 2008, Greenwood *et al*., 2013; Greenwood *et al*., 2016). The challenge, then, is testing whether animals that carry different versions of the same pleiotropic gene show behavioral changes that correlate with anatomical evolution.

Linkage

Evolution also coordinates multiple traits through the action of multiple, co-inherited genes. Linkage disequilibrium occurs when physical associations between two or more

genetic variants, often on the same chromosome, cause the variants to be inherited together (Saltz *et al.*, 2017). Like pleiotropy, linkage is a source of genetic correlation between behavior and anatomy.

Sex linkage is theorized to be one way evolution separates the development of sexually antagonistic traits between males and females (Rice, 1984). Sexually antagonistic traits involve phenotypes that are beneficial in one sex but deleterious in the other. The costly development of elaborate courtship displays and their correlated ornaments, for example, benefit males but not females in many animal species (Alcock and Rubenstein, 2019). Differences in dosage effects and sex determination cascades cause sex-linked genes to express sex-specific effects during development. Many sex-linked genes, then, are responsible for sexual dimorphism in both behavioral and anatomical development (Reinhold, 1998). In *Drosophila* and mice, Reinhold (1998) estimates as much as one-third of sexually dimorphic behavioral and anatomical differences are due to X effects. Between *Drosophila melanogaster* and *D. simulans*, divergence in gene expression is primarily explained by sex-biased gene expression, and an excess of female-biased genes are X-linked (Ranz *et al*., 2003). The repeated coevolution of behavior and anatomy within and between species, therefore, may be a consequence of species resolving sexual antagonism via mutations on the X chromosome. In 1978, Turner theorized this very scenario, suggesting that selection causes sex chromosomes to behave like sieves for mutations with sex-limited effects during the evolution of sexual dimorphism.

How do linked loci cause correlated differences within and between species? Early models inspired by the genetics of butterfly mimicry hypothesized that supergenes, multiple genes in tight linkage disequilibrium, were responsible for causing complex patterns of phenotypic evolution (Ford, 1964; Clark and Sheppard, 1972; Charlesworth and Charlesworth, 1975). In swallowtail butterflies (*Papilio polytes*), for example, both sexually dimorphic and female polymorphic wing pattern mimicry segregate as if controlled by a single locus (Clark and Sheppard, 1972). Surprisingly, genetic mapping localized these effects to numerous single nucleotide polymorphisms (SNPs) at a single gene, *doublesex* (*dsx*), rather than multiple tightly linked loci like Clark and Sheppard

(1972) hypothesized (Kunte *et al.*, 2014). *dsx* encodes a zinc-finger containing TF that controls sexual differentiation through alternative splicing in insects (Erdman and Burtis, 1993). An inversion mutation flanking the *dsx* locus in *P. polytes* reduced recombination at this region relative to the rest of the genome (Kunte *et al*., 2014). As has recently been shown in ruff (Lamichhaney *et al.*, 2016), sparrows (Tuttle *et al.*, 2016), and zebra finch (Kim *et al*., 2017), supergenes may exist as a consequence of inversions that facilitate the accumulation of mutations in tight linkage disequilibrium. In *P. polytes*, then, the *dsx* locus may also behave like a sieve, allowing the buildup of mutations that lead to correlated differences in wing patterning, possibly through complex alternative splicing mechanisms (Kunte *et al*., 2014).

Together these results suggest that genetic correlations controlling variation in both behavior and anatomy can be built through linkage and pleiotropy. In fact, it is not always clear how to separate both mechanisms, since multiple mutations in tight linkage can modify the function of a single pleiotropic gene, as in the case of *dsx*. Similarly, the evolution of sexual dimorphism within species and correlated divergence between might often be part of the same problem. That is, genetic mechanisms that separate the expression of phenotypes between males and females can also generate differences between species, as in the case of sex chromosome evolution. But, there are still many unresolved issues: Most of the evidence explaining how genes and genomes evolve within and between species to generate phenotypic differences in behavior and anatomy are correlative. While birds, fish, and butterflies show some of the most elaborate diversity patterns in mating displays and ornamentation, it is extremely difficult to perform casual genetic experiments in these systems. As a consequence, in nearly all cases, the mechanistic relationship between individual gene mutations and their pleiotropic effects on mating success remains unclear. Understanding these mechanisms is a requirement to connect genotype to phenotype and genotype to environment during correlated evolution.

Solving the problem in *Drosophila*

In *Drosophila*, males engage in courtship rituals involving wing, leg, and body movements near females to initiate mating (Hall, 1994). These movements are correlated with rapidly evolving anatomical changes within and between species, including pigmentation patterning on the wings (Kopp and True, 2002), secondary sexual structures on the legs (Kopp, 2011), and lipid profiles on the body (Yew and Chung, 2015). Genetic tools are available to modify each of these phenotypes in live, freely behaving animals (Duffy, 2002). In this thesis, I take advantage of these tools to answers questions about the genetic basis of developmental and evolutionary change in correlated behavior and anatomy. Specifically, I perform a series of genetic experiments to study how correlations between mating behaviors and pigmentation come about. Each chapter illustrates the power of *Drosophila* to learn how genes and genomes function in the context of ecologically important traits.

Thesis overview

In chapter two, I investigate how a single mutation in the *yellow* gene influences male mating success in *Drosophila melanogaster*. Using tissue specific RNAi manipulations in combination with GAL4 and GAL80 tools, I show that *yellow* expression specifically in male-specific leg structures called sex combs is required for mating success. Loss of sex comb melanization in *yellow* mutants causes structural changes that reduce a male's ability to grasp and mount females for copulation. These results highlight, unexpectedly, that anatomical changes themselves can modify animal behavior.

In chapter three, I show that the function of two pigmentation enzymes, Ebony and Tan, have reciprocal effects on cuticular hydrocarbon (CHC) synthesis. Specifically, loss of Ebony activity increases the abundance of long-chain CHCs, and loss of Tan activity increases the abundance of short-chain CHCs. These effects are partially explained by changes in dopamine signaling. Further, natural variation in *ebony* and *tan* expression

covaries with CHC profiles in the direction predicted by the mutants, suggesting that pigmentation and CHCs might evolve in coordination.

In chapter four, I perform QTL mapping between the sibling species *D. elegans* and *D. gunungcola* to study the genetic basis of divergence in wing pigmentation and mating display. Evolution on the X chromosome explains the majority of variation for both traits, due to the effects of co-localized QTLs. Fine-mapping revealed a ~400 kb region containing fifteen genes that behaves like a genetic switch controlling wing spot evolution. Through introgression mapping, I separated the effects of the wing spot locus from the effects of mating display, possibly as a consequence of epistasis. I also discovered new populations of *D. gunungcola* that perform mating displays similar to *D. elegans*, suggesting that behavioral divergence occurred more slowly than anatomical divergence between these species.

Finally, in the appendices, I include a series of supplemental figures accompanying each chapter and a review that synthesizes a database of genes and mutations contributing to pigmentation evolution in *Drosophila*.

References

Alcock, J., & Rubenstein, D. R. (2019). Animal behavior. Sinauer.

Barrett, R. D., Rogers, S. M., & Schluter, D. (2008). Natural selection on a major armor gene in threespine stickleback. *Science*, *322*(5899), 255-257.

Bayés, M., Hartung, A. J., Ezer, S., Pispa, J., Thesleff, I., Srivastava, A. K., & Kere, J. (1998). The anhidrotic ectodermal dysplasia gene (EDA) undergoes alternative splicing and encodes ectodysplasin-A with deletion mutations in collagenous repeats. *Human Molecular Genetics*, *7*(11), 1661-1669.

Brooks, D. R. & McLennan, D. A. (1991). Phylogeny, ecology, and behavior: a research program in comparative biology. University of Chicago press.

Butler, A. A., & Cone, R. D. (2002). The melanocortin receptors: lessons from knockout models. *Neuropeptides*, *36*(2-3), 77-84.

Charlesworth, D., & Charlesworth, B. (1975). Theoretical genetics of Batesian mimicry II. Evolution of supergenes. *Journal of Theoretical Biology*, *55*(2), 305-324.

Clarke, C., & Sheppard, P. M. (1972). The genetics of the mimetic butterfly Papilio polytes L. *Philosophical Transactions of the Royal Society of London. B, Biological Sciences*, *263*(855), 431-458.

Colosimo, P. F., Hosemann, K. E., Balabhadra, S., Villarreal, G., Dickson, M., Grimwood, J., ... & Kingsley, D. M. (2005). Widespread parallel evolution in sticklebacks by repeated fixation of ectodysplasin alleles. *Science*, *307*(5717), 1928-1933.

Cook, D. F. (1990). Differences in courtship, mating and postcopulatory behaviour between male morphs of the dung beetle *Onthophagus binodis* Thunberg (Coleoptera: Scarabaeidae). *Animal Behaviour*, *40*(3), 428-436.

Darwin, C. (2004). *On the origin of species*, 1859. Routledge.

Ducrest, A. L., Keller, L., & Roulin, A. (2008). Pleiotropy in the melanocortin system, coloration and behavioural syndromes. *Trends in Ecology & Evolution*, *23*(9), 502-510.

Duffy, J. B. (2002). GAL4 system in Drosophila: a fly geneticist's Swiss army knife. *Genesis*, *34*(1-2), 1-15.

Emlen, D. J. (1997). Alternative reproductive tactics and male-dimorphism in the horned beetle Onthophagus acuminatus (Coleoptera: Scarabaeidae). *Behavioral Ecology and Sociobiology*, *41*(5), 335-341.

Endler, J. A. (1983). Natural and sexual selection on color patterns in Poeciliid fishes. *Environmental Biology of Fishes*, *9*, 173-190.

Erdman, S. E., & Burtis, K. C. (1993). The *Drosophila* doublesex proteins share a novel zinc finger related DNA binding domain. *The EMBO Journal*, *12*(2), 527-535.

Evans, H. E. (1966). *The comparative ethology and evolution of the sand wasps*. Harvard University Press.

Ford EB. (1964). Ecological Genetics. Methuen: London.

Greenwood, A. K., Wark, A. R., Yoshida, K., & Peichel, C. L. (2013). Genetic and neural modularity underlie the evolution of schooling behavior in threespine sticklebacks. *Current Biology*, *23*(19), 1884-1888.

Greenwood, A. K., Mills, M. G., Wark, A. R., Archambeault, S. L., & Peichel, C. L. (2016). Evolution of schooling behavior in threespine sticklebacks is shaped by the *Eda* gene. *Genetics*, *203*(2), 677-681.

Gordon M (1931) Hereditary basis of melanosis in hybrid fishes. *The American Journal of Cancer*, *15*, 1495–1523.

Hall, J. C. (1994). The mating of a fly. *Science*, *264*(5166), 1702-1714.

Jenssen, T. A. (1977). Evolution of anoline lizard display behavior. *American Zoologist*, 17(1), 203-215.

Kallman KD (1975) The platyfish *Xiphophorus maculatus*. In: Handbook of Genetics, vol. 4 (ed. King RC), pp. 81–132. Plenum Press, New York, NY, USA.

Kallman KD (1989) Genetic control of size at maturity in Xiphophorus. In: Ecology and Evolution in Livebearing Fishes (eds Meffee GK, Snelson FF), pp. 163–184. Prentice-Hall, Englewood Cliffs, NJ. Kallman.

Kere, J., Srivastava, A. K., Montonen, O., Zonana, J., Thomas, N., Ferguson, B., ... & Chen, E. Y. (1996). X–linked anhidrotic (hypohidrotic) ectodermal dysplasia is caused by mutation in a novel transmembrane protein. *Nature Genetics*, *13*(4), 409.

Kim, K. W., Bennison, C., Hemmings, N., Brookes, L., Hurley, L. L., Griffith, S. C., ... & Slate, J. (2017). A sex-linked supergene controls sperm morphology and swimming speed in a songbird. *Nature Ecology & Evolution*, *1*(8), 1168.

Kopp, A., & True, J. R. (2002). Evolution of male sexual characters in the oriental *Drosophila melanogaster* species group. *Evolution & Development*, 4(4), 278-

291.

Kopp, A. (2011). *Drosophila* sex combs as a model of evolutionary innovations. *Evol Dev.*, 13(6):504-22.

Kühnen, P., Clément, K., Wiegand, S., Blankenstein, O., Gottesdiener, K., Martini, L. L., ... & Krude, H. (2016). Proopiomelanocortin deficiency treated with a melanocortin-4 receptor agonist. *New England Journal of Medicine*, *375*(3), 240-246.

Kunte, K., Zhang, W., Tenger-Trolander, A., Palmer, D. H., Martin, A., Reed, R. D., ... & Kronforst, M. R. (2014). *doublesex* is a mimicry supergene. *Nature*, 507(7491), 229.

Lamichhaney, S., Fan, G., Widemo, F., Gunnarsson, U., Thalmann, D. S., Hoeppner, M. P., ... & Chen, W. (2016). Structural genomic changes underlie alternative reproductive strategies in the ruff (*Philomachus pugnax*). *Nature Genetics*, 48(1), 84.

Lewis, J. (1998, December). Notch signaling and the control of cell fate choices in vertebrates. In Seminars in cell & developmental biology (Vol. 9, No. 6, pp. 583-589). Academic Press.

Liu, J., Garza, J. C., Li, W., & Lu, X. Y. (2013). Melanocortin-4 receptor in the medial amygdala regulates emotional stress-induced anxiety-like behaviour, anorexia and corticosterone secretion. *International Journal of Neuropsychopharmacology*, *16*(1), 105-120.

Louvi, A., & Artavanis-Tsakonas, S. (2006). Notch signalling in vertebrate neural development. *Nature Reviews Neuroscience*, *7*(2), 93.

Mayr, E. (1963). Animal Species and Evolution. Belknap Press, Cambridge.

Mikkola, M. L., & Thesleff, I. (2003). Ectodysplasin signaling in development. *Cytokine & Growth Factor Reviews*, *14*(3-4), 211-224.

Mills, M. G., Greenwood, A. K., & Peichel, C. L. (2014). Pleiotropic effects of a single gene on skeletal development and sensory system patterning in sticklebacks. *EvoDevo*, 5(1), 5.

Moczek, A. P., & Emlen, D. J. (2000). Male horn dimorphism in the scarab beetle, *Onthophagus taurus*: do alternative reproductive tactics favour alternative phenotypes*?*. *Animal Behaviour*, *59*(2), 459-466.

Montonen, O., Ezer, S., Saarialho-Kere, U. K., Herva, R., Karjalainen-Lindsberg, M. L., Kaitila, I., ... & Kere, J. (1998). The gene defective in anhidrotic ectodermal

dysplasia is expressed in the developing epithelium, neuroectoderm, thymus, and bone. *Journal of Histochemistry & Cytochemistry*, *46*(3), 281-289.

Nijhout, H. F. (1998). Insect hormones. Princeton University Press.

Nussey, S. S. (2001). Endocrinology: an integrated approach. CRC Press.

Ranz, J. M., Castillo-Davis, C. I., Meiklejohn, C. D., & Hartl, D. L. (2003). Sex-dependent gene expression and evolution of the *Drosophila* transcriptome. *Science*, 300(5626), 1742-1745.

Reinhold, K. (1998). Sex linkage among genes controlling sexually selected traits. *Behavioral Ecology and Sociobiology*, 44(1), 1-7.

Rice, W. R. (1984). Sex chromosomes and the evolution of sexual dimorphism. *Evolution*, *38*(4), 735-742.

Rideout, E. J., Dornan, A. J., Neville, M. C., Eadie, S., & Goodwin, S. F. (2010). Control of sexual differentiation and behavior by the *doublesex* gene in *Drosophila melanogaster*. *Nature Neuroscience*, *13*(4), 458.

Robinett, C. C., Vaughan, A. G., Knapp, J. M., & Baker, B. S. (2010). Sex and the single cell. II. There is a time and place for sex. *PLoS Biology*, *8*(5), e1000365.

Saltz, J. B., Hessel, F. C., & Kelly, M. W. (2017). Trait correlations in the genomics era. *Trends in Ecology & Evolution*, 32(4), 279-290.

Seimiya, M., & Gehring, W. J. (2000). The *Drosophila* homeobox gene *optix* is capable of inducing ectopic eyes by an eyeless-independent mechanism. *Development*, 127(9), 1879-1886.

Sillén-Tullberg, B. (1988). Evolution of gregariousness in aposematic butterfly larvae: a phylogenetic analysis. *Evolution*, *42*(2), 293-305.

Turner, J. R. (1978). Why male butterflies are non-mimetic: natural selection, sexual selection, group selection, modification and sieving. *Biological Journal of the Linnean Society*, *10*(4), 385-432.

Tuttle, E. M., Bergland, A. O., Korody, M. L., Brewer, M. S., Newhouse, D. J., Minx, P., ... & Gonser, R. A. (2016). Divergence and functional degradation of a sex chromosome-like supergene. *Current Biology*, *26*(3), 344-350.

Wagner, G. P., & Zhang, J. (2011). The pleiotropic structure of the genotype–phenotype map: the evolvability of complex organisms. *Nature Reviews Genetics*, *12*(3), 204.

West-Eberhard, M. J. (1983). Sexual selection, social competition, and speciation. *The Quarterly Review of Biology*, *58*(2), 155-183.

West-Eberhard, M. J. (2003). *Developmental plasticity and evolution*. Oxford University Press.

Wittkopp, P. J., & Beldade, P. (2009, February). Development and evolution of insect pigmentation: genetic mechanisms and the potential consequences of pleiotropy. In Seminars in Cell & Developmental Biology (Vol. 20, No. 1, pp. 65-71). Academic Press.

Yew, J. Y., & Chung, H. (2015). Insect pheromones: An overview of function, form, and discovery. *Progress in Lipid Research*, *59*, 88-10.

Zhan, C., Zhou, J., Feng, Q., Zhang, J. E., Lin, S., Bao, J., ... & Luo, M. (2013). Acute and long-term suppression of feeding behavior by POMC neurons in the brainstem and hypothalamus, respectively. *Journal of Neuroscience*, *33*(8), 3624-3632.

Zhang, J., & Wagner, G. P. (2013). On the definition and measurement of pleiotropy. *Trends in Genetics*, *29*(7), 383-384.

Zhang, L., Mazo-Vargas, A., & Reed, R. D. (2017). Single master regulatory gene coordinates the evolution and development of butterfly color and iridescence. *Proceedings of the National Academy of Sciences*, *114*(40), 10707-10712.

Chapter 2

The *yellow* Gene Influences *Drosophila* Male Mating Success Through Sex Comb Melanization[1]

Abstract

Drosophila melanogaster males perform a series of courtship behaviors that, when successful, result in copulation with a female. For over a century, mutations in the *yellow* gene, named for its effects on pigmentation, have been known to reduce male mating success. Prior work has suggested that *yellow* influences mating behavior through effects on wing extension, song, and/or courtship vigor. Here, we rule out these explanations, as well as effects on the nervous system more generally, and find instead that the effects of *yellow* on male mating success are mediated by its effects on pigmentation of male-specific leg structures called sex combs. Loss of *yellow* expression in these modified bristles reduces their melanization, which changes their structure and causes difficulty grasping females prior to copulation. These data illustrate why the mechanical properties of anatomy, and not just neural circuitry, must be considered to fully understand the development and evolution of behavior.

[1] This chapter is *in review* at *eLife* as: Massey, J. H., Chung, D., Siwanowicz, I., Stern, D. L., Wittkopp, P. J. The *yellow* gene influences *Drosophila* male mating success through sex comb melanization

Introduction

"The form of any behavior depends to a degree on the form of the morphology performing it" -Mary Jane West-Eberhard, 2003

Over 100 years ago in Thomas Hunt Morgan's fly room, Alfred Sturtevant described what is often regarded as the first example of a single gene mutation affecting behavior (Sturtevant, 1915; reviewed in Drapeau *et al.*, 2003; Cobb, 2007; Greenspan 2008): he noted that *yellow* mutant males, named for their loss of black pigment that gives their body a more yellow appearance (Figure 2-1A), mated successfully with wild-type females much less often than wild-type males. In 1956, in what is often regarded as the first ethological study (reviewed in Cobb, 2007; Greenspan 2008), Margaret Bastock compared courtship of *yellow* mutant and wild-type males and concluded that despite all courtship actions being present, loss of *yellow* function likely reduces courtship vigor or drive, leading to copulation inhibition (Bastock 1956). Despite more recent data consistent with this hypothesis (Drapeau et al. 2003), the precise mechanism by which the *yellow* gene affects male mating success in *D. melanogaster* has remained a mystery. Consequently, Bastock's statement about *yellow* from her 1956 paper is equally true today: *"It seemed worthwhile therefore to examine more closely one example of a gene mutation affecting behavior and to ask two questions, (1) how does it bring about its effect? [and], (2) what part might it play in evolution?"*

The *D. melanogaster yellow* gene encodes a protein hypothesized to act either structurally (Geyer *et al.*, 1986) or enzymatically (Wittkopp *et al.*, 2002) in the synthesis of dopamine melanin, and a Yellow homolog has been shown to bind dopamine and other biogenic amines in the sand fly *Lutzomyia longipalpis* (Xu *et al.*, 2011). The interaction between Yellow and dopamine might explain the protein's effects on male mating success because dopamine acts as a modulator of male courtship drive in *D. melanogaster* (Zhang *et al.*, 2016). These effects of dopamine are mediated by neurons expressing the gene *fruitless* (*fru*) (Zhang *et al.*, 2016), which is a master regulator of sexually dimorphic behavior in *D. melanogaster* that can affect every component of courtship and copulation (reviewed in Villella and Hall, 2008). *fru* has also been shown

to regulate expression of *yellow* in the central nervous system (CNS) of male *D. melanogaster* larvae (Drapeau *et al*., 2003). These observations suggest that the pleiotropic effects of *yellow* on male mating success might result from effects of *yellow* in the adult CNS, particularly in *fru*-expressing neurons. Consistent with this hypothesis, functional links between the pigment synthesis pathway and behavior mediated by the nervous system have previously been reported for other pigmentation genes (Hotta and Benzer, 1969; Heisenberg, 1971; Borycz *et al*., 2002; Richardt *et al*., 2002; True *et al*., 2005; Suh and Jackson, 2007).

Results and Discussion

fruitless-*expressing cells do not mediate the effect of* yellow *on male mating success*

D. melanogaster males perform multiple behaviors, including tapping, chasing, singing, and genital licking, before attempting to copulate with females by curling their abdomen and grasping the female (Figure 2-1B, Movie 1). In one-hour trials, we found that virgin males homozygous for a null allele of the *yellow* gene (*y1*) successfully mated with wild-type virgin females only 3% of the time, whereas wild-type males mated with wild-type virgin females 93% of the time (Figure 2-1C). Videos of mating trials indicated that the difference in mating success between wild-type and *yellow* males did not come from differences in courtship activity (Figure 2-1D-H) (compare Movies 1 and 2), but rather from differences in the ability of *yellow* and wild-type males to initiate copulation (compare Movies 3 and 4).

To determine whether *yellow* activity in *fru*-expressing cells is responsible for this difference in mating success, we used the UAS-GAL4 system (Brand and Perrimon, 1993) to drive expression of *yellow-RNAi* (Dietzl *et al.*, 2007) with fru^{GAL4} (Stockinger *et al*., 2005), knocking down native *yellow* expression in these cells. We also used fru^{GAL4} to drive *yellow* expression in *y1* mutants. In both cases, we found no significant effect on male mating success (Figure 2-2A,B), showing that expression of *yellow* in *fru*-expressing cells is neither necessary nor sufficient for *yellow's* effect on male mating success.

Doublesex-expressing cells require yellow *for normal male mating success*

To continue searching for cells responsible for *yellow*'s effects on mating, we examined a 209 bp sequence 5' of the *yellow* gene called the "mating-success regulatory sequence" (MRS) because deletion mapping indicated it was required for male mating success (Drapeau et al. 2006). We hypothesized that the MRS might contain an enhancer driving *yellow* expression and found that ChIP-seq data indicates the Doublesex (Dsx) transcription factor binds to this region *in vivo* (Clough *et al.*, 2014). Like *fru*, *dsx* expression is required to specify sex-specific behaviors in *D. melanogaster* (Rideout *et al*., 2010; Robinett *et al.*, 2010; reviewed in Villella and Hall, 2008; Yamamoto and Koganezawa, 2013), suggesting that *yellow* expression regulated by Dsx through the MRS enhancer might be responsible for its effects on male mating behavior. We found that reducing *yellow* expression in *dsx*-expressing cells with either of two different dsx^{GAL4} drivers (Robinett *et al.*, 2010; Rideout *et al.*, 2010) strongly reduced male mating success (Figure 2-2C, Supplementary Figure S2-1A), whereas restoring *yellow* activity in cells expressing dsx^{GAL4} in y^1 mutants significantly increased male mating success compared with y^1 controls (Figure 2-2D, Supplementary Figure S2-1B). Video recordings of male flies with reduced *yellow* expression in *dsx*-expressing cells showed the same mating defect observed in y^1 mutants: males seem to perform all courtship actions normally, but repeatedly failed to copulate (Movie 5). We therefore conclude that *yellow* expression is required in *dsx*-expressing cells for normal male mating behavior.

To determine whether the MRS sequence might be the enhancer mediating *yellow* expression in *dsx*-expressing cells that affect male mating success, we manipulated *yellow* expression with GAL4 driven by a 2.7kb DNA region located 5' of *yellow* that includes the wing, body, and putative MRS enhancers (Gilbert *et al.*, 2006, Supplementary Figure S2-2A). Altering *yellow* expression with this GAL4 driver modified pigmentation as expected but did not affect male mating success (Supplemental Figure S2-2B-D), possibly because this GAL4 line did not show any detectable expression in the adult CNS (Supplementary Figure S2-2E). To test more directly whether the MRS was necessary for male mating success, we deleted 152 bp of the 209 bp MRS sequence using CRISPR/Cas9 gene editing (Bassett *et al*., 2013) (Supplemental

Figure S2-2F,G). We found that this deletion had no significant effect on male mating success (Supplemental Figure S2-2H), contradicting the previous deletion mapping data (Drapeau *et al*., 2006). We conclude therefore that *yellow* expression in *dsx*-expressing cells affecting mating behavior must be mediated by other *cis*-regulatory sequences associated with the *yellow* gene.

dsx-*expressing cells outside the CNS require* yellow *for normal male mating success*

Although *dsx* is expressed broadly throughout the fly (Robinett *et al*., 2010; Rideout *et al*., 2010), we hypothesized that its expression in the nervous system would be responsible for *yellow*'s effects on mating because *yellow* has been reported to be expressed in the adult brain (Hinaux *et al*., 2018) and behavioral effects of other pigmentation genes are mediated by neurons (Hotta and Benzer, 1969; Heisenberg, 1971; Borycz et al., 2002; True *et al*., 2005). However, we found that suppressing *yellow* expression in the larval CNS, dopaminergic neurons, or serotonergic neurons (Supplementary Figure S2-3), or in all neurons (Figure 2-2E) or all glia (Figure 2-2F), had no significant effect on male mating success. Specifically reducing *yellow* expression in either all *dsx*-expressing neurons (Figure 2-2G) or all *dsx*-expressing glutamatergic neurons that are required for genital coupling (Pavlou *et al*., 2016) (Figure 2-2H) also had no significant effect on male mating success. In addition, when we examined *yellow* expression in adult brains, we were only able to observe non-specific signal at the anterior of the adult brain in females (Figure 2-2J,K). Given this lack of evidence that *yellow* is required in neuronal cells for normal male mating behavior, we limited dsx^{GAL4} activation of *yellow* expression in *y1* mutants to non-neuronal cells and found that these flies exhibited a substantial increase in male mating success compared with y^1 mutant males (Figure 2-2I), showing that *yellow* expression in non-neuronal *dsx*-expressing cells is required for normal male mating behavior.

To identify which non-neuronal *dsx*-expressing cells require *yellow* expression for normal male mating success, we screened ten *dsx*-enhancer GAL4 lines that each contains a different ~3 kb region of *dsx* noncoding sequence (Figure 2-2L; Pfeiffer *et al*., 2008). Two of these lines, *42D04-GAL4* and *40F03-GAL4*, significantly decreased male mating

success when driving *yellow-RNAi* (Figure 2-2M). These two GAL4 drivers contain overlapping sequences from intron 2 of *dsx* (Figure 2-2L), suggesting that their similar effects result from reduction of *yellow* expression in the same cells. Line *42D04-GAL4* had stronger effects than *40F03-GAL4* (Figure 2-2N), so we performed all further analyses with this line. Males with *yellow* reduced by *42D04-GAL4* performed courtship behavior in a pattern similar to y^1 mutant males: males performed all precopulatory courtship behaviors normally, but repeatedly failed to copulate, even after hours of attempts (Movie 6). These data indicate that some or all cells in which *42D04-GAL4* drives expression require *yellow* expression for normal male mating behavior.

Sex combs require yellow *expression for normal male mating success*

42D04-GAL4 drives expression in a sexually dimorphic pattern in multiple neurons of the adult male (Figure 2-3A,B) and female CNS (Supplemental Figure S2-4A,B), consistent with previously described dsx^{GAL4} expression in the posterior cluster, the abdominal cluster, and, in males, in the prothoracic TN1 neurons (Robinett *et al.*, 2010). *42D04-GAL4* also drives expression in male and female larval CNS and genital discs, with expression in the genital tissues persisting into the adult stage only in females (Supplemental Figure S2-4C-G). Finally, we observed *42D04-GAL4* expression at the base of the sex combs (also observed by Robinett *et al*. 2010), which are modified bristles used during mating (Cook, 1975; Ng and Kopp 2008; Hurtado-Gonzales *et al*., 2015) that are present only on the first tarsal segment of adult male forelegs (Figure 2-3C-F). Yellow protein is expressed in sex combs (Hinaux *et al*., 2018, Figure 2-3G,H), where it is presumably required for synthesis of black dopamine melanin in the sex comb "teeth". This expression of *yellow* in sex comb cells is driven by enhancer sequences in the *yellow* intron (Supplementary Figure S2-5), potentially explaining why manipulating *yellow* expression using GAL4 driven by sequences 5' of the *yellow* gene failed to affect mating. Driving expression of *yellow*-RNAi with *42D04-GAL4* eliminated expression of an mCherry tagged version of the native Yellow protein in sex combs and strongly reduced black melanin in the sex combs (Figure 2-3I-L) but not the abdomen (Supplemental Figure S2-4J).

To test the impact of *yellow* expression in sex combs on male mating behavior, we used *42D04-GAL4* to drive *yellow-RNAi,* but inhibited the function of *42D04-GAL4* in the CNS with *nysb-GAL80* (courtesy of Julie Simpson). These flies showed no GAL4 activity in the CNS (Figure 2-3M,N), but lost black melanin in the sex combs (Figure 2-3O) and had significantly reduced male mating success (Figure 2-3P). High-speed videos (1000 frames per second) revealed that *yellow* mutant (y^1) males fail repeatedly to grasp the female abdomen with their sex combs when attempting to mount and copulate (Movie 7), whereas wild-type males more readily grasp the female with their melanized sex combs and initiate copulation efficiently (Movie 8). These observations suggest that *yellow* expression in sex combs affects their melanization, which in turn affects their function.

Sex comb melanization is required for efficient grasping, mounting and copulation

To test whether sex comb melanization (as opposed to some other unknown effect of losing *yellow* expression in sex combs) is critical for male sexual behavior, we suppressed expression of *Laccase2* (Arakane *et al.*, 2005; Riedel *et al.*, 2011) in sex combs using *42D04-GAL4* and *Laccase2-RNAi* (Dietzl *et al.*, 2007). Laccase2 is required to oxidize dopamine into dopamine quinones and thus acts upstream of Yellow in the melanin synthesis pathway (Figure 2-4A; Riedel *et al*., 2011). Males with *Laccase2* suppressed in sex combs lacked both black and brown dopamine melanin, making these sex combs appear translucent (Figure 2-4B). These males displayed strongly reduced mating success compared with wild-type males (Figure 2-4C) and behavioral defects similar to those observed for y^1 mutants (Movies 9,10), including inefficient grasping of the female for mounting and copulation. We noticed, however, that flies with *Laccase2-RNAi* driven by *42D04-GAL4* also showed a loss of melanin in the aedeagus (Supplementary Figure S2-6A), which is the main part of the male genitalia used for copulation, despite no visible expression of *42D04-GAL4* in the adult male genitalia (Supplementary Figure S2-4G) nor changes in aedeagus pigmentation in y^1 mutants (Supplementary Figure 2-6A). We therefore used subsets of the *42D04* enhancer (Supplementary Figure S2-6B) to drive expression of *Laccase2-RNAi,* separating the effects of expression in the sex combs from expression in the genitalia (Supplementary

Figure S2-6C). Male mating success was reduced when *Laccase2* suppression reduced melanization in the sex combs, but not the genitalia (Supplementary Figure S2-6D-G).

How can sex comb melanization affect sex comb function? In insects, melanization impacts not only the color of the adult cuticle but also its mechanical stiffness (Xu et al., 1997; Kerwin et al., 1999; Vincent and Wegst, 2004; Andersen, 2005; Arakane *et al.*, 2005; Suderman *et al.*, 2006; Riedel *et al.*, 2011; Noh *et al.*, 2016). For example, expressing *Laccase2-RNAi* in *D. melanogaster* wings softens the cuticle to such a degree that the wings collapse (Riedel *et al.*, 2011). Butterflies lacking dopamine melanin due to loss of *yellow* or another gene required for melanin synthesis, *Dopa decarboxylase,* show changes in the fine structure of their wing scales (Matsuoka and Monteiro, 2018), and we also observed structural changes in *D. melanogaster* sex comb teeth lacking *yellow* or *Laccase2* expression using scanning electron microscopy (SEM), with a crack appearing in one of the *Laccase2-RNAi* comb teeth (Figure 2-4D). We conclude that these structural changes in sex combs are responsible for inhibiting the *yellow* mutant male's ability to grasp a female for mounting and copulation (Movie 10). Interestingly, Wilson *et al.* (1976) also proposed "that there may be a structural basis for the behavioural effects of the [*yellow*] mutant" based on their observations of behavior in *yellow* mutant males.

Data from other Drosophila species are also consistent with this structural hypothesis. Specifically, *yellow* mutants in *D. subobscura*, *D. pseudoobscura*, and *D. gaucha*, all of which have sex combs, show reduced male mating success (Rendel, 1944; Tan, 1946; Frias and Lamborot, 1970; Pruzan-Hotchkiss *et al.*, 1992) whereas *yellow* mutants in *Drosophila willistoni*, a species that lacks sex combs (Kopp, 2011; Atallah *et al.*, 2014), do not (Da Silva *et al.*, 2005). Sex comb morphology is highly diverse among species that have sex combs (Kopp, 2011), but these structures generally seem to be melanized (Supplementary Figure S2-7; Tanaka *et al.*, 2009) and used to grasp females (Movies 11-15). Our high-speed video recordings of mating in *D. anannasae*, *D. bipectinata*, *D. kikkawai*, *D. malerkotiana*, and *D. takahashi* show that differences in sex comb morphology (Supplementary Figure S2-7) correspond with differences in how (where on

the female and with which part of the male leg) the male grasps the female prior to copulation (Movies 11-15).

It remains unclear how *D. willistoni* males (and males of other species without sex combs) are able to efficiently grasp females prior to copulation (Movie 16). Differences in females might be part of the answer, however, as *D. melanogaster y1* mutant males are able to mate with *y1* mutant females at rates similar to wild-type males (Bastock 1956, Dow 1976, Heisler 1984, Liu et al., 2019; Supplementary Figure S2-8A). That said, removing all melanin from *D. melanogaster* sex combs by knocking down *Laccase-2* reduced mating efficiency with *y1* females, suggesting that the brown melanin remaining in *y1* sex-combs (Figure 2-4B) played a role in the mating success of *y1* males with *y1* females (Supplementary Figure S2-8B).

Taken together, our data show that melanization of a secondary sexual structure affects mating in *D. melanogaster*. Specifically, we find that the reduced mating success of *D. melanogaster yellow* mutant males, which was perceived as a behavioral defect for decades, is caused by changes in the morphology of the structures used during mating. These observations underscore that behavior cannot be understood by studying the nervous system alone; anatomy and behavior function and evolve as an interconnected system.

Materials and Methods

Fly stocks and maintenance

The following lines were used for this work: *y1* [which was backcrossed into a wild-type (*Canton-S*) line for 6 generations before starting our experiments; the *y1* allele contains an A to C transversion in the ATG initiation and is considered a null allele (Geyer *et al.*, 1990)]; *Canton-S* as wild-type (courtesy of Scott Pletcher); *UAS-yellow-RNAi* obtained from the Vienna Drosophila Resource Centre (VDRC) (Dietzl *et al.*, 2007, KK106068); *y1;UAS-y* (BDSC 3043); *elav-GAL4* (BDSC 49226); *nsyb-GAL4* (BDSC 39171); *repo-GAL4* (BDSC 7415); dsx^{GAL4} (Robinett *et al*., 2010) (courtesy of Bruce Baker); dsx^{GAL4}

(Rideout *et al.*, 2010) (courtesy of Stephen Goodwin); *fru*^{GAL4} (Stockinger *et al.*, 2005) (courtesy of Barry Dickson); the following Janelia enhancer trap GAL4 lines (Pfeiffer *et al*., 2008): *40A05-GAL4* (BDSC 48138), *41D01-GAL4* (BDSC 50123), *42D02-GAL4* (BDSC 41250), *41F06-GAL4* (BDSC 47584), *41A01-GAL4* (BDSC 39425), *42D04-GAL4* (BDSC 47588), *40F03-GAL4* (BDSC 47355), *39E06-GAL4* (BDSC 50051), *42C06-GAL4* (BDSC 50150), *40F04* (BDSC 50094); *y*^{mCherry} (courtesy of Nicolas Gompel); *nsyb-GAL80* (courtesy of Julie Simpson); *UAS-Laccase2-RNAi* obtained from the VDRC (Dietzl *et al.*, 2007, KK101687); *dsx*$^{GAL4-DBD}$ (Pavlou *et al*., 2016) (courtesy of Stephen Goodwin); *vGlut*$^{dVP16-AD}$ (Gao *et al*., 2008) (courtesy of Stephen Goodwin); BDSC 6993; BDSC 49365; BDSC 6927; BDSC 45175; BDSC 3740; BDSC 5820; BDSC 8848 (courtesy of Shinya Yamamoto); BDSC 7010 (courtesy of Shinya Yamamoto); *TPH-GAL4* (courtesy of Shinya Yamamoto); *wing-body-GAL4* (BDSC 44373); *D. melanogaster yellow 5' up EGFP reporter* (Kalay and Wittkopp, 2010) (courtesy of Gizem Kalay); *D. melanogaster yellow intron EGFP reporter* (Kalay and Wittkopp, 2010) (courtesy of Gizem Kalay); *vasa-Cas9* (BDSC 51324); *UAS-cytGFP* (courtesy of Janelia Fly Core); *pJFRC12-10XUAS-IVS-myr::GFP* (courtesy of Janelia Fly Core). All flies were grown at 23°C with a 12 h light-dark cycle with lights on at 8AM and off at 8PM on standard corn-meal fly medium.

Behavior

Mating assays

Virgin males and females were separated upon eclosion and aged for 4-7 d before each experiment. Experiments were carried out at 23°C on a 12 h light dark cycle with lights on at 8 AM and off at 8 PM on standard corn-meal fly medium. Males were isolated in glass vials, and females were group housed in standard plastic fly vials at densities of 20-30 flies. All mating assays were performed at 23°C between 8-11AM or 6-9PM. For each assay replicate, a single virgin male and female fly were gently aspirated into a 35 mm diameter Petri dish (Genesee Scientific, catalog #32-103) placed on top of a 17 inch LED light pad (HUION L4S) and immediately monitored for 60 min for courtship and copulation activity. All genotypes tested initiated courtship (including tapping, chasing,

wing extension, genital licking, and attempted copulation) towards the female. Any genotype that copulated within the 60 min window was noted. Except for the experiment described in Figure 2-8, all female targets in mating assays were wild-type (*Canton-S*). Percent mated in 60 min was then calculated as the number of replicates that mated divided by the total number of replicates and multiplied by 100.

Courtship analysis

For courtship analysis, 60 min videos were recorded using Canon VIXIA HF R500 camcorders mounted to Manfrotto (MKCOMPACTACN-BK) aluminum tripods. To calculate courtship indices in Figure 2-1 between wild-type and *y1* males, the amount of time males spent engaged in courtship: tapping, chasing, wing extension, genital licking, or attempted copulation was quantified for the first 10 min of the assay and divided by the total 10 min period. We chose to quantify courtship activity within the first 10 min of the assay, because wild-type (*Canton-S*) males will often begin copulating after this window, while *y1* males will continue to court throughout the entire 60 min period. Wing extension bouts were quantified by noting every unilateral wing extension bout for each genotype within the first 10 min of the assay.

Song analysis

Courtship song was recorded as described previously (Arthur *et* al., 2013). All genotypes were recorded simultaneously. Song data was segmented (Arthur *et al.*, 2013) and analyzed (http://www.github.com/dstern/BatchSongAnalysis) without human intervention. *P*-values for one-way ANOVAs were estimated with 10,000 permutations (http://www.mathworks.com/matlabcentral/ fileexchange/44307-randanova1).

High-speed video capture

For high-speed video capture of attempted mounting and copulation events, virgin males and females were isolated upon eclosion and aged for 4-7 d before each assay. Using a Fascam Photron SA4 (courtesy of Gwyneth Card) mounted with a 105 mm AF Micro Nikkor Nikon lens (courtesy of Gwyneth Card), we recorded individual pairs of males and females that were gently aspirated into a single well of a 96 well cell culture plate

(Corning 05-539-200) partially filled with 2% agarose and covered with a glass coverslip. We recorded mounting and copulation attempts at 1000 frames per second (fps) and played back at 30 fps. Most wild-type males attempted mounting 3-5 times before copulating, whereas *y1*, *yellow-RNAi,* and *Laccasse2-RNAi* males repeatedly attempted mounting without engaging in copulation, mirroring the videos we captured on the Canon VIXIA HF R500 at 30 fps.

Imaging sex combs and genitalia

Sex comb images highlighting different melanization states (Figure 2-3I, J, O; Figure 2-4B) were taken using a Zeiss Axio Cam ERc 5s mounted on a Zeiss Axio Observer A1 Inverted Microscope. Front legs were cut and placed sex comb side down on a microscope slide (Fisher brand 12-550-123) and imaged through a 40x objective. Images were processed using AxioVision LE software. Abdomens and genitalia images highlighting different melanization states of the aedeagus and female genital bristles were captured using a Canon EOS Rebel T6 camera mounted with a Canon MP-E 65 mm macro lens. Genitalia images were processed in Adobe Photoshop (version 19.1.5) (Adobe Systems Inc., San Jose, CA).

Focus Ion Beam Scanning Electron Microscope (FIB-SEM) images (Figure 2-4D) were taken by placing individual, dissected legs on carbon tape adhered to a SEM pin stud mount with sex combs facing up. The samples were then coated with a 20-nm Au layer using a Gatan 682 Precision Etching and Coating System, and imaged by SEM in a Zeiss Sigma system. The samples were imaged using a 3-nA electron beam with 1.5 kV landing energy at 2.5MHz.

Immunohistochemistry and confocal imaging

Central Nervous System

Dissections, immunohistochemistry, and imaging of fly central nervous systems were done as previously described (Aso *et al.*, 2014). In brief, brains and VNCs were dissected

in Schneider's insect medium and fixed in 2% paraformaldehyde (diluted in the same medium) at room temperature for 55 min. Tissues were washed in PBT (0.5% Triton X-100 in phosphate buffered saline) and blocked using 5% normal goat serum before incubation with antibodies. Tissues expressing GFP were stained with rabbit anti-GFP (ThermoFisher Scientific A-11122, 1:1000) and mouse anti-BRP hybridoma supernatant (nc82, Developmental Studies Hybridoma Bank, Univ. Iowa, 1:30), followed by Alexa Fluor® 488-conjugated goat anti-rabbit and Alexa Fluor® 568-conjugated goat anti-mouse antibodies (ThermoFisher Scientific A-11034 and A-11031), respectively. Tissues expressing mCherry-tagged Yellow protein ($y^{mCherry}$) were stained with rabbit anti-dsRed (Clontech 632496, 1:1000) and rat anti-*D*N-Cadherin (DN-Ex #8, Developmental Studies Hybridoma Bank, Univ. Iowa, 1:100) as neuropil marker, followed by Cy™3-conjugated goat anti-rabbit and Cy™5-conjugated goat anti-rat antibodies (Jackson ImmunoResearch 111-165-144 and 112-175-167), respectively. After staining and post-fixation in 4% paraformaldehyde, tissues were mounted on poly-L-lysine-coated cover slips, cleared, and embedded in DPX as described. Image z-stacks were collected at 1 µm intervals using an LSM710 confocal microscope (Zeiss, Germany) fitted with a Plan-Apochromat 20x/ 0.8 M27 objective. Images were processed in Fiji (http://fiji.sc/) and Adobe Photoshop (version 19.1.5) (Adobe Systems Inc., San Jose, CA).

Sex combs and genitalia

Adult flies were 2-7 d old and pupae were 96 h old after pupal formation (APF) for the EGFP reporter experiment summarized in Supplementary Figure S2-5. Flies were anesthetized on ice, submerged in 70% ethanol, rinsed twice in phosphate buffered saline with 0.1 % Triton X-100 (PBS-T), and fixed in 2% formaldehyde in PBS-T. Forelegs and genitalia/abdomen tips were removed with fine scissors and mounted in Tris-buffered (pH 8.0) 80% glycerol. Serial optical sections were obtained at 1.5 µm or 0.5 µm intervals on a Zeiss 880 confocal microscope with a LD-LCI 25x/0.8 NA objective (genitalia) or a Plan-Apochromat 40x/1.3 NA objective (appendages/tarsal sex combs). The native fluorescence of GFP, mCherry and autofluorescence of cuticle were imaged using 488, 594 and 633 lasers, respectively. Images were processed in Fiji (http://fiji.sc/),

Icy (http://icy.bioimageanalysis.org/) and Adobe Photoshop (version 19.1.5) (Adobe Systems Inc., San Jose, CA).

Statistics

Statistical tests were performed in R for Mac version 3.3.3 (R Core Team 2018) using Fisher's exact tests to test for statistically significant effects of 2 x 2 contingency tables, Chi-square tests to test for statistically significant effects of contingency tables greater than 2 x 2 with Bonferroni corrections for multiple comparisons, and two-tailed Student's t-tests to test for statistically significant effects of pairwise comparisons of continuous data with normally distributed error terms. For song analysis, one-way ANOVAs were performed in MATLAB version R2017a (The MathWorks, Inc.).

Generation of the mating regulatory sequence (MRS) deletion line

Using the 209 bp region mapped in Drapeau *et al*. (2006) between -300 and -91 bp upstream of *yellow*'s transcription start site, we designed two single guide RNA (gRNA) target sites at -291 bp and -140 bp that maximized the MRS deletion region, given constraints of identifying NGG PAM sites required for CRISPR/Cas9 gene editing (Supplementary Figure S2-1A,B). We in-vitro transcribed these gRNAs using a MEGAscript T7 Transcription Kit (Invitrogen) following the PCR-based protocol from Bassett *et al*. (2013). Two 1 kb homology arms were PCR amplified from the *yellow* locus immediately upstream and downstream of the gRNA target sites using the forward and reverse primers with NcoI and BglII tails, respectively, for the Left Arm (5'-TTACCATGGGGGATCAAGTTGAACCAC-3', 5'-GGAGATCTGGCCTTCATCGACATTTA-3') and the forward and reverse primers with Bsu36I and MluI tails, respectively, for the Right Arm (5'-TACATCCCTAAGGCCTGATTACCCGAACACT-3', 5'-TATACGCGTTGCCATGCTATTGGCTTC-3') and cloned into pHD-DsRed-attp (Gratz *et al*., 2014; Addgene Plasmid # 51019) in two steps, digesting first with NcoI and BglII (Left Arm) to transform the Left Arm and second with Bsu36I and MluI (Right Arm) to

transform the Right Arm, flanking the 3xP3::DsRed, attP, and LoxP sites. Homology arms were ligated into pHD-DsRed-attp using T4 DNA Ligase (ThermoFisher Scientific), and products were transformed into One Shot TOP10 (Invitrogen) DH5 alpha competent cells. Purified donor plasmid was then co-injected at 500 ng/uL with the two gRNAs at 100 ng/uL total concentration into a *vasa-Cas9* (BDSC 51324) line. Flies were then screened for DsRed expression in the eyes, and Sanger sequenced verified for a 3xP3::DsRed replacement of the MRS region (Supplementary Figure S2-2F). We confirmed that we deleted 152 bp of the 209 bp region based on Sanger sequencing the CRISPR/Cas9 cut sites (Supplementary Figure S2-2F). Next, we crossed $y^{\Delta MRS+3xP3::DsRed}$ with a Cre-expressing fly line (courtesy of Bing Ye, University of Michigan) to excise 3xP3::DsRed and screened for flies that lost DsRed expression in the eyes. Finally, we PCR-gel verified that DsRed was indeed removed in creation of the $y^{\Delta MRS}$ line using the forward and reverse primers, respectively (5'-CAGTCGCCGATAAAGATGAACACTG-3', 5'-CAAGGTGATCAGGGTCACAAGGATC-3') (Supplementary Figure S2-2G).

Generation of the *42D04-GAL4* enhancer sub-fragment pBPGUw lines

Enhancer sub-fragments (2 kb, 2 kb, 1.3 kb, 1.3 kb, and 1.3 kb for *42D04_A,B,C,D,E*-GAL4, respectively) were synthesized as IDT gene blocks (sequences copied below) based off of the 42D04 *D. melanogaster dsx* enhancer sequence (FBsf0000164494) (Supplementary Figure S2-7). The gene blocks were designed with 5' and 3' Gibson tails to facilitate Gibson assembly (Gibson *et al*., 2009) into the GAL4 plasmid pBPGUw (Pfeiffer *et al*., 2008; Addgene Plasmid #17575) after digestion with FseI and AatII. Products were transformed into Mix and Go! DH5 alpha competent cells (Zymo). Clones were selected by ampicillin resistance on Amp-LB plates (60mg/mL). Purified plasmids were injected at 500 ng/uL into the phiC31 integrase-expressing 86Fb landing site line *BDSC 24749* (courtesy of Rainbow Transgenics) for phiC31 attP-attB integration and screened for using a mini-white marker.

Acknowledgements

We thank members of the Wittkopp and Stern labs for helpful discussions. For fly strains, we thank Bruce Baker, Carmen Robinett, Stephen Goodwin, Barry Dickson, Scott Pletcher, Julie Simpson, Shinya Yamamoto, Bing Ye, Nicolas Gompel, Gizem Kalay, The Bloomington Drosophila Stock Center, The Vienna Drosophila RNAi Center, and the Janelia Fly Core for fly strains. For fly injections, we thank Rainbow Transgenics Inc. For technical support with Scanning Electron Microscopy (SEM), we thank Harald Hess and Song Pang. For use of the Photron for high-speed video capture, we thank Gwyneth Card and W. Ryan Williamson. CNS dissections, immunostaining, and imaging were performed by the Janelia Project Technical Resource team with special thanks to Gudrun Ihrke, Kari Close, and Christina Christoforou. We thank Nicolas Gompel, Abby Lamb, and Henry Ertl for comments on the manuscript. Funding: University of Michigan, Department of Ecology and Evolutionary Biology, Peter Olaus Okkelberg Research Award, National Institutes of Health (NIH) training grant T32GM007544, and Howard Hughes Medical Institute Janelia Graduate Research Fellowship to J.H.M.; NIH R01 GM089736 and 1R35GM118073 to PJW. Data and materials availability: All data is available in the main text or the supplementary materials.

References

Andersen, S. O. (2005). Cuticular sclerotization and tanning. In L.I. Gilbert, K. Iatrou, S.S. Gill (Eds.), *Comprehensive Molecular Insect Science* (pp. 145-175). Elsevier-Pergamon.

Arakane, Y., Muthukrishnan, S., Beeman, R. W., Kanost, M. R., & Kramer, K. J. (2005). Laccase 2 is the phenoloxidase gene required for beetle cuticle tanning. *Proceedings of the National Academy of Sciences*, *102*(32), 11337-11342.

Arthur, B. J., Sunayama-Morita, T., Coen, P., Murthy, M. & Stern, D. L. (2013). Multi-channel acoustic recording and automated analysis of *Drosophila* courtship songs. *BMC Biol. 11*, 11.

Aso, Y., Hattori, D., Yu, Y., Johnston, R. M., Iyer, N. A., Ngo, T. T., ... & Rubin, G. M. (2014). The neuronal architecture of the mushroom body provides a logic for associative learning. *Elife*, *3*, e04577.

Atallah, J., Vurens, G., Mavong, S., Mutti, A., Hoang, D., & Kopp, A. (2014). Sex-specific repression of dachshund is required for *Drosophila* sex comb development. *Developmental Biology*, *386*(2), 440-447.

Bassett, A. R., Tibbit, C., Ponting, C. P., & Liu, J. L. (2013). Highly efficient targeted mutagenesis of *Drosophila* with the CRISPR/Cas9 system. *Cell Reports*, *4*(1), 220-228.

Bastock, M. (1956). A gene mutation which changes a behavior pattern. *Evolution*, *10*(4), 421-439.

Borycz, J., Borycz, J. A., Loubani, M., & Meinertzhagen, I. A. (2002). *Tan* and *ebony* genes regulate a novel pathway for transmitter metabolism at fly photoreceptor terminals. *Journal of Neuroscience*, *22*(24), 10549-10557.

Brand, A. H., & Perrimon, N. (1993). Targeted gene expression as a means of altering cell fates and generating dominant phenotypes. *Development*, *118*(2), 401-415.

Clough, E., Jimenez, E., Kim, Y. A., Whitworth, C., Neville, M. C., Hempel, L. U., ... & Smith, H. E. (2014). Sex-and tissue-specific functions of *Drosophila doublesex* transcription factor target genes. *Developmental Cell*, *31*(6), 761-773.

Cobb, M. (2007). A gene mutation which changed animal behaviour: Margaret Bastock and the yellow fly. *Animal Behaviour*, *74*(2), 163-169.

Cook, R. (1975). Courtship of *Drosophila melanogaster*: rejection without extrusion. Behaviour, *52*(3-4), 155-171.

Da Silva, L. B., Leite, D. F., Valente, V. L. S., Rohde, C. 2005. Mating activity of yellow

and sepia *Drosophila willistoni* mutants. *Behav. Processes, 70,* 149–155.

Dietzl, G., Chen, D., Schnorrer, F., Su, K. C., Barinova, Y., Fellner, M., ... & Couto, A. (2007). A genome-wide transgenic RNAi library for conditional gene inactivation in *Drosophila*. *Nature*, *448*(7150), 151.

Dow, M. A. (1976). The genetic basis of receptivity of yellow mutantDrosophila melanogaster females. *Behavior genetics*, *6*(2), 141-143.

Drapeau, M. D., Cyran, S. A., Viering, M. M., Geyer, P. K., & Long, A. D. (2006). A cis-regulatory sequence within the yellow locus of *Drosophila melanogaster* required for normal male mating success. *Genetics*, *172*(2), 1009-1030.

Drapeau, M. D., Radovic, A., Wittkopp, P. J., & Long, A. D. (2003). A gene necessary for normal male courtship, *yellow*, acts downstream of *fruitless* in the *Drosophila melanogaster* larval brain. *Journal of Neurobiology*, *55*(1), 53-72.

Frias, D., and M. Lamborot. (1970). Reproductive isolation between the *yellow*, *white*, and ‘‘wild’’ stocks of *D. gaucha* at two temperatures (in Spanish). *Arch. Biol. Med. Exp. 7,* 67.

Gao, S., Takemura, S. Y., Ting, C. Y., Huang, S., Lu, Z., Luan, H., ... & Wang, J. W. (2008). The neural substrate of spectral preference in *Drosophila*. *Neuron*, *60*(2), 328-342.

Geyer, P. K., Spana, C., & Corces, V. G. (1986). On the molecular mechanism of gypsy-induced mutations at the *yellow* locus of *Drosophila melanogaster*. *The EMBO Journal*, *5*(10), 2657-2662.

Geyer, P. K., & Corces, V. G. (1987). Separate regulatory elements are responsible for the complex pattern of tissue-specific and developmental transcription of the *yellow* locus in *Drosophila melanogaster*. *Genes & Development*, *1*(9), 996-1004.

Geyer, P. K., Green, M. M., & Corces, V. G. (1990). Tissue-specific transcriptional enhancers may act in trans on the gene located in the homologous chromosome: the molecular basis of transvection in *Drosophila*. *The EMBO Journal*, *9*(7), 2247-2256.

Gibson, D. G., Young, L., Chuang, R. Y., Venter, J. C., Hutchison III, C. A., & Smith, H. O. (2009). Enzymatic assembly of DNA molecules up to several hundred kilobases. *Nature Methods*, *6*(5), 343.

Gilbert, M. K., Tan, Y. Y., & Hart, C. M. (2006). The *Drosophila* boundary element-associated factors BEAF-32A and 32B affect chromatin structure. *Genetics, 173*, 1365-1375.

Gratz, S. J., Ukken, F. P., Rubinstein, C. D., Thiede, G., Donohue, L. K., Cummings, A. M., & O'Connor-Giles, K. M. (2014). Highly specific and efficient CRISPR/Cas9-catalyzed homology-directed repair in *Drosophila*. *Genetics*, *196*(4), 961-971.

Greenspan, R. J. (2008). The origins of behavioral genetics. *Current Biology*, *18*(5), R192-R198.

Heisenberg, M. (1971). Separation of receptor and lamina potentials in the electroretinogram of normal and mutant *Drosophila*. *Journal of Experimental Biology*, *55*(1), 85-100.

Heisler, I. L. (1984). Inheritance of female mating propensities for yellow locus genotypes in *Drosophila melanogaster*. *Genetics Research*, *44*(2), 133-149.

Hinaux, H., Bachem, K., Battistara, M., Rossi, M., Xin, Y., Jaenichen, R., ... & Rodermund, L. (2018). Revisiting the developmental and cellular role of the pigmentation gene yellow in *Drosophila* using a tagged allele. *Developmental Biology*, *438*(2), 111-123.

Hotta, Y., & Benzer, S. (1969). Abnormal electroretinograms in visual mutants of Drosophila. *Nature*, *222*(5191), 354.

Hurtado-Gonzales, J. L., Gallaher, W., Warner, A., & Polak, M. (2015). Microscale laser surgery demonstrates the grasping function of the male sex combs in *Drosophila melanogaster* and *Drosophila bipectinata*. *Ethology*, *121*(1), 45-56.

Kalay, G., & Wittkopp, P. J. (2010). Nomadic enhancers: tissue-specific cis-regulatory elements of yellow have divergent genomic positions among *Drosophila* species. *PloS Genetics*, *6*(11), e1001222.

Kalay, G., Lusk, R., Dome, M., Hens, K., Deplancke, B., & Wittkopp, P. J. (2016). Potential direct regulators of the *Drosophila yellow* gene identified by yeast one-hybrid and RNAi screens. *G3: Genes, Genomes, Genetics*, *6*(10), 3419-3430.

Kerwin, J. L., Turecek, F., Xu, R., Kramer, K. J., Hopkins, T. L., Gatlin, C. L., & Yates III, J. R. (1999). Mass spectrometric analysis of catechol–histidine adducts from insect cuticle. *Analytical biochemistry*, *268*(2), 229-237.

Kopp, A. (2011). *Drosophila* sex combs as a model of evolutionary innovations. *Evol Dev.*, *13*(6):504-22.

Liu, J., Champer, J., Langmüller, A. M., Liu, C., Chung, J., Reeves, R., ... & Messer, P. W. (2019). Maximum likelihood estimation of fitness components in experimental evolution. *Genetics*, *211*(3), 1005-1017.

Luan, H., Peabody, N. C., Vinson, C. R., & White, B. H. (2006). Refined spatial manipulation of neuronal function by combinatorial restriction of transgene expression. *Neuron*, *52*(3), 425-436.

Martin, M., Meng, Y. B., & Chia, W. (1989). Regulatory elements involved in the tissue-specific expression of the *yellow* gene of *Drosophila*. *Molecular and General Genetics MGG*, *218*(1), 118-126.

Matsuoka, Y., & Monteiro, A. (2018). Melanin pathway genes regulate color and morphology of butterfly wing scales. *Cell Reports*, *24*(1), 56-65.

Ng, C. S., & Kopp, A. (2008). Sex combs are important for male mating success in *Drosophila melanogaster*. *Behavior Genetics*, *38*(2), 195.

Noh, M. Y., Koo, B., Kramer, K. J., Muthukrishnan, S., & Arakane, Y. (2016). Arylalkylamine N-acetyltransferase 1 gene (TcAANAT1) is required for cuticle morphology and pigmentation of the adult red flour beetle, *Tribolium castaneum*. *Insect Biochemistry and Molecular Biology*, *79*, 119-129.

Pavlou, H. J., Lin, A. C., Neville, M. C., Nojima, T., Diao, F., Chen, B. E., ... & Goodwin, S. F. (2016). Neural circuitry coordinating male copulation. *Elife*, *5*, e20713.

Pfeiffer, B. D., Jenett, A., Hammonds, A. S., Ngo, T. T. B., Misra, S., Murphy, C., ... & Mungall, C. (2008). Tools for neuroanatomy and neurogenetics in *Drosophila*. *Proceedings of the National Academy of Sciences*, *105*(28), 9715-9720.

Pruzan-Hotchkiss, A., Sato, K., Thompson, J. F. (1992). Genetic and behavioral studies on *yellow Drosophila*. *Behav. Genet. 22*, 747.

R Core Team. 2013. R: A Language and Environment for Statistical Computing. Available from: http://www.r-project.org/.

Rendel, J. M. (1944). Genetics and cytology of *Drosophila subobscura*. II. Normal and selective matings in *Drosophila subobscura*. *J. Genet. 46*, 287–302.

Richardt, A., Rybak, J., Störtkuhl, K. F., Meinertzhagen, I. A., & Hovemann, B. T. (2002). Ebony protein in the *Drosophila* nervous system: optic neuropile expression in glial cells. *Journal of Comparative Neurology*, *452*(1), 93-102.

Rideout, E. J., Dornan, A. J., Neville, M. C., Eadie, S., & Goodwin, S. F. (2010). Control of sexual differentiation and behavior by the *doublesex* gene in *Drosophila melanogaster*. *Nature Neuroscience*, *13*(4), 458.

Riedel, F., Vorkel, D., & Eaton, S. (2011). Megalin-dependent *yellow* endocytosis restricts melanization in the *Drosophila* cuticle. *Development*, *138*(1), 149-158.

Robinett, C. C., Vaughan, A. G., Knapp, J. M., & Baker, B. S. (2010). Sex and the single cell. II. There is a time and place for sex. *PloS Biology, 8*(5), e1000365.

Rogers, W. A., Grover, S., Stringer, S. J., Parks, J., Rebeiz, M., & Williams, T. M. (2014). A survey of the trans-regulatory landscape for *Drosophila melanogaster* abdominal pigmentation. *Developmental Biology, 385*(2), 417-432.

Siegal, M. L., and Hartl, D. L. (1996). Transgene coplacement and high efficiency site-specific recombination with the Cre/loxP system in *Drosophila*. *Genetics, 144*, 715–726.

Stockinger, P., Kvitsiani, D., Rotkopf, S., Tirián, L., & Dickson, B. J. (2005). Neural circuitry that governs *Drosophila* male courtship behavior. *Cell, 121*(5), 795-807.

Sturtevant, A. H. (1915). Experiments on sex recognition and the problem of sexual selection in *Drosophila*. *Journal of Animal Behaviour, 5*, 351e366.

Suderman, R. J., Dittmer, N. T., Kanost, M. R., & Kramer, K. J. (2006). Model reactions for insect cuticle sclerotization: cross-linking of recombinant cuticular proteins upon their laccase-catalyzed oxidative conjugation with catechols. *Insect Biochemistry and Molecular Biology, 36*(4), 353-365.

Suh, J., & Jackson, F. R. (2007). *Drosophila ebony* activity is required in glia for the circadian regulation of locomotor activity. *Neuron, 55*(3), 435-447.

Tan, C. C. (1946). Genetics of sexual isolation between *Drosophila pseudoobscura* and *Drosophila persimilis*. *Genetics 31*, 558–573.

Tanaka, K., Barmina, O., & Kopp, A. (2009). Distinct developmental mechanisms underlie the evolutionary diversification of *Drosophila* sex combs. *Proceedings of the National Academy of Sciences, 106*(12), 4764-4769.

True, J. R., Yeh, S. D., Hovemann, B. T., Kemme, T., Meinertzhagen, I. A., Edwards, T. N., ... & Li, J. (2005). *Drosophila tan* encodes a novel hydrolase required in pigmentation and vision. *PloS Genetics, 1*(5), e63.

Villella, A., & Hall, J. C. (2008). Neurogenetics of courtship and mating in *Drosophila*. *Advances in Genetics, 62*, 67-184.

Vincent, J. F., & Wegst, U. G. (2004). Design and mechanical properties of insect cuticle. *Arthropod Structure & Development, 33*(3), 187-199.

West-Eberhard, M. J. (2003). Developmental plasticity and evolution. Oxford University Press.

Williams, T. M., Selegue, J. E., Werner, T., Gompel, N., Kopp, A., & Carroll, S. B. (2008). The regulation and evolution of a genetic switch controlling sexually dimorphic traits in *Drosophila*. *Cell*, *134*(4), 610-623.

Wilson, R., Burnet, B., Eastwood, L., & Connolly, K. (1976). Behavioural pleiotropy of the *yellow* gene in *Drosophila melanogaster*. *Genetics Research*, *28*(1), 75-88.

Wittkopp, P. J., True, J. R., & Carroll, S. B. (2002). Reciprocal functions of the *Drosophila* Yellow and Ebony proteins in the development and evolution of pigment patterns. *Development*, *129*(8), 1849-1858.

Xu, R., Huang, X., Hopkins, T. L., & Kramer, K. J. (1997). Catecholamine and histidyl protein cross-linked structures in sclerotized insect cuticle. *Insect Biochemistry and Molecular Biology*, *27*(2), 101-108.

Xu, X., Oliveira, F., Chang, B. W., Collin, N., Gomes, R., Teixeira, C., ... & Ribeiro, J. M. (2011). Structure and function of a "Yellow" protein from saliva of the sand fly *Lutzomyia longipalpis* that confers protective immunity against Leishmania major infection. *Journal of Biological Chemistry*, *286*(37), 32383-32393.

Yamamoto, D., & Koganezawa, M. (2013). Genes and circuits of courtship behaviour in *Drosophila* males. *Nature Reviews Neuroscience*, *14*(10), 681.

Zhang, S. X., Rogulja, D., & Crickmore, M. A. (2016). Dopaminergic circuitry underlying mating drive. *Neuron*, *91*(1), 168-181.

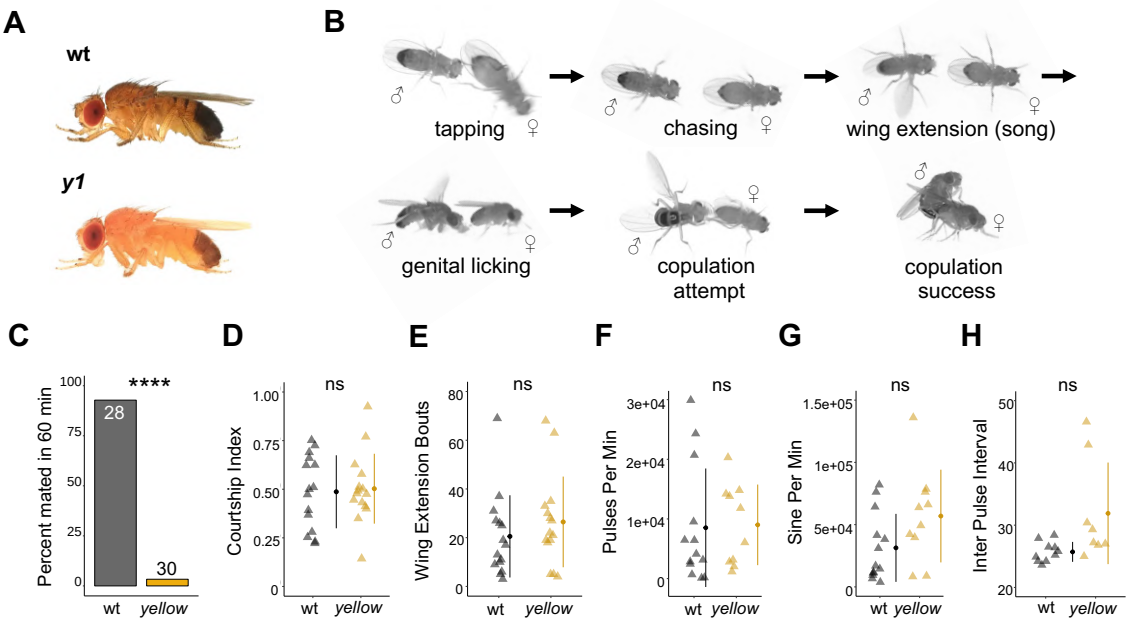

Figure 2-1 The *Drosophila melanogaster yellow* gene is required for male mating success

(**A**) Photographs comparing wild-type and yellow (y1) body pigmentation (Nicolas Gompel). (**B**) Snapshots from videos illustrating D. melanogaster courtship behaviors. (**C**) y1 males (yellow) showed significantly lower mating success levels compared to wild-type males (black) in non-competitive, one-hour trials. Sample sizes are shown at the top of each barplot. (**D**-**H**) y1 males showed similar levels of courtship activity and song compared to wild-type males. (**D**) Courtship index: the proportion of time a male engages in courtship activity divided by the total observation period. (**E**) Wing extension bouts: the number of unilateral wing extensions during the observation period. (**F**) Pulses per minute. (**G**) Sine per minute. (**H**) Inter pulse interval. (**D**-**H**) Show individual points that represent single fly replicates. Circles represent means and lines SD. Significance was measured using Fisher's exact test in (**C**), Student's t-tests (two-tailed) in (**D**,**E**), and one-way ANOVA in (**F**-**H**). ****P<0.0001. n.s., not significant.

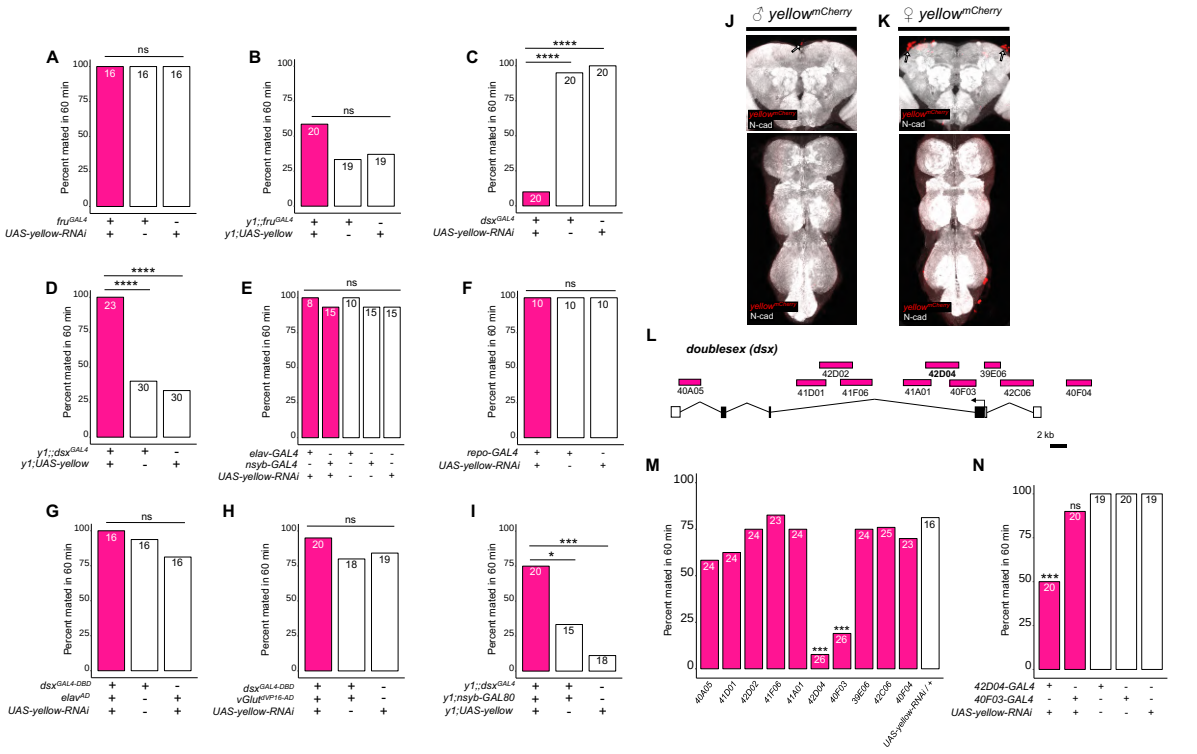

Figure 2-2 *yellow* expression in non-neuronal *doublesex*-expressing cells, but not *fruitless*-expressing cells, is necessary and sufficient for male mating success

(A,**B)** Neither expressing *yellow-RNAi* nor *yellow-cDNA* in *fru*-expressing cells using fru^{GAL4} (Stockinger *et al*., 2005) affected male copulation. (**C**) Expressing *yellow-RNAi* in *dsx*-expressing cells using dsx^{GAL4} (Robinett *et al*., 2010) significantly inhibited male mating success. (**D**) Expressing *yellow* in *dsx*-expressing cells using dsx^{GAL4} in a *y1* mutant background was sufficient to restore male mating success. (**E**,**F**) Expressing *yellow-RNAi* using pan-neuronal (*elav-GAL4* and *nsyb-GAL4*) and pan-glia (*repo-GAL4*) drivers did not affect male mating success. (**G**) Restricting *yellow-RNAi* expression to *dsx*-expressing neurons using the split-GAL4 technique, combining $dsx^{GAL4\text{-}DBD}$ (Pavlou *et al*., 2016) with $elav^{VP16\text{-}AD}$ (Luan *et al*., 2006), did not affect male mating success. (**H**) Restricting *yellow-RNAi* expression to *dsx*-expressing glutamatergic neurons using the split-GAL4 technique, combining $dsx^{GAL4\text{-}DBD}$ (Pavlou *et al*., 2016) with $vGlut^{dVP16\text{-}AD}$ (Gao *et al*., 2008) did not affect male mating success. (**I**) Expressing *yellow* in *dsx*-expressing cells restricted outside the CNS using dsx^{GAL4} and *nsyb-GAL80* (courtesy of Julie Simpson) in a *y1* mutant background significantly increased male mating success. (**J**,**K**) Brain and ventral nerve cord of adult male and female $y^{mCherry}$ flies stained with anti-N-Cadherin (N-cad) antibody labeling neuropil (white) and anti-DsRed antibody labeling Yellow::mCherry (red). We observed sparse, inconsistent signal outside the CNS at the top of the brain in males (white arrow), and especially females (white arrow), but we were unable to confirm a previous report that $y^{mCherry}$ is expressed in the adult brain (Hinaux *et al*., 2018). (**L**) Diagram of the male exon structure of the *dsx* locus highlighting 10 genomic fragments between 1.7 and 4 kb used to clone Janelia enhancer trap GAL4 drivers (Pfeiffer *et al*., 2008). Black boxes indicate coding exons. White boxes indicate 5' and 3' UTRs, and the arrow in exon 2 denotes the transcription start site. (**M**) Expressing *yellow-RNAi* using each Janelia *dsx-GAL4* driver identified *42D04-GAL4* and *40F03-GAL4* as affecting male mating success when compared with the *yellow-RNAi* control. (**N**) A replicate experiment comparing *42D04-GAL4* and *40F03-GAL4* effects on male mating success with both GAL4 and UAS parental controls confirmed the significant effect of *42D04-GAL4* but not *40F03-GAL4*. We attribute differences in the *40F03-GAL4* effect between (**M**) and (**N**) to between experiment variability in the levels of male mating success; each common genotype tested in (**M**), for example, mated at higher levels in (**N**), but *42D04-GAL4* consistently showed a significant effect relative to controls. Sample sizes are shown at the top of each barplot. Significance was measured using Chi-square tests with Bonferroni corrections for multiple comparisons. **P*<0.05, ****P*<0.00, *****P*<0.0001. n.s., not significant.

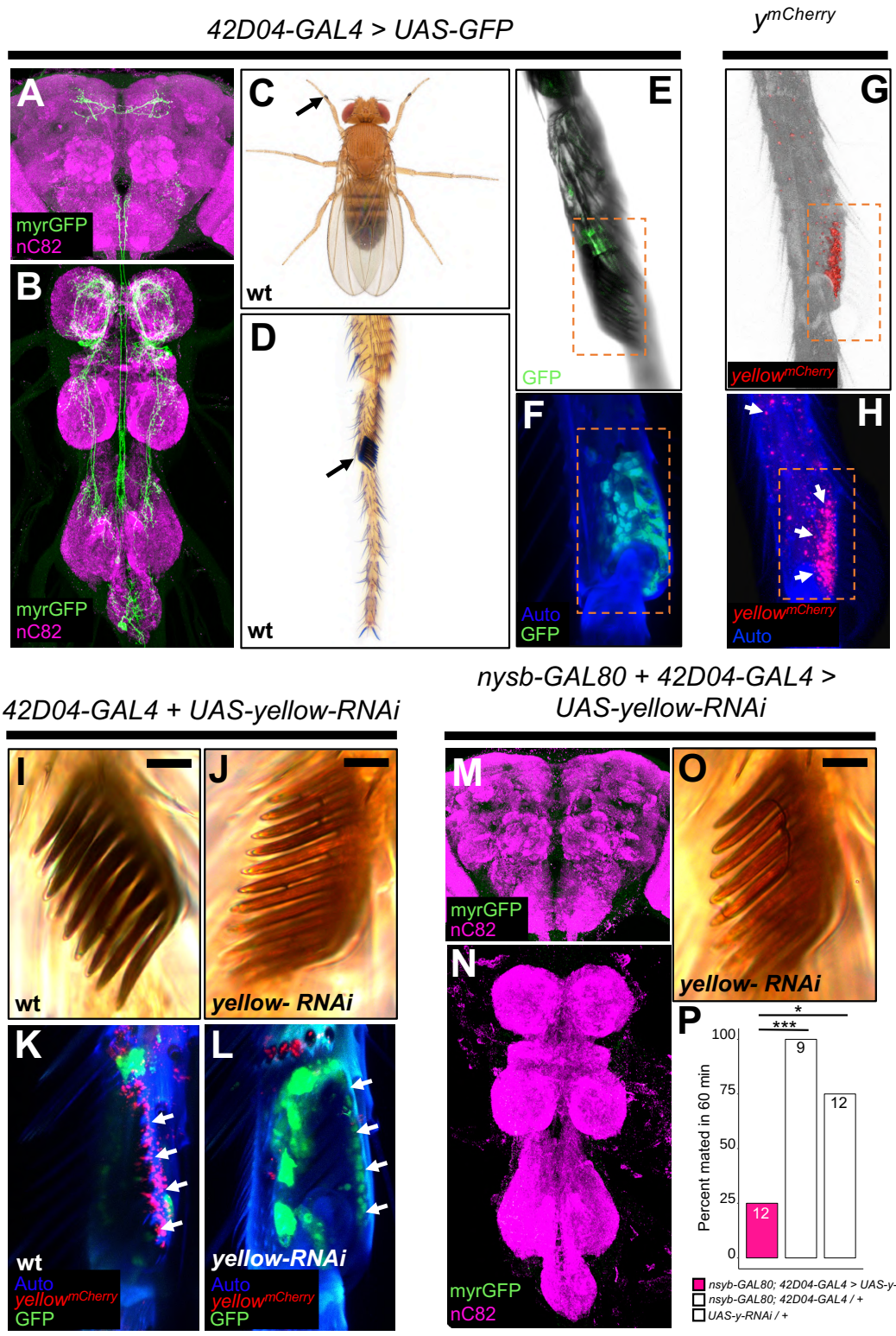
42D04-GAL4 > UAS-GFP
y mCherry
A
myrGFP
nC82
B
myrGFP
nC82
C
wt
D
wt
E
GFP
F
Auto
GFP
G
yellow mCherry
H
yellow mCherry
Auto
42D04-GAL4 + UAS-yellow-RNAi
nysb-GAL80 + 42D04-GAL4 >
UAS-yellow-RNAi
I
wt
J
yellow- RNAi
K
wt
Auto
yellow mCherry
GFP
L
yellow-RNAi
Auto
yellow mCherry
GFP
M
myrGFP
nC82
N
myrGFP
nC82
O
yellow- RNAi
P
Percent mated in 60 min
100
75
50
25
0
12
9
12
*
***
nsyb-GAL80; 42D04-GAL4 > UAS-y-RNAi
nsyb-GAL80; 42D04-GAL4 / +
UAS-y-RNAi / +

Figure 2-3 *yellow* expression in non-neuronal *42D04-GAL4* expressing cells is necessary for sex comb melanization and male mating success

(**A**,**B**) Brain and ventral nerve cord of adult male fly stained with anti-GFP (green) antibody for myrGFP expressed using *42D04-GAL4* and counterstained with anti-nC82 (magenta) for neuropil. (**C**) Wild-type (wt) *D. melanogaster* adult male fly highlighting the location of sex combs (Nicolas Gompel). (**D**) Close up of a wild-type (wt) sex comb on the first tarsal segment (ts1) of the front leg (courtesy of Nicolas Gompel). (**E**) Bright field illumination of a male front leg expressing cytGFP (green) in sex-comb cells using *42D04-GAL4*. (**F**) Confocal image of the sex comb cells expressing cytGFP (green) with *42D04-GAL4* and leg cuticle autofluorescence (blue). (**G**) Confocal image of a $y^{mCherry}$ male leg highlighting native $y^{mCherry}$ sex comb expression (red). (**H**) Zoomed in confocal image shown in (**G**) with leg cuticle autofluorescence (blue) and native $y^{mCherry}$ sex comb expression (red). (**I**) Wild-type (wt) sex comb. (**J**) Loss of black melanin in sex combs in males expressing *yellow-RNAi* using *42D04-GAL4*. (**K**) Co-localization of $y^{mCherry}$ (red) at the base of the sex comb cells expressing cytGFP (green) with *42D04-GAL4*. (**L**) Loss of $y^{mCherry}$ (red) at the base of the sex comb cells expressing cytGFP (green) and *yellow-RNAi* using *42D04-GAL4*. (**M**,**N**) Brain and ventral nerve cord of adult male expressing *nsyb-GAL80* to block GAL4 activity in the CNS, stained with anti-GFP (green) antibody for myrGFP expressed using *42D04-GAL4*, and counterstained with anti-nC82 (magenta) for neuropil. (**O**) Loss of black melanin in sex combs in *nsyb-GAL80* males expressing *yellow-RNAi* using *42D04-GAL4*. (**P**) Expressing *yellow-RNAi* using *42D04-GAL4* in males expressing *nsyb-GAL80* significantly inhibited male mating success. Scale bars in (**I**), (**J**), and (**O**) measure 12.5 μm. Sample sizes are shown at the top of each barplot. Significance was measured using Chi-square tests with Bonferroni corrections for multiple comparisons. **P*<0.05, ****P*<0.001.

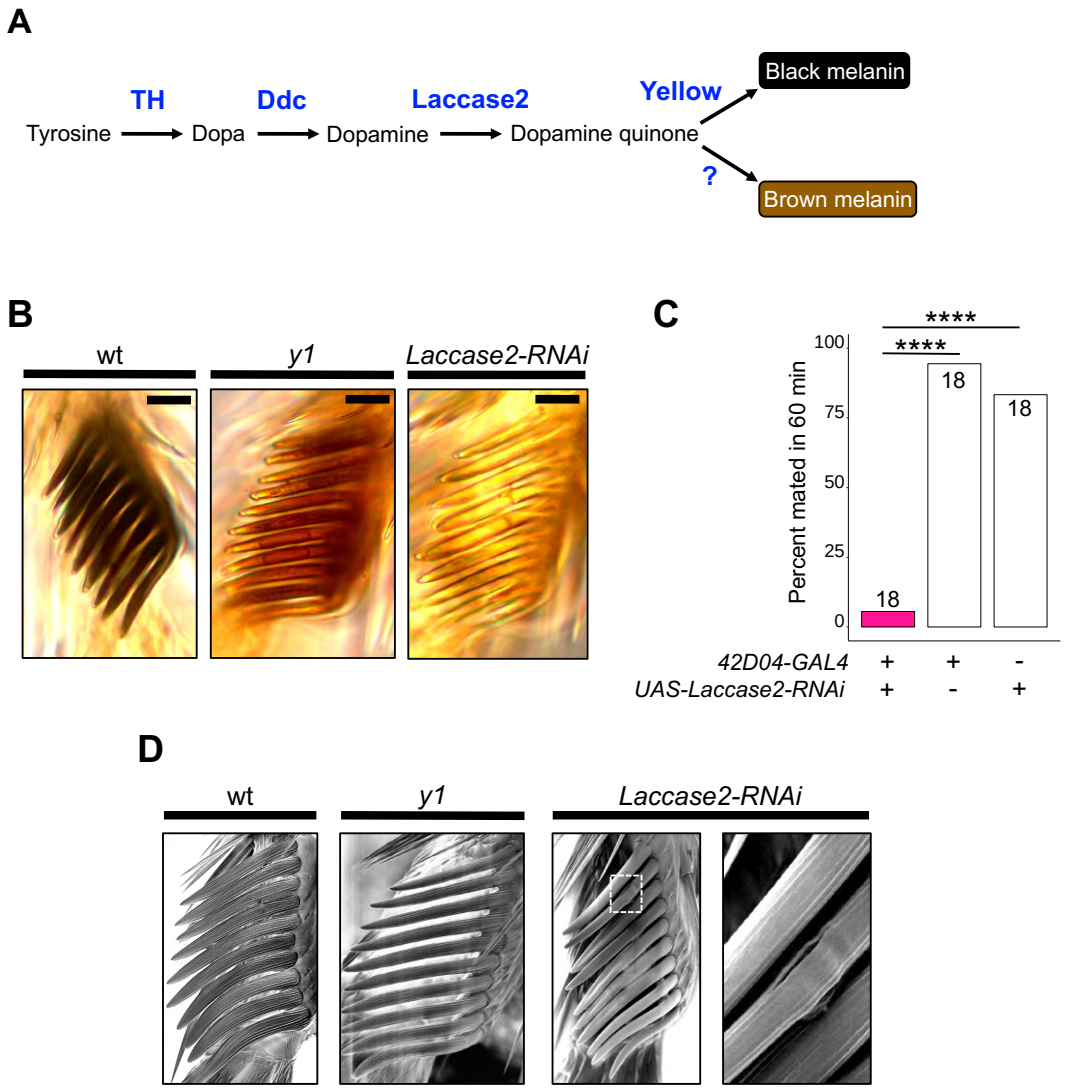

Figure 2-4 Sex comb melanization is specifically required for male mating success

(**A**) Simplified version of the insect melanin synthesis pathway. (**B**) Light microscopy images of sex combs from wild-type (wt), *y1*, and *42D04-GAL4; UAS-Laccase2-RNAi* males. Expressing *Laccase2-RNAi* in sex combs completely blocked melanin synthesis. (**C**) Expressing *Laccase2-RNAi* using *42D04-GAL4* in males significantly inhibited male mating success. (**D**) Scanning Electron Microscopy (SEM) of sex coms from wild-type (wt), *y1*, and *Laccase2-RNAi* males (expressed using *42D04-GAL4*). Compared to wild-type, sex comb teeth in *y1* mutants appeared thinner and smoother, whereas*Laccase2-RNAi* sex comb teeth appeared even smoother than *y1* mutants, and one comb tooth had a visible crack in the cuticle (white rectangle, enlarged on the right). Scale bars in (**B**) measure 12.5 µm. Sample sizes are shown at the top of each barplot. Significance in was measured using Chi-square tests with Bonferroni corrections for multiple comparisons. ****$P<0.0001$.

Chapter 3

Pleiotropic Effects of *ebony* and *tan* on Pigmentaiton and Cuticular Hydrocarbon Composition in *Drosophila melanogaster*[1]

Abstract

Pleiotropic genes are genes that affect more than one trait. For example, many genes required for pigmentation in the fruit fly *Drosophila melanogaster* also affect traits such as circadian rhythms, vision, and mating behavior. Here, we present evidence that two pigmentation genes, *ebony* and *tan,* which encode enzymes catalyzing reciprocal reactions in the melanin biosynthesis pathway, also affect cuticular hydrocarbon (CHC) composition in *D. melanogaster* females. More specifically, we report that *ebony* loss-of-function mutants have a CHC profile that is biased toward long (>25C) chain CHCs, whereas *tan* loss-of-function mutants have a CHC profile that is biased toward short (<25C) chain CHCs. Moreover, pharmacological inhibition of dopamine synthesis, a key step in the melanin synthesis pathway, reversed the changes in CHC composition seen in *ebony* mutants, making the CHC profiles similar to those seen in *tan* mutants. These observations suggest that genetic variation affecting *ebony* and/or *tan* activity might cause correlated changes in pigmentation and CHC composition in natural populations. We tested this possibility using the *Drosophila* Genetic Reference Panel (DGRP) and found that CHC composition covaried with pigmentation as well as levels of *ebony* and

[1] This chapter is published as: Massey, J. H., Akiyama, N., Bien, T., Dreisewerd, K., Wittkopp, P. J., Yew, J. Y., & Takahashi, A. (2019). Pleiotropic effects of ebony and tan on pigmentation and cuticular hydrocarbon composition in Drosophila melanogaster. *Frontiers in Physiology*, *10*, 518.

tan expression in newly eclosed adults in a manner consistent with the *ebony* and *tan* mutant phenotypes. These data suggest that the pleiotropic effects of *ebony* and *tan* might contribute to covariation of pigmentation and CHC profiles in *Drosophila*.

Introduction

When organisms adapt to novel environments, genetic changes often cause multiple traits to evolve. In some cases, organisms invading similar environments undergo similar shifts for suites of traits. In the threespine stickleback, for example, marine populations independently invading freshwater lake habitats have repeatedly evolved similar changes in defensive armor, behavior, and body shape (Walker and Bell, 2000; Schluter *et al*., 2004; Wark *et al*. 2011). Such correlated evolution might result from (i) selection favoring a particular suite of traits (i.e. selection targeting multiple unlinked loci), (ii) selection favoring a trait that is genetically linked to genes affecting other traits, or (iii) selection favoring a trait that varies due to genetic variation at a pleiotropic gene affecting multiple traits. In the case of the threespine stickleback, genetic variation linked to a single major gene, *Eda*, has been found to explain correlated differences in these traits among populations (Albert *et al*., 2008; Greenwood *et al*., 2016), suggesting that pleiotropy has played a role. Studies in various other plant and animal species also support the hypothesis that pleiotropy contributes to the coevolution of correlated traits (e.g., McKay *et al*., 2003; McLean *et al*., 2011; Duveau and Felix 2012; Nagy *et al*. 2018).

In insects, genes determining body color are often pleiotropic. For example, in *Drosophila*, the *yellow* gene is required for the synthesis of black melanin and also affects mating behavior (Bastock, 1956; Drapeau *et al*., 2003; Drapeau *et al*., 2006). The genes *pale* and *Dopa-decarboxylase*, which encode enzymes that synthesize tyrosine-derived precursors for pigmentation, are also pleiotropic, affecting both body color and immunity (reviewed in Wittkopp and Beldade, 2009; Takahashi, 2013). In addition, prior work suggests that pigmentation genes might also affect cuticular hydrocarbon (CHC) profiles, which can affect desiccation (Gibbs, 1997; Gibbs, 1998; Foley and Telonis-Scott, 2011) and mate choice (reviewed in Yew and Chung, 2015). Specifically, a

receptor for the tanning hormone *bursicon* and levels of the biogenic amine dopamine, which both affect cuticle pigmentation in *Drosophila melanogaster*, have been shown to influence CHC composition (Marican *et al.*, 2004; Wicker-Thomas and Hamann, 2008; Flaven-Pouchon *et al.* 2016).

Here, we test whether the *ebony* and *tan* genes of *D. melanogaster*, which are required for the synthesis of dark melanins and yellow sclerotins from dopamine, respectively, also affect CHC composition. The *ebony* gene encodes a protein that converts dopamine into N-β-alanyl dopamine (NBAD), and the *tan* gene encodes a protein that catalyzes the reverse reaction, converting NBAD back into dopamine (Figure 3-1A). We report that loss-of-function mutations in both *ebony* and *tan* altered CHC length composition relative to wild-type flies in opposing directions. These opposing effects on CHC length composition are consistent with *ebony* and *tan's* opposing biochemical functions in dopamine metabolism (Figure 3-1A). Indeed, pharmacological inhibition of dopamine synthesis in *ebony* mutants caused a *tan*-like CHC length profile. To examine the possibility that variation in *ebony* and/or *tan* activity might cause correlated changes in pigmentation and CHC composition in a natural population, we used lines from the *Drosophila* Genetic Reference Panel (DGRP) to test for covariation between pigmentation and CHC composition. We found that CHC length composition covaried not only with pigmentation but also with levels of *ebony* and *tan* expression in a manner consistent with the mutant analyses. In the discussion, we compare our data to studies of clinal variation in CHC composition and pigmentation to determine whether the pleiotropic effects we see might have contributed to correlated evolution of these traits.

Materials and Methods

Fly stocks and maintenance

The following lines were used: P excision line tan^{20A} (True et al., 2005) (courtesy of John True, Stony Brook University); the *UAS-ebony-RNAi* effector line was obtained from the Vienna Drosophila Resource Centre (Dietzl et al., 2007, KK106278); dsx^{GAL4} (Rideout et al., 2010) (courtesy of Stephen Goodwin, Oxford University); *OK72-GAL4* (Ferveur et al., 1997) (courtesy of Scott Pletcher, University of Michigan); *pannier-GAL4* (Calleja et

al. 2000) was obtained from the Bloomington Drosophila Stock Center (BDSC 3039); *vasa-Cas9* (Gratz et al., 2014, BDSC 51324) (courtesy of Rainbow Transgenics Inc.). All flies were grown at 23°C with a 12 h light-dark cycle on standard corn-meal fly medium.

DGRP stocks

The following inbred D. melanogaster lines from the DGRP (Ayroles et al. 2009; Mackay et al. 2012; Huang et al. 2014) were used in this study: *RAL-208, RAL-303, RAL-324, RAL-335, RAL-357, RAL-358, RAL-360, RAL-365, RAL-380, RAL-399, RAL-517, RAL-555, RAL-705, RAL-707, RAL-732, RAL-774, RAL-786, RAL-799, RAL-820, RAL-852, RAL-714, RAL-437, RAL-861* and *RAL-892*. These lines consist of the set of 20 lines used in Miyagi et al. (2015) and additional 3 dark lines (*RAL-714, RAL-437, and RAL-861*), which were added to avoid line specific effects from a limited number of dark lines. All flies were grown at 25°C with a 12 h light-dark cycle on standard corn-meal fly medium.

Generation of ebony CRISPR lines

New loss-of-function ebony mutants were constructed by synthesizing two single guide RNAs (gRNA), using a MEGAscript T7 Transcription Kit (Invitrogen), following the PCR-based protocol from Bassett et al. (2014), that target ebony's first coding exon and co-injecting these at a total concentration of 100 ng/μL into embryos of a D. melanogaster *vasa-Cas9* line (Gratz et al., 2014; BDSC 51324) (Supplementary Figure S3-1). These gRNAs were previously found to generate a high level of heritable germline transformants (Ren et al., 2014; Supplementary Figure S3-1). We screened for germline transformants based on body pigmentation and confirmed via Sanger sequencing three unique ebony loss-of-function alleles, $ebony^{CRISPR(1,2)}$ containing a 55 bp deletion, and $ebony^{CRISPR(3)}$ and $ebony^{CRISPR(4)}$, each containing an in-frame 3 bp deletion (Supplementary Figure S3-1). Each deletion caused flies to develop dark body pigmentation, indicating loss of Ebony activity (Figure 3-1B, Supplementary Figure S3-2A).

CHC extraction and measurements

For Figures 3-1 and 3-2 and Supplementary Figures S3-2–S3-5, CHCs were extracted and analyzed as described below (CHC names and formulas are summarized in Supplementary Table S3-1). For the analyses using the DGRP (Figures 3-3 and 3-4, Supplementary Figure S3-6), all CHC data for females were obtained from Dembeck et al. (2015b); however, in the case of GC/MS peaks composed of more than two combined CHC components that differed in CHC chain length, the non-branched CHC chain length was used. Also, CHCs that were not detected in all strains were removed from the analyses.

Extraction

For each experiment, five replicate CHC samples of virgin female flies were prepared for each genotype or pharmacological treatment group. All *ebony* and *tan* mutant CHC extractions were performed on 3–4 d old virgin females. We restricted our analysis to virgin females, because previous evidence studies suggested that a link between dopamine and CHC composition occurs in females but not males (Marican et al., 2004; Wicker-Thomas and Hamann, 2008). For pharmacological experiments, 1–2 d old virgin females were treated for 4 d prior to CHC extraction. For GAL4/UAS experiments (Brand and Perrimon, 1993), virgin females were tested at 10–12 d. For each sample, 5 flies were placed in a single glass vial (Wheaton 224740 E–C Clear Glass Sample Vials) on ice. 120 µL of hexane (Sigma Aldrich, St Louis, MO, USA) spiked with 10 µg/mL of hexacosane (Sigma Aldrich) was added to each vial and sealed with a cap. Vials were incubated at room temperature for 20 mins. 100 µL of the cuticular extract was removed, transferred into a clean vial (Wheaton 0.25 mL with low volume insert), and stored at -20ºC.

GC/MS analysis

Gas chromatography mass spectrometry (GC/MS) analysis was performed on a 7820A GC system equipped with a 5975 Mass Selective Detector (Agilent Technologies, Inc., Santa Clara, CA, USA) and a HP-5ms column ((5%-Phenyl)-methylpolysiloxane, 30 m length, 250 µm ID, 0.25 µm film thickness; Agilent Technologies, Inc.). Electron ionization (EI) energy was set at 70 eV. One microliter of the sample was injected in

splitless mode and analyzed with helium flow at 1 mL/ min. The following parameters were used: column was set at 40°C for 3 min, increased to 200°C at a rate of 35°C/min, then increased to 280°C at a rate of 20°C/min for 15 min. The MS was set to detect from m/z 33 to 500. Chromatograms and spectra were analyzed using MSD ChemStation (Agilent Technologies, Inc.). CHCs were identified on the basis of retention time and EI fragmentation pattern. The relative abundance for each CHC signal was calculated by normalizing the area under each CHC peak to the area of the hexacosane signal. To eliminate multicollinearity among sample peak amounts, a log-contrast transformation was applied to the resulting proportional values, using nC27 as the denominator (Yew et al., 2011; Blow and Allen, 1998):

$$\textbf{logcontrast CHC}_n = \textbf{log 10}\left(\frac{\textbf{proportion (CHC}_n\textbf{)}}{\textbf{proportion (C27 alkane)}}\right)$$

To determine the relative change in CHC length between two genotypes, experimental groups, or groups of DGRP strains, the difference in relative intensity of individual CHC intensities of each group was calculated:

$$\textbf{Difference} = \textbf{logcontrast CHC}_a - \textbf{logcontrast CHC}_b$$

These values were then plotted against CHC chain length.

Ultraviolet laser desorption ionization mass spectrometry (UV-LDI MS)

For intact fly analysis, individual animals were attached to a glass cover slip using adhesive pads (G304, Plano, Wetzlar, Germany). The cover slips were mounted on a custom-milled sample holder containing a rectangular, 1.8 mm deep well. Sample height was adjusted by choosing a stack of 0.2 mm-thick adhesive pads (G3347, Plano). Mass spectra were generated using a prototype orthogonal-extracting mass spectrometer (oTOF-MS) as described previously (Yew et al. 2011). The oTOF-MS was equipped with a modified oMALDI2 ion source (AB Sciex, Concord, Canada) and an N_2 laser (λ = 337 nm) operated at a pulse repetition rate of 30 Hz. N_2 was used as buffer gas at p = 2 mbar. This elevated pressure is critical to achieve an efficient collisional cooling environment for generation of weakly-bound $[M + K]^+$ ions that constituted the major molecular ion

species. Before starting the actual measurements, external mass calibration was achieved with red phosphorus, resulting in a mass accuracy of approximately 25 ppm. Approximately 900 laser shots were placed at one position to achieve a mass spectrum (30 s @30 Hz). All spectra were acquired in positive ion mode and processed using MS Analyst software (Analyst QS 2.0, AB Sciex, Concord, Canada).

Pharmacology Experiments

For pharmacological treatments, standard corn-meal fly medium was liquefied and cooled to ca. 60°C before the addition of each respective drug or solvent control. Ten 1–2 d old virgin females were placed in the vials for 4 d. To inhibit tyrosine hydroxylase activity, we prepared a 36 mM alpha methyl tyrosine (L-AMPT) (Sigma Aldrich) diet. The pH of the solution was adjusted with concentrated HCl until the drug dissolved. A solvent control diet solution was prepared using identical procedures. For the dopamine treatments, 1 mM and 10 mM L-dopa precursor (Methyl L-DOPA hydrochloride) (Sigma Aldrich) were dissolved in water before adding to liquefied fly media.

RNA extraction

Female virgin flies were collected within 1 h of eclosion, and the heads were removed in RNAlater (Ambion) to separate the effect from transcripts in non-epidermal head tissues. The remaining head-less body samples were stored in RNAlater at -80°C until use. Three body samples from each line were placed in a 2 mL microtube with 400 µL TRIzol Reagent (Thermo Fisher Scientific, Tokyo, Japan) and an equivalent volume of 1.2 mm zirconia silica beads (Bio Medical Science). After shaking the tube at 3,200 rpm for 2 min using a Beads Crusher µT-12 (TAITEC, Koshigaya, Japan), 160 µl chloroform was added and mixed thoroughly. Total RNA in the aqueous phase was subsequently purified using silica-gel (Wakocil 5SIL, Wako, Osaka, Japan) based on the method of Boom et al. (1990) and was quantified using a Nanodrop 2000c spectrophotometer (Thermo Fisher Scientific).

Quantitative real-time PCR (qRT-PCR)

First strand cDNA was synthesized from 1 µg total RNA by using a PrimeScript RT Reagent Kit with gDNA Eraser (Takara Bio, Kusatsu, Japan). qRT-PCR was performed in a 25 µl reaction volume with SYBR Premix Ex Taq II Tli RNaseH Plus (Takara Bio) on a Thermal Cycler Dice TP800 (Takara Bio). Primer pairs used for RT-qPCR were ebony: 5′−CTTAGTGTGAAACGGCCACAG−3′ and 5′−GCAGCGAACCCATCTTGAA−3′; tan: 5′−GTTGAGGGGCTTCGATAAGA−3′ and 5′−GTCCTCCGGAAAGATCCTG−3′; Act57B: 5′−CGTGTCATCCTTGGTTCGAGA−3′ and 5′−ACCGCGAGCGATTAACAAGTG−3′; Rp49: 5′−TCGGATCGATATGCTAAGCTG−3′ and 5′−TCGATCCGTAACCGATGTTG−3′. Act57B and Rp49 were used as internal control. Two replicate PCR reactions were performed for each cDNA sample and three biological replicates were obtained for each line.

Grouping DGRP lines based on pigmentation scores and ebony/tan expression levels

The DGRP lines (N = 155) with both pigmentation scores in Dembeck et al. (2015a) and CHC profiles in Dembeck et al. (2015b) were grouped into dark, intermediate, and light pigmentation lines using the pigmentation scores of the abdominal tergites from Dembeck et al. (2015a). The scores ranged from 0 for no dark pigmentation to 4 for 100% dark pigmentation in increments of 0.5, and were averaged across 10 individuals per line. Pigmentation grouping was done based on the score delimitations that split the lines most evenly into three groups. For the 5^{th} tergite (A5), lines were categorized into following groups: dark ($1.5 < \text{score}$, N = 53), intermediate ($1 < \text{score} \leq 1.5$, N = 56), and light ($\text{score} \leq 1$, N = 49). For the 6^{th} tergite (A6), lines were categorized into following groups: dark ($3 < \text{score}$, N = 51), intermediate ($2 < \text{score} \leq 3$, N = 55), light ($\text{score} \leq 2$, N = 49).

The 23 DGRP lines with varying ebony and tan expression levels were grouped into low, intermediate, and high expression lines using the qRT-PCR data. Since the normalized quantities are continuous values, grouping was done based on standard deviations (SD). For the ebony expression, lines were categorized into following groups: low (expression

< mean - 0.5SD, N = 6), intermediate (mean - 0.5SD ≤ expression ≤ mean + 0.5SD, N = 9), and high (mean + 0.5SD < expression, N = 8). For the tan expression, lines were categorized into following groups: low (expression < mean - 0.5SD, N = 10), intermediate (mean - 0.5SD ≤ expression ≤ mean + 0.5SD, N = 7), and high (mean + 0.5SD < expression, N = 6).

Statistics

All statistical tests were performed in R for Mac version 3.3.3 (R Core Team 2018) using one-way ANOVAs to test for statistically significant effects between more than two groups and post-hoc Tukey HSD tests for multiple pairwise comparisons. We used Spearman's rank correlation coefficient ρ to test for the significance of the association. All pairwise tests were two-tailed, and the level of significance was set as $\alpha = 0.05$.

Results

Loss-of-function mutations in ebony and tan have reciprocal effects on CHC length profiles

To determine whether the ebony gene affects cuticular hydrocarbons (CHCs), we created three new ebony mutant alleles via CRISPR/Cas9 gene editing. One allele, $ebony^{CRISPR(1,2)}$, contained a 55 bp deletion that caused a frame-shift in ebony's coding sequence (Supplementary Figure S3-1C). Flies homozygous for this $ebony^{CRISPR(1,2)}$ allele showed dark body pigmentation similar to that described previously for loss-of-function ebony mutants (Bridges and Morgan, 1923) (Figure 3-1B). We measured CHC profiles in 3–4 d old $ebony^{CRISPR(1,2)}$ virgin females using gas chromatography (GC/MS) and found that $ebony^{CRISPR(1,2)}$ flies showed lower levels of total alkanes relative to 3–4 d old virgin females from the strain the guide RNAs were injected into (i.e., un-injected *vasa-Cas9*) (Figure 3-1C, One-way ANOVA: $F_{9,40} = 4494$, $P < 2.0 \times 10^{-16}$; post-hoc Tukey HSD was significant for alkanes: $P < 1.0 \times 10^{-5}$).

We then tested whether $ebony^{CRISPR(1,2)}$ females had different proportions of individual CHCs. We calculated the average difference in individual log-contrast transformed CHC

relative intensities (see Materials and Methods) between *ebony*$^{CRISPR(1,2)}$ flies and un-injected *vasa-Cas9* control flies and plotted these values against CHC chain length (varying from 21 carbons (C) to 29C) (Figure 3-1D, Supplementary Table S3-1). We found that *ebony*$^{CRISPR(1,2)}$ flies tended to show lower levels of short chain CHCs (<25C) and higher levels of long chain CHCs (>25C), suggesting that disrupting the function of ebony causes a CHC lengthening effect (Figure 3-1D, Spearman's $\rho = 0.83$, $P < 1.0 \times 10^{-5}$).

The two other *ebony* alleles generated using CRISPR/Cas9 gene editing *(ebony*$^{CRISPR(3)}$ and *ebony*$^{CRISPR(4)}$) each had a single 3 bp in-frame deletion in the first coding exon (Supplementary Figure S3-1D,E), suggesting that they might have less severe effects on Ebony activity than the *ebony*$^{CRISPR(1,2)}$ allele containing a 55 bp deletion causing a frame-shift. Consistent with this prediction, these ebony mutants also showed darker body pigmentation than wild-type flies (Supplementary Figure S3-2A), but did not show any bias toward longer CHCs (Supplementary Figure S3-2B,C, *ebony*$^{CRISPR(3)}$: Spearman's $\rho = 0.22$, $P = 0.34$; *ebony*$^{CRISPR(4)}$: Spearman's $\rho = 0.07$, $P = 0.78$).

To better understand the effects of reduced ebony expression on CHCs, we knocked down ebony expression in specific cell types using *ebony-RNAi* (Dietzl et al., 2007). First, we drove expression of *ebony-RNAi* with the *dsx*^{GAL4} driver (Rideout et al., 2010), which causes RNAi expression in the cuticle, fat body, CNS, and oenocytes among other tissues. We observed darker pigmentation in *dsx*^{GAL4} > *UAS-ebony-RNAi* flies than control flies (data not shown), suggesting that the *ebony-RNAi* effectively targeted and knocked down ebony expression. These *dsx*^{GAL4} > *UAS-ebony-RNAi* flies also showed a pattern of CHC lengthening similar to the *ebony*$^{CRISPR(1,2)}$ mutants when compared to *dsx*^{GAL4} / + control flies but not when compared to *UAS-ebony-RNAi* / + control flies. This result might be due to leaky *UAS-ebony-RNAi* expression in the latter control flies that makes their profiles more similar to those of *dsx*^{GAL4} > *UAS-ebony-RNAi* flies (Supplementary Figure S3-3A, B, relative to *dsx*^{GAL4} / + control: Spearman's $\rho = 0.58$, $P < 0.007$; relative to *UAS-ebony-RNAi* / + control: Spearman's $\rho = 0.19$, $P = 0.42$).

We hypothesized that the effect on CHCs might be due to reducing ebony expression specifically in oenocytes because these cells synthesize many CHC precursor compounds (Wigglesworth, 1970). Therefore, we drove expression of *ebony-RNAi* using the *OK72-GAL4* driver that is also expressed in oenocytes (Ferveur et al., 1997). These flies showed no significant difference in CHC length profiles (Supplementary Figure S3-3C, Spearman's $\rho = -0.01$, $P = 0.96$), suggesting that ebony expression in non-oenocyte tissues expressing doublesex affects the overall length proportion of CHCs.

Next, we asked whether loss-of-function mutations in the tan gene also affect CHC composition. Specifically, we examined CHC composition in 3–4 d old virgin females carrying a tan^{20A} null allele, which contains an imprecise P-element excision that results in a 953 bp deletion that includes the presumptive promoter region (True et al., 2005). Because tan encodes a protein that catalyzes the reverse of the reaction catalyzed by Ebony (Figure 3-1A), we predicted that tan mutants might show the opposite effects on CHC composition. Similar to the $ebony^{CRISPR(1,2)}$ mutants, tan^{20A} females showed differences in the overall abundance of alkanes, but also total CHCs, monoenes, and methyl branched CHCs (Figure 3-1E, One-way ANOVA: $F_{9,40} = 3586$, $P < 2.0 \times 10^{-16}$; post-hoc Tukey HSD was significant for total summed CHCs: $P < 0.01$, total summed alkanes: $P < 0.001$, total summed monoenes: $P < 0.001$, and total summed methyl branched: $P < 0.001$). More importantly, tan^{20A} (w^{1118} tan^{20A}) females tended to show higher levels of short chain CHCs relative to long chain CHCs when compared to w^{1118} *Canton-S* (CS) control flies, as predicted (Figure 3-1F, Spearman's $\rho = -0.62$, $P = 0.0043$). Together, these results suggest that *ebony* and *tan* have reciprocal effects on both pigmentation synthesis (reviewed in True, 2003 and True et al., 2005) and CHC length profiles. We note that this conclusion contradicts Wicker-Thomas and Hamann (2008)'s report that CHC profiles were similar in *ebony* or *tan* loss-of-function mutants and wild-type flies; however, the ebony and tan alleles used in this prior work might not have been nulls.

Pharmacological inhibition of tyrosine hydroxylase activity reverses the CHC lengthening effect in $ebony^{CRISPR(1,2)}$ *flies*

We hypothesized that ebony and tan might have reciprocal effects on CHC length profiles because of their effects on dopamine metabolism. For example, because ebony encodes a protein that converts dopamine into NBAD (Figure 3-1A), we hypothesized that loss-of-function *ebony* mutants might accumulate dopamine (as reported in Hodgetts and Konopka, 1973) and that this dopamine might be shunted into other pathways, possibly affecting CHC lengthening. To explore this hypothesis, we fed 1–2 d old adult female $ebony^{CRISPR(1,2)}$ flies a tyrosine hydroxylase inhibitor, alpha methyl tyrosine (L-AMPT), for four days to determine whether inhibiting dopamine synthesis would reverse the CHC lengthening pattern we observed in $ebony^{CRISPR(1,2)}$ flies. Relative to $ebony^{CRISPR(1,2)}$ solvent-fed control flies, $ebony^{CRISPR(1,2)}$ flies fed 36 mM L-AMPT did indeed reverse the CHC lengthening pattern we observed in $ebony^{CRISPR(1,2)}$ flies, resulting in a shortening of CHCs similar to that observed in tan^{20A} flies (Figure 3-2A, Spearman's $\rho = -0.48$, $P = 0.03$). Feeding 1–2 d old adult flies L-AMPT did not, however, affect body pigmentation (data not shown), consistent with body pigmentation being determined prior to and soon after eclosion (Hovemann et al., 1998). We also fed $ebony^{CRISPR(4)}$ flies a 36 mM dose of L-AMPT to see if we could induce CHC shortening in an ebony mutant with unchanged CHC length composition. Similar to $ebony^{CRISPR(1,2)}$ fed flies, we detected a significant negative correlation when comparing $ebony^{CRISPR(4)}$ fed flies to an $ebony^{CRISPR(4)}$ solvent-fed control (Supplementary Figure S3-4, Spearman's $\rho = -0.57$, $P = 0.009$).

We next hypothesized that tan^{20A} flies might have lower levels of circulating dopamine, because *tan* encodes a protein that converts NBAD back into dopamine (Figure 3-1A). To determine whether elevating dopamine levels in *tan* mutants would affect CHCs, we fed tan^{20A} females a dopamine precursor, methyl L-DOPA hydrochloride (L-DOPA precursor), to see if elevating dopamine levels could reverse the CHC shortening pattern we observed in tan^{20A} flies; however, neither the 1 mM nor 10 mM L-DOPA precursor treatments seemed to affect CHC length profiles when compared to tan^{20A} solvent-fed control flies (Figure 3-2B, C, Spearman's $\rho = 0.17$, $P = 0.50$; Spearman's $\rho = 0.01$, $P = 0.97$, respectively). We also fed tan^{20A} flies a higher 100 mM dose of the L-DOPA precursor, but all of these flies died before CHC extraction; these flies also showed

darker cuticle pigmentation consistent with elevated dopamine. Finally, we fed 1 mM and 10 mM doses of L-DOPA precursor to wild-type (w^{1118} *CS*) females to see if we could induce CHC lengthening in a wild-type genetic background; instead, we observed a slight CHC shortening effect for the 1 mM dose and no effect for the 10 mM dose (Supplementary Figure S3-5, Spearman's $\rho = -0.52$, $P = 0.02$; Spearman's $\rho = -0.36$, $P = 0.12$, respectively). Together, these results indicate that inhibiting tyrosine hydroxylase activity in *ebony* mutants causes a CHC shortening effect like that observed in tan^{20A} flies; however, increasing dopamine levels through feeding does not cause a CHC lengthening effect.

UV-LDI MS data suggests that ebony's effects on pigmentation and CHC length profiles are not linked at the level of the cuticle

Pigmentation synthesis in insect cuticles involves the secretion of biogenic amines (such as dopamine) by epidermal cells into the developing cuticle where they are oxidized into quinones that can form melanins or sclerotins that crosslink proteins (Figure 3-1A; reviewed in True, 2003 and Riedel et al., 2011). To determine whether ebony's effects on CHC length profiles depend on their function in pigmentation and sclerotization of the fly cuticle, we measured the relative abundance of individual CHCs in virgin females with different levels of pigmentation across the body. We crossed *pannier-GAL4* (Calleja et al. 2000) females with males from the *UAS-ebony-RNAi* effector line to generate flies with a dark, heavily melanized stripe down the dorsal midline (Figure 3-3A). We then used UV laser desorption/ionization mass spectrometry (UV-LDI MS) to take repeated measurements of CHCs along the thorax of females, targeting inside and outside the dark stripe (Figure 3-3A). Although we observed an upward trend in abundance from short to long CHCs, we did not detect a significant CHC lengthening effect like that observed between $ebony^{CRISPR(1,2)}$ flies and un-injected vasa-Cas9 females (Figure 3-3B, Spearman's $\rho = 0.58$, $P = 0.13$). Within the black cuticle, most CHCs detected by UV-LDI MS showed a decrease in abundance relative to brown cuticle (Figure 3-3B). This result suggests that ebony does not affect CHC length profiles through the pigmentation/sclerotization synthesis pathway, at least at the level of CHC/pigment deposition in the cuticle.

Abdominal pigmentation covaries with CHC length profiles in the Drosophila Genetic Reference Panel (DGRP)

The effects of *ebony* and *tan* mutants on CHC profiles described above suggest that variation in these genes might contribute to variation in both pigmentation and CHC profiles. Recently, Dembeck et al. (2015a,b) analyzed the genetic architecture of abdominal pigmentation and CHC composition in female *D. melanogaster* lines from the Drosophila Genetic Reference Panel (DGRP): Dembeck et al. (2015a) quantified abdominal pigmentation intensity in the 5th and 6th abdominal tergites (A5 and A6), and Dembeck et al. (2015b) investigated CHC profiles from the majority of the panel, but the relationship between the two traits was not examined. Using data from the 155 DGRP lines for which both pigmentation scores and CHC profiles were published, we tested the hypothesis that natural variation in pigmentation covaries with natural variation in CHC length profiles. In order to investigate CHC composition in a way that was comparable to the experiments described above, we divided the 155 DGRP lines into dark (N = 53), intermediate (N = 56), and light (N = 46) pigmentation groups using the 5th abdominal tergite (A5) pigmentation scores (0–4) from Dembeck et al (2015a). Next, we tested whether females from dark, intermediate, or light pigmentation groups showed differences in their abundance of CHCs with different chain lengths relative to the 155 DGRP line average. We found that the group with the darkest A5 pigmentation showed lower levels of short chain CHCs and higher levels of long chain CHCs relative to the 155 line average (Figure 3-4A, Spearman's $\rho = 0.44$, $P < 0.01$); the group with intermediate A5 pigmentation showed no relationship with CHC chain length (Figure 3-4B, Spearman's $\rho = 0.002$, $P = 0.98$); and the group with lightest A5 pigmentation showed the opposite pattern as the dark group (Figure 3-4C, Spearman's $\rho = -0.57$, $P = 1.0 \times 10^{-3}$). We also compared CHC profiles in dark (N = 51), intermediate (N = 55), and light (N = 49) groups based on pigmentation of the 6th abdominal tergite (A6), and found that, unexpectedly, the dark group did not show a significant CHC lengthening effect (Supplementary Figure S3-6A, Spearman's $\rho = 0.19$, $P = 0.25$), and the intermediate group showed a CHC lengthening effect (Supplementary Figure S3-6B, Spearman's $\rho = 0.44$, $P < 0.01$). However, the light group showed a significant CHC shortening effect as

expected (Supplementary Figure S3-6C, Spearman's $\rho = -0.68$, $P < 1.0 \times 10^{-5}$). These data suggest that darkly pigmented DGRP females show a pattern of CHC lengthening similar to the darkly pigmented loss-of-function *ebony*$^{CRISPR(1,2)}$ flies, and lightly pigmented DGRP females show a pattern of CHC shortening similar to lightly pigmented loss-of-function *tan*^{20A} flies.

ebony and tan expression covaries with CHC length profiles in the DGRP

The DGRP genome-wide association (GWAS) study from Dembeck et al. (2015a) revealed that top variants associated with pigmentation are in *ebony*, *tan*, and *bab1*, consistent with variation in ebony expression level observed in the DGRP lines (Miyagi et al. 2015) and associations between pigmentation and these genes in studies of other D. melanogaster populations (Rebeiz et al. 2009a,b; Telonis-Scott et al. 2011; Takahashi and Takano-Shimizu 2011; Bastide et al. 2013; Endler et al. 2016; 2018). We therefore hypothesized that the differences in CHC length profiles seen in darkly and lightly pigmented DGRP females might be a consequence of expression variation at *ebony* and/or *tan*.

Using qRT-PCR, we quantified ebony and tan expression within 1 h after eclosion, which is when pigments determining adult body color are actively produced, in a sample of 23 DGRP lines that showed variable pigmentation. We then tested whether variation in *ebony* and *tan* expression covaried with CHC length profiles by categorizing the 23 DGRP lines into groups of low, intermediate, and high *ebony* or *tan* expression levels based on the qRT-PCR results, examining the average difference in individual CHC abundances between each expression group relative to the 23 line average, and plotting these values against CHC chain length (Figure 3-5).

Consistent with our hypothesis, the DGRP lines with low ebony expression showed lower levels of short chain CHCs, lines with high *ebony* expression showed higher levels of short chain CHCs, and lines with intermediate expression showed no change in CHC profiles (Figure 3-5A–C, Spearman's $\rho = 0.67$, $P < 1.0 \times 10^{-6}$, Spearman's $\rho = -0.61$, $P < 1.0 \times 10^{-5}$, Spearman's $\rho = -0.10$, $P = 0.50$, respectively). Reciprocally, the DGRP lines

with low or intermediate *tan* expression showed a slight increase in short chain CHCs, and lines with high tan expression showed a significant decrease in short chain CHCs (Figure 3-5D,F, Spearman's $\rho = -0.29$, $P = 0.05$, Spearman's $\rho = -0.32$, $P = 0.03$, Spearman's $\rho = 0.50$, $P < 0.001$, respectively). Taken together, our results suggest that differences in *ebony* and *tan* gene expression have pleiotropic effects on both pigmentation and CHC length profiles that might cause these traits to covary in natural *D. melanogaster* populations.

Discussion

Pigmentation genes are often pleiotropic, with effects on vision, circadian rhythms, immunity, and mating behavior (reviewed in Wittkopp and Beldade, 2009; Takahashi, 2013). Here, we show that *ebony* and *tan* also affect CHC production, with the two genes altering CHC length profiles in opposing directions: $ebony^{CRISPR(1,2)}$ mutants had significantly higher levels of long chain CHCs, and tan^{20} mutants had significantly higher levels of short chain CHCs. Our results suggest 1) that *ebony* and *tan* have a previously undescribed role in CHC synthesis and/or deposition and 2) that pleiotropy of both genes might influence the covariation of pigmentation and CHC composition.

Considering the pleiotropic effects of ebony and tan through changes in dopamine metabolism

Previous work has shown that changes in dopamine metabolism influence CHC composition in Drosophila melanogaster. Specifically, females homozygous for loss-of-function *Dopa-decarboxylase* (*Ddc*) temperature-sensitive alleles showed changes in CHC composition that could be reversed with dopamine feeding (Marican et al., 2004; Wicker-Thomas and Hamann, 2008). Additionally, inhibiting dopamine synthesis by feeding wild-type females the tyrosine hydroxylase inhibitor L-AMPT altered CHC composition in a similar direction as the loss-of-function alleles (Marican et al., 2004; Wicker-Thomas and Hamann, 2008). We found that feeding with L-AMPT affects CHC length composition, causing $ebony^{CRISPR(1,2)}$ and $ebony^{CRISPR(3)}$ mutants to have a more tan^{20}-like CHC length profile (Figure 3-2A and Supplementary Figure S3-4). This result suggests that *ebony* and *tan* may affect CHC length composition through dopamine

metabolism, but feeding *tan*^{20} and wild-type females dopamine did not lead to CHC lengthening (Figure 3-2B,C and Supplementary Figure S3-5). Why did L-AMPT feeding affect CHC length composition while dopamine feeding did not? One possible reason is that L-AMPT is a potent inhibitor of tyrosine hydroxylase activity (Spector et al., 1965), which processes tyrosine that flies ingest, whereas dopamine feeding might not cause significant changes in dopamine abundance in tissues relevant to CHC synthesis.

Another gene suggesting a possible link between CHC composition and dopamine is the *D. melanogaster apterous* gene. Loss of apterous gene function causes an increase in the proportion of long chain CHCs (Wicker and Jallon, 1995), and *apterous* mutants also show high levels of dopamine (Gruntenko et al., 2003; Grutenko et al., 2005; Grutenko et al., 2012). These mutants also show low levels of juvenile hormone (JH) (Altaratz et al., 1991), and treating decapitated females with methoprene to increase JH synthesis caused a decrease in long chain CHCs (Wicker and Jallon, 1995). The CHC lengthening and increased dopamine levels seen in *apterous* mutants resemble *ebony* mutants, but it is unknown whether *ebony* mutants show altered JH profiles. Further evidence supporting a role of JH and other ecdysteroids in determining CHC chain length comes from houseflies (Blomquist et al., 1987). In *D. melanogaster*, ecdysteroid signaling was found to be required not only for CHC synthesis but also survival of the oenocyte cells that synthesize CHCs (Chiang et al., 2016). An interesting future direction would be to test whether changes in dopamine metabolism in *ebony* or *tan* mutants influence CHC length composition through JH signaling. More broadly, a thorough genetic analysis focused on tissue-specific manipulation of dopamine is needed to deepen our understanding about its role in CHC synthesis.

CHC lengthening in ebony mutants does not seem to depend on changes at the level of the cuticle

Data from our tyrosine hydroxylase inhibition experiments supported the hypothesis that elevated dopamine levels in *ebony* mutants (as reported in Hodgetts and Konopka, 1973) affect CHC lengthening; however, it remains unclear which cells require *ebony* expression (and possibly dopamine metabolism) to influence CHC synthesis. We

hypothesized that *ebony*-dependent changes of the fly cuticle itself might affect CHC deposition during fly development or CHC extraction in the laboratory, and found that all but one detected CHC showed an overall decrease in abundance in dark cuticle relative to light cuticle. We note that these differences might be due to changes in the physical properties of dark versus light cuticle as they interact with the UV-LDI instrument. We also note that $ebony^{CRISPR(3)}$ and $ebony^{CRISPR(4)}$ mutants had darkly pigmented cuticle like $ebony^{CRISPR(1,2)}$ mutants but CHC length profiles similar to wild-type flies, suggesting that *ebony* and *tan*'s effects on CHC length composition can be separated from their role in pigmentation synthesis. For example, ebony expression in glia is necessary for normal circadian rhythms in *D. melanogaster* but not pigmentation (Suh and Jackson, 2007). It is also possible that *ebony* actually affects CHC composition through changes in pigmentation precursors within epidermal cells underneath the cuticle, which might not have been detected by our UV-LDI MS analysis in the thorax. We tested whether knocking down *ebony* in oenocytes in the abdomen affected CHC length composition and found that it did not, thus the specific cells required for ebony and tan's effects on CHC synthesis remain unknown.

Patterns of CHC composition and pigmentation along clines in natural populations

Identifying the pleiotropic effects of ebony and tan on pigmentation and CHCs is important because it suggests that these genes might contribute to the covariation of both traits in natural populations. For example, selection for *ebony*- or *tan*-dependent pigmentation variation might also cause variation in CHC length composition without selection acting directly on this trait. Alternatively, selection for long chain CHCs with higher melting temperatures (Gibbs and Pomonis, 1995; Gibbs, 1998) in drier climates might cause a correlated increase in pigmentation intensity. Indeed, we found that variation in abdominal pigmentation covaries with both *ebony* and *tan* gene expression as well as CHC length profiles in directions predicted by *ebony* and *tan* mutants among the DGRP lines, which were derived from flies isolated from a single, natural population (Ayroles et al. 2009; Mackay et al. 2012; Huang et al. 2014). However, this finding does not necessarily imply variation in both traits is caused by the same gene(s) nor that these traits will always co-evolve; for example, individuals with dark pigmentation may

coincidentally possess alleles that are in linkage disequilibrium that cause a CHC lengthening phenotype. Comparing the phenotypic frequency of pigmentation and CHC length composition phenotypes within and between the same populations that are undergoing adaptation to common environments will help answer this question. In Africa, for example, *D. melanogaster* populations repeatedly show a strong positive correlation between elevation and dark pigmentation, suggesting that environments at high altitudes might select for darkly pigmented flies (or some other trait that correlates with pigmentation) (Pool and Aquadro, 2007; Bastide et al., 2014). It will be interesting to know whether these populations also show an increase in abundance of long chain CHCs.

Both pigmentation and CHC length profiles vary along altitudinal and latitudinal clines in natural *Drosophila* populations, suggesting that ecological factors such as humidity or temperature play a role in shaping variation in at least one of these traits. At higher altitudes or latitudes, populations often showed darker pigmentation profiles in Europe, India, and Australia (Heed and Krishnamurthy, 1959; David et al., 1985; Capy et al., 1988; Das, 1995; Munjal et al., 1997; Parkash and Munjal, 1999; Pool and Aquadro, 2007; Telonis-Scott et al., 2011; Parkash et al., 2008a; Parkash et al., 2008b; Matute and Harris, 2013). In Africa, however, latitude and pigmentation intensity showed a negative correlation, so this relationship is not universal (Bastide et al., 2014). For CHCs, Rajpurohit et al. (2017) reported that *D. melanogaster* populations at higher latitudes showed more short chain CHCs, whereas populations at lower latitudes showed more long chain CHCs in the United States. Frentiu and Chenoweth (2010) similarly found that populations at high latitudes along a cline in Australia showed more short chain CHCs and fewer long chain CHCs. These patterns do not match predictions based on the pleiotropy we observed: flies at higher latitudes tend to have darker pigmentation and higher levels of short chain CHCs whereas $ebony^{CRISPR(1,2)}$ mutants, for example, have darker pigmentation and lower levels of short chain CHCs. To the best of our knowledge, pigmentation (nor *ebony* or *tan* expression) and CHC length composition have not been simultaneously measured in flies from the same cline, making it difficult to discern whether pigmentation and CHC composition covary in the wild in ways predicted by the

mutant data. For example, Frentiu and Chenoweth (2010) measured CHCs from populations along the east coast of Australia, but they did not include populations from higher latitude coastal regions with darker pigmentation and lower ebony expression in newly eclosed adults (Telonis-Scott et al. 2011). Comparing variation in both traits within and between populations along latitudinal and/or altitudinal clines will make it clearer if and to what extent pigmentation and CHC composition covary and whether variation in these features is accompanied by changes in ebony and tan expression.

Acknowledgements

We thank members of the Takahashi, Wittkopp, and Yew labs and Aki Ejima for helpful discussions; John True, Stephen Goodwin, Scott Pletcher, Rainbow Transgenics Inc., the Bloomington Drosophila Stock Center, and the Vienna Drosophila RNAi Center for fly stocks; and Rainbow Transgenics Inc., for fly injections. This work was supported by a University of Michigan, Department of Ecology and Evolutionary Biology, Nancy W. Walls Research Award, National Institutes of Health training grant T32GM007544, and Howard Hughes Medical Institute Janelia Graduate Research Fellowship awarded to J.H.M; the German Research Foundation (grant DR 416/10-1) awarded to K.D.; National Institutes of Health grant 1R35GM118073 awarded to P.J.W.; Department of Defense, U.S. Army Research Office W911NF1610216 and National Institutes of Health grant 1P20GM125508 awarded to J.Y.Y.; The Sumitomo Foundation Grant for Basic Science Research Projects 160999 to A.T.

References

Albert, A. Y., Sawaya, S., Vines, T. H., Knecht, A. K., Miller, C. T., *et al.* (2008). The genetics of adaptive shape shift in stickleback: pleiotropy and effect size. *Evolution, 62,* 76-85.

Altaratz, M., Applebaum, S. W., Richard, D. S., Gilbert, L. I., & Segal, D. (1991). Regulation of juvenile hormone synthesis in wild-type and apterous mutant *Drosophila*. *Molecular and Cellular Endocrinology, 81,* 205-216.

Ayroles, J. F., Carbone, M. A., Stone, E. A., Jordan, K. W., Lyman, R. F., Magwire, M. M., ... & Mackay, T. F. (2009). Systems genetics of complex traits in *Drosophila melanogaster*. *Nature Genetics, 41,* 299-307.

Bassett, A. R., Tibbit, C., Ponting, C. P., Liu, J-L. 2013. Highly efficient targeted mutagenesis of *Drosophila* with CRISPR/Cas9 system. *Cell Reports, 4,* 220-228.

Bastide, H., Betancourt, A., Nolte, V., Tobler, R., Stöbe, P., Futschik, A., & Schlötterer, C. (2013). A genome-wide, fine-scale map of natural pigmentation variation in *Drosophila melanogaster*. *PLoS Genetics, 9,* e1003534.

Bastide, H., Yassin, A., Johanning, E. J. Pool, J. E. (2014). Pigmentation in *Drosophila melanogaster* reaches its maximum in Ethiopia and correlates most strongly with ultra-violet radiation in sub-Saharan Africa. *BMC Evolutionary Biology, 14,* 179.

Bastock, M. (1956). A gene mutation which changes a behavior pattern. *Evolution, 10,* 421-439.

Boom, R. C. J. A., Sol, C. J., Salimans, M. M., Jansen, C. L., Wertheim-van Dillen, P. M., & Van der Noordaa, J. P. M. E. (1990). Rapid and simple method for purification of nucleic acids. *Journal of Clinical Microbiology, 28,* 495-503.

Blomquist, G. J., Dillwith, J. W., & Adams, T. S. (1987). Biosynthesis and endocrine regulation of sex pheromone production in Diptera. In *Pheromone Biochemistry* (pp. 217-250).

Blows MW, Allen RA (1998). Levels of mate recognition within and between two *Drosophila* species and their hybrids. *American Naturalist, 152,* 826–837.

Brand, A. H., & Perrimon, N. (1993). Targeted gene expression as a means of altering cell fates and generating dominant phenotypes. *Development, 118,* 401-415.

Bridges, C. B., & Morgan, T. H. (1923). *Third-chromosome group of mutant characters of Drosophila melanogaster.* Carnegie Institution Of Washington: Washington.

Calleja, M., Herranz, H., Estella, C., Casal, J., Lawrence, P., Simpson, P., & Morata, G.

(2000). Generation of medial and lateral dorsal body domains by the pannier gene of *Drosophila*. *Development, 127*, 3971-3980.

Capy, P., David, J. R., & Robertson, A. (1988). Thoracic trident pigmentation in natural populations of Drosophila simulans: a comparison with *D. melanogaster*. *Heredity, 61*, 263.

Chiang, Y. N., Tan, K. J., Chung, H., Lavrynenko, O., Shevchenko, A., & Yew, J. Y. (2016). Steroid hormone signaling is essential for pheromone production and oenocyte survival. *PLoS Genetics*, *12*, e1006126.

Das, A. (1995). Abdominal pigmentation in *Drosophila melanogaster* females from natural Indian populations. *Journal of Zoological Systematics and Evolutionary Research*, *33*(2), 84-87.

David, J. R., Capy, P., Payant, V., & Tsakas, S. (1985). Thoracic trident pigmentation in *Drosophila melanogaster*: differentiation of geographical populations. *Génétique, Sélection, Évolution*, *17*, 211.

Dembeck, L. M., Huang, W., Magwire, M. M., Lawrence, F., Lyman, R. F., & Mackay, T. F. (2015). Genetic architecture of abdominal pigmentation in *Drosophila melanogaster*. *PLoS Genetics*, *11*, e1005163.

Dembeck, L. M., Böröczky, K., Huang, W., Schal, C., Anholt, R. R., & Mackay, T. F. (2015). Genetic architecture of natural variation in cuticular hydrocarbon composition in *Drosophila melanogaster*. *Elife, 4*, e09861.

Dietzl, G., Chen, D., Schnorrer, F., Su, K. C., Barinova, Y., Fellner, M., ... & Couto, A. (2007). A genome-wide transgenic RNAi library for conditional gene inactivation in *Drosophila*. *Nature, 448*, 151-156.

Drapeau, M. D., Radovic, A., Wittkopp, P. J., & Long, A. D. (2003). A gene necessary for normal male courtship, *yellow*, acts downstream of fruitless in the *Drosophila melanogaster* larval brain. *Journal of Neurobiology, 55*, 53-72.

Drapeau, M. D., Cyran, S. A., Viering, M. M., Geyer, P. K., & Long, A. D. (2006). A cis-regulatory sequence within the yellow locus of *Drosophila melanogaster* required for normal male mating success. *Genetics, 172*, 1009-1030.

Duveau, F., & Félix, M. A. (2012). Role of pleiotropy in the evolution of a cryptic developmental variation in *Caenorhabditis elegans*. *PLoS Biology, 10*, e1001230.

Endler, L., Betancourt, A. J., Nolte, V., & Schlötterer, C. (2016). Reconciling differences in pool-GWAS between populations: a case study of female abdominal pigmentation in *Drosophila melanogaster*. *Genetics*, *202*, 843-855.

Endler, L., Gibert, J. M., Nolte, V., & Schlötterer, C. (2018). Pleiotropic effects of regulatory variation in *tan* result in correlation of two pigmentation traits in *Drosophila melanogaster*. *Molecular Ecology, 27*, 3207-3218.

Ferveur, J. F., Savarit, F., O'kane, C. J., Sureau, G., Greenspan, R. J., & Jallon, J. M. (1997). Genetic feminization of pheromones and its behavioral consequences in *Drosophila* males. *Science*, *276*, 1555-1558.

Flaven-Pouchon, J., Farine, J-P., Ewer, J., Ferveur, J-F. (2016). Regulation of cuticular hydrocarbon profile maturation by *Drosophila* tanning hormone, bursicon, and its interaction with desaturase activity. *Insect Biochemistry and Molecular Biology, 79*, 87-96.

Foley, B. R., & Telonis-Scott, M. (2011). Quantitative genetic analysis suggests causal association between cuticular hydrocarbon composition and desiccation survival in *Drosophila* melanogaster. *Heredity, 106*, 68.

Frentiu, F. D., Chenoweth, S. F. (2010). Clines in cuticular hydrocarbons in two Drosophila species with independent population histories. *Evolution*, *64*, 1784-1794.

Gibbs, A., & Pomonis, J. G. (1995). Physical properties of insect cuticular hydrocarbons: the effects of chain length, methyl-branching and unsaturation. *Comparative Biochemistry and Physiology Part B: Biochemistry and Molecular Biology*, *112*, 243-249.

Gibbs, A. G., Chippindale, A. K., & Rose, M. R. (1997). Physiological mechanisms of evolved desiccation resistance in *Drosophila melanogaster*. *Journal of Experimental Biology*, *200*, 1821-1832.

Gibbs, A. G. (1998). Water-proofing properties of cuticular lipids. *American Zoologist*, 38, 471-482.

Gratz, S. J., Ukken, F. P., Rubinstein, C. D., Thiede, G., Donohue, L. K., Cummings, A. M., & O'Connor-Giles, K. M. (2014). Highly specific and efficient CRISPR/Cas9-catalyzed homology-directed repair in *Drosophila*. *Genetics*, *196*, 961-971.

Greenwood, A. K., Mills, M. G., Wark, A. R., Archambeault, S. L., Peichel, C. L. (2016). Evolution of schooling behavior in threespine sticklebacks is shaped by the *Eda* gene. *Genetics*, *203*, 677-681.

Gruntenko, N. E., Chentsova, N. A., Andreenkova, E. V., Bownes, M., Segal, D., Adonyeva, N. V., & Rauschenbach, I. Y. (2003). Stress response in a juvenile hormone-deficient *Drosophila melanogaster* mutant apterous. *Insect Molecular Biology, 12*, 353-363.

Gruntenko, N. E., Karpova, E. K., Alekseev, A. A., Chentsova, N. A., Saprykina, Z. V., Bownes, M., & Rauschenbach, I. Y. (2005). Effects of dopamine on juvenile hormone metabolism and fitness in *Drosophila virilis*. *Journal of Insect Physiology*, *51*, 959-968.

Gruntenko, N. E., Laukhina, O. V., Bogomolova, E. V., Karpova, E. K., Menshanov, P. N., Romanova, I. V., & Rauschenbach, I. Y. (2012). Downregulation of the dopamine D2-like receptor in corpus allatum affects juvenile hormone synthesis in *Drosophila melanogaster* females. *Journal of Insect Physiology*, *58*, 348-355.

Heed, W. B., & Krishnamurthy, N. B. (1959). Genetic studies on the cardini group of *Drosophila* in the West Indies. *Univ. Texas Publ*, 5914, 155-179.

Hodgetts, R. B., & Konopka, R. J. (1973). Tyrosine and catecholamine metabolism in wild-type *Drosophila melanogaster* and a mutant, *ebony*. *Journal of Insect Physiology*, *19*, 1211-1220.

Hovemann, B. T., Ryseck, R. P., Walldorf, U., Störtkuhl, K. F., Dietzel, I. D., & Dessen, E. (1998). The *Drosophila ebony* gene is closely related to microbial peptide synthetases and shows specific cuticle and nervous system expression. *Gene*, *221*, 1-9.

Huang, W., Massouras, A., Inoue, Y., *et al.* (2014) Natural variation in genome architecture among 205 *Drosophila melanogaster* Genetic Reference Panel lines. *Genome Research*, *24*, 1193–1208.

Mackay, T. F., Richards, S., Stone, E. A., Barbadilla, A., Ayroles, J. F., Zhu, D., ... & Richardson, M. F. (2012). The *Drosophila melanogaster* genetic reference panel. *Nature*, *482*, 173-178.

Marican, C., Duportets, L., Birman, S., Jallon, J. M. (2004). Female-specific regulation of cuticular hydrocarbon biosynthesis by dopamine in *Drosophila melanogaster*. *Insect Biochemistry and Molecular Biology*, *34*, 823-830.

Matute, D. R., & Harris, A. (2013). The influence of abdominal pigmentation on desiccation and ultraviolet resistance in two species of *Drosophila*. *Evolution*, *67*, 2451-2460.

Mckay, J. K., Richards, J. H., and Mitchell-Olds, T. (2003). Genetics of drought adaptation in *Arabidopsis thaliana*: I. Pleiotropy contributes to genetic correlations among ecological traits. *Molecular Ecology*, *12*, 1137-1151.

McLean, C. Y., Reno, P. L., Pollen, A. A., Bassan, A. I., Capellini, T. D., Guenther, C., ... & Wenger, A. M. (2011). Human-specific loss of regulatory DNA and the evolution of human-specific traits. *Nature*, *471*, 216.

Miyagi, R., Akiyama, N., Osada, N., & Takahashi, A. (2015). Complex patterns of *cis*-regulatory polymorphisms in *ebony* underlie standing pigmentation variation in *Drosophila melanogaster*. *Molecular Ecology*, *24*, 5829–5841.

Munjal, A. K., Karan, D., Gibert, P., Moreteau, B., Parkash, R., & David, J. R. (1997). Thoracic trident pigmentation in *Drosophila melanogaster*: latitudinal and altitudinal clines in Indian populations. *Genetics Selection Evolution*, *29*, 601.

Nagy, O., Nuez, I., Savisaar, R., Peluffo, A. E., Yassin, A., Lang, M., ... & Courtier-Orgogozo, V. (2018). Correlated evolution of two copulatory organs via a single *cis*-regulatory nucleotide change. *Current Biology*, *28*, 3450-3457.

Parkash, R., & Munjal, A. K. (1999). Phenotypic variability of thoracic pigmentation in Indian populations of *Drosophila melanogaster*. *Journal of Zoological Systematics and Evolutionary Research*, *37*, 133-140.

Parkash, R., Rajpurohit, S., & Ramniwas, S. (2008a). Changes in body melanisation and desiccation resistance in highland vs. lowland populations of *D. melanogaster*. *Journal of Insect Physiology*, *54*, 1050-1056.

Parkash, R., Sharma, V., & Kalra, B. (2008b). Climatic adaptations of body melanisation in *Drosophila melanogaster* from Western Himalayas. *Fly*, *2*, 111-117.

Pool, J. E., & Aquadro, C. F. (2007). The genetic basis of adaptive pigmentation variation in *Drosophila melanogaster*. *Molecular Ecology*, *16*, 2844-2851.

R Core Team. 2013. R: A Language and Environment for Statistical Computing. Available from: http://www.r-project.org/.

Rajpurohit, S., Hanus, R., Vrkoslav, V., Behrman, E. L., Bergland, A. O., Petrov, D., Cvacka, J., Schmidt, P. S. (2017). Adaptive dynamics of cuticular hydrocarbons in *Drosophila*. *J. Evol. Biol*. *30*, 66-80.

Rebeiz, M., Pool, J. E., Kassner, V. A., Aquadro, C. F., & Carroll, S. B. (2009a). Stepwise modification of a modular enhancer underlies adaptation in a *Drosophila* population. *Science*, *326*, 1663–1667.

Rebeiz, M., Ramos-Womack, M., Jeong, S., Andolfatto, P., Werner, T., True, J., et al. (2009b). Evolution of the *tan* locus contributed to pigment loss in *Drosophila santomea*: A response to Matute et al. *Cell*, *139*, 1189–1196.

Ren, X., Yang, Z., Xu, J., Sun, J., Mao, D., Hu, Y., ... & Deng, P. (2014). Enhanced specificity and efficiency of the CRISPR/Cas9 system with optimized sgRNA parameters in *Drosophila*. *Cell Reports*, *9*, 1151-1162.

Rideout, E. J., Dornan, A. J., Neville, M. C., Eadie, S., & Goodwin, S. F. (2010). Control of sexual differentiation and behavior by the *doublesex* gene in *Drosophila melanogaster*. *Nature Neuroscience, 13*, 458.

Riedel, F., Vorkel, D., & Eaton, S. (2011). Megalin-dependent yellow endocytosis restricts melanization in the *Drosophila* cuticle. *Development, 138*, 149-158.

Schluter, D., Clifford, E. A., Nemethy, M., McKinnon, J. S. (2004). Parallel evolution and inheritance of quantitative traits. *Am. Nat., 163*, 809-822.

Spector, S., Sjoerdsma, A., & Udenfriend, S. (1965). Blockade of endogenous norepinephrine synthesis by α-methyl-tyrosine, an inhibitor of tyrosine hydroxylase. *Journal of Pharmacology and Experimental Therapeutics, 147*, 86-95.

Suh, J., & Jackson, F. R. (2007). *Drosophila ebony* activity is required in glia for the circadian regulation of locomotor activity. *Neuron, 55*, 435-447.

Takahashi, A. (2013). Pigmentation and behavior: potential association through pleiotropic genes in *Drosophila*. *Genes & genetic systems, 88*, 165-174.

Takahashi, A., Takano-Shimizu, T. (2011). Divergent enhancer haplotype of *ebony* on inversion In(3R)Payne associated with pigmentation variation in a tropical population of *Drosophila melanogaster*. *Molecular Ecology, 20*, 4277-4287.

Telonis-Scott, M., Hoffmann, A. A., & Sgro, C. M. (2011). The molecular genetics of clinal variation: A case study of ebony and thoracic trident pigmentation in *Drosophila melanogaster* from eastern Australia. *Molecular Ecology, 20*, 2100–2110.

True, J. R. (2003). Insect melanism: the molecules matter. *Trends in Ecology & Evolution, 18*, 640-647.

True, J. R., Yeh, S-D., Hovemann, B. T., Kemme, T., Meinertzhagen, I. A., Edwards, T. N., Liou, S-R., Han, Q., Li, J. (2005). Drosophila *tan* encodes a novel hydrolase required in pigmentation and vision. *PLoS Genetics, 1*, e63.

Walker, J. A., and M. A. Bell. (2000). Net evolutionary trajectories of body shape evolution within a microgeographic radiation of threespine sticklebacks (*Gasterosteus aculeatus*). *J. Zool., 252*, 293-302.

Wark, A. R., A. K. Greenwood, E. M. Taylor, K. Yoshida, and Peichel, C. L. (2011). Heritable differences in schooling behavior among threespine sticklebacks revealed by a novel assay. *PLoS One, 6*, e18316.

Wicker, C., & Jallon, J. M. (1995). Hormonal control of sex pheromone biosynthesis in

Drosophila melanogaster. *Journal of Insect Physiology, 41*, 65-70.

Wigglesworth, V. B. (1970). Structural lipids in the insect cuticle and the function of the oenocytes. *Tissue and Cell*, *2*, 155-179.

Wittkopp, P. J., & Beldade, P. (2009). Development and evolution of insect pigmentation: genetic mechanisms and the potential consequences of pleiotropy. *Seminars in Cell & Developmental Biology*, *20*, 65-71.

Yew, J. Y., Dreisewerd, K., De Oliveira, C. C., & Etges, W. J. (2011). Male-specific transfer and fine scale spatial differences of newly identified cuticular hydrocarbons and triacylglycerides in a *Drosophila* species pair. *PLoS One*, *6*, e16898.

Yew, J. Y., & Chung, H. (2015). Insect pheromones: An overview of function, form, and discovery. *Progress in Lipid Research, 59*, 88-10.

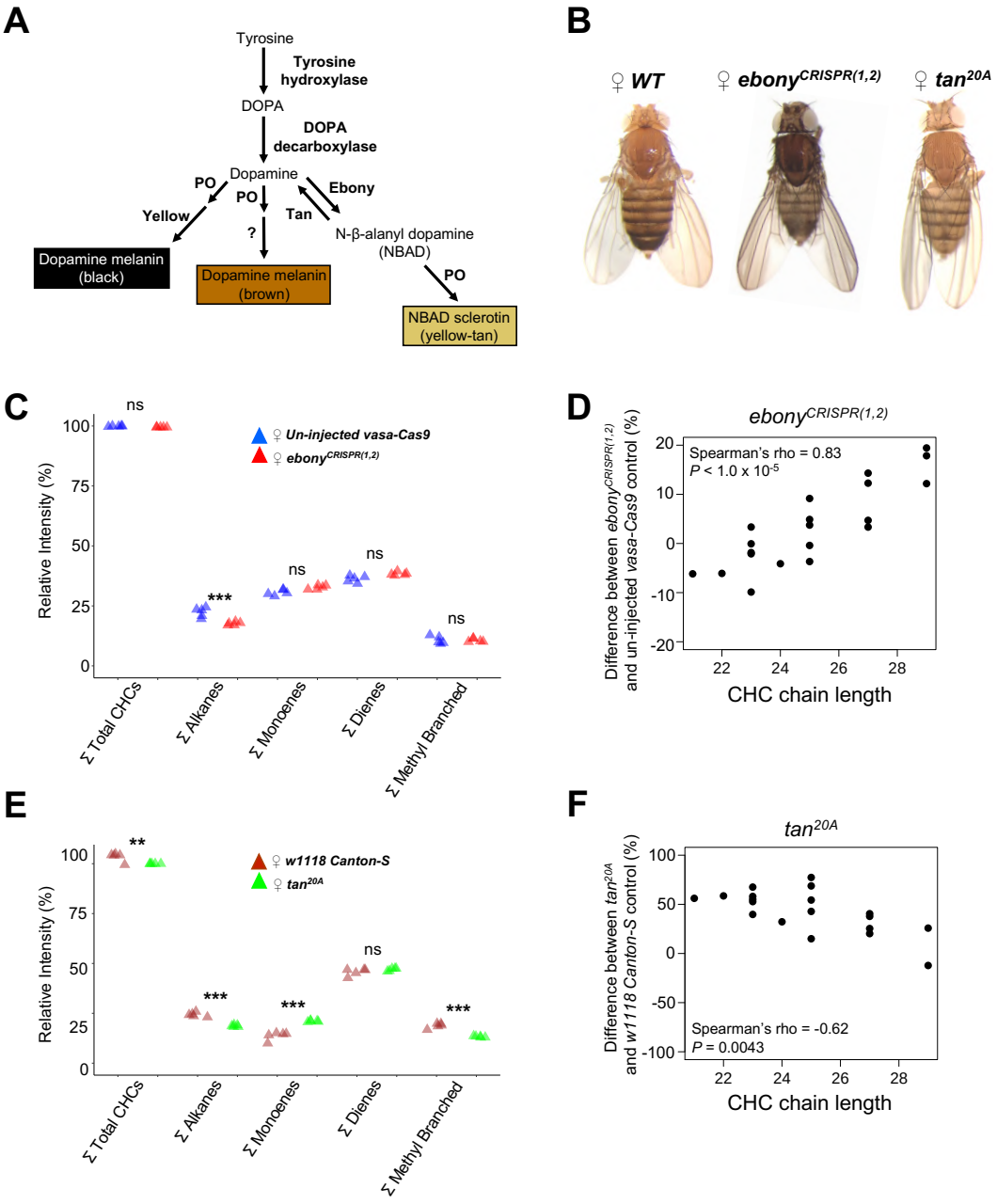
A
Tyrosine
Tyrosine hydroxylase
DOPA
DOPA decarboxylase
Dopamine
PO
PO
Ebony
Tan
Yellow
?
N-β-alanyl dopamine (NBAD)
PO
Dopamine melanin (black)
Dopamine melanin (brown)
NBAD sclerotin (yellow-tan)
B
♀ WT
♀ ebonyCRISPR(1,2)
♀ tan20A
C
Relative Intensity (%)
♀ Un-injected vasa-Cas9
♀ ebonyCRISPR(1,2)
ns
***
ns
ns
ns
Σ Total CHCs
Σ Alkanes
Σ Monoenes
Σ Dienes
Σ Methyl Branched
D
ebonyCRISPR(1,2)
Difference between ebonyCRISPR(1,2) and un-injected vasa-Cas9 control (%)
Spearman's rho = 0.83
P < 1.0 x 10-5
CHC chain length
E
Relative Intensity (%)
♀ w1118 Canton-S
♀ tan20A
**
***
***
ns
***
Σ Total CHCs
Σ Alkanes
Σ Monoenes
Σ Dienes
Σ Methyl Branched
F
tan20A
Difference between tan20A and w1118 Canton-S control (%)
Spearman's rho = -0.62
P = 0.0043
CHC chain length

Figure 3-1 *ebony* and *tan* affect pigmentation and CHC composition in female *Drosophila melanogaster*

(**A**) Insect sclerotization and pigmentation synthesis pathway. Ebony converts dopamine into N-β-alanyl dopamine (NBAD) which is oxidized into yellow-colored NBAD sclerotin. Tan catalyzes the reverse reaction, converting NBAD back into dopamine that can be oxidized into black and brown melanins. (**B**) Photographs highlighting the effects of $ebony^{CRISPR(1,2)}$ (darker) and tan^{20A} (lighter) on body pigmentation compared to the un-injected *vasa-Cas9* control line (*WT*). (**C**) Summary of $ebony^{CRISPR(1,2)}$ effects on total summed CHC classes relative to *un-injected vasa-Cas9* control females. (**D**) Difference in log-contrast of relative CHC intensity between $ebony^{CRISPR(1,2)}$ and *un-injected vasa-Cas9* control flies. (**E**) Summary of tan^{20A} effects on total summed CHC classes relative to w^{1118} *Canton-S* control females. For (**D**) and (**E**), each triangle represents a single replicate of CHCs extracted from five pooled individuals (N = 5 replicates per genotype). (**F**) Difference in log-contrast of relative CHC intensity between tan^{20A} and w^{1118} *Canton-S* control flies. Results of Tukey HSD post-hoc tests following One-way ANOVA are shown: * $P < 0.05$, ** $P < 0.01$, *** $P < 0.001$.

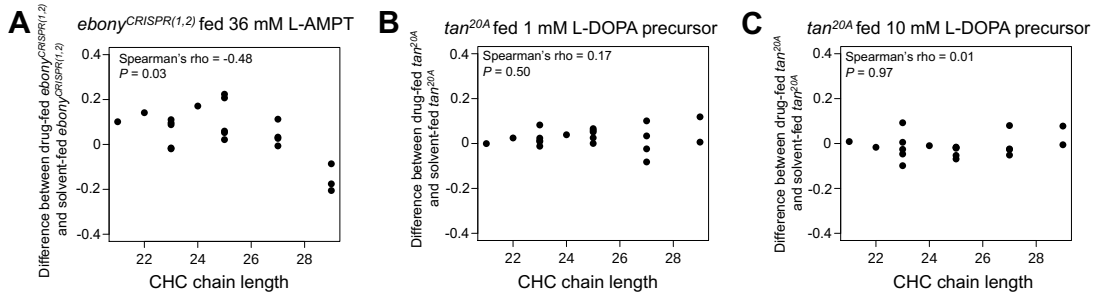

Figure 3-2 Effects of pharmacological treatments on CHC lengthening in *ebony*$^{CRISPR(1,2)}$ and *tan*^{20A} mutants

(**A**) Difference in log-contrast of relative CHC intensity between *ebony*$^{CRISPR(1,2)}$ females fed 36mM alpha methyl tyrosine (L-AMPT) and *ebony*$^{CRISPR(1,2)}$ females fed a solvent control. (**B**) Difference in log-contrast relative of CHC intensity between *tan*^{20A} females fed 1 mM methyl L-DOPA hydrochloride (L-DOPA precursor) and *tan*^{20A} females fed a solvent control. (**C**) Difference in log-contrast of relative CHC intensity between *tan*^{20A} females fed 10 mM L-DOPA precursor and *tan*^{20A} females fed a solvent control.

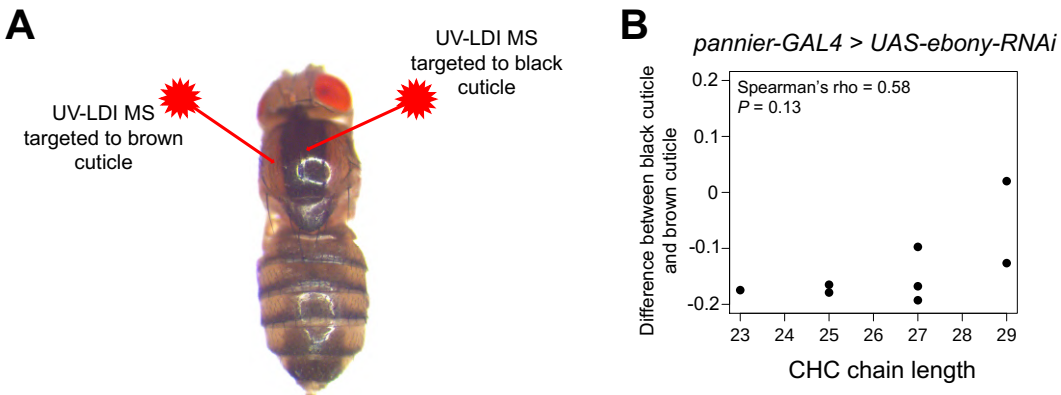

Figure 3-3 UV laser desorption/ionization mass spectrometry (UV-LDI MS) did not detect differences in short versus long CHCs between lightly and darkly pigmented cuticle

Female *pannier-GAL4* flies were crossed to *UAS-ebony-RNAi* males to generate flies with a dark, heavily melanized stripe down the dorsal midline. (**A**) The UV-LDI MS lasers were targeted to light brown or dark black cuticle within the same fly (N = 3 biological replicates). (**B**) Difference in relative CHC intensity between black and brown cuticle.

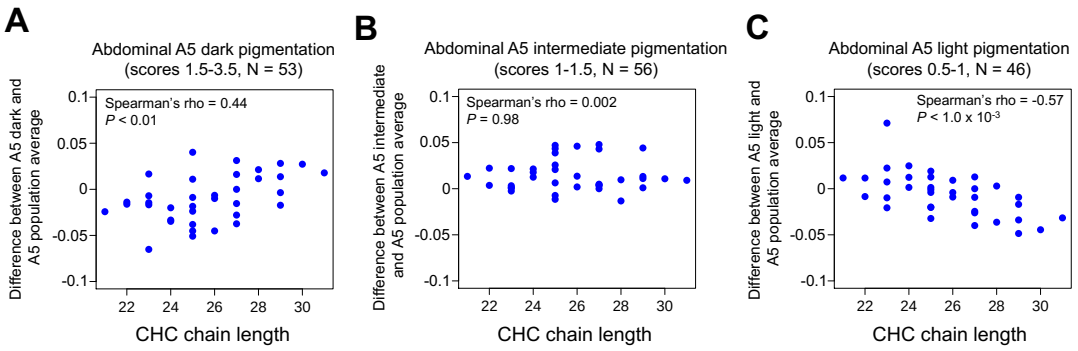

Figure 3-4 Abdominal pigmentation co-varies with CHC length profiles in the *Drosophila* Genetic Reference Panel (DGRP)

Pigmentation scores and CHC data were obtained from Dembeck *et al.* (2015a,b). (**A**) Difference in log-contrast of relative CHC intensity between DGRP females with darkly-pigmented 5th abdominal tergites (A5) (1.5 < score, N = 53) and the 155 line average. (**B**) Difference in log-contrast of relative CHC intensity between DGRP females with intermediately-pigmented A5 (1 < score ≤ 1.5, N = 56) and the 155 line average. (**C**) Difference in log-contrast of relative CHC intensity between DGRP females with lightly-pigmented A5 (score ≤ 1, N = 49) and the 155 line average.

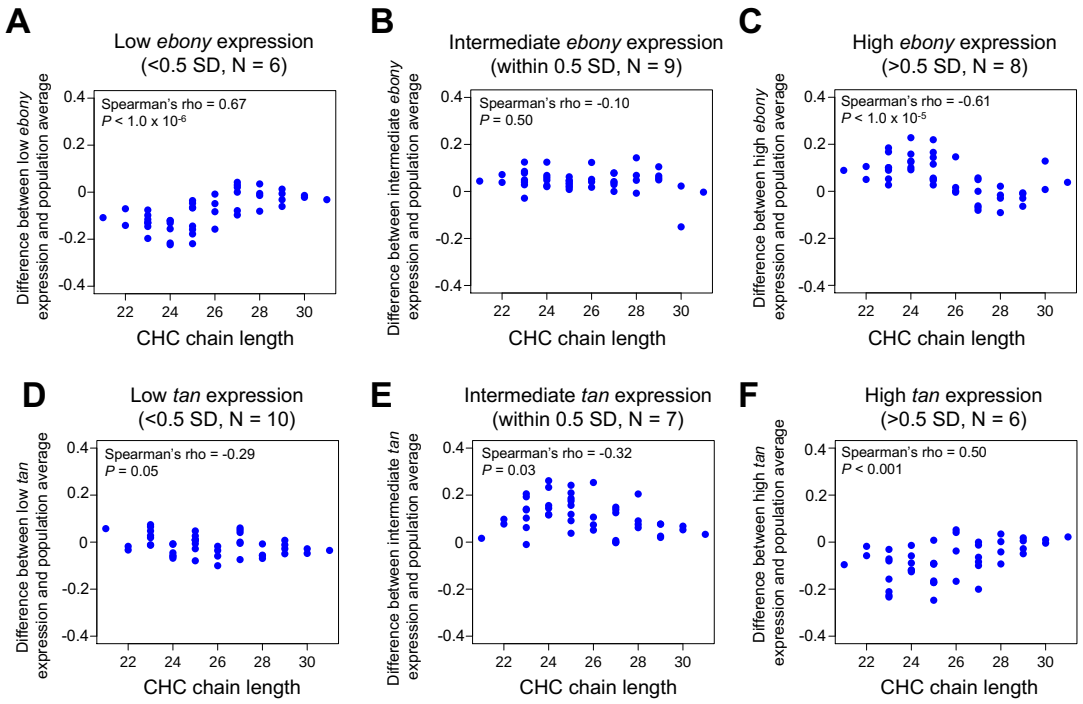

Figure 3-5 Variation in *ebony* and expression co-varies with CHC length profiles in the DGRP

CHC data was obtained from Dembeck *et al*. (2015b), and *ebony* and *tan* expression was quantified via qRT-PCR for 23 DGRP lines. (**A**) Difference in log-contrast of relative CHC intensity between DGRP females with low *ebony* expression and the 23 line average. (**B**) Difference in log-contrast of relative CHC intensity between DGRP females with intermediate *ebony* expression and the 23 line average. (**C**) Difference in log-contrast of relative CHC intensity between DGRP females with low *ebony* expression and the 23 line average. (**D**) Difference in log-contrast of relative CHC intensity between DGRP females with low *tan* expression and the 23 line average. (**E**) Difference in log-contrast of relative CHC intensity between DGRP females with intermediate *tan* expression and the 23 line average. (**F**) Difference in log-contrast of relative CHC intensity between DGRP females with high *tan* expression and the 23 line average.

Chapter 4

Genetic Dissection of Correlated Divergence in Wing Pigmentation and Mating Display

Abstract

Species differences in sexual traits involve correlated changes in morphology and behavior. The evolution of mating displays in particular often highlight diverse pigmentation patterns that distinguish males from females and closely related species. How the genome evolves to cause these correlated changes is not well understood. We investigated the genetic basis of correlated divergence in wing pigmentation and mating display between the sibling species *D. elegans* and *D. gunungcola.* Divergence in both traits map to a co-localized region on the X chromosome. Within this region, we mapped a single, ~440 kb locus that behaves like a genetic switch controlling wing spot divergence. Divergence in mating display also involved loci on the autosomes. Introgression mapping on the X chromosome and field observations suggest that wing spot and mating display divergence can be separated, possibly as a consequence of epistatic interactions between the X and autosomes.

Introduction

Animals often use colorful morphological structures to communicate with prospective mates during courtship. Most famously, male peacocks display their elaborately decorated plumage during courtship rituals to lure females (Petrie *et al*., 1991; Petrie and Halliday, 1994; but see Takahashi *et al*., 2008). In vertebrates and invertebrates, pigmented bodies or wings often evolve together with specific components of courtship behavior that animals use to display their colorful anatomy (Loxton, 1979; Endler, 1991; Sinervo et al., 2000; White et al., 2015). These correlated differences evolve both within and between populations, frequently distinguishing males from females or closely related species (Gray and McKinnon, 2007; McKinnon and Pierotti, 2010). Little is known about how pigmented body parts and courtship behaviors evolve together at the level of the genome. In just a few cases, linkage mapping and genome-wide association studies (GWAS) have shown that loci affecting pigmentation patterning tend to co-localize with loci affecting variation in mating behaviors (Lindholm and Breden, 2002; Kronforst *et al*., 2006; Thomas *et al*., 2008; Kupper *et al*., 2016; Lamichhaney *et al*., 2016; Merrill *et al*., 2019; reviewed in McKinnon and Pierotti, 2010). That is, physical linkage of genes or mutations on the same chromosome underlie phenotypic correlations between mating behavior and pigmentation. Interestingly, these loci also tend to explain much of the variation observed for both traits. A key challenge is determining how frequently these patterns of genomic architecture underlie correlated evolution and whether the same pleiotropic or separate linked loci are involved.

Disentangling whether pleiotropic or physically linked loci underlie patterns of correlated evolution between pigmentation and mating behavior is important for understanding how genomes create, maintain, and shape adaptive differences between sexes and species. If two beneficial traits are genetically correlated due to separate, physically linked loci, simulations predict that natural or sexual selection (e.g., through predation or female choice) must actively work to minimize recombination to maintain linkage (Charlesworth and Charlesworth, 1976); it has been hypothesized that one solution to this problem might involve the evolution of chromosomal inversions that suppress recombination between two or more linked loci (Kirkpatrick and Barton, 2006). Alternatively, mutations

at a single pleiotropic gene could cause correlated components of pigmentation and mating behavior to evolve simultaneously. The likelihood that mutation or recombination disrupt genetic correlations, however, will likely depend on locus-specific rates of recombination, mutation, and the distance between physically linked loci (Paaby and Rockmann, 2013). Distinguishing between these genetic modes of phenotypic evolution will require, in part, mapping species correlated differences at higher resolution in an attempt to recombine tightly linked loci.

In the Oriental *Drosophila melanogaster* species group, male-specific wing spots are phylogenetically correlated with mating displays (Kopp and True, 2002). Males that possess wing spots tend to perform elaborate wing display dances during courtship, turning their dorsal wing surfaces toward the female and waving them up and down; males without spots lack display behavior (Kopp and True, 2002). Correlated gains or losses of both traits have evolved repeatedly (Kopp and True, 2002). In two closely related species from this group, *D. elegans* (Bock and Wheeler, 1972) males possess wing spots and perform wing displays (Figure 4-1A), while males in its sibling species, *D. gunungcola* (Sultana *et al*., 1999), have lost both (Figure 4-1A) (Kopp and True, 2002; Prud'homme *et al*., 2006; Yeh *et al*., 2006). Previously, Yeh *et al*., (2006) and Yeh and True (2014) took advantage of the fact *D. elegans* and *D. gunungcola* form fertile F1 hybrid female offspring in the lab to study the genetic basis of wing spot and wing display divergence. Through linkage mapping, they discovered that evolution of linked loci on the X chromosome contributed to divergence in both traits (Yeh and True, 2014). It remains unclear, however, whether the same or different loci on the X chromosome underlie correlated differences in wing spot and wing display between these species.

To further dissect the genetic basis of wing spots and wing display divergence between *D. elegans* and *D. gunungcola*, we generated several hundred backcross recombinant male progeny segregating for both traits. We assembled chromosome-length scaffolds of *D. elegans* and applied Multiplexed Shotgun Genotyping (MSG) (Andolfatto *et al*., 2011) to estimate recombination crossover positions across the genome; we also generated quantitative measures of both wing spots and wing display behavior to estimate the effect

size of loci contributing to divergence. Finally, we generated advanced, recombinant introgressions on the X chromosome in an attempt to separate quantitative trait loci (QTL) underlying wing spots and wing display behavior.

Materials and Methods

Fly stocks

Species stocks were kept on a 12 h light-dark cycle at 23ºC on University of Michigan R food diet (http://lab-express.com/flyfoodsupplies.htm#rfood), containing molasses as a sugar source. The *D. elegans HK* (Hong Kong) and *D. gunungcola SK* (Sukarami) lines used in this study were a gift from John True (Stony Brook University). Fisherbrand filter paper (cat# 09-790-2A) was added to the food when 3rd instar L3 larvae developed to facilitate pupation.

Generating hybrid progeny

Virgin male and females of *D. elegans HK* and *D. gunungcola SK* were isolated upon eclosion and stored in groups of ten for one week on University of Michigan M food (http://lab-express.com/flyfoodsupplies.htm#rfood), standard cornmeal diet with 20% higher agar content. Virgin males from *D. elegans HK* were crossed to virgin females from *D. gunungcola SK*, and virgin males from *D. gunungcola SK* were crossed to virgin females from *D. elegans HK* in groups of ten males and ten females to generate fertile F1 female and sterile F1 male hybrids. These crosses generally took 3-4 weeks to produce hybrid progeny. The switch from R food to M food for interspecific crosses was necessary, because R food tended to accumulate condensation and bacterial growth much faster than M food when few flies occupied a vial. Since crossing *D. elegans HK* and *D. gunungcola SK* to generate F1 hybrids tends to take several more weeks than within species crosses, the switch to M food diet allowed for maximum breeding time and the development of dozens of hybrid progeny. Once hybrid females eclosed from both interspecific cross directions, they were pooled into the same vial and aged for ten days. We did not keep track of F1 hybrid female maternity, because previous work (Yeh and True, 2014) found no effect of F1 hybrid maternity on trait means in F2 backcross

populations. Multiple high density groups of ~60 hybrid females were then backcrossed to ~60 virgin male *D. elegans HK* flies in individual vials on M food diet to create the *D. elegans HK* backcross recombinant population (724 individuals). To create the *D. gunungcola SK* backcross recombinant population (241 individuals), groups of ~60 hybrid females were backcrossed to ~60 virgin male *D. gunungcola SK* flies in individual vials on M food diet; this backcross was significantly less successful at producing recombinant progeny than the *D. elegans HK* backcross direction.

Behavioral assays

Virgin *D. elegans HK* females aged at least 10 days were isolated upon eclosion and stored in groups of 30-40 for courtship assays. F1 hybrid and recombinant backcross males were isolated individually in M food vials using CO2 upon eclosion for at least 5 days before each courtship assay. For each assay, a single individual male was gently aspirated into a custom designed 70 mm diameter bowl arena adapted from methods described in Simon and Dickinson (2010). Next, a single virgin *D. elegans HK* female was aspirated into the chamber and videotaped for 20 min immediately after, using a Canon VIXIA HF R500. Videos were recorded between 0900 and 1600 at 23ºC. *D. elegans HK* virgin females were used in all courtship assays in case any *D. elegans HK* female cues were necessary to elicit male wing display behavior. After each assay, both the male and female were aspirated back into an M food vial for up to 5 days after which each male was frozen in individual 1.5 mL Eppendorf tubes for wing spot quantification (see Quantification of wing spots), genomic DNA (gDNA) extraction, and sequencing (see Library preparation and sequencing). All courtship videos (~900 total, available upon request) were transferred to external hard drives for wing display quantification (see Quantification of wing display behavior).

Quantification of wing display behavior

F1 hybrid and recombinant males from both backcross directions performed variable wing display behaviors during courtship (Figure 4-2D, as described previously in Yeh *et al.*, 2006; Yeh and True, 2014). To generate quantitative measurements of wing display variation between individuals, each courtship video was played using QuickTime

(version 10.4) (Apple Inc., Cupertino, CA) software in a MacOS environment and digital screenshots were manually taken for each wing display bout, defined as bilateral wing extensions performed near the female (Supplemental Figure S4-1). Next, for each individual fly, wing display screenshots were compared to each other to identify the maximum wing display bout per fly, defined by comparing the distance between the tips of each wing relative to the center of the fly. These maximum wing display screenshots were then imported into ImageJ software (version 1.50i) (Wayne Rasband, National Institutes of Health, USA; http://rsbweb.nih.gov/ij/) to manually measure the "Maximum wing display angle" for F1 hybrid and recombinant males. In ImageJ, each screenshot image was inverted using the "Find Edges" function to enhance the contrast between the arena background and the edges of the fly wings (Supplemental Figure S4-1). Next, the "Polygon Selections" tool was used to fit an ellipse around the fly body using the "Fit Ellipse" function (Supplemental Figure S4-1). A Macros function (Supplementary File S4-2) was then used to generate major and minor axes inside the ellipse to identify the center of the fly body (Supplemental Figure S4-1). Finally, the "Angle Tool" was used to measure the "Maximum wing display angle" centering the vertex at the intersection of the major and minor axes and extended from wing tip to wing tip (Supplemental Figure S4-1). "Maximum wing display angle" varied between ~50º and ~220º between backcross recombinant individuals (Figure 4-2D).

Quantification of wing spots

Since wing spots fully form ~24 h after eclosion in *D. elegans HK*, all parental male *D. elegans HK*, *D. gunungcola SK*, F1 hybrids, and backcross recombinants were aged at least 7 days before being frozen at -20C in 1.5 mL Eppendorf tubes. Next, using a 20 Gauge stainless steel syringe tip (Techcon) (cat# TE720100PK) the right wing of each fly was cut away from the thorax and placed on a glass microscope slide (Fisherbrand) (cat# 12-550-15) to image using either a Leica MZFLIII stereoscope equipped with a Leica DC480 microscope camera or a Canon EOS Rebel T6 camera equipped with a Canon MP-E 65 mm macro lens. Each camera was calibrated using an OMAX 0.1 mm slide micrometer to define pixel density in ImageJ software. JPEG images of wings were imported into ImageJ to measure wing spot size relative to total wing area (wing spot size

/ total wing area). Total wing area (wing length x wing width) was approximated using length and width proxies (Figure 4-2A) following methods described in Yeh and True (2014). Using the "Polygon Selections" tool, the margins of black pigmentation defining each "Wing spot size" (Figure 4-2A) was traced and the polygon area quantified in mm^2 using the "Measure" function. "Wing spot size" varied between 0.15 mm^2 and 0 mm^2 (spotless) between recombinant individuals.

Library preparation and sequencing

We estimated chromosome ancestry "genotypes" for 724 *D. elegans HK* backcross progeny and 241 *D. gunungcola SK* backcross progeny with a single Multiplexed Shotgun Genotyping (MSG) (Andolfatto *et al*., 2011) library using 965 barcoded adaptors following methods described in Cande *et al*., (2012). In brief, to extract gDNA from all male backcross individuals, single flies were placed into individual wells of 96-well (Corning) (cat# 3879) plates containing a single steel grinding bead (Qiagen) (cat# 69989). Eleven plates in total were prepared for 965 individual gDNA extractions. gDNA was isolated and purified using the solid tissue extraction procedure from a Zymo Quick-DNA 96 Kit (cat# D3012) and a paint shaker to homogenize tissue. gDNA was tagmented using a hyperactive version of Tn5 transposase charged with annealed adaptor oligos following the methods described in (Picelli *et al*., 2014). Unique barcoded adaptor sequences were ligated to each sample of tagmented gDNA with 14 cycles of PCR using NEB OneTaq 2x Master Mix (cat# M0482S), and all samples were pooled into a single multiplexed sequencing library. Agencourt AMPure XP beads (Beckman Coulter) (cat# A63881) were used to size select ~150-800 bp fragments and eluted in 35 uL of molecular grade water (Corning) (cat# MT46000CI). The library was quantified by qPCR and sequenced in a single lane of Illumina HiSeq by the Janelia Quantitative Genomics Team.

In addition to generating the backcross sequencing library, both *D. elegans HK* and *D. gunungcola SK* parental species were sequenced at 20x coverage using an Illumina MiSeq Reagent Kit (v.3, 600 cycle PE) to facilitate genome assembly. In brief, gDNA was extracted using a Zymo Quick-DNA Microprep Kit (cat# D4074) from 10 pooled

females for each species and quantified on a Qubit 2.0 (Invitrogen). These samples were sent to the University of Michigan DNA Sequencing Core to prepare 300 bp PE libraries, which were quantified by qPCR and sequenced in a single lane of Illumina MiSeq.

Genome assembly

In brief, Illumina reads from all 965 F2 backcross recombinants were used to perform MSG on the Baylor College of Medicine *D. elegans* genome assembly (https://www.ncbi.nlm.nih.gov/bioproject/62315). Using custom script in R and Python (https://github.com/masseyj/elegans), the recombination fraction between the Baylor and MSG contigs was calculated and plotted to manually tabulate joins and splits between newly assembled contigs. These new contigs were then used to assemble chromosome length scaffolds in *D. elegans*.

Marker generation with Multiplexed Shotgun Genotyping

Following methods described previously (Andolfatto *et al*., 2011; Cande *et al*., 2012), we used the MSG software pipeline (https://github.com/JaneliaSciComp/msg/tree/master/instructions) to perform data parsing and chromosome ancestry estimation to generate markers for QTL analysis. In brief, using data from the Illumina backcross sequencing library (see File S4-1 for the number of reads per individual), we mapped reads to the assembled *D. elegans HK* and *D. gunungcola SK* parental genomes to estimate chromosome ancestry for each backcross individual. We generated 3,425 and 3,121 markers for the *D. elegans HK* and *D. gunungcola SK* backcrosses, respectively (Supplementary Files S4-3, S4-4), for QTL analysis.

QTL analysis

QTL analysis was performed using R/qtl (Broman *et al*., 2003) in R for Mac version 3.3.3 (R Core Team 2018) in a MacOS environment. Ancestry data for both backcross directions were imported into R/qtl using a custom script (https://github.com/dstern/read_cross_msg), which directly imports the conditional probability estimates by the Hidden Markov Model (HMM) of MSG (Andolfatto *et al*.,

2011) into R/qtl. We performed genome scans with a single QTL model using the "scanone" function of R/qtl and Haley-Knott regression (Haley and Knott, 1992) for "Wing spot size" and "Maximum wing display angle". Significance of QTL peaks at α = 0.01 was determined by performing 1000 permutations of the data. Effect sizes for each QTL peak were individually estimated by comparing the mean "Wing spot size" or "Maximum wing display angle" between individuals that inherited either *D. elegans HK* or *D. gunungcola SK* alleles at each QTL peak position. Since we detected multiple QTL peaks on separate chromosomes for "Maximum wing display angle", we tested for the presence of epistatic interactions using two methods: First, we performed a two-way ANOVA comparing the effect of each QTL peak in multiple QTL peak genetic backgrounds and found no evidence of an interaction (Figure 4-2F). Second, we performed genome-wide pairwise tests using the "scantwo" function of R/qtl and Haley-Knott regression to test for non-additive interactions across all markers and found no significant LOD scores for any marker pairs (Supplementary Figure S4-2, Supplementary Table S4-1; Supplementary Table S4-2).

Note, for several QTL peaks, we noticed that a significant proportion of the chromosome reached the LOD significance threshold even though the QTL peak intervals were much smaller. For example, the 95% Bayes credible interval (Broman and Sen , 2009) for the *D. elegans* backcross wing spot QTL on the X chromosome is only 435,676 bp even though the majority of the chromosome (~25 Mbp) climbs above the LOD threshold at 3.56. We attribute this pattern, in part, to low recombination frequencies in both backcross directions. On average, we detected only two crossover events genome-wide per fly (Supplementary Figure S4-3).

Annotating the wing spot QTL interval

To annotate genes within the ~440 Kbp fine-mapped wing spot locus (Figure 4-3B, we performed nucleotide BLAST (BLASTn) (Johnson *et al.*, 2008) searches against the *D. melanogaster* genome (taxid: 7227) using ~10 Kbp windows of assembled *D. elegans* chromosome regions spanning the QTL interval. Using the "GBrowse" tool on Flybase (Thurmond *et al.*, 2019), we mapped regions of microsynteny to identify the orientation

of each gene and exported the respective *D. melanogaster* coding region (CDS) FASTA sequence to align with the *D. elegans* X chromosome.

Generating X chromosome advanced recombinant introgressions

To isolate the QTL effects for "Wing spot size" and "Maximum wing display angle" localized to the X chromosome according to the *D. elegans HK* backcross experiment (Figure 4-2), F1 hybrid females were generated using the procedures described above. F1 hybrid females were then backcrossed towards *D. elegans HK*, and F2 backcross males lacking wing spots were isolated to measure "Maximum wing display angles" during courtship as described above. This procedure was repeated for seven generations to generate F3-F9 backcross individuals: F2 backcross females were backcrossed towards *D. elegans HK*, and F3 backcross males lacking wing spots were isolated to measure "Maximum wing display angles" (and so on to F9; Figure 4-4A). At each generation, an attempt was made to create stable introgression lines of advanced recombinant males lacking wing spots, but all failed to produce offspring, suggesting that *D. gunungcola SK* genomic regions on the X chromosome might also be linked to sterility factors. After seven generations of backcrossing, gDNA from all backcross males lacking wing spots was extracted and sequenced for MSG as described above. Backcross males lacking wing spots from F4-F9 were homozygous for *D. elegans HK* genomic regions across all autosomes but varied for the amount of *D. gunungcola SK* genome regions on the X chromosome (Supplementary Figure S4-4). Due to low levels of recombination (Supplementary Figure S4-3), however, the vast majority of introgressed individuals contained large 5-15 Mbp linked blocks of *D. gunungcola SK* X chromosome (Figure 4-4B).

Video capture of D. elegans and D. gunungcola in Indonesia

D. elegans is distributed across Southeast Asia, including Japan, Malaysia, Hong Kong, the Philippines, Taiwan, and Indonesia, often occupying Ipomoea or Brugmansia flowers. *D. gunungcola* is distributed throughout Indonesia in regions that partly overlap with *D. elegans* (Hirai and Kimura, 1997; Sultana *et al*., 1999; Ishii *et al*., 2002; Suwito *et al*., 2002). Using Canon VIXIA HF R500 camcorders mounted to Manfrotto (cat#

MKCOMPACTACN-BK) aluminum tripods, we captured videos of *D. elegans* and *D. gunungcola* courting conspecific females on *Ipomoea indica* and *Brugmansia candida* flowers at National Central University (Taoyuan City, Taiwan), Bumiaji (Indonesia), and Coban Rondo (Indonesia).

Statistics

Statistical tests were performed in R for Mac version 3.3.3 (R Core Team 2018) using Student's t-test (two-tailed) to test for statistically significant effects of pairwise comparisons of continuous data with normally distributed error terms. For tests comparing more than two groups, one-way ANOVAs were performed with post-hoc Tukey HSD for pairwise comparisons adjusted for multiple comparisons. See "QTL analysis" methods for statistical tests used during QTL mapping.

Results and Discussion

Evolution of loci on the X chromosome contributed to divergence in wing spots and wing display behavior

D. elegans males perform elaborate wing display dances in front of females during courtship, highlighting the presence of darkly pigmented wing spots (Figure 4-1A). Its sibling species, *D. gunungcola*, lost wing spots (Prud'homme *et al*., 2006) and lack the ability to perform wing displays (Figure 4-1A,B). Although these species diverged 2-2.8 Myr (Prud'homme *et al*., 2006), they are still capable of reproducing to form viable F1 hybrids in the lab (Yeh *et al*., 2006; Yeh and True, 2014). To compare the effects of evolution on the X chromosome to divergence in wing spots and wing display behavior, we quantified variation in wing spot size and wing display behavior between reciprocal F1 hybrid males, inheriting their X chromosome from either *D. elegans* or *D. gunungcola* mothers and autosomes from both species' parents. As previously reported (Yeh *et al*., 2006; Yeh and True, 2014), F1 hybrid males inheriting the X chromosome from *D. elegans* mothers (F1E) possessed wing spots (although smaller than *D. elegans*), while F1 hybrid males inheriting the X chromosome from *D. gunungcola* mothers (F1G) did not (Figure 4-1B,C). We also confirmed reports (Yeh *et al*., 2006; Yeh and True, 2014) of

differences in wing display behavior between F1E and F1G hybrids. While both F1 hybrids performed wing displays during courtship, F1G hybrid males performed much more variable wing displays (Figure 4-1B). Specifically, F1G hybrids failed to open their wings as widely as F1E hybrids during display performance (Figure 4-1B). We quantified variation in wing display behavior between F1 hybrids by measuring the maximum bilateral wing display angles (Figure 4-1B) during courtship (see Methods), finding that F1E hybrids performed wing displays similar to *D. elegans* males, while F1G males showed, on average, lower display angles (Figure 4-1C). Together these data confirm previous reports (Yeh *et al.*, 2006; Yeh and True, 2014) that evolution on the X chromosome contributed significantly to divergence in wing spot size and wing display behavior between *D. elegans* and *D. gunungcola.*

Evolution at a single locus explains the majority of wing spot divergence, but evolution at multiple, additive loci contributed to wing display divergence

To identify the location of loci contributing to divergence in wing spot size and wing display behavior on the X chromosome and autosomes, we quantified variation in both traits (Figure 4-2A,D) in hundreds of F2 backcross recombinant male flies and estimated genome-wide chromosome ancestry using MSG (Andolfatto *et al.*, 2011) for quantitative trait locus (QTL) mapping (Broman and Sen, 2009) . Scanning for single, additive QTL in the *D. elegans* backcross population, we identified highly significant QTL peaks on the X chromosome for both wing spot size and wing display behavior as predicted based on our comparisons between reciprocal F1 hybrids (Figure 4-2B,E; Table 4-1). Scanning for single, additive QTL in the *D. gunungcola* backcross population similarly revealed a highly significant QTL peak on the X chromosome for wing spot size but only a marginally significant QTL peak for wing display behavior (Figure 4-2B,E; Table 4-1). In both backcross directions, we identified a QTL peak on Muller Element B for wing display behavior and a peak on Muller Element E for the *D. gunungcola* backcross (Figure 4-2E; Table 4-1).

The X-linked QTL peak for wing spot size in both backcross directions explains almost all of the difference in wing spot size between *D. elegans* and *D. gunungcola* (Figure 4-

2C). QTL peaks for wing display behavior showed smaller effects (Figure 4-2F). Since we detected QTL peaks on separate chromosomes for wing display behavior in both backcross directions, we estimated the effect size of each to test for any possible epistatic interactions. In the *D. elegans* backcross, the effects from X chromosome and Muller Element B QTL peaks were approximately additive; that is, for the *D. elegans* backcross, we did not detect a significant interaction when comparing the effect of the X-linked QTL peak in either homozygous or heterozygous genetic backgrounds at the Muller Element B QTL peak (Figure 4-2F). Similarly, we did not detect significant interactions between QTL peaks at Muller Element B and E for the *D. gunungcola* backcross (Figure 4-2F). We also performed a two-dimensional genome scan (see Methods) in both backcross directions to test for genome-wide evidence of epistatic loci contributing to wing display divergence and found no significant interactions (Supplementary Figure S4-2; Supplementary Table S4-1; Supplementary Table S4-2). Thus, the wing display QTLs behave approximately additively in both backcrosses, while divergence in wing spot size is primarily controlled by a single major locus.

Some QTL peaks for wing display behavior were present in only one backcross direction (Figure 4-2E). This is likely a consequence of performing an F2 backcross rather than an F2 intercross to map QTL. For example, the peak on Muller Element E in the *D. gunungcola* backcross is likely caused by *D. gunungcola* recessive alleles that are detectable in only the *D. gunungcola* backcross. The absence of a large effect X chromosome QTL peak in the *D. gunungcola* backcross is less clear (Figure 4-2E). Although we did not detect evidence of epistatic loci contributing to wing display divergence in our two-dimensional genome scan (Supplementary Figure S4-2; Supplementary Table S4-1; Supplementary Table S4-2), it is possible that the presence of many small-effect *D. gunungcola* alleles in the *D. gunungcola* backcross masked the effect of the X chromosome. Our current sample size (N = 147) is likely too small to measure these effects. It is clear, however, that evolution at loci on multiple chromosomes contributed to wing display divergence between *D. elegans* and *D. gunungcola* (Figure 4-2E; ; Table 4-1).

The wing spot locus maps to a narrow 440 kb region containing omb

The interval estimates (Table 4-1) for the QTL peaks explaining wing spot size variation in both backcross directions mapped to a narrow region on the X chromosome. We aligned X chromosomes from recombinants with crossover positions immediately flanking the wing spot QTL peak to more closely compare the effect of this region on wing spot size (Figure 4-3A). Strikingly, the ~440 kbp wing spot locus seems to act like a switch, turning on or off the wing spot between recombinants varying in *D. elegans* and *D. gunungcola* alleles at this region (Figure 4-3A). To identify potential candidate genes contributing to this switch effect, we annotated the loci within this region (see Methods) and discovered it contains *omb* (Figure 4-3B), a T-box-containing transcription factor (Pflugfelder *et al*., 1992a; Pflugfelder *et al*., 1992b) previously implicated in pigmentation development (Thompson, 1959; Kopp and Duncan, 1997), pigmentation evolution (Brisson *et al*., 2004), and distal wing patterning (Grim and Pflugfelder, 1996). In *D. melanogaster*, gain- and loss-of-function *omb* alleles cause expansion and contraction of abdominal pigmentation bands, respectively (Kopp and Duncan, 1997). In *D. polymorpha*, variation in abdominal pigmentation patterning is strongly associated with polymorphisms at the *omb* locus (Brisson *et al*., 2004). *omb*, therefore, is the strongest candidate gene for wing spot divergence; however, we cannot presently rule out the other 14 genes mapped within this region.

Surprisingly, wing spot divergence did not map to *yellow*, a pigmentation candidate gene that was previously thought to contribute to wing spot divergence between *D. elegans* and *D. gunungcola* (Prud'homme *et al.*, 2006; reviewed in Massey and Wittkopp, 2016). Like *omb*, *yellow* has been implicated in pigmentation development (Geyer *et al.*, 1986; Geyer *et al*., 1987; Wittkopp *et al*., 2002a; Wittkopp *et al.*, 2002b) and evolution (Gompel *et al.*, 2005; Prud'homme *et al.*, 2006). Yellow protein expression prefigures wing spot patterning in multiple spotted *Drosophila* species (Wittkopp *et al*., 2002b; Gompel *et al*., 2005; Prud'homme *et al*., 2006). Using wing GFP reporter constructs in *D. melanogaster*, Prud'homme *et al.* (2006) mapped variation in wing GFP patterning to a few divergent nucleotides at the *D. elegans* and *D. gunungcola yellow* wing enhancer region, suggesting that *D. gunungcola* lost wing spots, at least in part, due to *cis*-

regulatory evolution at *yellow*. In *D. elegans, yellow* maps to 11.41 Mbp on the X chromosome, ~650 Kbp downstream of the fine-mapped wing spot region (Figure 4-3A). In two instances, recombinants that inherited the entire *D. gunungcola yellow* locus in physical linkage with the *D. elegans* wing spot region still possessed dark wing spots (Figure 4-3A). To test whether divergence in wing spot size alone, rather than wing spot presence, maps closer to *yellow*, we removed spotless recombinants from our analyses and found that the position of the QTL peak did not change for the *D. elegans* backcross (Supplementary Figure S4-4; Supplementary Table S4-3). For the *D. gunungcola* backcross, however, we discovered new QTL peaks on Muller Element C and E that explained variation in wing spot size, independent of wing spot presence (Supplementary Figure S4-4; Supplementary Table S4-3; Masset *et al*., in prep). These results suggest that recessive *D. gunungcola* alleles linked to Muller Element C and E contributed to wing spot size evolution (Massey *et al*., In prep). *cis*-regulatory evolution at *yellow*, however, likely did not play as significant a role in wing spot divergence between *D. elegans* and *D. gunungcola* as previously anticipated (Prud'homme *et al*., 2006).

Spotless advanced recombinants perform D. elegans-like wing display behavior

In the *D. elegans* backcross, QTL peaks explaining both wing spot size and wing display behavior co-localize on the X chromosome (Figure 4-2B,E). To disentangle whether this genetic correlation is a consequence of physical linkage between loci affecting each trait independently or a single, pleiotropic gene, we introgressed regions of the *D. gunungcola* X chromosome into a *D. elegans* genetic background through repeated backcrossing (Figure 4-4A, see Methods). At backcross generations F4-F9, we quantified maximum wing display angles for spotless recombinants and estimated genome-wide chromosome ancestry using MSG (Andolfatto *et al.*, 2011). By the third backcross, recombinants were only segregating for *D. elegans* and *D. gunungcola* alleles on the X chromosome and were homozygous for *D. elegans* autosomes (Supplementary Figure S4-5). Although we repeated backcrossing for eight generations, we recovered very few uniquely recombined X chromosomes. Instead, likely due to low levels of recombination (Supplementary Figure S4-3), the vast majority of spotless recombinants inherited similar 5-15 Mbp X chromosome haplotypes from *D. gunungcola* (Figure 4-4B). Still, one of these haplotypes

contained an estimated crossover position in between the *D. elegans* backcross wing display and wing spot QTL peaks, inheriting the *D. elegans* wing display QTL peak in physical linkage with the *D. gunungcola* QTL peak (Figure 4-4B). Unexpectedly, these, and all of the advanced backcross recombinants, performed wing displays indistinguishable from *D. elegans* wing display behavior (Figure 4-4B). That is, spotless recombinants performed maximum wing display angles as well as *D. elegans* whether or not they inherited *D. gunungcola* loci linked near the wing display QTL peak (Figure 4-4B). These results suggest that in the process of introgressing the wing spot QTL peak from *D. gunungcola* into an *D. elegans* genetic background, the effects of the X-linked wing display QTL were lost.

Why does introgressing the *D. gunungcola* wing spot locus into a *D. elegans* genetic background fail to cause correlated changes in wing display behavior? One possibility is that *D. gunungcola* loci linked to the Muller Element B QTL peak must be present in the same genetic background as *D. gunungcola* X-linked loci to detect effects on wing display behavior. In the *D. elegans* backcross, however, wing display QTL peaks localized to these chromosomes behaved approximately additively with each other, suggesting that each locus should affect wing display variation independent of the other (Figure 4-2F). Another possibility is that small effect *D. gunungcola* autosomal loci that we failed to detect in the F2 backcross experiment potentiate the X chromosome effect on wing display divergence. Alternatively, we might have failed to capture the true X-linked wing display locus in the process of introgression. Regardless, spotless advanced recombinants that inherited the X-linked *D. gunungcola* wing spot locus (and several Mbp of linked loci) performed maximum wing display angles indistinguishable from *D. elegans* (Figure 4-4B), suggesting that through either undetected epistatic interactions or physical linkage these correlated traits are separable.

D. gunungcola lacking wing spots perform wing displays in the wild

When *D. elegans* and *D. gunungcola* diverged 2-2.8 Myr (Prud'homme *et al.*, 2006), did wing spots or wing display behavior evolve first, or did they evolve simultaneously? That is, were wing spots and wing displays ever separated in nature? Since wing display

behavior likely diverged due to multiple loci (Figure 4-2E; Table 4-1), and wing spots due to a single major locus (Figure 4-2B; Table 4-1), we hypothesized that the evolution of wing display behavior likely took longer than the evolution of wing spots. Currently, only one *D. gunungcola* line exists in the laboratory (Sultana *et al*., 1999), and it does not perform any type of wing display during courtship (Figure 4-1A; Kopp and True, 2002; Yeh *et al*., 2006; Yeh and True, 2014), making it impossible to test this hypothesis with presently available stocks. To determine whether *D. gunungcola* populations in the wild are still segregating for wing spot or wing display variation, we isolated new lines from Indonesia and recorded videos of their courtship behavior on flowers (see Methods). *D. gunungcola* isolated at all field sites lacked wing spots (unpublished observation); however, we also observed for the first time *D. gunungcola* males performing wing displays towards conspecific females (Figure 4-5). Males approached females, initiating bilateral wing extensions during courtship, however, unlike *D. elegans* wing displays in the wild (Figure 4-5), *D. gunungcola* males did not turn their dorsal wing surfaces towards the female (Figure 4-5) and instead held their wings out flat similar to F1G courting males (Figure 4-1B). These are the first, to our knowledge, observations of *D. gunungcola* performing wing display behavior. These results suggest that loci affecting wing display variation are still segregating in natural *D. gunungcola* populations, while the genetic loss of wing spots appears to be fixed. Within these *D. gunungcola* populations, therefore, wing spot divergence preceded the loss of wing display behavior.

Conclusions

In the laboratory, *D. elegans* and *D. gunungcola* show divergent wing spot and wing display behavior (Figure 4-1A). QTL mapping identified a single major locus, including the *omb* gene, on the X chromosome that acts like a genetic switch controlling wing spot loss in *D. gunungcola* (Figure 4-3). Divergence in wing display behavior involved a major locus on the X chromosome but also multiple loci on the autosomes that behave approximately additively with each other (Figure 4-2E,F). Although the X-linked QTL regions for wing spots and wing display behavior co-localized, introgressing the wing spot locus from *D. gunungcola* into *D. elegans* did not cause a correlated change in wing display behavior (Figure 4-4). Different genetic mechanisms, therefore, likely caused

divergence in wing spots and wing display behavior between *D. elegans* and *D. gunungcola*: A single genetic switch mechanism controls wing spot loss in *D. gunungcola*, however, multiple loci (both on the X and autosomes) contributed to wing display divergence, and the X-linked *D. gunungcola* wing spot locus on its own is insufficient to cause wing display differences (Figure 4-4).

The precise mechanism underlying the genetic correlation linking wing spot and wing display divergence to the X chromosome remains unclear. Isolating the effects of the wing spot locus independent of the wing display region through introgression (Figure 4-4) suggests that physical linkage between X-linked genes is responsible for the genetic co-localization pattern. During introgression, for example, the causal wing display locus might have been lost due to recombination. This would suggest, contrary to the *D. elegans* backcross results (Table 4-1), that the causal wing display locus maps to a region downstream of 15 Mb, since the *D. gunungcola* introgression regions spanned ~0-15 Mb (Figure 4-4). Alternatively, divergence in wing spot and wing display might involve the same pleiotropic gene or tightly linked loci; while the *D. gunungcola* wing spot locus is sufficient to turn off the wing spot in *D. elegans*, the wing display locus may interact epistatically with *D. gunungcola* autosomal wing display loci that together reduce wing display angles. This would require that both loci are present in the same genetic background to affect wing display variation. Presently, our data do not support this hypothesis, given all wing display loci behaved approximately additively in the backcross experiments (Figure 4-2F; Supplementary Figure S2; Supplementary Table S-1; Supplementary Table S-2). Nevertheless, our current estimates of epistasis are likely significantly underpowered. Future studies aiming to fine-map the causal wing display locus, therefore, will likely only succeed if *D. gunungcola* autosomal loci (possibly linked to Muller Element B) are present in the same genetic background as the mapping population.

Wing spot and wing display divergence were previously described as being perfectly phylogenetically correlated in the Oriental *Drosophila melanogaster* species group (Kopp and True, 2002). Males in species that possess wing spots perform wing displays in front

of females during courtship, and males in species that lack wing spots do not. We mapped the genomic architecture of interspecific divergence for both traits between *D. elegans* and *D. gunungcola* to test whether or not these traits are genetically and phenotypically separable. We learned that both traits can be separated, possibly due to epistatic interactions between the X and autosomes. A complimentary approach to solving this problem is to ask whether both traits have ever been separated in natural populations. Surprisingly, we discovered that *D. gunungcola* populations in the wild are still segregating for components of wing display behavior yet appear to be fixed for the loss of wing spots (Figure 4-5). These observations suggest that *D. gunungcola* completely lost wing spots before they completely lost wing displays. Interestingly, however, wild *D. gunungcola* males do not perform wing displays as well as *D. elegans* (Figure 4-5). Males appear to lack the ability to turn their dorsal wing surfaces toward the female during wing displays, and wing waving behavior is much slower, resembling F1G hybrid courtship (Figure 4-1B). The components of wing display behavior that have diverged in natural *D. gunungcola* populations, therefore, are the actions that appear to make wing spots clearly visible during courtship. In future work, mapping how well males turn their dorsal wing surfaces during wing display within and between multiple *D. gunungcola* and *D. elegans* populations will likely help disentangle the genetic mechanisms underlying correlated divergence patterns between these species.

Acknowledgements

We thank members of the Wittkopp and Stern labs for helpful discussions. For fly strains, we thank John True. We also thank Shu-Dan Yeh for helpful discussions, advice about rearing *D. elegans* and *D. gunungcola*, for laying the groundwork to study both species in the wild, and for hosting J.H.M. in Taiwan and Indonesia. Funding: University of Michigan, Department of Ecology and Evolutionary Biology, Peter Olaus Okkelberg Research Award, National Institutes of Health (NIH) training grant T32GM007544, and Howard Hughes Medical Institute Janelia Graduate Research Fellowship to J.H.M.; NIH R01 GM089736 and 1R35GM118073 to PJW.

References

Andolfatto, P., Davison, D., Erezyilmaz, D., Hu, T. T., Mast, J., Sunayama-Morita, T., & Stern, D. L. (2011). Multiplexed shotgun genotyping for rapid and efficient genetic mapping. *Genome Research*, *21*(4), 610-617.

Bock, I. R., and Wheeler, M. R. (1972) The *Drosophila melanogaster* species group. University of Texas Publication 7213, 1–102.

Brisson, J. A., Templeton, A. R., & Duncan, I. (2004). Population genetics of the developmental gene *optomotor-blind* (*omb*) in *Drosophila polymorpha*: evidence for a role in abdominal pigmentation variation. *Genetics*, *168*(4), 1999-2010.

Broman KW, Wu H, Sen S, Churchill GA (2003) R/qtl: QTL mapping in experimental crosses. *Bioinformatics, 19*: 889–890.

Broman, K. W., & Sen, S. (2009). A Guide to QTL Mapping with R/qtl (Vol. 46). New York: Springer.

Cande, J., Andolfatto, P., Prud'homme, B., Stern, D. L., & Gompel, N. (2012). Evolution of multiple additive loci caused divergence between *Drosophila yakuba* and *D. santomea* in wing rowing during male courtship. *PLoS One*, *7*(8), e43888.

Charlesworth, D., & Charlesworth, B. (1976). Theoretical genetics of Batesian mimicry II. Evolution of supergenes. *Journal of Theoretical Biology*, *55*(2), 305-324.

Endler, J. A. (1991). Variation in the appearance of guppy color patterns to guppies and their predators under different visual conditions. *Vision Research*, *31*(3), 587-608.

Geyer, P. K., Spana, C., & Corces, V. G. (1986). On the molecular mechanism of gypsy-induced mutations at the *yellow* locus of *Drosophila melanogaster*. *The EMBO Journal*, *5*(10), 2657-2662.

Geyer, P. K., & Corces, V. G. (1987). Separate regulatory elements are responsible for the complex pattern of tissue-specific and developmental transcription of the *yellow* locus in *Drosophila melanogaster*. *Genes & Development*, *1*(9), 996-1004.

Gompel, N., Prud'homme, B., Wittkopp, P. J., Kassner, V. A., & Carroll, S. B. (2005). Chance caught on the wing: cis-regulatory evolution and the origin of pigment patterns in *Drosophila*. *Nature*, *433*(7025), 481.

Gray, S. M., & McKinnon, J. S. (2007). Linking color polymorphism maintenance and speciation. *Trends in Ecology & Evolution*, *22*(2), 71-79.

Grimm, S. and Pflugfelder, G. O. (1996). Control of the gene *optomotor-blind* in *Drosophila* wing development by *decapentaplegic* and *wingless*. *Science*, *271*,

1601-04.

Haley CS, Knott SA (1992). A simple regression method for mapping quantitative trait loci in line crosses using flanking markers. *Heredity, 69*: 315–324.

Hirai Y, Kimura MT (1997). Incipient reproductive isolation between two morphs of *Drosophila elegans* (Diptera: Drosophilidae). *Biol J Linn Soc, 61*: 501–513.

Ishii K, Hirai Y, Katagiri C, Kimura MT (2002). Mate discrimination and cuticular hydrocarbons in *Drosophila elegans* and *D. gunungcola*. *Zool Sci, 19*: 1191–1196.

Johnson, M., Zaretskaya, I., Raytselis, Y., Merezhuk, Y., McGinnis, S., & Madden, T. L. (2008). NCBI BLAST: a better web interface. Nucleic Acids Research, 36(suppl_2), W5-W9.

Kirkpatrick, M., & Barton, N. (2006). Chromosome inversions, local adaptation and speciation. *Genetics*, *173*(1), 419-434.

Kopp, A., & Duncan, I. (1997). Control of cell fate and polarity in the adult abdominal segments of *Drosophila* by *optomotor-blind*. *Development*, *124*(19), 3715-3726.

Kopp, A., & True, J. R. (2002). Evolution of male sexual characters in the oriental *Drosophila melanogaster* species group. *Evolution & Development*, *4*(4), 278-291.

Kronforst, M. R., Young, L. G., Kapan, D. D., McNeely, C., O'Neill, R. J., & Gilbert, L. E. (2006). Linkage of butterfly mate preference and wing color preference cue at the genomic location of wingless. *Proceedings of the National Academy of Sciences*, *103*(17), 6575-6580.

Küpper, C., Stocks, M., Risse, J. E., dos Remedios, N., Farrell, L. L., McRae, S. B., ... & Kitaysky, A. S. (2016). A supergene determines highly divergent male reproductive morphs in the ruff. *Nature Genetics*, *48*(1), 79.

Lamichhaney, S., Fan, G., Widemo, F., Gunnarsson, U., Thalmann, D. S., Hoeppner, M. P., ... & Chen, W. (2016). Structural genomic changes underlie alternative reproductive strategies in the ruff (Philomachus pugnax). *Nature Genetics*, *48*(1), 84.

Lindholm, A., & Breden, F. (2002). Sex chromosomes and sexual selection in poeciliid fishes. *The American Naturalist*, *160*(S6), S214-S224.

Loxton, R. G. (1979). On display behaviour and courtship in the praying mantis *Ephestiasula amoena* (Bolivar). *Zoological Journal of the Linnean Society*, *65*(1), 103-110.

Massey, J. H., & Wittkopp, P. J. (2016). The genetic basis of pigmentation differences within and between *Drosophila* species. In Current topics in developmental biology (Vol. 119, pp. 27-61). Academic Press.

McKinnon, J. S., & Pierotti, M. E. (2010). Colour polymorphism and correlated characters: genetic mechanisms and evolution. *Molecular Ecology, 19*(23), 5101-5125.

Merrill, R. M., Rastas, P., Martin, S. H., Melo, M. C., Barker, S., Davey, J., ... & Jiggins, C. D. (2019). Genetic dissection of assortative mating behavior. *PLoS Biology*, 17(2), e2005902.

Paaby, A. B., & Rockman, M. V. (2013). The many faces of pleiotropy. *Trends in Genetics, 29*(2), 66-73.

Petrie, M., Tim, H., & Carolyn, S. (1991). Peahens prefer peacocks with elaborate trains. *Animal Behaviour, 41*(2), 323-331.

Petrie, M., & Halliday, T. (1994). Experimental and natural changes in the peacock's (*Pavo cristatus*) train can affect mating success. *Behavioral Ecology and Sociobiology, 35*(3), 213-217.

Pflugfelder, G. O., Roth, H. and Poeck, B. (1992a). A homology domain shared between *Drosophila optomotor-blind* and mouse Brachyury is involved in DNA binding. *Biochem. Biophys. Res. Comm*., *186*, 918-25.

Pflugfelder, G. O., Roth, H., Poeck, B., Kersher, S., Schwarz, H., Jonschker, B. and Heisenberg, M. (1992b). The lethal (1) *optomotor-blind* gene of *Drosophila melanogaster* is a major organizer of optic lobe development: Isolation and characterization of the gene. *Proc. Nat. Acad. Sci*., *89*, 1199-1203.

Picelli, S., Björklund, Å. K., Reinius, B., Sagasser, S., Winberg, G., & Sandberg, R. (2014). Tn5 transposase and tagmentation procedures for massively scaled sequencing projects. *Genome Research, 24*(12), 2033-2040.

Prud'Homme, B., Gompel, N., Rokas, A., Kassner, V. A., Williams, T. M., Yeh, S. D., ... & Carroll, S. B. (2006). Repeated morphological evolution through cis-regulatory changes in a pleiotropic gene. *Nature, 440*(7087), 1050-1053.

R Core Team. 2013. R: A Language and Environment for Statistical Computing. Available from: http://www.r-project.org/.

Simon, J. C., & Dickinson, M. H. (2010). A new chamber for studying the behavior of *Drosophila*. *Plos One*, 5(1), e8793.

Sinervo, B., Miles, D. B., Frankino, W. A., Klukowski, M., & DeNardo, D. F. (2000). Testosterone, endurance, and Darwinian fitness: natural and sexual selection on the physiological bases of alternative male behaviors in side-blotched lizards. *Hormones and Behavior*, *38*(4), 222-233.

Sultana, F., Kimura, M. T., & Toda, M. J. (1999). Anthophilic *Drosophila* of the *elegans* species-subgroup from Indonesia, with description of a new species (Diptera: Drosophilidae). *Entomological Science, 2*, 121-126.

Suwito A, Ishida TA, Hattori K, Kimura MT (2002). Environmental adaptations of two flower breeding species of *Drosophila* from Java, Indonesia. *Entomol Sci*, 5: 399–406.

Takahashi, M., Arita, H., Hiraiwa-Hasegawa, M., & Hasegawa, T. (2008). Peahens do not prefer peacocks with more elaborate trains. *Animal Behaviour, 75*(4), 1209-1219.

Thomas, J. W., Cáceres, M., Lowman, J. J., Morehouse, C. B., Short, M. E., Baldwin, E. L., ... & Martin, C. L. (2008). The chromosomal polymorphism linked to variation in social behavior in the white-throated sparrow (*Zonotrichia albicollis*) is a complex rearrangement and suppressor of recombination. *Genetics*, *179*(3), 1455-1468.

Thompson, P. E. (1959). Drosophila. Info. Service 33, 99

Thurmond, J., Goodman, J. L., Strelets, V. B., Attrill, H., Gramates, L. S., Marygold, S. J., ... & Kaufman, T. C. (2018). FlyBase 2.0: the next generation. *Nucleic Acids Research*, *47*(D1), D759-D765.

White, T. E., Zeil, J., & Kemp, D. J. (2015). Signal design and courtship presentation coincide for highly biased delivery of an iridescent butterfly mating signal. *Evolution*, *69*(1), 14-25.

Wittkopp, P. J., Vaccaro, K., & Carroll, S. B. (2002a). Evolution of *yellow* gene regulation and pigmentation in *Drosophila*. *Current Biology*, *12*(18), 1547-1556.

Wittkopp, P. J., True, J. R., & Carroll, S. B. (2002). Reciprocal functions of the Drosophila *yellow* and *ebony* proteins in the development and evolution of pigment patterns. *Development*, *129*(8), 1849-1858.

Yeh, S. D., Liou, S. R., & True, J. R. (2006). Genetics of divergence in male wing pigmentation and courtship behavior between Drosophila elegans and D. gunungcola. Heredity, 96(5), 383.

Yeh, S. D., & True, J. R. (2014). The genetic architecture of coordinately evolving male wing pigmentation and courtship behavior in Drosophila elegans and Drosophila

gunungcola. G3: Genes, Genomes, Genetics, 4(11), 2079-2093.

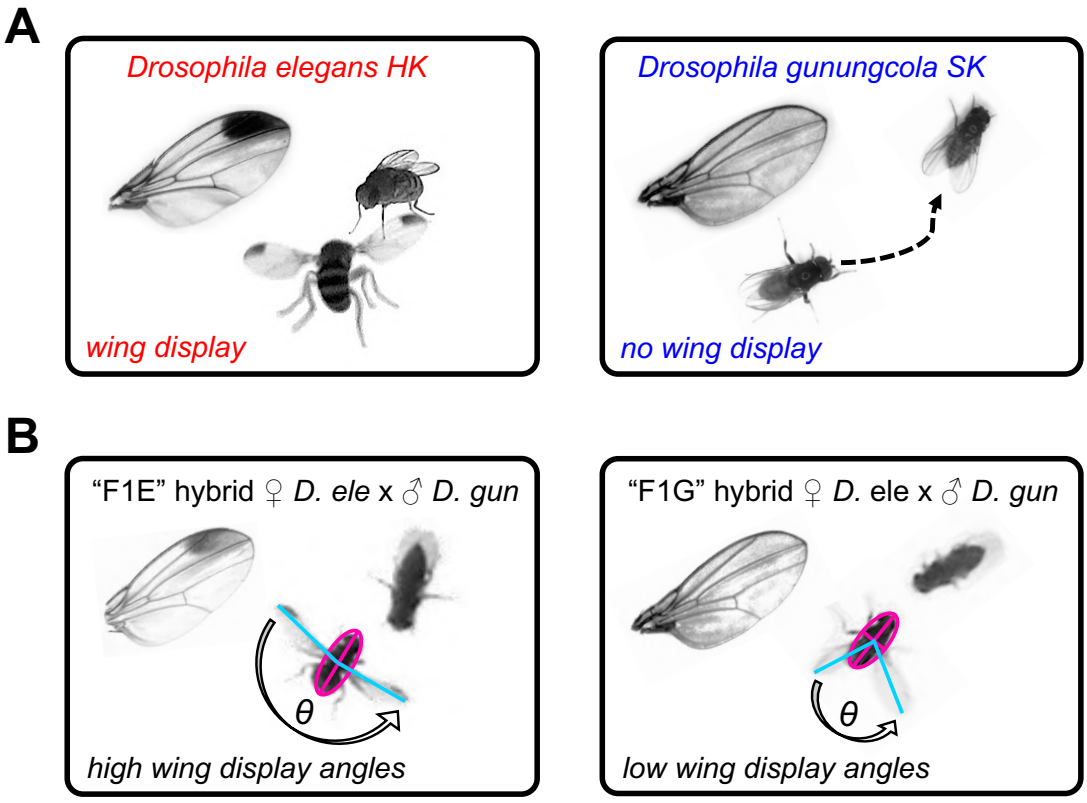
A
Drosophila elegans HK
wing display
Drosophila gunungcola SK
no wing display
B
"F1E" hybrid ♀ D. ele x ♂ D. gun
θ
high wing display angles
"F1G" hybrid ♀ D. ele x ♂ D. gun
θ
low wing display angles

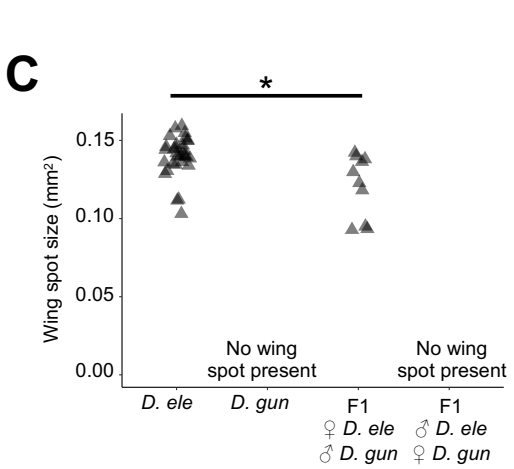
C
*
Wing spot size (mm²)
0.15
0.10
0.05
0.00
No wing spot present
No wing spot present
D. ele
D. gun
F1 ♀ D. ele ♂ D. gun
F1 ♂ D. ele ♀ D. gun

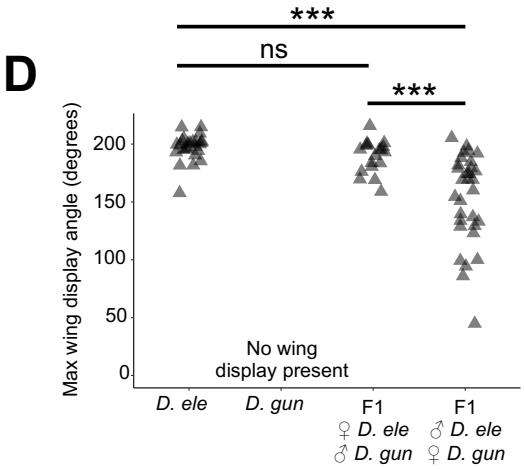
D
***
ns
***
Max wing display angle (degrees)
200
150
100
50
0
No wing display present
D. ele
D. gun
F1 ♀ D. ele ♂ D. gun
F1 ♂ D. ele ♀ D. gun

Figure 4-1 Wing pigmentation and wing display behavior in *D. elegans*, *D. gunungcola*, and F1 hybrids

(A) Males in *D. elegans* (left) possess wing spots and perform bilateral wing display behaviors in front of females during courtship (VIDEO). Males in *D. gunungcola* (right) lost wing spots (Prud'homme and Gompel *et al*., 2006) and do not perform wing displays (VIDEO). (B) F1 hybrid males inheriting their X chromosome from *D. elegans* mothers (F1E, left) possess wing spots and perform wing display behavior like *D. elegans* (VIDEO). F1 hybrid males inheriting their X chromosome from *D. gunungcola* mothers (F1G, right) are spotless and perform wing displays with low bilateral wing angles (VIDEO). (C) Quantification of wing spot size (see Methods) in male *D. elegans* and F1E. Wing spots are slightly larger in *D. elegans* than F1E (Student's t-test; $t = -2.8057$; $df = 11.43$; $p = 0.017$; two-tailed). (D) Quantification of maximum bilateral wing display angles during courtship (see Methods) in male *D. elegans* and F1 hybrids. F1G hybrids showed lower maximum wing display angles than *D. elegans* and F1E hybrids (One-way ANOVA: $F_{2,71} = 20.92$; $p < 7.18 \times 10^{-8}$; post-hoc Tukey HSD was significant between *D. elegans* and F1G: $p < 2.0 \times 10^{-7}$ and between F1E and F1G: $p < 7.1 \times 10^{-5}$). Gray triangles represent individual replicates. * $P < 0.05$, *** $P < 0.001$.

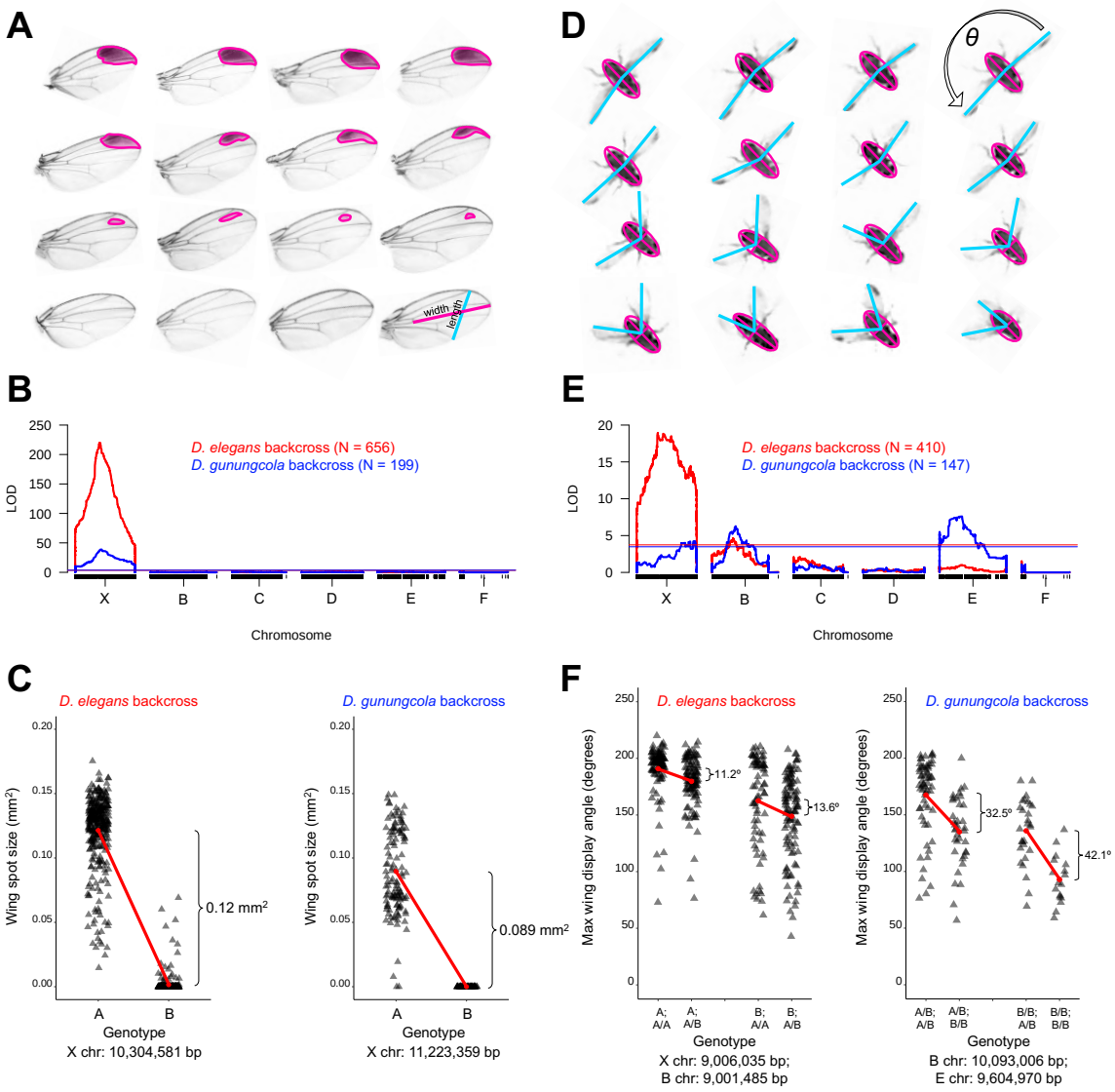
A
width
length
D
θ
B
D. elegans backcross (N = 656)
D. gunungcola backcross (N = 199)
LOD
250
200
150
100
50
0
X
B
C
D
E
F
Chromosome
E
D. elegans backcross (N = 410)
D. gunungcola backcross (N = 147)
LOD
20
15
10
5
0
X
B
C
D
E
F
Chromosome
C
D. elegans backcross
Wing spot size (mm²)
0.20
0.15
0.10
0.05
0.00
0.12 mm²
A
B
Genotype
X chr: 10,304,581 bp
D. gunungcola backcross
Wing spot size (mm²)
0.20
0.15
0.10
0.05
0.00
0.089 mm²
A
B
Genotype
X chr: 11,223,359 bp
F
D. elegans backcross
Max wing display angle (degrees)
250
200
150
100
50
0
11.2°
13.6°
A; A/A
A; A/B
B; A/A
B; A/B
Genotype
X chr: 9,006,035 bp;
B chr: 9,001,485 bp
D. gunungcola backcross
Max wing display angle (degrees)
250
200
150
100
50
0
32.5°
42.1°
A/B; A/B
A/B; B/B
B/B; A/B
B/B; B/B
Genotype
B chr: 10,093,006 bp;
E chr: 9,604,970 bp

Figure 4-2 QTL analysis and effect plots for wing pigmentation and wing display behavior in *D. elegans* and *D. gunungcola* backcross males

(A) Wing spots vary in size and shape in *D. elegans* and *D. gunungcola* backcross recombinants. Wing spots were traced (pink) and quantified relative to proxies for total wing area (length x width) using ImageJ (VERSION) software (see Methods). (B) Wing pigmentation QTL map for the *D. elegans* (red) and *D. gunungcola* (blue) backcross. LOD (logarithm of the odds) is indicated on the y-axis. The x-axis represents the physical map of Muller Elements X, B, C, D, E, and F based on the *D. elegans* assembled genome. Individual SNP markers are indicated with black tick marks along the x-axis. Horizontal red and blue lines mark p = 0.01 for the *D. elegans* and *D. gunungcola* backcross, respectively. (C) Effect plots for the X chromosome QTL peak from the *D. elegans* backcross (left) and *D. gunungcola* backcross (right). (D) Maximum wing display angles varied in *D. elegans* and *D. gunungcola* backcross recombinants. Maximum wing display angles were quantified by measuring the angle between each wing tip using ImageJ (VERSION) software (see Methods). (E) Maximum wing display QTL map for the *D. elegans* (red) and *D. gunungcola* (blue) backcross. LOD is indicated on the y-axis. The x-axis represents the physical map of Muller Elements X, B, C, D, E, and F based on the *D. elegans* assembled genome. Individual SNP markers are indicated with black tick marks along the x-axis. Horizontal red and blue lines mark p = 0.01 for the *D. elegans* and *D. gunungcola* backcross, respectively. (F) Effect plots for the X chromosome and Muller Element B QTL peaks from the *D. elegans* backcross (left) and for the Muller Element B and E QTL peaks from the *D. gunungcola* backcross (right). No epistatic interaction was detected comparing the combined effects of each QTL peak on maximum wing display angle (see Methods) (Two-way ANOVA: $F_{1,402} = 0.146$; p = 0.70 for the *D. elegans* backcross; Two-way ANOVA: $F_{1,141} = 0.875$; p = 0.35 for the *D. gunungcola* backcross). Gray triangles represent individual replicates.

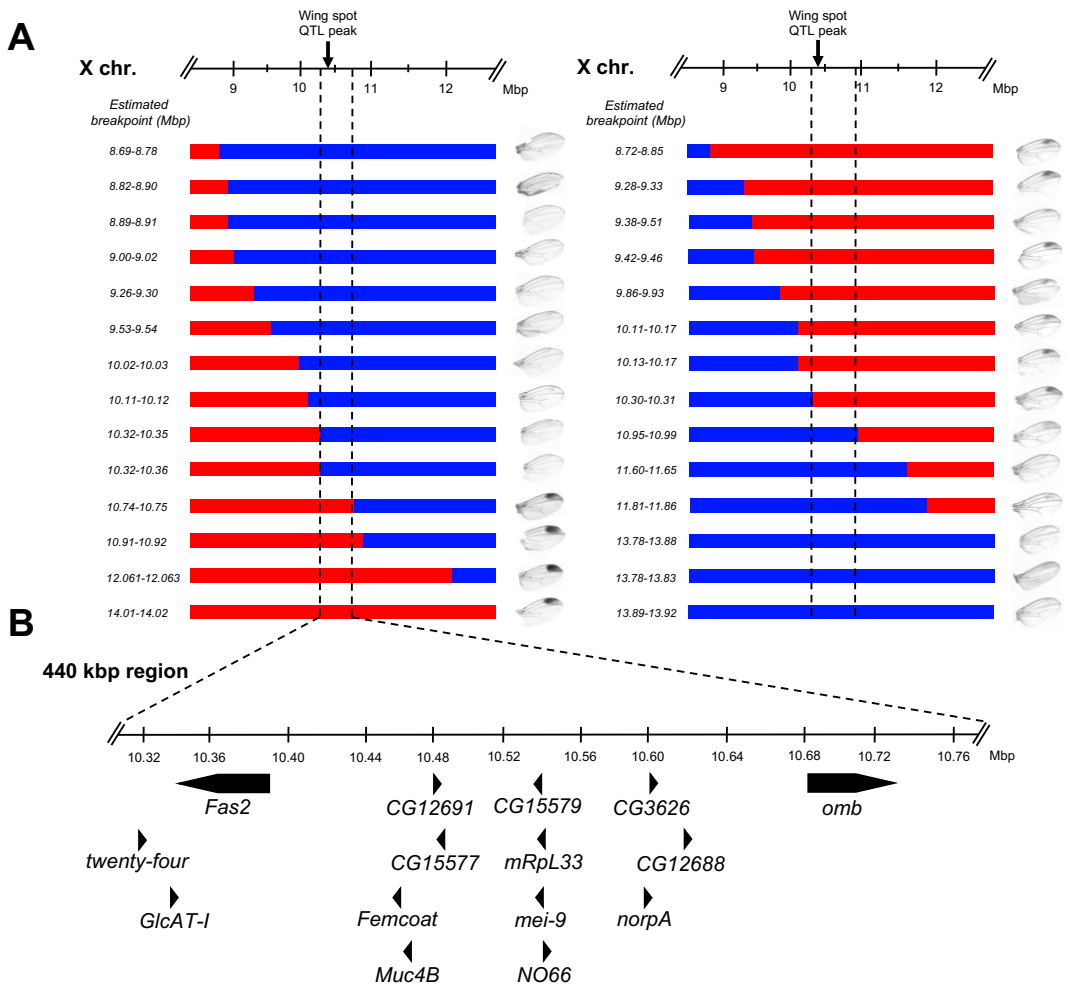

Figure 4-3 Fine-mapping the wing spot locus

(A) *D. elegans* and *D. gunungcola* backcross recombinants containing X chromosome breakpoints immediately flanking the wing spot QTL peak were aligned to compare the effects of each on wing pigmentation. Regions in red represent *D. elegans* linked loci, and regions in blue represent *D. gunungcola* linked loci. Recombinants possessing *D. elegans* loci to the left of ~10.32 Mbp (left panel) are spotless, while recombinants possessing *D. elegans* loci to the right of ~10.74 Mbp (left panel) possess dark wing spots. Similarly, recombinants possessing *D. gunungcola* loci to the right of ~10.95 Mbp (right panel) are spotless. The effect of the fine-mapped wing spot locus between ~10.32 and ~10.74 Mbp seems to act like a switch, turning on or off wing pigmentation. (B) Two recombinants define the wing spot locus to a ~440 Kbp region containing 15 candidate genes. *omb* is the strongest wing pigmentation candidate gene given evidence from prior work (see Results and Discussion).

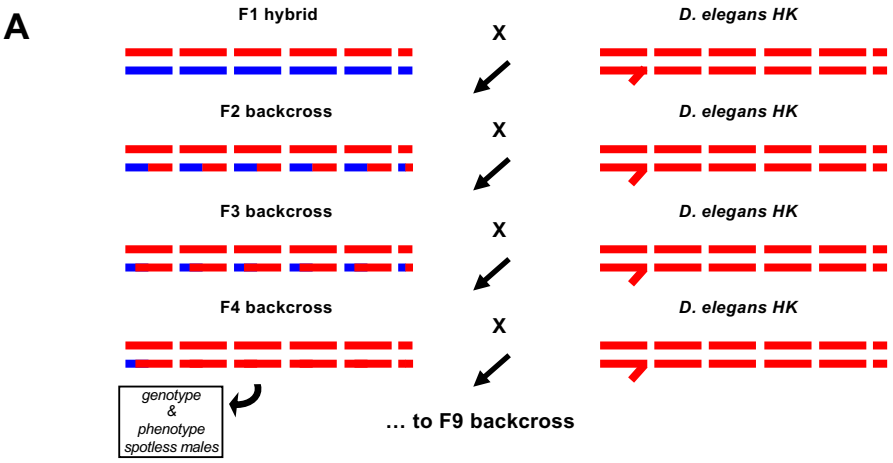
A
F1 hybrid
X
D. elegans HK
F2 backcross
X
D. elegans HK
F3 backcross
X
D. elegans HK
F4 backcross
X
D. elegans HK
genotype & phenotype spotless males
... to F9 backcross

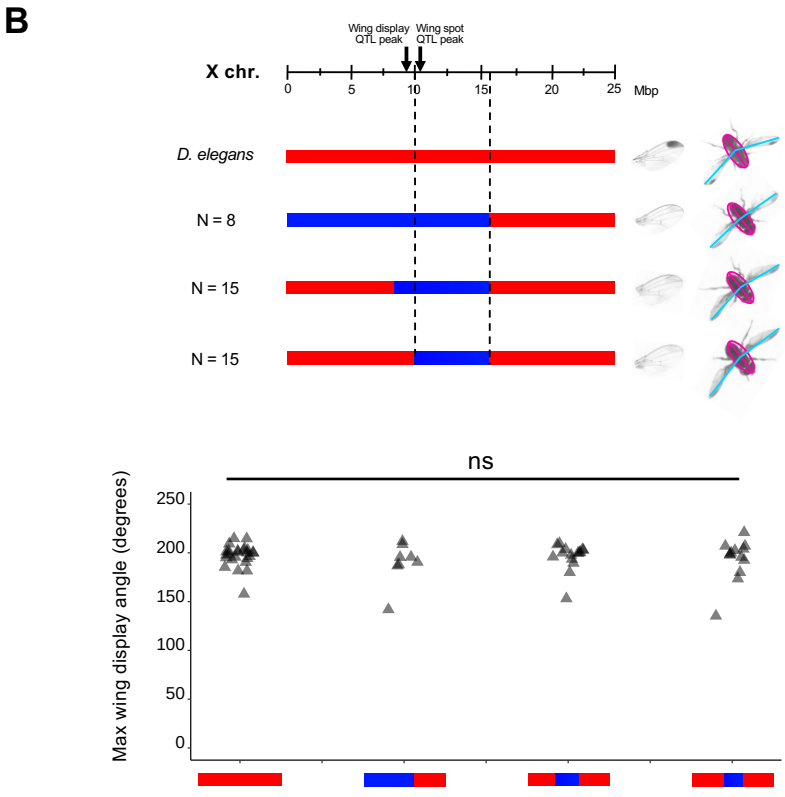
B
Wing display QTL peak
Wing spot QTL peak
X chr.
0
5
10
15
20
25
Mbp
D. elegans
N = 8
N = 15
N = 15
ns
Max wing display angle (degrees)
250
200
150
100
50
0

Figure 4-4 Introgression-mapping the X-linked wing spot and wing display loci

(A) Schematic illustrating the crossing procedure used to generate advanced recombinant introgressions (see Methods). Briefly, hybrid females (*D. elegans* genome in red, *D. gunungcola* genome in blue) were repeatedly backcrossed towards *D. elegans* males to generate F2-F9 advanced recombinant males. At backcross generations F4-F9, males lacking wing spots were placed in courtship assays with virgin *D. elegans* females (see Methods) to quantify maximum wing display angles and then genotyped via MSG (Andolfatto *et al*., 2011). By the third backcross generation, advanced recombinants were only segregating for different species alleles on the X chromosome and were homozygous *D. elegans* on the autosomes (FIGURE). (B, Top panel) Due to low levels of recombination (FIGURE), replicates of only three unique introgression haplotypes were recovered. None of the haplotypes possessed dark wing spots (although a light wing spot "shadow" is visible, perhaps due to phenol oxidase expression in the wing spot region) as a consequence of inheriting *D. gunungcola* loci (blue) linked to the wing spot QTL peak. (B, Bottom panel) Quantification of max wing display angles from the haplotypes in the top panel. Max wing display angles for each haplotype were not different than *D. elegans* males (One-way ANOVA: $F_{3,57} = 0.451$; $p = 0.72$). Gray triangles represent individual replicates. n.s., not significant.

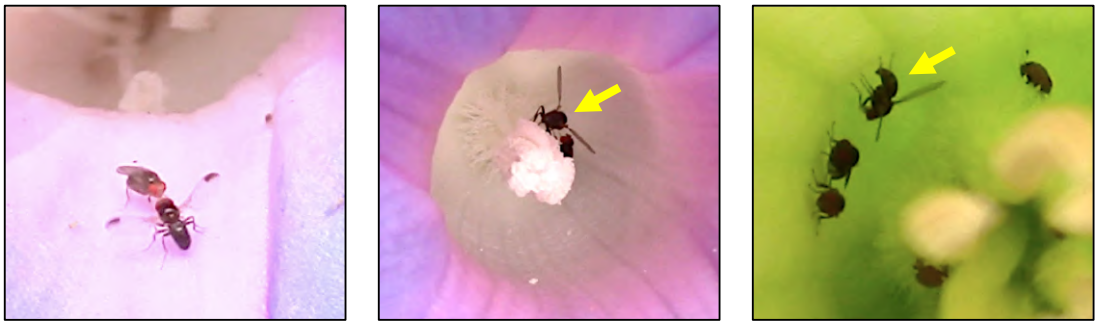

D. elegans *D. gunungcola* *D. gunungcola*

Figure 4-5 *D. gunungcola* perform a type of wing display on flowers in the wild

Both male *D. elegans* (left) and male *D. gunungcola* (middle and right) perform a type of wing display behavior towards females on *Ipomoea indica* (left, middle) and *Brugmansia candida* (right) flowers in Taiwan (*D. elegans*) and Indonesia (*D. gunungcola*). *D. gunungcola* males completely lack wing spots, and their wing displays are slower and have lower angles (wings were extended out flat at ~180º) than *D. elegans.*

Trait	Backcross	Chromosome	QTL interval (bp)[a]	QTL peak (bp)	LOD
Wing spot size	*D. elegans*	X	10,297,836-10,744,020	10,304,581	220
Max wing display angle	*D. elegans*	X	8,729,737-15,691,924	9,006,035	18.9
Max wing display angle	*D. elegans*	B	5,773,911-13,325,000	9,001,485	4.66
Wing spot size	*D. gunungcola*	X	10,474,499-11,584,862	11,223,359	38.9
Max wing display angle	*D. gunungcola*	X	16,885,658-25,539,528	24,196,217	4.23
Max wing display angle	*D. gunungcola*	B	7,078,659-12,180,268	10,093,006	6.28
Max wing display angle	*D. gunungcola*	E	3,813,413-11,535,144	9,604,970	7.59

[a] LOD drop 1.5 support interval

Table 0-1 QTLs detected for wing spot size and maximum wing display angle divergence

Chapter 5

Discussion and Future Directions

As facts accumulated it became evident that each gene produces not a single effect, but in some cases a multitude of effects on the characters of the individual.

-Thomas Hunt Morgan, 1935

Several results summarized in this thesis were unexpected. First, dissecting the effects of the *yellow* gene on male mating success revealed a previously unrecognized function for melanin in *Drosophila* reproductive behavior; second, quantifying the effects of *ebony* and *tan* knockout alleles on cuticular hydrocarbon (CHC) composition demonstrated a new function for pigmentation genes in lipid synthesis; and third, performing unbiased, high-resolution quantitative trait locus (QTL) mapping in interspecific hybrids identified new genes involved in pigmentation evolution and new mechanisms associated with behavioral evolution. All together, this thesis provides novel, causal evidence describing how gene pleiotropy manifests through the action of pigmentation enzymes to coordinate behavior and anatomy and how the genome evolves to generate species differences in these traits. Conclusions from each chapter compel multiple, future directions.

What a single mutation teaches us about behavior and evolution

For decades, pigmentation mutants in plants and animals have served developmental and evolutionary biologists as clear examples of how genotypes connect to phenotypes (Bateson, 1903; Bridges and Morgan, 1923; Wright, 1987; Jackson *et al*., 1994; Wittkopp *et al*., 2002; Wittkopp *et al*., 2003; Lin and Fisher, 2007; Hubbard *et al*., 2010). What has

remained a puzzle is how mutations affecting pigmentation act pleiotropically to disrupt behavior patterns (Takahashi, 2013). In chapter two, I set out to solve one of these mysteries by applying sophisticated genetic tools in *Drosophila melanogaster* to a classic problem: How and why do *yellow* mutant males mate less successfully than wild-type flies? My results for this chapter are clear and unexpected: *yellow* flies mate poorly because they lack melanin in a structure that is required to grasp females for mating success. These results illustrate not only how a single gene mutation disrupts fly reproduction, but also why males possess sex combs.

Melanized appendages are ubiquitous in nature. From insect legs to bird talons to bear claws, animal species repeatedly rely on melanized structures to hunt food and capture mates. While the shapes of these structures and the behaviors that use them evolve rapidly (Emlen *et al.*, 2005; Bush and Hu, 2006; Fowler *et al.*, 2009; Kopp, 2011), their melanization state appears relatively conserved. Natural and sexual selection, therefore, likely filter out mutations that disrupt melanin synthesis in appendages used for foraging and reproduction, but mutations that change their shape and how they are used might be favored in certain environments. In *Drosophila*, for example, mutations causing within and between species differences in pigmentation are restricted to tissue-specific *cis*-regulatory regions of genes important for pigmentation development (Massey and Wittkopp, 2016). Previously, it has been hypothesized that this pattern was a consequence of pigmentation gene pleiotropy (Wittkopp and Beldade, 2009; Takahashi, 2013): Pigmentation enzymes also affect biogenic amine metabolism and brain function, so mutations affecting protein coding regions are likely deleterious. Results from chapter two, however, imply that Yellow protein evolution is more likely constrained due to its specific contribution in melanizing a secondary sexual structure. In fact, there is little evidence that Yellow functions in the fly brain at all (but see Drapeau *et al.*, 2003). Taken together, these data suggest that mutations impacting structural evolution can directly lead to behavioral differences, independent of the nervous system.

Recently, Matsuoka and Monteiro (2018) discovered that mutations disrupting pigmentation synthesis in the butterfly wing also altered wing scale morphology.

Similarly, in barn owls and snakes, changes in feather and scale pigmentation, respectively, are correlated with changes in structure (Roulin *et al*., 2013; Spinner *et al*., 2013). The behavioral role of animal color pattern evolution has often been discussed in the framework of mating signals and camouflage (Cuthill *et al*., 2017), but application of scanning electron microscopy (SEM) and high-speed photography suggest that pigmentation-dependent structural changes themselves might influence how birds fly and snakes slither. In some cases, then, interactions between a species' abiotic environment (e.g., wind speed or surface roughness) could be the primary force shaping color pattern evolution rather than sexual/social selection by mates or competitors. Swimming performance assays in water striders, for example, illustrate how anatomical evolution influences ecologically-relevant behavioral variation: Water striders possessing leg fans due to expression of a single gene swim more quickly upstream than water striders without fans (Santos *et al*., 2017). These results again highlight the importance of characterizing the behavioral consequences of genes controlling structural evolution.

The precise mechanism that links gene function to phenotypic development and evolution is understood for only a few genes in a few organisms (e.g., Hoekstra *et al*., 2006; Barrett *et al*., 2008; Frankel *et al*., 2011). It will remain difficult to describe why we see certain patterns of molecular evolution without this information. It will also remain difficult to understand the ecological purpose of certain phenotypes. In the case of the *yellow* gene, characterizing the behavioral consequences of a single loss-of-function mutation revealed both how *yellow* functions in behavior and why flies possess sex combs. While we were searching in the fly brain for clues, the genetic data led us to an unexpected result, teaching us something new about the biology of the fly. But, the *yellow* mutation taught us another lesson: The details connecting genes and mutations to fitness matter; they help explain the reason phenotypes are evolving (or not) in the first place.

Cuticle structure and function: Consequences of pigmentation gene pleiotropy

The reason *yellow* mutants were ever implicated in behavior was because an undergraduate student named Alfred Sturtevant carefully observed their abnormal mating patterns in fly bottles (Sturtevant, 1915). But, genes function in phenotypic development and evolution in numerous unobservable ways. Insects, for example, primarily communicate through chemical signaling (Blomquist and Bagnères, 2010). Sex, mating status, developmental stage, and behavioral state are all communicated through chemical pheromones in many fly, butterfly, and bee species (Blomquist and Bagnères, 2010). In *Drosophila*, pheromones are derived from lipid metabolism just beneath the cuticle that requires, in part, the function of Desaturase enzymes in specialized secretory cells called oenocytes along the abdomen (Makki *et al*., 2014). Lipids in the form of short- and long-chain hydrocarbons are secreted into the hardening cuticle after eclosion, coating the fly body in a complex mixture of compounds that elicit behavioral responses in hetero- and conspecifics (Billeter *et al.*, 2009). In chapter three, I hypothesized that pigmentation enzymes, which are also secreted into the developing cuticle, might interact with lipid metabolism and pheromone production as a consequence of changes in the cuticle structure post eclosion. Surprisingly, we discovered that flies inheriting loss-of-function mutations in the enzymes Ebony and Tan showed reciprocal effects on short- versus long-chain cuticular hydrocarbon (CHC) abundance, suggesting that pigmentation and CHC synthesis might interact in the developing insect cuticle. Subsequent experiments also revealed that natural variation in *ebony* and *tan* expression co-varied with CHC synthesis in directions predicted by the mutants.

As in chapter two, results from chapter three suggest that structural changes themselves can change animal behavior. For example, in *D. melanogaster*, we observed significantly elevated levels of 7,11-heptacosadiene [a female derived pheromone important in species recognition (Billeter *et al.*, 2009)] in *ebony* mutants and significantly decreased levels in *tan* mutants. Although we did not perform behavioral assays in these experiments, we speculate that changes in pigmentation intensity across the fly body could influence how well hetero- and conspecific animals perceive pheromone signals in nature. Since 7,11-heptacosadiene often inhibits courtship from species that do not synthesize it (Billeter *et al*., 2009), for example, flies evolving lighter body pigmentation as a consequence of

ebony expression might be harassed more often by heterospecific males due to pleiotropic changes in CHC production. Future experiments could test these hypotheses by quantifying social interactions among hetero- and conspecific flies varying in body pigmentation and 7,11-heptacosadiene abundance.

Pigmentation genes have also been implicated in vertebrate pheromone production. In mice, pleiotropic effects of alpha-melanocyte-stimulating hormone (α-MSH) stimulate both pigmentation and aggressive behaviors (Cone *et al.*, 1996; Morgan *et al*., 2004a,b). α-MSH signaling at melanocortin receptor 1 (MC1R) in the epidermis promotes pigmentation, while signaling at MC5R in the preputial gland promotes aggression (Cone *et al.*, 1996; Morgan *et al*., 2004a,b). Surprisingly, the mechanism that links α-MSH signaling to aggression is by stimulating the release of an aggression-promoting pheromone in male urine via MC5R (Morgan *et al*., 2004a,b). α-MSH acts pleiotropically on pigmentation and pheromone production, because it is capable of binding multiple receptors with tissue-specific expression patterns and physiological functions (Cone *et al*., 1996). It is possible that Ebony and Tan behave similarly. Rather than changing the structure of the cuticle, Ebony and Tan might instead influence CHC production through physiological changes. Since both enzymes participate in dopamine metabolism, for example, their effects on pigmentation and CHC synthesis might stem from changes in circulating dopamine levels in the hemolymph. Future studies should focus on dissecting how dopamine, Ebony, and Tan participate in lipid synthesis.

The pleiotropic impact of pigmentation genes in invertebrate and vertebrates is likely larger in magnitude than previously anticipated. Is this because pigmentation synthesis affects numerous other traits, or is it because pigmentation genes are also pheromone and behavior genes? In the case of α-MSH and its five receptors, the answer seems to be the latter, since α-MSH can affect multiple phenotypes by activating receptors in varied tissues. For Ebony and Tan, it is hard to say. Distinguishing between these two scenarios is important, however, because each implies different genetic and phenotypic modes for how behavior and pigmentation evolve. Mutations in the protein coding region of MC1R, for example, have repeatedly caused pigmentation to evolve but not behavior (Martin and

Orgogozo, 2013). Why is MC1R a hotspot for pigmentation evolution but not its ligand α-MSH? This is likely because α-MSH is capable of binding five different receptors in vertebrates, whereas the phenotypic effects of MC1R activation are restricted to the melanocytes (Cone *et al*., 1996). Mutations affecting α-MSH function must coordinate with numerous downstream processes. In humans, for example, loss-of-function mutations in the pre–pro–opiomelanocortin (POMC) gene, which generates α-MSH, causes a range of phenotypic effects from red hair color to obesity to adrenal insufficiency (Krude *et al*., 1998). These data suggest that protein coding changes at MC1R are repeatedly permissible because MC1R expression is restricted to a subset of α-MSH-positive tissue. As discussed above, protein coding changes at Ebony, Tan, and Yellow have never been implicated in pigmentation evolution in *Drosophila,* but there are numerous instances of tissue-specific, *cis*-regulatory changes affecting pigmentation at these genes (Massey *et al*., 2016). The biochemical function of Ebony, Tan, and Yellow likely restrict the position of new mutations influencing pigmentation evolution to non-coding regions of DNA. Unlike α-MSH, these enzymes do not rely on receptors expressed in pigmentation-specific cells to carry out their function. Instead, their synthesized products (dopamine derivatives) participate directly in pigmenting the cuticle (Wright 1987). As illustrated in chapters one and two, mutations disrupting their coding sequence impact phenotypes important in reproduction. Gene pleiotropy, therefore, manifests in different ways in different taxa depending on the function of the gene in question, which in turn influences how mutations can shape their contribution to phenotypic evolution.

How behavioral and anatomical divergence map onto the genome

While chapters two and three focused on the specific effects of single-gene loss-of-function mutations in behavior and anatomy, chapter four investigated how the genome more generally organizes phenotypic evolution at these traits. Surprisingly, QTL mapping identified a small region on the X chromosome that explains the majority of variation for wing spot and wing display divergence between *D. elegans* and *D. gunungcola*. These

results confirmed previous evidence suggesting a role for the X chromosome in divergence between these species (Yeh *et al*., 2006; Yeh and True, 2014). We then attempted to dissect the genetic basis of these QTL effects on both traits, discovering that, in isolation, the QTL controlling wing spot divergence did not control wing display divergence. Rather, the effects of the X-linked wing display QTL seemed to require the effects of QTL on the autosomes to be detected. These results, unexpectedly, implied that epistasis played an important role in behavioral divergence between *D. elegans* and *D. gunungcola*.

Multiple studies have investigated how correlated behavioral and anatomical evolution map onto the genome. In one example, QTL affecting schooling position in the threespine stickleback co-localized with QTL affecting the evolution of bony plates and the number of neuromasts in a locomotor sense organ (Greenwood *et al*., 2013). Similarly, in cavefish, QTL affecting eye size co-localized with QTL affecting locomotor behavior and sensory receptor number (Yoshizawa *et al*., 2012). And, in Heliconius butterflies, QTL affecting wing pigmentation co-localized with QTL affecting mate preference (Kronforst *et al*., 2006). Genetic dissections in these systems is exceedingly difficult, however, and to date no study has succeeded in disentangling whether physical linkage or gene pleiotropy underlie patterns of co-localized QTL for behavioral and anatomical divergence. But, preliminary results from multiple introgression analyses suggest a pattern: When behavioral QTL are repeatedly backcrossed from one genetic background into another, their effects tend to disappear (see results in chapter four; Jessica Cande, pers. comm; Yun Ding, pers. comm; Dolph Schluter, pers. comm). Behavioral QTL might often behave epistatically with loci that in combination build behavioral differences within and between species. Despite these “negative results” future studies should publish their attempts at fine-mapping behavioral QTL even if they ultimately fail, since these data will help determine if this is a common pattern.

How might epistatic interactions shape the evolution of behavior and its correlated anatomical traits? In the case of *D. elegans* and *D. gunungcola* divergence, previous work indicates that wing spots and wing displays were lost in *D. gunungcola* (Prud’homme *et*

al., 2006). Results from chapter four suggest that mutations disrupting the wing spot QTL on the X chromosome led to wing spot loss in *D. gunungcola*, but, these same (or physically linked) mutations did not by themselves cause wing display loss. Without genotype or phenotype information from more ancestral *D. gunungcola* populations, it is difficult to predict exactly how the genetic architecture for wing spots and wing displays evolved over time, however, field observations of wild *D. gunungcola* (all of which lack wing spots) courtship behavior suggest that elements of wing display behavior remain intact in the *D. gunungcola* genome. It is exciting to speculate that these observations reflect something about the epistatic nature of wing display divergence between these species. That is, data from chapter four suggest that multiple mutations on multiple chromosomes are required for wing display divergence in *D. gunungcola*, but mutations at a single locus are required for wing spot divergence. These preliminary results compel future work to study the genetic basis of natural phenotypic variation within and between *D. gunungcola* populations.

More generally, epistatic interactions between QTL affecting behavior have important implications for how behaviors might evolve. Results from epistatic analysis within individual proteins, for example, indicate that epistasis can limit the paths of mutations altering gene function, since the effects of new mutations change depending on their location within the protein (reviewed in Phillips, 2008). In a similar way, epistatic interactions among behavioral QTL might impact which genes or which types of mutations cause behaviors to evolve depending on their combined function in the nervous system. In addition, epistatic signatures in QTL mapping studies might reflect genetic robustness for the behavioral trait under investigation. In *D. elegans*, for example, advanced interspecific recombinants that inherited more than 5 Mb of *D. gunungcola* DNA on the X chromosome performed wing displays normally. If wing displays impact male mating success, sexual selection in the *D. elegans* genome could have created redundant mechanisms to maintain wing display performance in the face of new mutations. In any case, far more work needs to focus on the biological implications of epistatic interactions underlying the evolution of behavior and other complex traits.

Conclusions

In this thesis I performed a series of genetic analyses aimed at dissecting the mechanisms controlling correlations between mating behavior and pigmentation in *Drosophila*. Each chapter yielded surprising data about the interactions between these traits. Together, these results underscore a major theme: Understanding the specific function genes play in development and evolution helps reveal not only how and why phenotypes change within and between species but also new insights into the nature of phenotypes themselves.

References

Barrett, R. D., Rogers, S. M., & Schluter, D. (2008). Natural selection on a major armor gene in threespine stickleback. *Science*, *322*(5899), 255-257.

Bateson, W. (1903). *The present state of knowledge of colour-heredity in mice and rats*. publisher not identified.

Billeter, J. C., Atallah, J., Krupp, J. J., Millar, J. G., & Levine, J. D. (2009). Specialized cells tag sexual and species identity in *Drosophila melanogaster*. *Nature*, *461*(7266), 987.

Blomquist, G. J., & Bagnères, A. G. (Eds.). (2010). *Insect hydrocarbons: biology, biochemistry, and chemical ecology*. Cambridge University Press.

Bush, J. W., & Hu, D. L. (2006). Walking on water: biolocomotion at the interface. *Annu. Rev. Fluid Mech.*, *38*, 339-369.

Bridges, C. B., & Morgan, T. H. (1923). *The third-chromosome group of mutant characters of Drosophila melanogaster* (No. 327). Carnegie Institution of Washington.

Cone, R. D., Lu, D., Koppula, S., Vage, D. I., Klungland, H., Boston, B., ... & Kesterson, R. A. (1996). The melanocortin receptors: agonists, antagonists, and the hormonal control of pigmentation. *Recent progress in hormone research*, *51*, 287-317.

Cuthill, I. C., Allen, W. L., Arbuckle, K., Caspers, B., Chaplin, G., Hauber, M. E., ... & Mappes, J. (2017). The biology of color. *Science*, *357*(6350), eaan0221.

Drapeau, M. D., Radovic, A., Wittkopp, P. J., & Long, A. D. (2003). A gene necessary for normal male courtship, *yellow*, acts downstream of fruitless in the *Drosophila melanogaster* larval brain. *Journal of Neurobiology*, *55*(1), 53-72.

Emlen, D. J., Marangelo, J., Ball, B., & Cunningham, C. W. (2005). Diversity in the weapons of sexual selection: horn evolution in the beetle genus Onthophagus (Coleoptera: Scarabaeidae). *Evolution*, *59*(5), 1060-1084.

Fowler, D. W., Freedman, E. A., & Scannella, J. B. (2009). Predatory functional morphology in raptors: interdigital variation in talon size is related to prey restraint and immobilisation technique. *PloS One*, *4*(11), e7999.

Frankel, N., Erezyilmaz, D. F., McGregor, A. P., Wang, S., Payre, F., & Stern, D. L. (2011). Morphological evolution caused by many subtle-effect substitutions in regulatory DNA. *Nature*, *474*(7353), 598.

Greenwood, A. K., Wark, A. R., Yoshida, K., & Peichel, C. L. (2013). Genetic and neural modularity underlie the evolution of schooling behavior in threespine

sticklebacks. *Current Biology*, *23*(19), 1884-1888.

Hoekstra, H. E., Hirschmann, R. J., Bundey, R. A., Insel, P. A., & Crossland, J. P. (2006). A single amino acid mutation contributes to adaptive beach mouse color pattern. *Science*, *313*(5783), 101-104.

Hubbard, J. K., Uy, J. A. C., Hauber, M. E., Hoekstra, H. E., & Safran, R. J. (2010). Vertebrate pigmentation: from underlying genes to adaptive function. *Trends in Genetics*, *26*(5), 231-239.

Jackson, I. J., Budd, P., Horn, J. M., Johnson, R., Raymond, S., & Steel, K. (1994). Genetics and molecular biology of mouse pigmentation. *Pigment cell research*, *7*(2), 73-80.

Kopp, A. (2011). *Drosophila* sex combs as a model of evolutionary innovations. *Evolution & development*, *13*(6), 504-522.

Kronforst, M. R., Young, L. G., Kapan, D. D., McNeely, C., O'Neill, R. J., & Gilbert, L. E. (2006). Linkage of butterfly mate preference and wing color preference cue at the genomic location of wingless. *Proceedings of the National Academy of Sciences*, *103*(17), 6575-6580.

Krude, H., Biebermann, H., Luck, W., Horn, R., Brabant, G., & Grüters, A. (1998). Severe early-onset obesity, adrenal insufficiency and red hair pigmentation caused by POMC mutations in humans. *Nature Genetics*, *19*(2), 155.

Martin, A., & Orgogozo, V. (2013). The loci of repeated evolution: a catalog of genetic hotspots of phenotypic variation. *Evolution*, *67*(5), 1235-1250.

Lin, J. Y., & Fisher, D. E. (2007). Melanocyte biology and skin pigmentation. *Nature*, *445*(7130), 843.

Makki, R., Cinnamon, E., & Gould, A. P. (2014). The development and functions of oenocytes. *Annual Review of Entomology*, *59*, 405-425.

Massey, J. H., & Wittkopp, P. J. (2016). The genetic basis of pigmentation differences within and between *Drosophila* species. In *Current topics in developmental biology* (Vol. 119, pp. 27-61). Academic Press.

Morgan, T. H. (1935). The relation of genetics to physiology and medicine. *The Scientific Monthly*, *41*(1), 5-18.

Morgan, C., Thomas, R. E., & Cone, R. D. (2004a). Melanocortin-5 receptor deficiency promotes defensive behavior in male mice. *Hormones and behavior*, *45*(1), 58-63.

Morgan, C., Thomas, R. E., Ma, W., Novotny, M. V., & Cone, R. D. (2004b).

Melanocortin-5 receptor deficiency reduces a pheromonal signal for aggression in male mice. *Chemical senses*, *29*(2), 111-115.

Phillips, P. C. (2008). Epistasis—the essential role of gene interactions in the structure and evolution of genetic systems. *Nature Reviews Genetics*, *9*(11), 855.

Prud'Homme, B., Gompel, N., Rokas, A., Kassner, V. A., Williams, T. M., Yeh, S. D., ... & Carroll, S. B. (2006). Repeated morphological evolution through cis-regulatory changes in a pleiotropic gene. *Nature*, *440*(7087), 1050.

Roulin, A., Mangels, J., Wakamatsu, K., & Bachmann, T. (2013). Sexually dimorphic melanin-based colour polymorphism, feather melanin content, and wing feather structure in the barn owl (*Tyto alba*). *Biological Journal of the Linnean Society*, *109*(3), 562-573.

Santos, M. E., Le Bouquin, A., Crumière, A. J., & Khila, A. (2017). Taxon-restricted genes at the origin of a novel trait allowing access to a new environment. *Science*, *358*(6361), 386-390.

Spinner, M., Kovalev, A., Gorb, S. N., & Westhoff, G. (2013). Snake velvet black: hierarchical micro-and nanostructure enhances dark colouration in *Bitis rhinoceros*. *Scientific reports*, *3*, 1846.

Sturtevant, A. H. (1915). Experiments on sex recognition and the problem of sexual selection in *Drosophila*. *Journal of Animal Behaviour*, *5*, 351e366.

Takahashi, A. (2013). Pigmentation and behavior: potential association through pleiotropic genes in *Drosophila*. *Genes & genetic systems*, *88*(3), 165-174.

Wittkopp, P. J., True, J. R., & Carroll, S. B. (2002). Reciprocal functions of the *Drosophila* yellow and ebony proteins in the development and evolution of pigment patterns. *Development*, *129*(8), 1849-1858.

Wittkopp, P. J., Carroll, S. B., & Kopp, A. (2003). Evolution in black and white: genetic control of pigment patterns in *Drosophila*. *Trends in Genetics*, *19*(9), 495-504.

Wittkopp, P. J., & Beldade, P. (2009, February). Development and evolution of insect pigmentation: genetic mechanisms and the potential consequences of pleiotropy. In *Seminars in cell & developmental biology* (Vol. 20, No. 1, pp. 65-71). Academic Press.

Wright, T. R. (1987). The genetics of biogenic amine metabolism, sclerotization, and melanization in Drosophila melanogaster. In *Advances in genetics* (Vol. 24, pp. 127-222). Academic Press.

Yeh, S. D., Liou, S. R., & True, J. R. (2006). Genetics of divergence in male wing

pigmentation and courtship behavior between *Drosophila elegans* and *D. gunungcola*. *Heredity*, *96*(5), 383.

Yeh, S. D., & True, J. R. (2014). The genetic architecture of coordinately evolving male wing pigmentation and courtship behavior in *Drosophila elegans* and *Drosophila gunungcola*. *G3: Genes, Genomes, Genetics*, *4*(11), 2079-2093.

Yoshizawa, M., Yamamoto, Y., O'Quin, K. E., & Jeffery, W. R. (2012). Evolution of an adaptive behavior and its sensory receptors promotes eye regression in blind cavefish. *BMC Biology*, *10*(1), 108.

Appendices

Appendix A

Supplementary Figures and Tables for Chapter 2

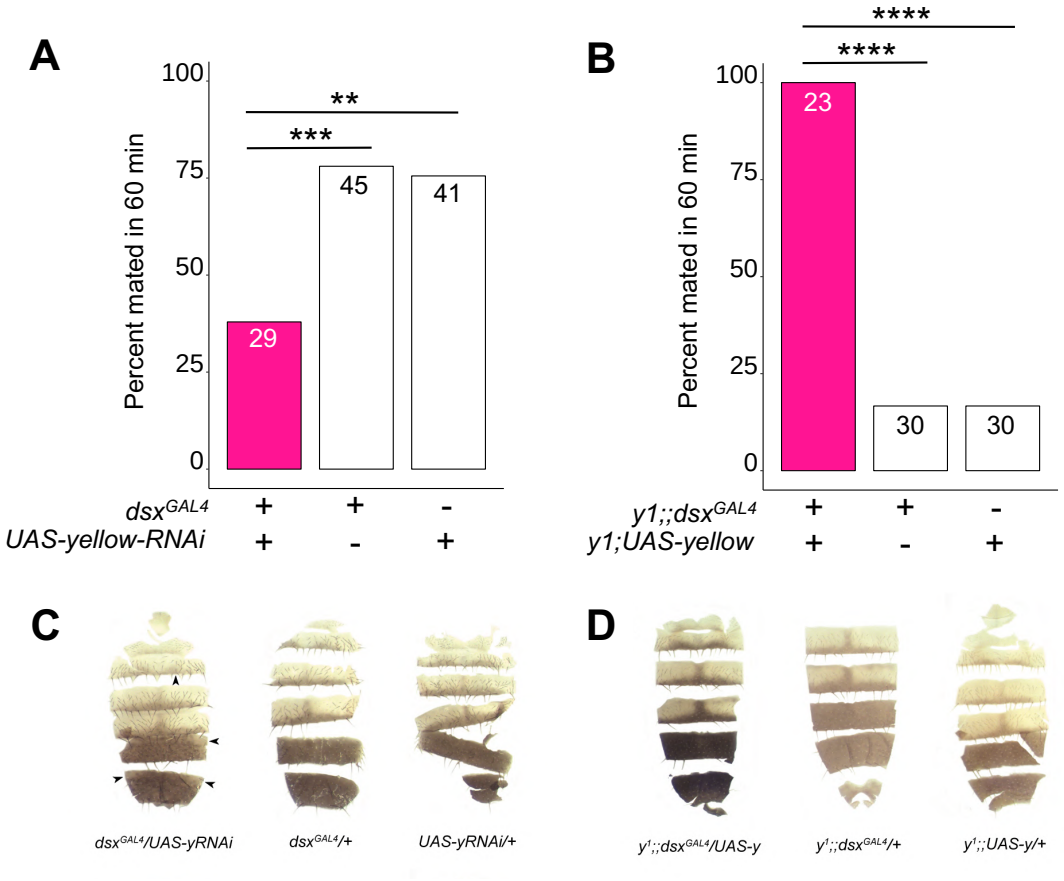

Supplemental Figure S2-1 *yellow* expression in *dsx*-expressing cells is necessary and sufficient for male mating success

(**A**) Expressing *yellow-RNAi* in *dsx*-expressing cells using dsx^{GAL4} (Rideout *et al*., 2010) significantly inhibited male mating success. (**B**) Expressing *yellow* in *dsx*-expressing cells using dsx^{GAL4} in a *y1* mutant background was sufficient to restore male mating success. (**C**) Expressing *yellow-RNAi* using dsx^{GAL4} (Rideout *et al.*, 2010) partially reduced black melanin levels in the male A5 and A6 abdominal tergites, consistent with prior work (Williams *et al*. 2008, Rogers *et al*. 2014, Kalay *et al*. 2016). (**D**) Expressing *yellow* using dsx^{GAL4} partially elevated black melanin levels in the male A5 and A6 abdominal tergites. Sample sizes are shown at the top of each barplot. Significance was measured using Chi-square tests with Bonferroni corrections for multiple comparisons. $^{**}P<0.01$, $^{***}P<0.001$, $^{****}P<0.001$.

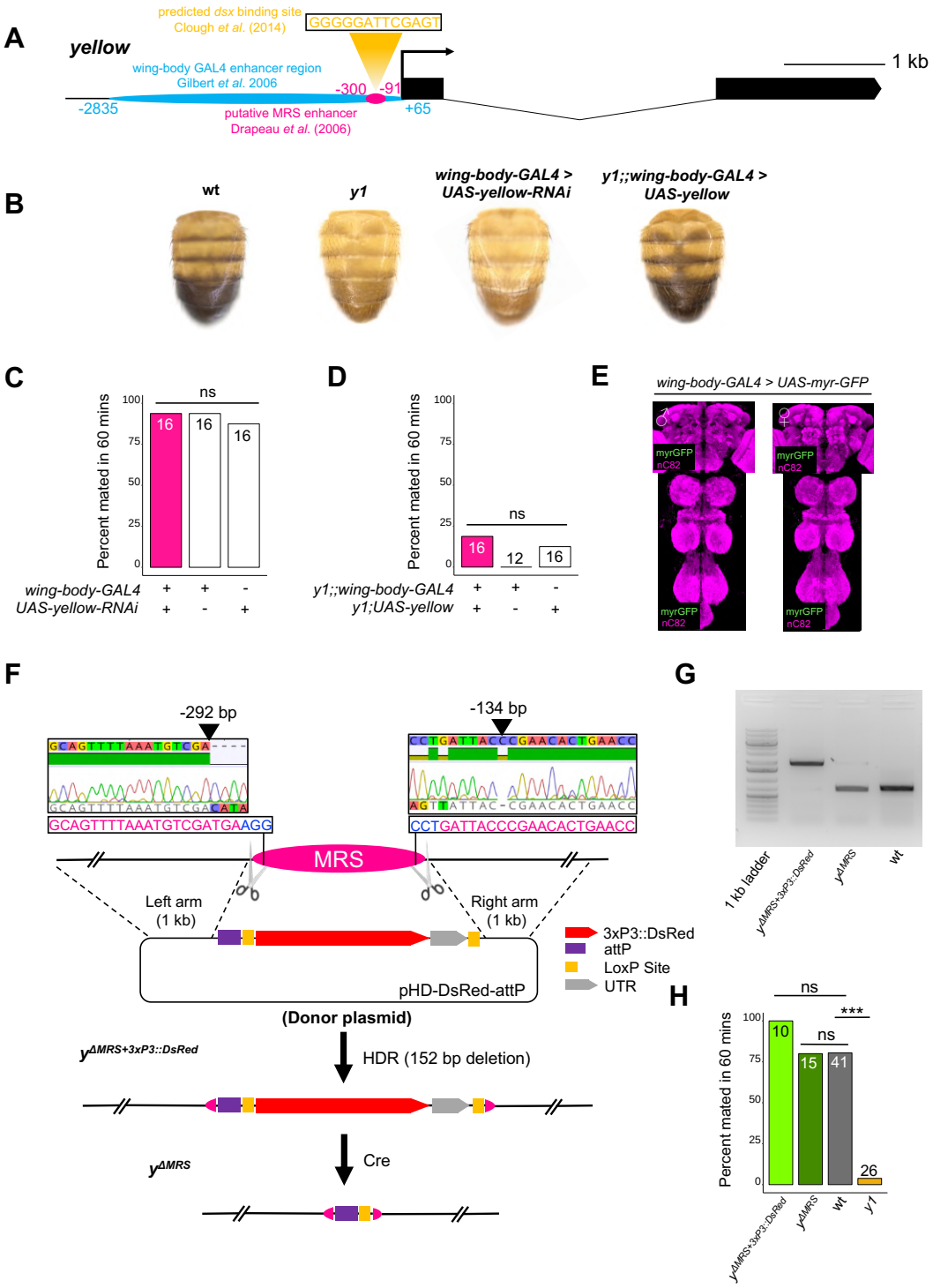
A
yellow
predicted dsx binding site
Clough et al. (2014)
GGGGGATTCGAGT
wing-body GAL4 enhancer region
Gilbert et al. 2006
-2835
-300
-91
+65
putative MRS enhancer
Drapeau et al. (2006)
1 kb
B
wt
y1
wing-body-GAL4 > UAS-yellow-RNAi
y1;;wing-body-GAL4 > UAS-yellow
C
Percent mated in 60 mins
ns
16
16
16
wing-body-GAL4
UAS-yellow-RNAi
D
Percent mated in 60 mins
ns
16
12
16
y1;;wing-body-GAL4
y1;UAS-yellow
E
wing-body-GAL4 > UAS-myr-GFP
myrGFP
nC82
F
-292 bp
-134 bp
GCAGTTTTAAATGTCGATGAAGG
CCTGATTACCCGAACACTGAACC
MRS
Left arm
(1 kb)
Right arm
(1 kb)
3xP3::DsRed
attP
LoxP Site
UTR
pHD-DsRed-attP
(Donor plasmid)
yΔMRS+3xP3::DsRed
HDR (152 bp deletion)
yΔMRS
Cre
G
1 kb ladder
yΔMRS+3xP3::DsRed
yΔMRS
wt
H
Percent mated in 60 mins
ns
***
ns
10
15
41
26
yΔMRS+3xP3::DsRed
yΔMRS
wt
y1

Supplemental Figure S2-2 The mating regulatory sequence (MRS) from Drapeau *et al.* (2006) does not affect male mating success

(**A**) Diagram of the *yellow* locus highlighting the putative "mating regulatory sequence" (MRS) (pink) region mapped in Drapeau *et al.* (2006) and a predicted *dsx* binding site (yellow) identified by ChIP-seq in Clough *et al.* (2014). The predicted binding site was identified based on *in vivo* Doublesex occupancy data (PWM score = 88.7) localized between 356,273 and 356,286 bp on the X chromosome (see Supplementary Table S2 in Clough *et al*., 2014). The wing-body enhancer region is indicated in blue, which was cloned upstream of GAL4 in Gilbert *et al*. (2006) to make the *wing-body-GAL4* line. (**B**) Expressing *yellow*-RNAi using *wing-body-GAL4* reduced black melanin to *y1* levels, and expressing *yellow* in a *y1* mutant background using *wing-body-GAL4* restores black melanin synthesis to wild-type (wt) levels. (**C**) Expressing *yellow*-RNAi using *wing-body-GAL4* did not inhibit male mating success. (**D**) Expressing *yellow* using *wing-body-GAL4* in a *y1* mutant background did not restore male mating success. (**E**) Brain and VNC of adult male and female flies stained with anti-GFP (green) antibody for myrGFP expressed using *wing-body-GAL4* and counterstained with anti-nC82 (magenta) for neuropil. (**F**) Diagram illustrating the CRISPR/Cas9-facilitaed homology-directed repair (HDR) strategy used to excise and replace the MRS (pink) with pHD-DsRed-attP (red) (Gratz *et al*., 2014). Two sgRNAs (pink letters) were designed towards target PAM sites (blue letters) at the most 5' and 3' bounds of the MRS (scissors). Sanger sequencing chromatograms illustrate the location of each cut site (black arrows) relative to the transcription start site. DsRed was removed using Cre-lox recombinase (Siegal and Hartl 1996). (**G**) PCR validation of DsRed removal and MRS deletion. (**H**) Excising the putative MRS did not inhibit male male mating success. Sample sizes are shown at the top of each barplot. Significance was measured using Chi-square tests with Bonferroni corrections for multiple comparisons. ***$P<0.001$. n.s., not significant.

BDSC Stock #	GAL4 expression pattern
6993	GAL4 expressed in larval brain, Bolwig's nerve and salivary glands.
49365	Expresses GAL4 under the control of DNA sequences in or near Lim3
6927	GAL4 expression pan-neural in late embryos, in a subset of motor neurons in 3rd instar larvae, and enriched in mushroom bodies in adults.
45175	Expresses GAL4 under the control of DNA sequences in or near InR
3740	GAL4 pattern in third instar larva: brain - optic proliferative center, laminar precursor cells, not in discs.
5820	GAL4 expressed in neuroblasts and neurons.
8848 (ple-GAL4)	Expresses GAL4 in dopaminergic cells (gift from Shinya Yamamoto)
7010 (Ddc-GAL4)	Expresses GAL4 in dopaminergic and serotonergic neurons under the control of Ddc (gift from Shinya Yamamoto)
TPH-GAL4	Expresses GAL4 in serotinergic cells (gift from Shinya Yamamoto)

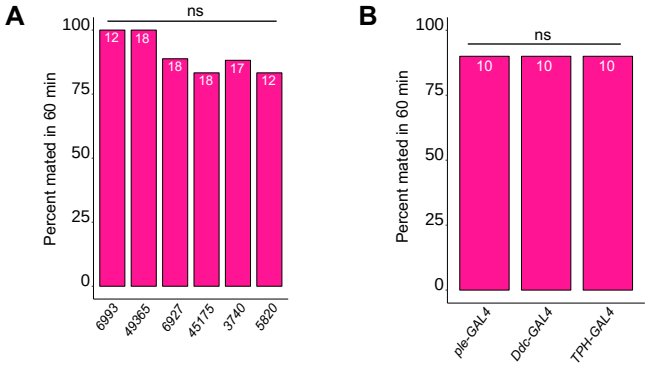

Supplemental Figure S2-3 Expressing *yellow-RNAi* in subsets of CNS tissue does not affect male mating success

(**A**,**B**) Expressing *yellow*-RNAi using a series of CNS, dopaminergic, and serotonergic GAL4 drivers did not affect male mating success. Significance was measured using Chi-square tests with Bonferroni corrections for multiple comparisons. Sample sizes are shown at the top of each barplot. Significance was measured using Chi-square tests with Bonferroni corrections for multiple comparisons. n.s., not significant.

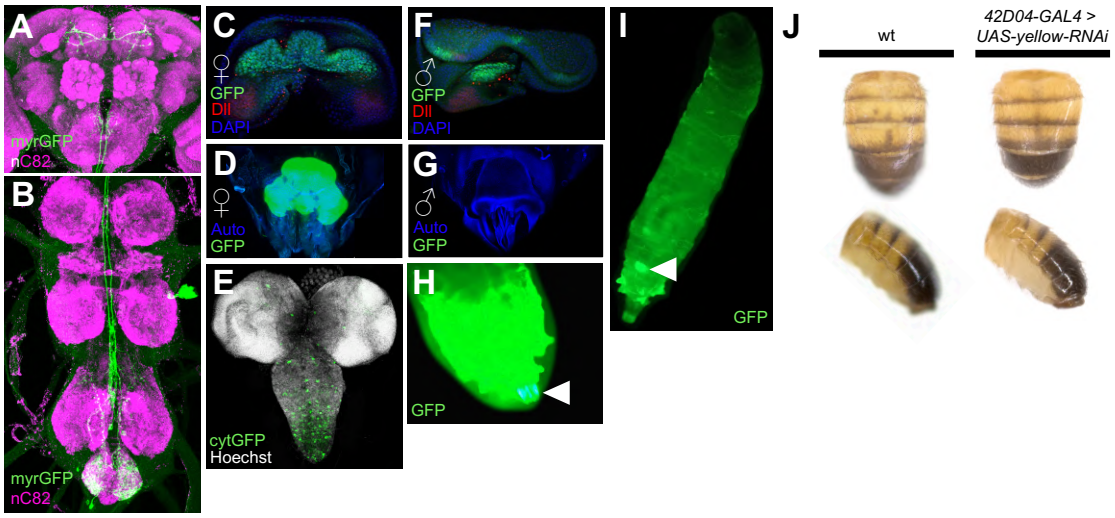

Supplemental Figure S2-4 Expression pattern of *42D04-GAL4*

(**A**,**B**) Brain and VNC of adult female fly stained with anti-GFP (green) antibody for myrGFP expressed using *42D04-GAL4* and counterstained with anti-nC82 (magenta) for neuropil. (**C**) L3 larval female genital disc stained with anti-GFP (green) antibody for cytGFP expressed using *42D04-GAL4*, anti-Dll (red) for Distal-less expression, and counterstained with DAPI (blue) for DNA (courtesy of Janelia Fly Light). (**D**) Adult female genitalia native cytGFP (green) expressed using *42D04-GAL4*. (**E**) L3 CNS native cytGFP (green) expressed using *42D04* (**F**) L3 larval male genital disc stained with anti-GFP (green) antibody for cytGFP expressed using *42D04-GAL4*, anti-Dll (red) for Distal-less expression, and counterstained with DAPI (blue) for DNA (courtesy of Janelia Fly Light). (**G**) Adult male genitalia did not show native cytGFP expression using *42D04-GAL4*. (**H**) L3 larval posterior spiracle (white arrowhead) native cytGFP (green) expression. (**I**) L3 larva whole body highlighting native cytGFP (green) expression in the genital disc (white arrowhead). (**J**) Expressing *yellow*-RNAi using *42D04-GAL4* does not affect body pigmentation relative to wild-type (wt) flies.

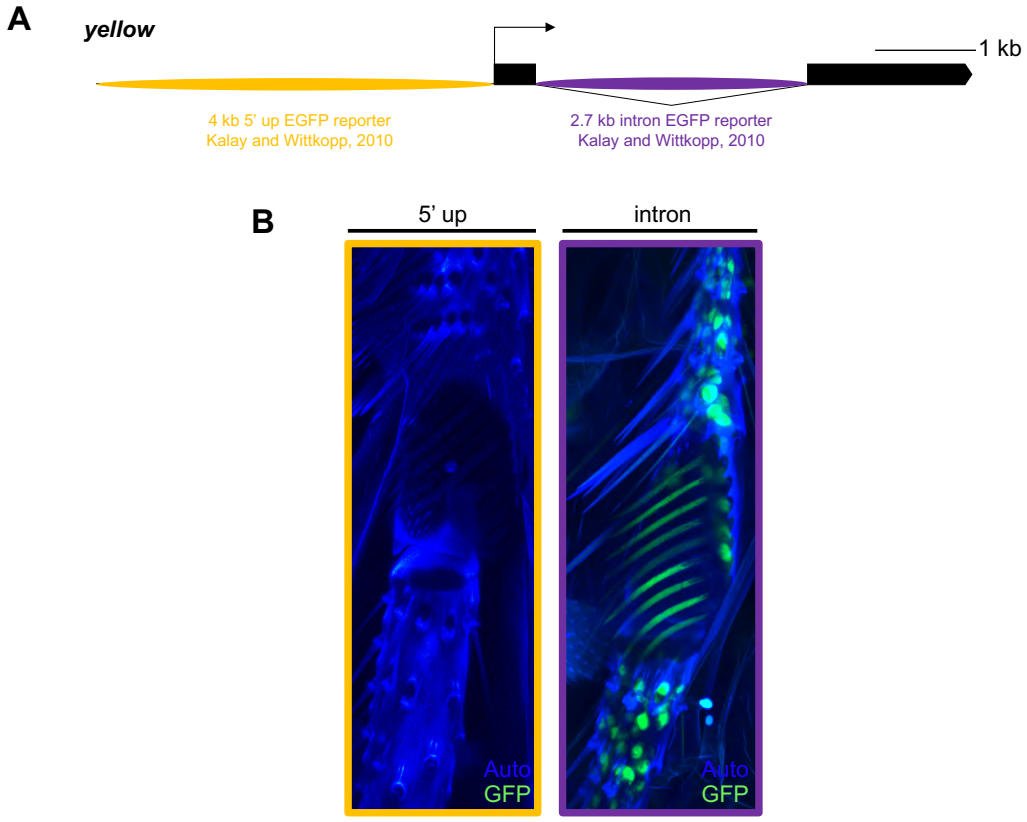

Supplemental Figure 2-5 *yellow* EGFP reporters localize yellow sex comb expression to the intronic bristle enhancer

(**A**) Diagram of the *yellow* locus highlighting two *D. melanogaster* enhancer regions [5' up including the wing, body, and putative MRS enhancers reported in Geyer and Corces (1987), Martin *et al*., (1989), and Drapeau *et al*., (2006); and intron, including the bristle and putative sex comb enhancer reported in Geyer and Corces (1987) and Martin *et al*., (1989)] that were cloned upstream of an EGFP reporter in Kalay and Wittkopp (2010). (**B**) Confocal image of a 96 h old (APF) pupal sex comb expressing cytGFP under the control of the 5' up enhancer region. (**C**) Confocal image of a 96 h APF pupal sex comb expressing cytGFP under the control of the intronic enhancer region, highlighting expression in bristle sockets, sex comb sockets, and sex comb teeth.

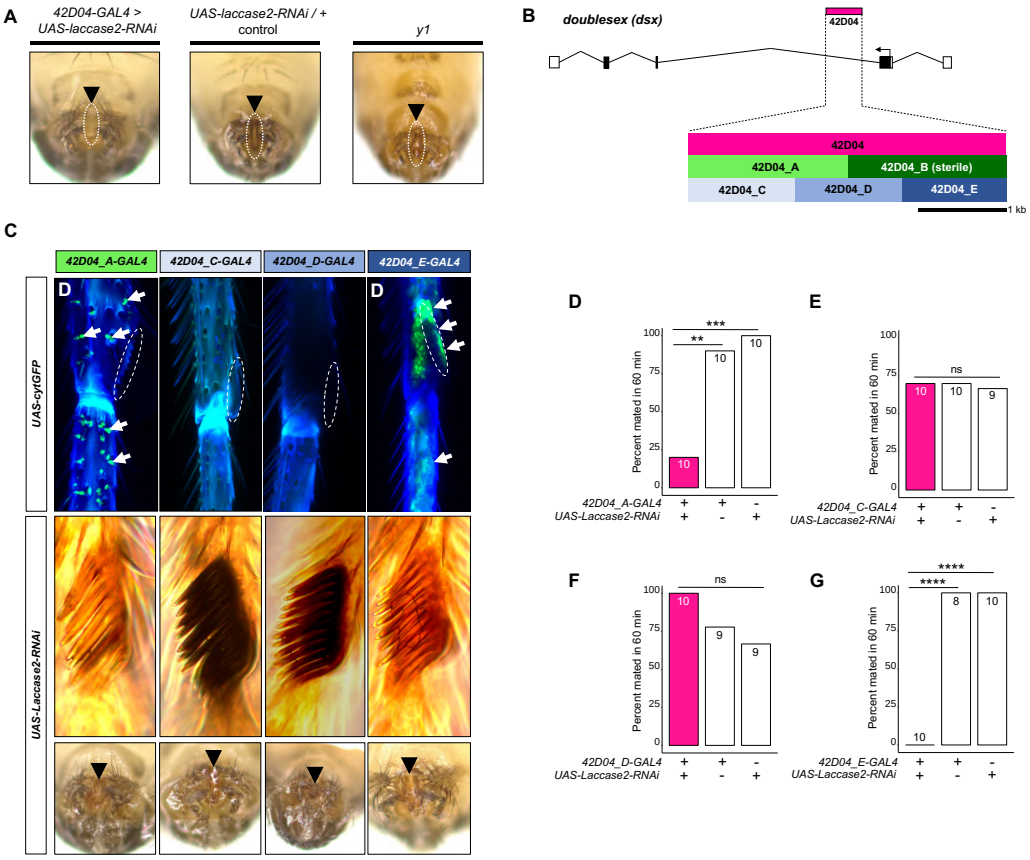

Supplemental Figure S2-6 Genetic dissection of the *42D04-GAL4* enhancer confirms the specific role of sex comb melanization, and not the aedeagus, in male mating success

(**A**) Expressing *Laccase2-RNAi* using *42D04-GAL4* blocked melanin synthesis in the aedeagus. (**B**) Diagram of the male exon structure of the *dsx* locus highlighting the strategy used to dissect the *42D04-GAL4* expression pattern. Five new GAL4 lines were created by synthesizing different sized sub-fragments of the *42D04-GAL4* enhancer fragment and cloning them upstream of GAL4 (see Supplemental Materials and Methods). Note, *42D04_B-GAL4* could not be maintained, since female flies expressing GAL4 using this enhancer region were all sterile and showed necrotic growths on their genitalia. (**C**) Expression pattern of *42D04_A,C,D, and E-GAL4* lines. Expressing cytGFP using *42D04_A-GAL4* showed GFP (green) localized to bristle sockets, and *42D04_E-GAL4* shows bright GFP in the sex comb and lower leg region. *42D04_C-GAL4* and *42D04_D-GAL4* did not show GFP expression in the legs. Expressing *Laccase2-RNAi* using *42D04_A-GAL4* and *42D04_E-GAL4* blocked melanin synthesis in the sex combs but not the aedeagus. (**D**) Expressing *Laccase2-RNAi* using *42D04_A-GAL4* and *42D04_E-GAL4* inhibited male mating success. Sample sizes are shown at the top of each barplot. Significance was measured using Chi-square tests with Bonferroni corrections for multiple comparisons. ***P*<0.01, ****P*<0.001, *****P*<0.001. n.s., not significant.

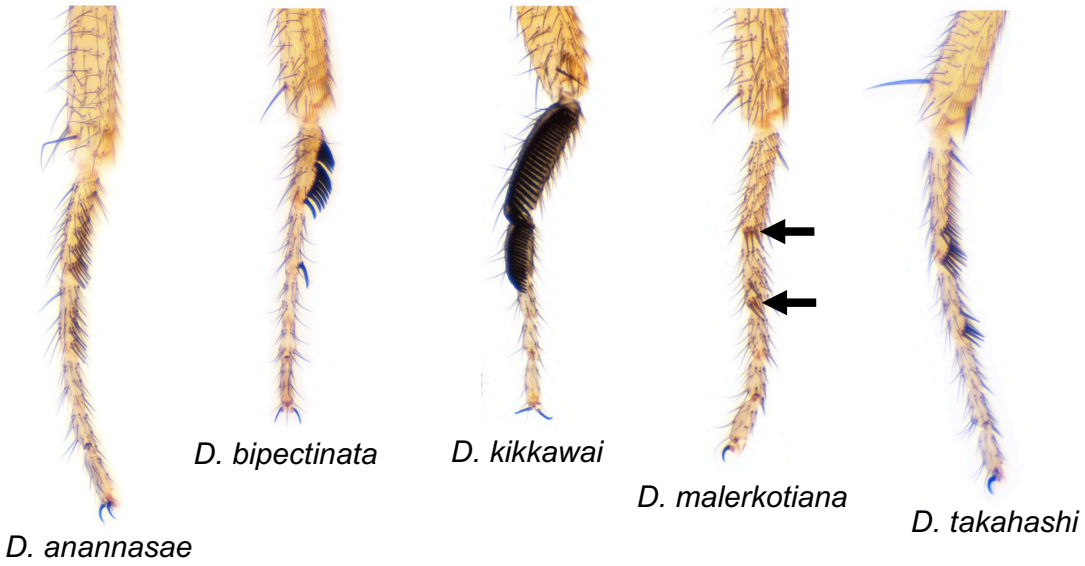

Supplemental Figure S2-7 *Drosophila* species with varying sex comb morphology used for high-speed video assays

D. anannasae, *D. bipectinata*, *D. kikkawai*, *D. malerkotiana*, and *D. takahahi* male front forelegs, highlighting variation in sex comb morphology (Nicolas Gompel).

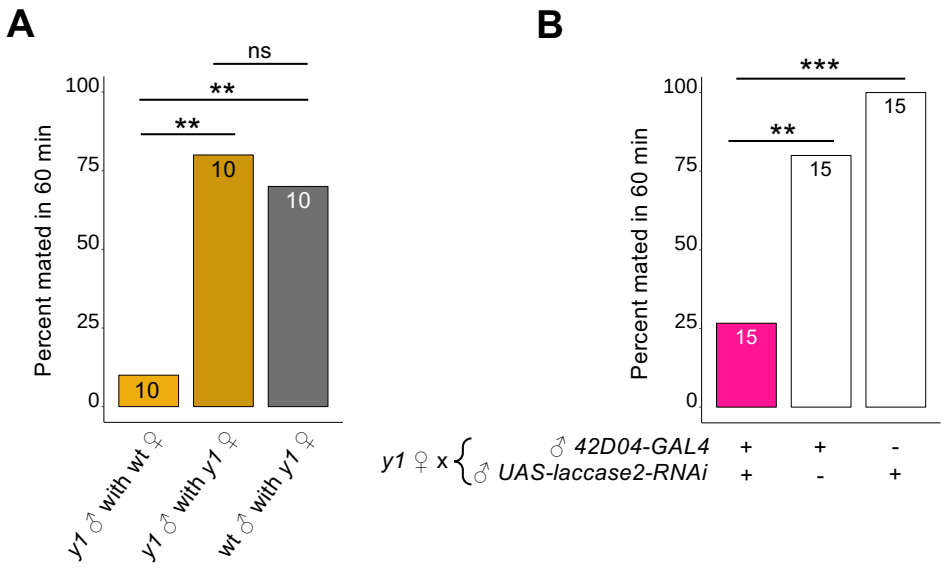

Supplementary Figure S2-8 Sex comb melanization is required for male mating success with *y1* females

(**A**) *y1* males showed increased male mating success with *y1* females. (**B**) Expressing *Laccase2-RNAi* using *42D04-GAL4* in males significantly inhibited male mating success with *y1* females. Significance was measured using Chi-square tests with Bonferroni corrections for multiple comparisons. ***P*<0.01, ****P*<0.001. n.s., not significant.

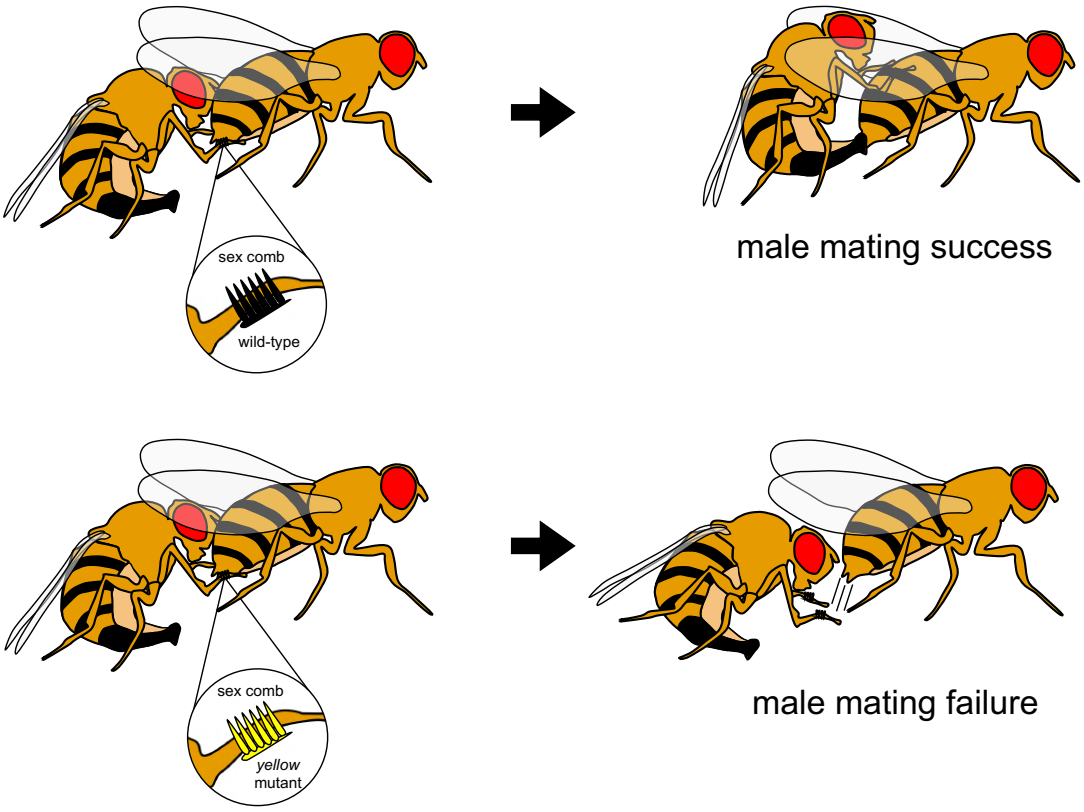

Chapter 2 Graphical Abstract

Appendix B

Supplementary Figures and Tables for Chapter 3

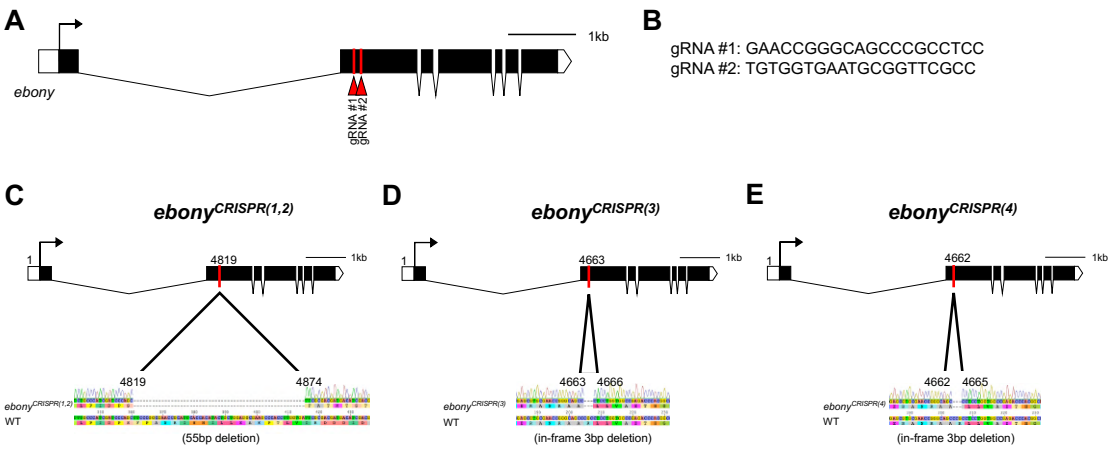

Supplemental Figure S3-1 Effects of CRISPR/Cas9 gene editing on *ebony* coding region

(**A**) Schematic of the *ebony* gene in *Drosophila melanogaster*, highlighting the sites of two gRNAs (red lines) targeted to the first coding exon. (**B**) DNA target sequences used to synthesize two gRNAs to direct Cas9 to *ebony*'s first coding exon. Both target sequences were previously published in Ren *et al*. (2014), showing the highest heritable germline transformation rate. (**C**) $ebony^{CRISPR(1,2)}$ contains a 55 bp deletion in the first coding exon that caused a frame-shift in *ebony*'s coding sequence. (**D**) $ebony^{CRISPR(3)}$ contains an in-frame 3 bp deletion in the first coding exon. (**E**) $ebony^{CRISPR(4)}$ contains an in-frame 3bp deletion in the first coding exon, shift 1 bp upstream of the $ebony^{CRISPR(3)}$ deletion.

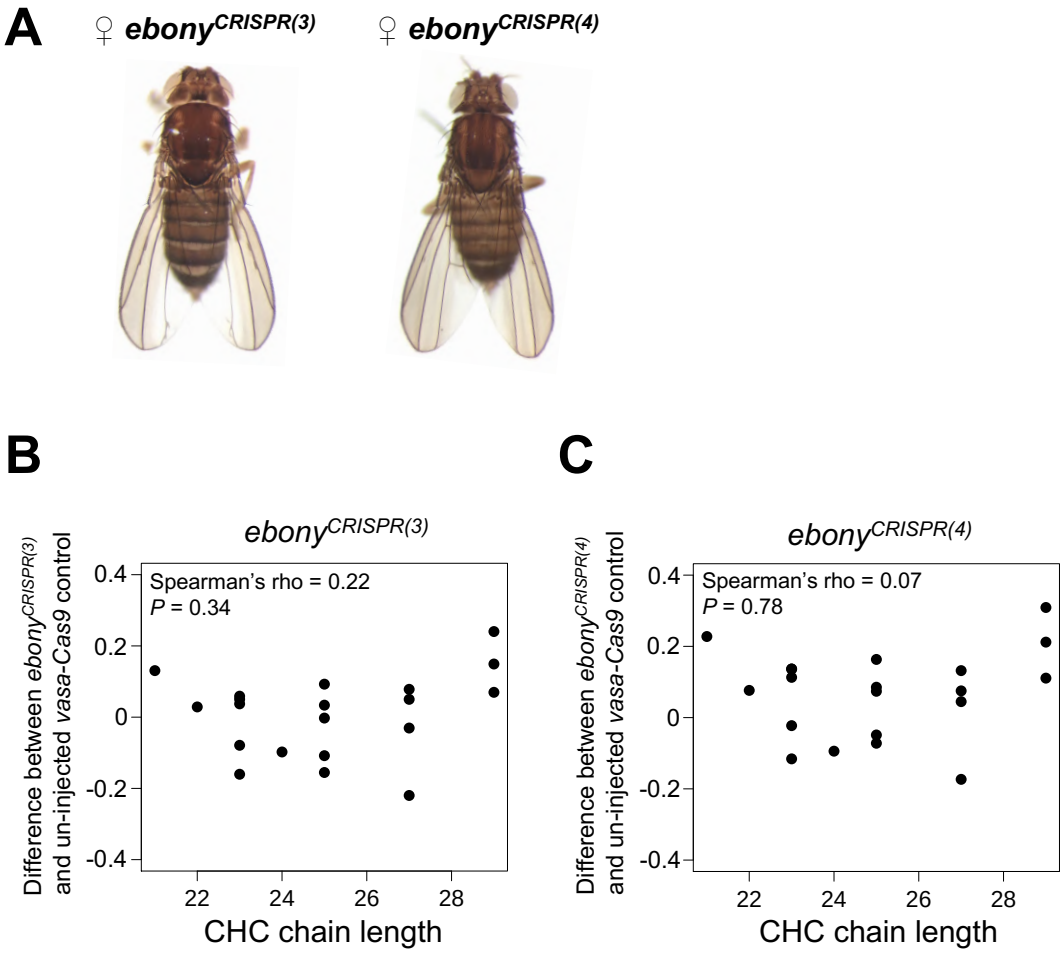

Supplemental Figure S3-2 *ebony*$^{CRISPR(3)}$ and *ebony*$^{CRISPR(4)}$ show darker body pigmentation but no CHC lengthening effect

(**A**) Photographs highlighting the effects of *ebony*$^{CRISPR(3)}$ and *ebony*$^{CRISPR(4)}$ mutations on body pigmentation. (**B**) Difference in log-contrast of relative CHC intensity between *ebony*$^{CRISPR(3)}$ and un-injected vasa-Cas9 control flies. (**C**) Difference in log-contrast of relative CHC intensity between *ebony*$^{CRISPR(4)}$ and un-injected vasa-Cas9 control flies.

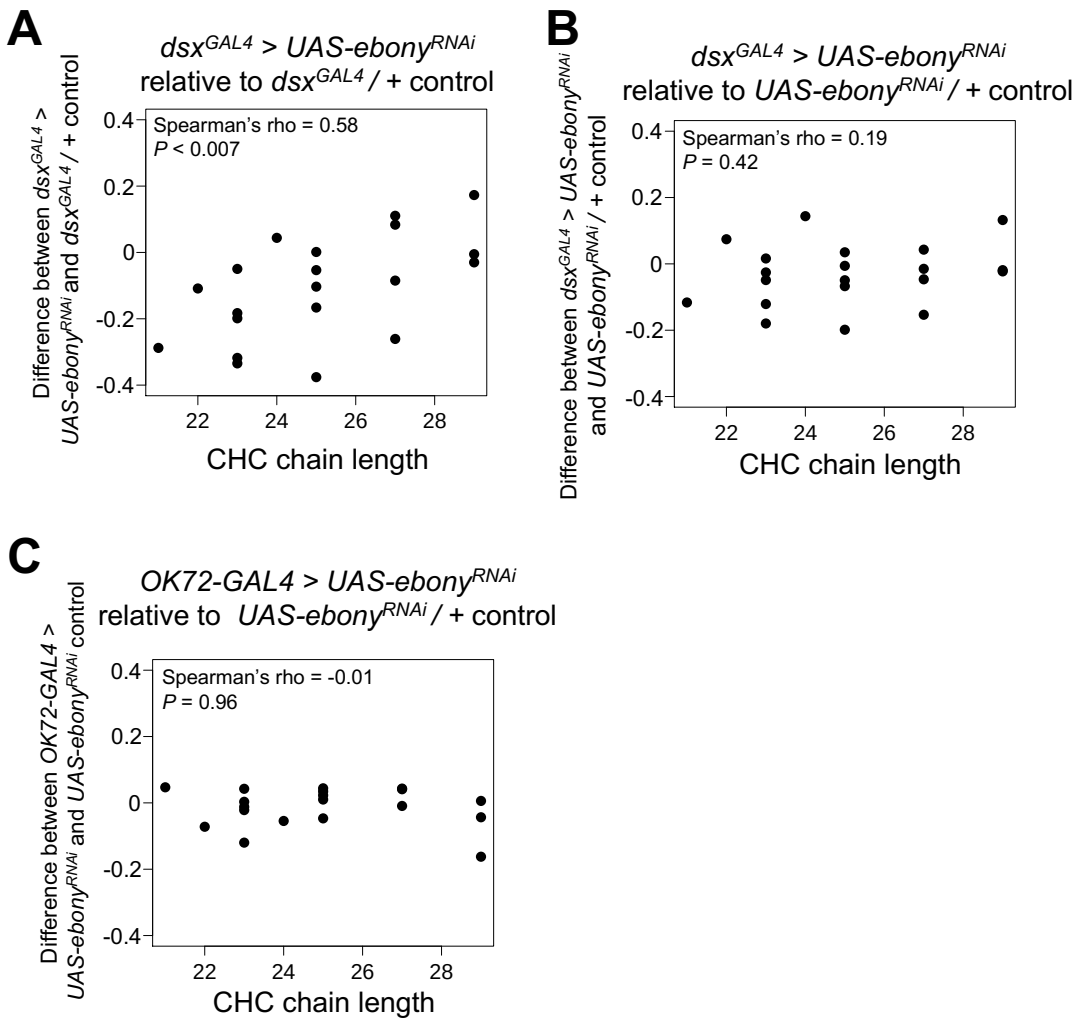

Supplemental Figure S3-3 *ebony* knock down in *doublesex*-expressing cells causes CHC lengthening

Female GAL4 lines were crossed with either the male *UAS-ebony-RNAi* effector line or a *w1118 CS* control line, and males from the *UAS-ebony-RNAi* effector line were crossed to the same *w1118 CS* control line for comparison. (**A**) Difference in log-contrast of relative CHC intensity between females expressing *ebony-RNAi* under the control of the dsx^{GAL4} and dsx^{GAL4} / + control females. (**B**) Difference in log-contrast of relative CHC intensity between females expressing *ebony-RNAi* under the control of dsx^{GAL4} and *UAS-ebony-RNAi* / + control females. (**C**) Difference in log-contrast of relative CHC intensity between females expressing *ebony-RNAi* under the control of the oenocyte driver *OK72-GAL4* and *UAS-ebony-RNAi* / + control females.

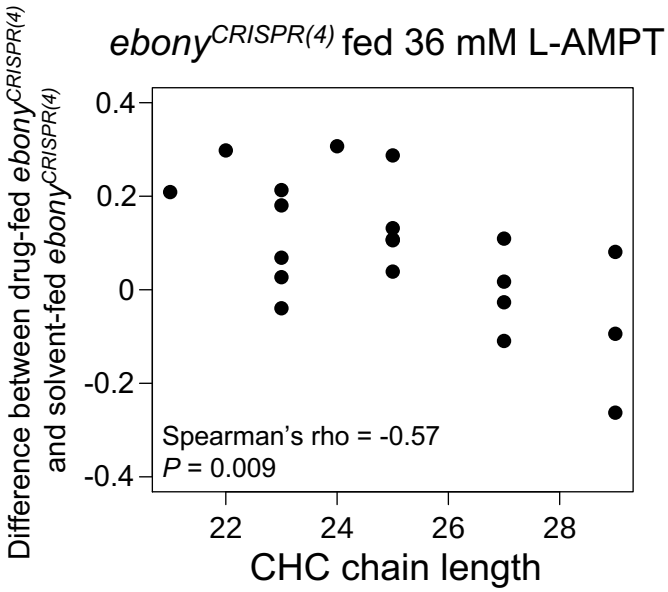

Supplemental Figure S3-4 Feeding *ebony*$^{CRISPR(4)}$ females L-AMPT causes CHC shortening

Difference in log-contrast of relative CHC intensity between *ebony*$^{CRISPR(4)}$ females fed 36mM alpha methyl tyrosine (L-AMPT) and *ebony*$^{CRISPR(4)}$ females fed a solvent control.

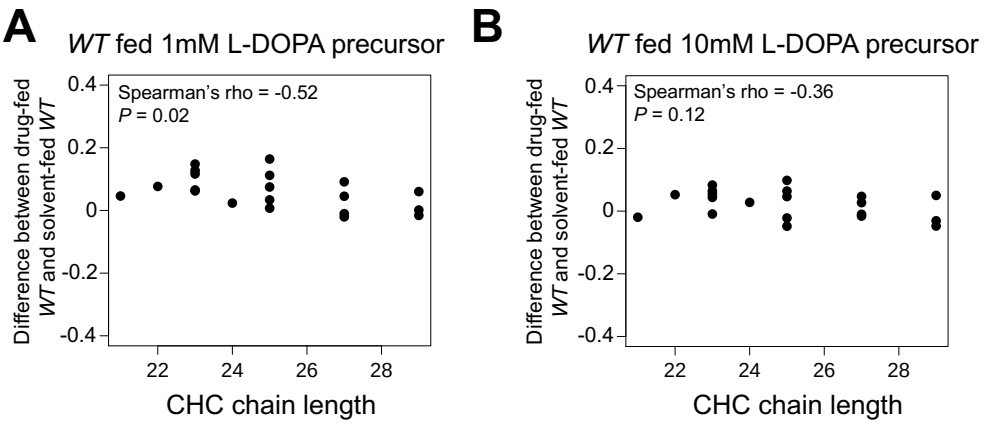

Supplemental Figure S3-5 Feeding WT (w^{1118} *CS*) females L-DOPA precursor causes a slight CHC shortening effect

(**A**) Difference in log-contrast of relative CHC intensity between *wild-type* (w^{1118} *CS*) fed 1mM methyl L-DOPA hydrochloride (L-DOPA precursor) and w^{1118} *CS* fed a solvent control. (**B**) Difference in log-contrast of relative CHC intensity between *wild-type* (w^{1118} *CS*) fed 10mM L-DOPA precursor and w^{1118} *CS* fed a solvent control.

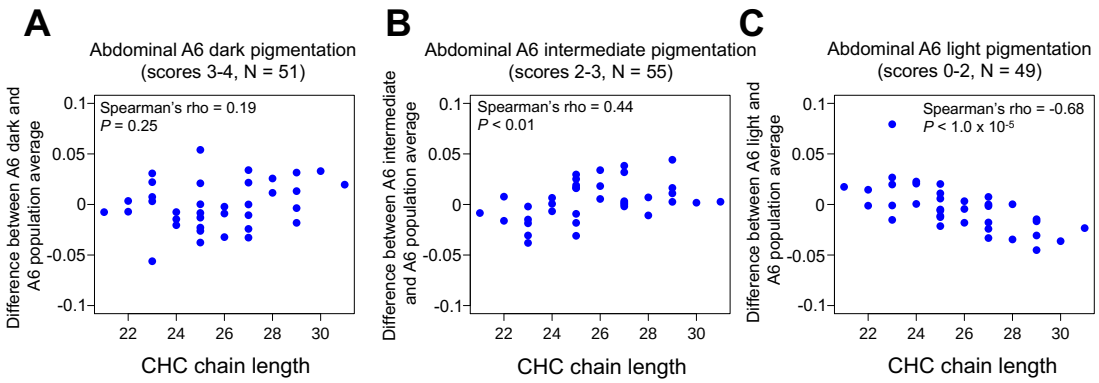

Supplemental Figure S3-6 DGRP lines with lightly pigmented A6 abdominal tergites show a CHC shortening effect

Pigmentation scores and CHC data were obtained from Dembeck *et al.* (2015a,b). (**A**) Difference in log-contrast of relative CHC intensity between DGRP females with darkly-pigmented 6th abdominal tergites (A6) (3 < score, N = 51) and the 155 line average. (**B**) Difference in log-contrast of relative CHC intensity between DGRP females with intermediately-pigmented A6 (2 < score ≤ 3, N = 55) and the 155 line average. (**C**) Difference in log-contrast of relative CHC intensity between DGRP females with lightly-pigmented A6 (score ≤ 2, N = 49) and the 155 line average.

Category	Elemental Formula	Common Notation[†]
alkane	C21 H44	nC21
monoene	C22 H44	C22:1
alkane	C22 H44	nC22
methyl branched	C22 H46	23Br
diene	C23 H44	7.11TD
monoene	C23 H46	9-T
monoene	C23 H46	7-T
monoene	C23 H46	5-T
alkane	C23 H46	nC23
alkane	C24 H50	nC24
methyl branched	C24 H50	25Br
diene	C25 H48	7.11PD
monoene	C25 H50	9-P
monoene	C25 H50	7-P
alkane	C25 H52	nC25
alkane	C26 H54	internal standard
methyl branched	C26 H54	27Br
diene	C27 H52	7.11HD
monoene	C27 H54	9-H
monoene	C27 H54	7-H
alkane	C27 H56	nC27
methyl branched	C28 H58	29Br
diene	C29 H56	7.11ND
alkane	C29 H60	nC29

[†]Br: methyl branched; T: tricosene; P: pentacosene; H: heptacosene; TD: tricosadiene; PD: pentacosadiene; ND: nonacosadiene

Supplemental Table S3-1 Common CHCs in female *D. melanogaster*

Appendix C

Supplementary Figures and Tables for Chapter 4

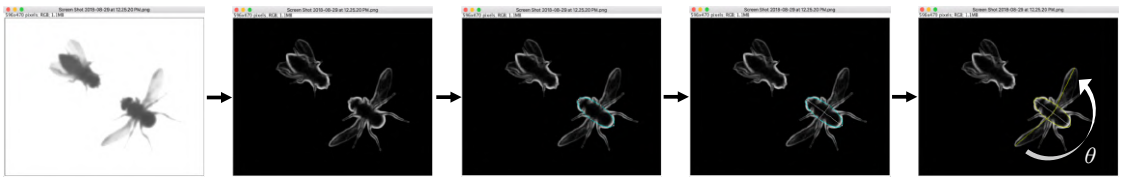

Supplemental Figure S4-1 ImageJ procedure for measuring maximum wing display angles

Screenshots of each wing display were captured for every recombinant courtship video. The maximum wing display bout was identified for each fly by quickly comparing screenshots that varied in wing display angles (from wing tip to wing tip) and picking by eye the display with the largest angle. Next, for each fly, the maximum wing display angle was quantified in ImageJ by using the 1) Find Edges function, 2) polygon tool to Fit Ellipse around the fly body, 3) Ellipse Macros (Supplemental File S2) to fit the major and minor axes of the ellipse, and 4) draw Angle tool, fitting the angle vertex at the major and minor axes intersection to calculate the wing display angle from wing tip to wing tip.

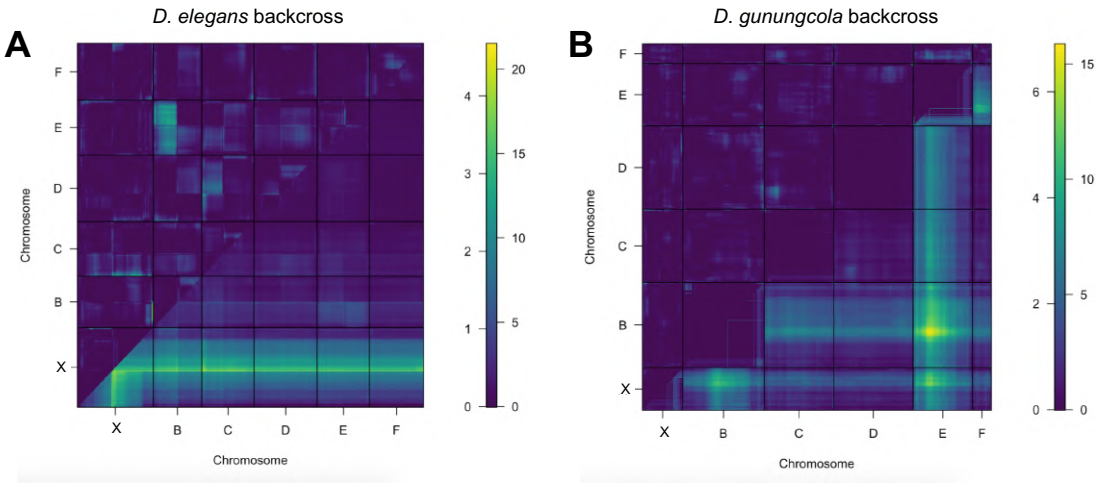

Supplemental Figure S4-2 LOD scores estimated from a two-dimensional, two QTL scan of maximum wing display angles

(A) For the *D. elegans* backcross, the Interaction LODi (see Supplementary Table S1) is displayed in the upper left triangle; the Full LODf (see Supplementary Table S1) is displayed in the lower right triangle. The color scale on the right indicates LOD values for LODi (left) and LODf (right). (B) For the *D. gunungcola* backcross, the Interaction LODi (see Supplementary Table S2) is displayed in the upper left triangle; the Full LODf (see Supplementary Table S2) is displayed in the lower right triangle. The color scale on the right indicates LOD values for LODi (left) and LODf (right).

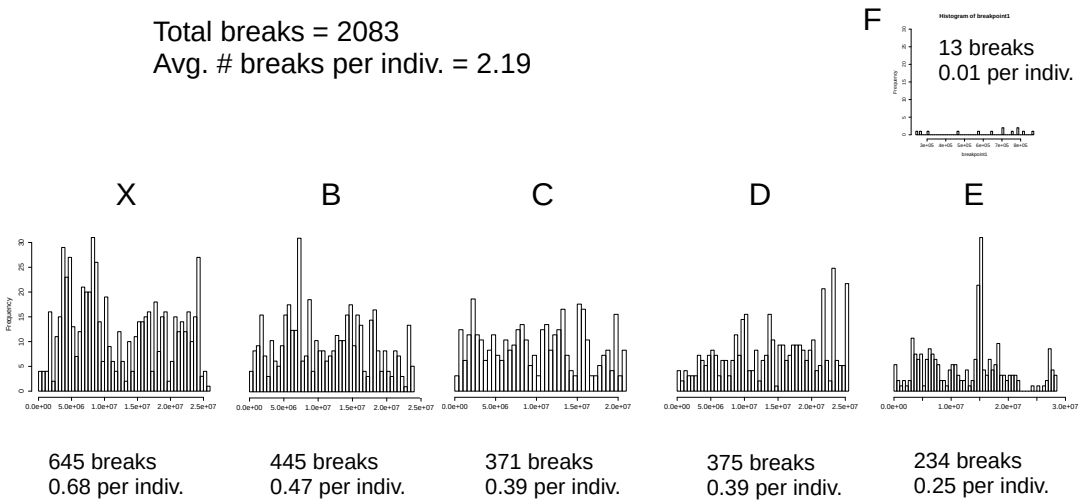

Supplemental Figure S4-3 Genome-wide frequency and distribution of recombination breakpoints

Each histogram summarizes the frequency and distribution of recombination breakpoints for every Muller Element. The x-axis represents the physical map of each Muller Element measured in bp. On average, there were only two breakpoints per genome per individual recombinant.

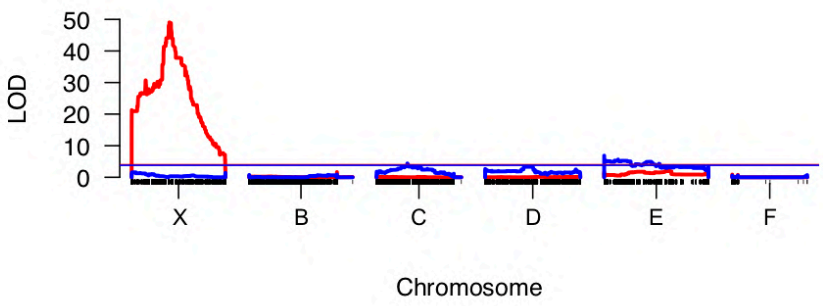

Supplemental Figure S4-4 QTL analysis for wing spot size, excluding spotless individuals

Wing pigmentation QTL map for the *D. elegans* (red) and *D. gunungcola* (blue) backcross, excluding spotless recombinants. LOD (logarithm of the odds) is indicated on the y-axis. The x-axis represents the physical map of Muller Elements X, B, C, D, E, and F based on the *D. elegans* assembled genome. Individual SNP markers are indicated with black tick marks along the x-axis. Horizontal red and blue lines mark p = 0.01 for the *D. elegans* and *D. gunungcola* backcross, respectively.

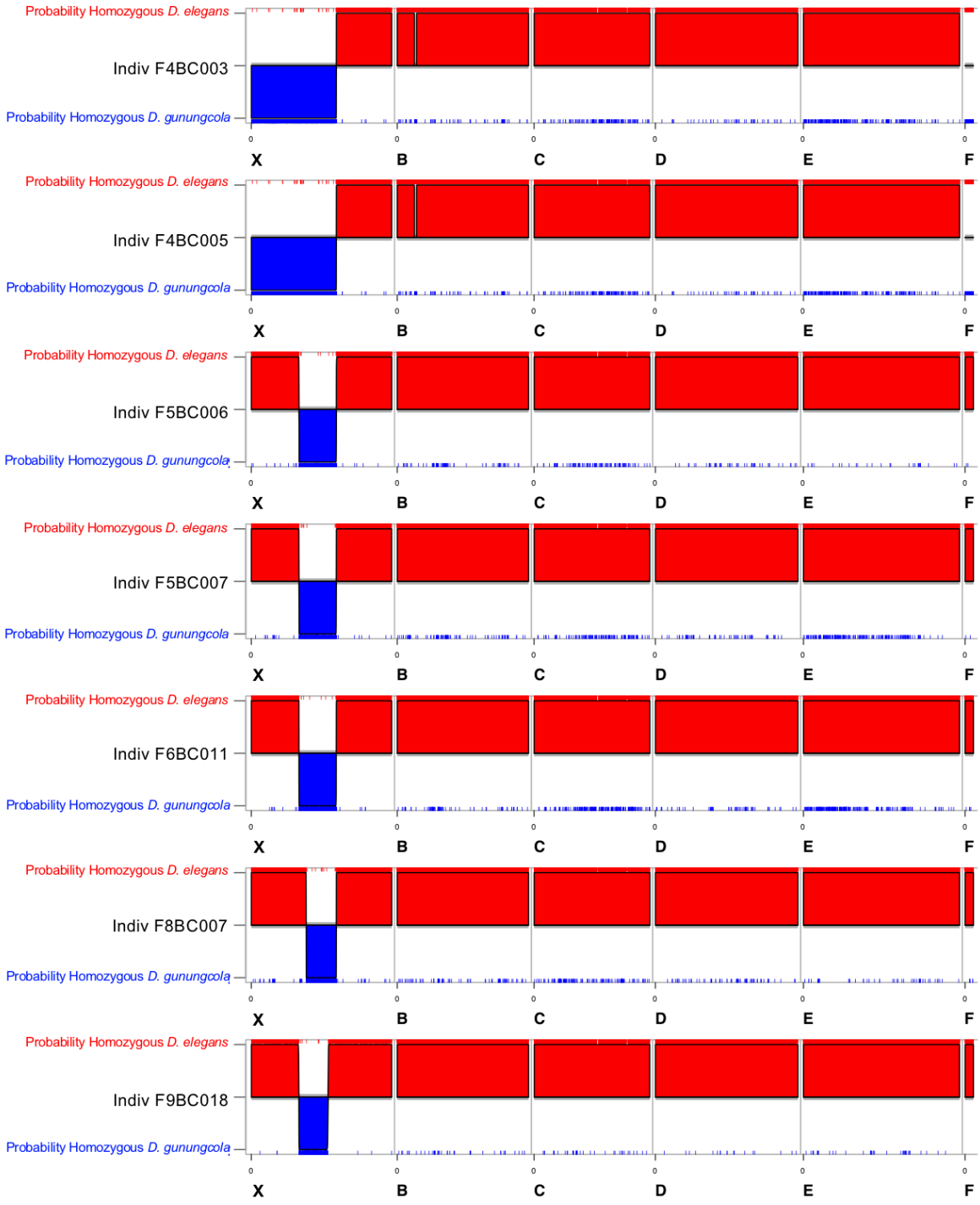
Probability Homozygous D. elegans
Indiv F4BC003
Probability Homozygous D. gunungcola
X B C D E F
Probability Homozygous D. elegans
Indiv F4BC005
Probability Homozygous D. gunungcola
X B C D E F
Probability Homozygous D. elegans
Indiv F5BC006
Probability Homozygous D. gunungcola
X B C D E F
Probability Homozygous D. elegans
Indiv F5BC007
Probability Homozygous D. gunungcola
X B C D E F
Probability Homozygous D. elegans
Indiv F6BC011
Probability Homozygous D. gunungcola
X B C D E F
Probability Homozygous D. elegans
Indiv F8BC007
Probability Homozygous D. gunungcola
X B C D E F
Probability Homozygous D. elegans
Indiv F9BC018
Probability Homozygous D. gunungcola
X B C D E F

Supplemental Figure S4-5 Representative genome-wide ancestry assignments for seven individuals from the X chromosome introgression experiment

The ancestry states are shown for each Muller element for representative male individuals from F4-F9 backcross generations. The posterior probability that a region is homozygous (Andolfatto *et al*., 2011) for *D. elegans* (red) or *D. gunungcola* (blue) is plotted along the y-axis. Individual SNP markers are indicated with red or blue tick marks along the x-axis. Crossover positions are indicated by a switch from red to blue or blue to red along each chromosome, representing a shift from *D. elegans* to *D. gunungcola* ancestry or *D. gunungcola* to *D. elegans* ancestry, respectively.

Chromosomes	Full[a]	Two QTL[b]	Interaction[c]	Full Additive[d]	Two Additive[e]
X:X	20.02***	1.947	0.0144	20.006***	1.933
X:B	21.33***	3.253	0.0161	21.311***	3.237*
X:C	21.49***	3.412	1.6614	19.824***	1.750
X:D	18.84***	0.763	0.1868	18.649***	0.576
X:E	19.36***	1.289	0.6103	18.752***	0.678
X:F	19.09***	1.016	0.1577	18.931***	0.858
B:B	4.71*	0.788	0.2569	4.453*	0.531
B:C	5.57**	1.644	0.0926	5.474**	1.551
B:D	6.14**	2.216	1.5895	4.549*	0.627
B:E	6.77**	2.845	1.7483	5.019**	1.096
B:F	5.01**	1.083	0.7518	4.254*	0.331
C:C	3.20	1.116	0.1116	3.091	1.004
C:D	4.49*	2.405	1.8687	2.623	0.536
C:E	3.27	1.187	0.5495	2.724	0.637
C:F	2.46	0.371	0.0888	2.369	0.282
D:D	2.31	1.938	0.0584	2.250	1.880
D:E	2.04	1.255	0.8588	1.176	0.396
D:F	1.46	1.090	0.7354	0.725	0.355
E:E	4.82*	4.044*	1.4233	3.401	2.620
E:F	1.71	0.929	0.5999	1.109	0.329
F:F	3.13	2.798	0.7486	2.381	2.049

*P < 0.05, ** P < 0.01, *** P < 0.001

[a] Maximum LOD score for the full model with interactions allowed

[b] Difference between the Full LOD and the maximum single-QTL LOD for the chromosome pair

[c] Difference between the maximum Full and Full Additive LODs

[d] Maximum LOD score for two QTLs with only additive interactions allowed

[e] Difference in LODs between the Full Additive model and the maximum single QTL model for the chromosome pair

Supplemental Table S4-1 Results of two-QTL scan for max wing display angle in D. elegans backcross

Chromosomes	Full[a]	Two QTL[b]	Interaction[c]	Full Additive[d]	Two Additive[e]
X:X	5.44**	1.212	0.56884	4.87	0.643
X:B	10.75***	5.288	0.00381	10.74***	5.285**
X:C	5.65**	1.423	0.00193	5.65**	1.421
X:D	5.29**	1.059	0.53058	4.76*	0.529
X:E	13.10***	5.490**	0.26490	12.83***	5.225**
X:F	5.60**	1.373	0.39196	5.21**	0.981
B:B	7.61**	2.152	1.23537	6.38**	0.917
B:C	6.97**	1.512	0.40271	6.57**	1.109
B:D	6.42**	0.958	0.68002	5.74**	0.278
B:E	14.70***	7.098**	0.15974	14.54***	6.938**
B:F	6.48**	1.024	0.03732	6.45**	0.987
C:C	3.11	1.977	0.18173	2.93	1.795
C:D	2.82	1.694	1.37202	1.45	0.322
C:E	9.20**	1.596	0.40867	8.79**	1.187
C:F	3.03	1.899	1.01448	2.01	0.884
D:D	2.25	1.907	0.61844	1.63	1.288
D:E	8.24**	0.630	0.02843	8.21**	0.601
D:F	2.29	1.386	0.98636	1.30	0.400
E:E	8.53**	0.922	0.50165	8.03**	0.421
E:F	10.84***	3.237	2.08462	8.76**	1.152
F:F	3.55	2.652	1.05307	2.50	1.599

*P < 0.05, ** P < 0.01, *** P < 0.001

[a] Maximum LOD score for the full model with interactions allowed

[b] Difference between the Full LOD and the maximum single-QTL LOD for the chromosome pair

[c] Difference between the maximum Full and Full Additive LODs

[d] Maximum LOD score for two QTLs with only additive interactions allowed

[e] Difference in LODs between the Full Additive model and the maximum single QTL model for the chromosome pair

Supplemental Table S4-2 Results of two-QTL scan for max wing display angle in D. gunungcola backcross

Trait	Backcross	Chromosome	QTL interval (bp)[a]	QTL peak (bp)	LOD
Wing spot size	*D. elegans*	X	10,117,675-10,748,234	10,303,766	49.1
Wing spot size	*D. gunungcola*	C	6,655,757-12,279,025	8,420,192	4.37
Wing spot size	*D. gunungcola*	E	10,907-4,009,870	12,292	6.85

[a] LOD drop 1.5 support interval

Supplemental Table S4-3 QTLs detected for wing spot size, excluding spotless individuals

Appendix D

Book chapter: The genetic basis of pigmentation differences within and between species

CHAPTER TWO

The Genetic Basis of Pigmentation Differences Within and Between *Drosophila* Species

J.H. Massey, P.J. Wittkopp[1]
University of Michigan, Ann Arbor, MI, United States
[1]Corresponding author: e-mail address: wittkopp@umich.edu

Contents

Abstract

In *Drosophila*, as well as in many other plants and animals, pigmentation is highly variable both within and between species. This variability, combined with powerful genetic and transgenic tools as well as knowledge of how pigment patterns are formed biochemically and developmentally, has made *Drosophila* pigmentation a premier system for investigating the genetic and molecular mechanisms responsible for phenotypic evolution. In this chapter, we review and synthesize findings from a rapidly growing body of case studies examining the genetic basis of pigmentation differences in the abdomen, thorax, wings, and pupal cases within and between *Drosophila* species. A core set of genes, including genes required for pigment synthesis (eg, *yellow*, *ebony*, *tan*, *Dat*) as well as developmental regulators of these genes (eg, *bab1*, *bab2*, *omb*, *Dll*, and *wg*), emerge as the primary sources of this variation, with most genes having been shown to contribute to pigmentation differences both within and between species. In cases where specific genetic changes contributing to pigmentation divergence

Current Topics in Developmental Biology, Volume 119
ISSN 0070-2153
http://dx.doi.org/10.1016/bs.ctdb.2016.03.004

were identified in these genes, the changes were always located in noncoding sequences and affected *cis*-regulatory activity. We conclude this chapter by discussing these and other lessons learned from evolutionary genetic studies of *Drosophila* pigmentation and identify topics we think should be the focus of future work with this model system.

1. INTRODUCTION

Heritable changes in DNA sequence within and among species explain much of life's diversity. Identifying these changes and understanding how they impact development to generate phenotypic differences remains a major challenge for evolutionary biology. A growing number of case studies have localized the specific genes involved in trait variation both within and among species, and some have described how individual mutations affect the developmental pathways underlying phenotypic differences. With a catalog of studies describing more than 1000 alleles contributing to morphological, physiological, or behavioral evolution of diverse traits in diverse species now available, researchers have begun to synthesize the genetic and developmental mechanisms underlying phenotypic evolution in search of genetic and molecular patterns that underlie the evolutionary process (Carroll, 2008; Kopp, 2009; Martin & Orgogozo, 2013; Stern & Orgogozo, 2008; Streisfeld & Rausher, 2011).

One finding from this synthesis is that different types of traits tend to evolve through different molecular mechanisms. For example, changes in *cis*-regulatory DNA sequences that regulate gene expression contribute to morphological differences within and among species more often than they contribute to differences in physiological traits, while the converse is true for changes in the amino acid sequence of proteins (Stern & Orgogozo, 2008, 2009). Another finding to emerge from this synthesis is that some traits have evolved multiple times independently using the same genetic changes (eg, xenobiotic resistance), whereas other traits have evolved similar changes using different mutations in the same gene (eg, coat color) or using different genes (Martin & Orgogozo, 2013). Differences in the genetic basis of phenotypic diversity also seem to exist within and between species, with changes in *cis*-regulatory sequences playing a larger role in interspecific than intraspecific differences (Coolon, Mcmanus, Stevenson, Graveley, & Wittkopp, 2014; Stern & Orgogozo, 2008; Wittkopp, Haerum, & Clark, 2008).

In this chapter, we examine patterns in the genetic and molecular mechanisms responsible for phenotypic evolution that emerge from focusing on a collection of studies investigating changes in a single trait within and among species in the same genus. Specifically, we review and synthesize the collection of case studies dissecting the genetic basis of body color (pigmentation) in *Drosophila*, emphasizing a comparison of genetic and molecular mechanisms that vary within and among *Drosophila* species. *Drosophila* pigmentation is an ideal trait for such an analysis because (i) pigmentation is one of the most variable traits within and among species (Kopp, 2009; Wittkopp, Carroll, & Kopp, 2003), (ii) much is known about the genes involved in pigment synthesis as well as those that control expression of these genes during *Drosophila* development (Kopp, 2009; Takahashi, 2013; True, 2003; Wittkopp, Carroll, et al., 2003), and (iii) specific genes and genetic changes have been identified as contributing to differences in *Drosophila* pigmentation that have evolved over multiple timescales and in multiple lineages (Table 1). These differences in pigmentation that have been dissected genetically include examples of trait divergence, convergent evolution, and evolutionary novelty.

2. DEVELOPMENT OF *DROSOPHILA* PIGMENTATION

In *Drosophila* (as well as in many other insects; True, 2003; Wittkopp & Beldade, 2009; Zhan et al., 2010), body color results from a combination of dark black and brown melanins as well as light yellow-tan and colorless sclerotins (True, 2003; Wittkopp, Carroll, et al., 2003; Wright, 1987). These four types of pigments are produced by a branched biochemical pathway that processes tyrosine obtained from the diet (Fig. 1). Tyrosine is first converted into DOPA (L-3,4-dihydroxyphenylalanine) by a tyrosine hydroxylase (TH) encoded by the *pale* gene. This DOPA is then converted into dopamine through a reaction catalyzed by the dopa decarboxylase enzyme encoded by the *Ddc* gene. Prior reviews have suggested that DOPA can also be polymerized into a black melanin through a process involving the Yellow protein (Kopp, 2009; Wittkopp, Carroll, et al., 2003), but recent data show that the formation of black pigment requires the function of *Ddc* (J.-M. Gibert, personal communication) and is thus likely produced from dopamine rather than DOPA, as has also been previously suggested (Riedel, Vorkel, & Eaton, 2011; Walter et al., 1996). Dopamine can then have one of four fates: it can be converted into a black melanin through a

Table 1 The Loci of Pigmentation Evolution in *Drosophila*

Level of Variation	Pigmentation Trait	Species	Gene(s)	Gene Function	Type of Mutation(s)	References
Within species	Abdominal	*D. melanogaster*	*bab*	TF	*cis*-Regulatory	Rogers et al. (2013)
Within species	Abdominal	*D. melanogaster*	*bab1*	TF	*cis*-Regulatory	Bastide et al. (2013)
Within species	Abdominal	*D. melanogaster*	*bab1*	TF	*cis*-Regulatory	Endler, Betancourt, Nolte, and Schlötterer (2016)
Within species	Abdominal	*D. melanogaster*	*bab*	TF	Unknown	Kopp, Graze, Xu, Carroll, and Nuzhdin (2003)
Within species	Abdominal	*D. melanogaster*	*bab1*	TF	*cis*-Regulatory	Bickel, Kopp, and Nuzhdin (2011)
Within species	Abdominal	*D. melanogaster*	*bab2*	TF	*cis*-Regulatory	Bickel et al. (2011)
Within species	Abdominal	*D. melanogaster*	*ebony*	Enzyme	*cis*-Regulatory	Johnson et al. (2015)
Within species	Abdominal	*D. melanogaster*	*ebony*	Enzyme	*cis*-Regulatory	Pool and Aquadro (2007)
Within species	Abdominal	*D. melanogaster*	*ebony*	Enzyme	*cis*-Regulatory	Rebeiz, Pool, Kassner, Aquadro, and Carroll (2009)
Within species	Abdominal	*D. polymorpha*	*omb*	TF	Unknown	Brisson, Templeton, and Duncan (2004)
Within species	Abdominal	*D. melanogaster*	*tan*	Enzyme	*cis*-Regulatory	Bastide et al. (2013)
Within species	Abdominal	*D. melanogaster*	*tan*	Enzyme	*cis*-Regulatory	Endler et al. (2016)
Within species	Abdominal	*D. erecta*	*tan*	Enzyme	*cis*-Regulatory	Yassin et al. (2016)
Within species	Abdominal	*D. polymorpha*	Two genes	Unknown	Unknown	Martinez and Cordeiro (1970)

Within species	Abdominal	*D. melanogaster*	84 genes	Multiple	*cis*-Regulatory	Dembeck, Huang, Magwire, et al. (2015)
Within species	Abdominal	*D. baimaii* *D. bicornuta* *D. burlai* *D. truncata*	Unknown	NA	Unknown	Ohnishi and Watanabe (1985)
Within species	Abdominal	*D. malerkotliana*	At least three QTL	NA	Unknown	Ng, Hamilton, Frank, Barmina, and Kopp (2008)
Between species	Abdominal	*D. melanogaster* *D. yakuba* *D. fuyamai* *D. auraria*	*bab*	TF	*cis*-Regulatory	Rogers et al. (2013)
Between species	Abdominal	*D. willistoni* *D. melanogaster*	*bab1*	TF	*cis*-Regulatory	Williams et al. (2008)
Between species	Abdominal	*D. auraria* *D. serrata*	*ebony*	Enzyme	*cis*-Regulatory	Johnson et al. (2015)
Between species	Abdominal	*D. americana* *D. novamexicana*	*ebony*	Enzyme	Unknown	Wittkopp et al. (2009)
Between species	Abdominal	*D. yakuba* *D. santomea*	*tan*	Enzyme	*cis*-Regulatory	Jeong et al. (2008)
Between species	Abdominal	*D. americana* *D. novamexicana*	*tan*	Enzyme	*cis*-Regulatory	Wittkopp et al. (2009)

Continued

Table 1 The Loci of Pigmentation Evolution in *Drosophila*—cont'd

Level of Variation	Pigmentation Trait	Species	Gene(s)	Gene Function	Type of Mutation(s)	References
Between species	Abdominal	*D. melanogaster* *D. subobscura* *D. virilis*	*yellow*	Unknown	*cis*-Regulatory	Wittkopp et al. (2002)
Between species	Abdominal	*D. melanogaster* *D. kikkawai*	*yellow*	Unknown	*cis*-Regulatory	Jeong, Rokas, and Carroll (2006)
Between species	Abdominal	*D. prostipennis* *D. melanogaster*	*yellow*	Unknown	*cis*-Regulatory	Ordway, Hancuch, Johnson, Wiliams, and Rebeiz (2014)
Between species	Abdominal	*D. yakuba* *D. santomea*	At least four QTL	NA	Unknown	Carbone, Llopart, deAngelis, Coyne, and Mackay (2005)
Between species	Abdominal	*D. yakuba* *D. santomea*	At least five QTL	NA	Unknown	Llopart, Elwyn, Lachaise, and Coyne (2002)
Between species	Abdominal	*D. arawakan* *D. nigrodunni*	Unknown	NA	Unknown	Hollocher, Hatcher, and Dyreson (2000)
Between species	Abdominal	*D. tenebrosa* *D. suboccidentalis*	At least two QTL	NA	Unknown	Bray, Werner, and Dyer (2014)
Within species	Thorax	*D. melanogaster*	*ebony*	Enzyme	*cis*-Regulatory	Miyagi, Akiyama, Osada, and Takahashi (2015)
Within species	Thorax	*D. melanogaster*	*ebony*	Enzyme	*cis*-Regulatory	Takahashi, Takahashi, Ueda, and Takano-Shimizu (2007)
Within species	Thorax	*D. melanogaster*	*ebony*	Enzyme	*cis*-Regulatory	Takahashi and Takano-Shimizu (2011)

Within species	Thorax	*D. melanogaster*	*ebony*	Enzyme	*cis*-Regulatory	Telonis-Scott, Hoffmann, and Sgro (2011)
Between species	Thorax	*D. guttifera* *D. melanogaster*	*wg*	Cell–cell signaling	*cis*-Regulatory	Koshikawa et al. (2015)
Between species	Wing	*D. biarmipes* *D. melanogaster*	*yellow*	Unknown	*cis*-Regulatory	Gompel, Prud'homme, Wittkopp, Kassner, and Carroll (2005)
Between species	Wing	*D. elegans* *D. gunungcola* *D. mimetica* *D. tristes*	*yellow*	Unknown	*cis*-Regulatory	Prud'homme et al. (2006)
Between species	Wing	*D. guttifera* *D. melanogaster*	*wg*	Cell–cell signaling	*cis*-Regulatory	Koshikawa et al. (2015)
Between species	Wing	*D. elegans* *D. gunungcola*	At least three QTL	NA	Unknown	Yeh and True (2014)
Between species	Pupariam	*D. virilis* *D. americana*	*Dat*	Enzyme	*cis*-Regulatory	Ahmed-Braimah and Sweigart (2015)

This table summarizes case studies that have examined the genetic basis of pigmentation differences within and between species of *Drosophila*.

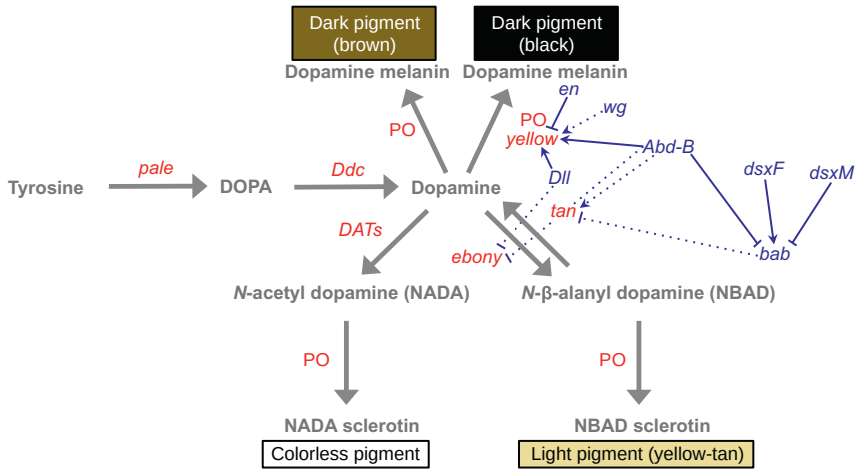

Fig. 1 Developmental and biochemical control of pigmentation in *Drosophila*. A simplified version of the biochemical pathway controlling pigment biosynthesis in insects is shown with regulators controlling expression of individual pigment synthesis genes in at least one *Drosophila* species overlaid. Genes colored *red* (placed next to thick arrows) are part of the pigment biosynthesis pathway, metabolites are colored *gray*, and *gray arrows* indicate chemical reactions during pigmentation synthesis. Genes colored *blue* (at ends of thin pointed and blunt arrows) are part of the regulatory network that directly (*solid arrows*) or indirectly (*broken arrows*) modulate enzyme expression during pigmentation development in *Drosophila*. *Pointed* and *blunt arrows* indicate positive and negative regulatory interactions, respectively. The pigment biosynthesis pathway is conserved among all *Drosophila*, but the regulatory relationships shown often function in only a subset of *Drosophila* species (Arnoult et al., 2013; Gompel et al., 2005).

process involving the Yellow protein and phenol oxidases (POs); converted into a brown melanin through a process involving POs, but not *yellow*; into a yellow-tan sclerotin through the activity of Ebony converting dopamine into beta-alanyl dopamine (NBAD) and POs polymerizing it into NBAD sclerotin, or into a colorless pigment through the activity of dopamine-acetyl-transferases (DATs) converting dopamine into *N*-acetyl dopamine (NADA) and POs polymerizing it into NADA sclerotin. One of these reactions, the conversion of dopamine into NBAD, is reversible, with the reverse reaction catalyzed by the Tan protein. Disruption of the *tan* gene reduces the production of dark melanins, indicating that the conversion of NBAD back into dopamine is a necessary step in the development of pigmentation. Changing relative expression levels of *yellow*, *ebony*, and/or *tan* can shift the balance between dark (black, brown) and yellow-tan pigments

as this branched biochemical pathway produces more of one type at the expense of the other (Wittkopp et al., 2009; Wittkopp, True, & Carroll, 2002).

Pigments produced by this biochemical pathway are deposited into the developing cuticle during late pupal and early adult stages (Kraminsky et al., 1980; Sugumaran, Giglio, Kundzicz, Saul, & Semensi, 1992; Walter et al., 1996; Wittkopp, Carroll, et al., 2003). The spatial distribution of these pigments is determined in a nearly cell autonomous manner by spatially regulated transcription of genes such as *yellow*, *tan*, and *ebony*. As discussed in detail later, changes in the expression patterns of these genes often underlie evolutionary changes in pigmentation. Genes regulating expression of these pigment synthesis genes are thus also potential targets for genetic divergence contributing to pigmentation diversity. Five transcription factors (*bric-a-brac* (*bab*), *abdominal-B* (*Abd-B*), *doublesex* (*dsx*), *Distal-less* (*Dll*), and *Engrailed* (*en*)) have been shown to regulate expression of pigment synthesis genes (*yellow*, *ebony*, *tan*) in *Drosophila* either directly (by binding to transcription factor binding sites located in enhancers controlling the gene's expression) or indirectly (by influencing abundance, activity, or binding of direct regulators; Fig. 1; Arnoult et al., 2013; Gompel et al., 2005; Jeong et al., 2006; Kopp, Duncan, Godt, & Carroll, 2000; Williams et al., 2008). For example, in at least one *Drosophila* species each, En (Gompel et al., 2005), Dll (Arnoult et al., 2013), and Abd-B (Jeong et al., 2006) have all been shown to directly bind to *yellow* enhancers, whereas Abd-B and Dsx (including both the male (dsxM) and female (dsxF) forms of dsx) have been shown to directly bind to enhancers of the *bab* gene (Williams et al., 2008). It is not yet known whether Bab proteins directly bind to enhancers of any pigment synthesis genes, but it is clear that Bab proteins affect expression of pigment synthesis genes in some manner (Kopp, 2009). Similarly, Wingless (Wg, a ligand for a signal transduction pathway) (Koshikawa et al., 2015; Werner, Koshikawa, Williams, & Carroll, 2010) has also been shown to influence expression of at least one pigment synthesis gene (Fig. 1), although questions remain about the precise molecular mechanisms by which it does so. Additional transcription factors with effects on abdominal pigmentation in *Drosophila melanogaster* have been identified in recent RNAi screens (Kalay, 2012; Rogers et al., 2014), but the ways in which they alter expression of pigment synthesis genes remain unknown. Elucidating the structure and complexity of the gene network regulating expression of pigment synthesis genes (and hence pigmentation) remains one of the biggest challenges for understanding the development and evolution of *Drosophila* pigmentation within and between species.

3. TISSUE-SPECIFIC REGULATION OF PIGMENTATION

Null mutations disrupting the function of proteins required for pigment synthesis such as TH, DDC, Yellow, Tan, Ebony, DATs, and POs alter pigmentation throughout the fly, whereas mutations in specific enhancers of these genes and mutations affecting transcriptional regulators of these genes typically alter pigmentation in only some parts of the fly. Evolutionary changes in pigmentation are often restricted to specific body parts, suggesting that such changes are likely to result from these latter types of mutations. One reason for this may be that null mutations in pigment synthesis genes often also alter behavior and/or other phenotypes in addition to pigmentation (Takahashi, 2013; True, 2003; Wittkopp & Beldade, 2009), making null mutations unlikely to survive in natural populations. The presence of tissue-specific enhancers for pigment synthesis genes coupled with differences in the sets of regulators that interact with each enhancer provide genetic mechanisms for overcoming these pleiotropic constraints and altering pigmentation independently in different body parts. Because the developmental control of pigmentation in different body regions often involves different regulatory genes, we have chosen to structure our review of the genetic mechanisms underlying pigmentation differences within and between *Drosophila* species by body part, examining the evolution of abdominal pigmentation, thorax pigmentation, wing pigmentation, and pupal pigmentation in *Drosophila* separately below.

4. ABDOMINAL PIGMENTATION

Abdominal pigment patterns (especially those on the dorsal side of the abdomen) are conspicuous and highly variable within and among species (Wittkopp, Carroll, et al., 2003; Rebeiz, Pool, et al., 2009; Rebeiz, Ramos-Womack, et al., 2009). It is not surprising then that most studies of genetic mechanisms underlying pigmentation differences in *Drosophila* have attempted to explain differences in intra- and interspecific abdominal pigmentation. These abdominal pigment patterns are displayed in a series of overlapping tergites that can vary in pigment color, pattern, and intensity among individuals and sexes in the same population, different populations, and different species (Kronforst et al., 2012; Wittkopp, Carroll, et al., 2003). For example, in *D. melanogaster* females, the most prominent abdominal tergites (A2–A6) show a "stripe" of dark melanins at the posterior edge of the

Fig. 2 Abdominal pigmentation in *D. melanogaster*. The dorsal abdomen of *D. melanogaster* is shown for wild-type adult females (*left*) and males (*right*). Note the dark pigment stripe visible at the posterior edge of abdominal segments A2–A6 in females and A2–A4 in males as well as the more complete melanization in tergites A5 and A6 of males relative to females.

segment as well as a peak of this dark color along the dorsal midline (Fig. 2, left). In male *D. melanogaster*, this pattern is seen in the A2, A3, and A4 tergites, but A5 and A6 are much more completely covered by dark melanins (Fig. 2, right). Sexually dimorphic pigmentation is absent in many species, however, with both sexes showing the same pigmentation pattern in all segments (Kopp et al., 2000). The pattern of pigmentation within each segment can also vary, with modifications to the shape of the stripe, unique patterns such as spots, and melanins distributed evenly throughout the abdomen as seen in different species (Wittkopp, Carroll, et al., 2003). Differences in abdominal pigmentation are generally assumed to result from adaptation, but the selection pressures responsible for the evolution of a particular pattern in a particular species remain unclear. Potential selection pressures proposed for divergent abdominal pigmentation include sexual selection resulting from mate choice as well as environmental factors that differ across gradients of altitude, latitude, temperature, humidity, and UV radiation (Bastide, Yassin, Johanning, & Pool, 2014; Brisson, De Toni, Duncan, & Templeton, 2005; Capy, David, & Robertson, 1988; Clusella-Trullas & Terblanche, 2011; Kopp et al., 2000; Matute & Harris, 2013; True, 2003; Wittkopp et al., 2011).

4.1 Genetic Basis of Abdominal Pigmentation Differences Within a Species

In *D. melanogaster*, the most studied of all *Drosophila* species, abdominal pigmentation often varies within and among populations. For example, in sub-Saharan Africa, *D. melanogaster* collected from low elevations showed lighter

abdominal pigmentation than *D. melanogaster* collected from high elevations (Pool & Aquadro, 2007); these differences persisted when rearing these flies in the lab, demonstrating that the differences in pigmentation were caused by genetic differences rather than phenotypic plasticity. Genetic analysis implicated one or more loci on the X and 3rd chromosomes in this pigmentation difference, and analysis of the pigment synthesis gene *ebony*, which is required for the synthesis of yellow-tan pigments and is located on the 3rd chromosome, revealed distinct haplotypes in populations from different altitudes that correlated with these differences in abdominal pigmentation. Nucleotide diversity levels within this region suggested that natural selection has elevated the frequency of dark *ebony* alleles in one of the populations sampled from Uganda, possibly facilitating adaptation to different altitudes (Pool & Aquadro, 2007). Further analysis identified a *cis*-regulatory element in this region that controls *ebony* expression in the abdomen and showed that the allele of this sequence from a lightly pigmented fly drives higher levels of *ebony* expression than the allele of this sequence found in a more darkly pigmented fly (Rebeiz, Pool, et al., 2009), consistent with Ebony's function in the synthesis of light-colored sclerotin (Walter et al., 1996). This region was also found to have recently accumulated multiple mutations in the Uganda population that appear to have given rise to an allele of large effect that contributes to divergence of abdominal pigmentation (Rebeiz, Pool, et al., 2009).

Genetic differences in *ebony cis*-regulatory sequences also appear to contribute to variable abdominal pigmentation in other populations of *D. melanogaster* and other species (Bastide et al., 2013; Dembeck, Huang, Magwire, et al., 2015; Endler et al., 2016; Johnson et al., 2015). For example, an association study using the Drosophila Genetic Reference Panel (DGRP) of *D. melanogaster* strains isolated from a population in Raleigh, North Carolina (Mackay et al., 2012) found a significant correlation between a noncoding variant located within a known *cis*-regulatory element of *ebony* and pigmentation variation within this population (Dembeck, Huang, Magwire, et al., 2015). Weak associations with noncoding SNPs in *ebony cis*-regulatory elements were also observed for European populations of *D. melanogaster* (Bastide et al., 2013; Dembeck, Huang, Carbone, & Mackay, 2015; Endler et al., 2016), with the most highly ranked SNP associated with *ebony* in Bastide et al. (2013) located in a sequence that inhibits *ebony* expression in male abdominal segments during development (Rebeiz, Pool, et al., 2009; Rebeiz, Ramos-Womack, et al., 2009). Outside of *D. melanogaster*, genetic variation linked to *ebony* has been shown to be

associated with polymorphic abdominal pigmentation within *Drosophila americana* (Wittkopp et al., 2009) and *Drosophila auraria* (Johnson et al., 2015). In this latter species, specific alleles of *ebony cis*-regulatory sequences were identified in light and dark individuals, and transgenic analyses of reporter genes were used to demonstrate the effects of these variable sites on *ebony* expression (Johnson et al., 2015). These *cis*-regulatory changes in *D. auraria* are located in a sequence that represses pigmentation in males (Johnson et al., 2015), but does not overlap with the male-specific enhancer (MSE) identified previously in *D. melanogaster* (Rebeiz, Pool, et al., 2009; Rebeiz, Ramos-Womack, et al., 2009).

The *tan* gene, which plays the opposite role of *ebony* in pigment synthesis, promoting production of dark brown melanin at the expense of yellow-tan sclerotin, also contributes to pigmentation variation within *Drosophila* species. In fact, the study that found evidence of an association between *ebony* genotype and abdominal pigmentation within the DGRP collection also identified multiple SNPs within noncoding regions near *tan* that were associated with differences in abdominal pigmentation in this population of *D. melanogaster* (Dembeck, Huang, Magwire, et al., 2015). Three of these noncoding SNPs were also found to be associated with abdominal pigmentation in European populations and an African population of *D. melanogaster* (Bastide et al., 2013; Endler et al., 2016). These SNPs were located within a *cis*-regulatory element known as the MSE (Jeong et al., 2008) that drives expression in *D. melanogaster* in the abdominal stripes as well as throughout the A5 and A6 abdominal segments with male-specific pigmentation. *tan cis*-regulatory evolution at the MSE was also recently implicated in a sex-specific color dimorphism involving abdominal pigmentation differences within *Drosophila erecta* (Yassin et al., 2016). This final case study is particularly interesting because ancient balancing selection was shown to likely be responsible for maintaining alternative alleles at the *tan* MSE and thus both light and dark morphs of female *D. erecta* (Yassin et al., 2016).

Genetic changes contributing to polymorphic pigmentation are not always caused by pigmentation synthesis genes such as *ebony* and *tan*; changes in regulatory genes upstream of the pigmentation synthesis pathway contribute to pigmentation differences segregating within a species as well. These sources of variation include genetic changes at the *bab* locus, a locus originally discovered to be an important regulator of abdominal pigmentation differences between sexes in *D. melanogaster* (Kopp et al., 2000). Null mutations in *bab* cause the development of a male-like pigmentation pattern in the A5 and A6 abdominal segments of female *D. melanogaster*, suggesting that

bab acts to repress male-specific abdominal pigmentation in females (Kopp et al., 2000). Using quantitative trait locus (QTL) mapping coupled with quantitative complementation tests to examine the genetic basis of abdominal pigmentation differences in a population of *D. melanogaster* from Winters, California, Kopp et al. (2003) found genetic variation at *bab* had a major effect on abdominal pigmentation differences in females. The *bab* locus includes two genes, *bab1* and *bab2*, each of which acts as a transcriptional regulator, and it was unclear in Kopp et al. (2003) if variation affecting *bab1* and/or *bab2* was responsible for variation in abdominal pigmentation. To address this uncertainty, Bickel et al. (2011) sequenced the *bab* region in multiple inbred lines from the California population and found that noncoding SNPs at both *bab1* and *bab2* were associated with abdominal pigmentation differences. Specifically, SNPs associated with pigmentation were found in the first intron of *bab1* and near the promoter region of *bab2*. In the DGRP collection, European populations, and an African population of *D. melanogaster*, only SNPs in the first intron of *bab1* were associated with abdominal pigmentation variation (Bastide et al., 2013; Dembeck, Huang, Carbone, et al., 2015; Dembeck, Huang, Magwire, et al., 2015; Endler et al., 2016). A *cis*-regulatory element controlling sex-specific expression of *bab1* in the A5–A7 segments in *D. melanogaster* males (repression) and females (induction) was also identified in the first intron of *bab1* (Williams et al., 2008) and overexpression of *bab1* during late pupal development was shown to be sufficient to suppress dark pigmentation (Salomone, Rogers, Rebeiz, & Williams, 2013), suggesting that the associated sites might alter pigmentation by altering expression of *bab1*. Indeed, Rogers et al. (2014) found that different alleles of this element were present in lightly and darkly pigmented *D. melanogaster* that drove different patterns of gene expression that correlate with pigmentation in the manner expected given *bab*'s role as a repressor of dark pigmentation. A small number of derived sequence changes were found to be responsible for these differences in *cis*-regulatory activity (Rogers et al., 2014). Genetic variation linked to another regulator of pigmentation, *omb*, has also been found to be associated with polymorphic body color in *Drosophila polymorpha*, but much less is known about this association, including whether coding or noncoding changes are more likely to be responsible for the association (Brisson et al., 2004).

Together, the studies described earlier demonstrate that genetic variation contributing to variable abdominal pigmentation within a species has repeatedly accumulated at noncoding regions near the *ebony*, *tan*, and *bab1* genes.

In fact, in the European *D. melanogaster* population studied in Bastide et al. (2013), 79% of the most strongly associated SNPs mapped to noncoding regions linked to *ebony*, *tan*, and *bab1*. Other loci also clearly contribute to polymorphic abdominal pigmentation, however (Dembeck, Huang, Carbone, et al., 2015; Dembeck, Huang, Magwire, et al., 2015; Ng et al., 2008), and some of these loci have recently begun to be identified in *D. melanogaster* (Dembeck, Huang, Carbone, et al., 2015; Dembeck, Huang, Magwire, et al., 2015). The developmental role that these newly identified genes (eg, *pinstripe*, *triforce*, *plush*, and *farmer*) play in pigment patterning remains unknown.

4.2 Genetic Basis of Abdominal Pigmentation Differences Between Species

Differences in pigmentation between species have evolved over longer timescales than differences in pigmentation within a species, suggesting that even phenotypically similar changes in pigmentation might have a distinct genetic basis within and between species (Orr, 2001). For example, different genes and/or different types of changes in the same genes might tend to contribute to phenotypic differences that have evolved over longer evolutionary timescales (Orr, 2001; Stern & Orgogozo, 2009). By directly comparing the genetic basis of intra- and interspecific pigmentation differences, we can better understand how the variants underlying polymorphism within a species give rise to divergence between species. In this section, we review what is known about the genetic basis of abdominal pigmentation differences between species.

The genetic basis of pigmentation differences between species can be dissected genetically using the same methods used to identify genes contributing to intraspecific polymorphism if two species with differences in pigmentation are closely related enough that they can still be crossed and produce viable offspring in the laboratory. One such species pair is *D. yakuba* and *D. santomea*, which are estimated to have begun diverging ~400,000 years ago (Cariou, Silvain, Daubin, Da Lage, & Lachaise, 2001) (Fig. 3). *D. yakuba* exhibits stripes of dark melanins in A2–A6 in both sexes as well as more complete dark pigmentation in segments A5 and A6 of males similar to *D. melanogaster* (Fig. 2B), whereas *D. santomea* lacks dark melanin in these regions in both sexes (Jeong et al., 2008). QTL mapping was used to identify regions of the genome contributing to abdominal pigmentation divergence between these two species. In Llopart et al. (2002), five QTLs were identified, one of which was on the X chromosome and

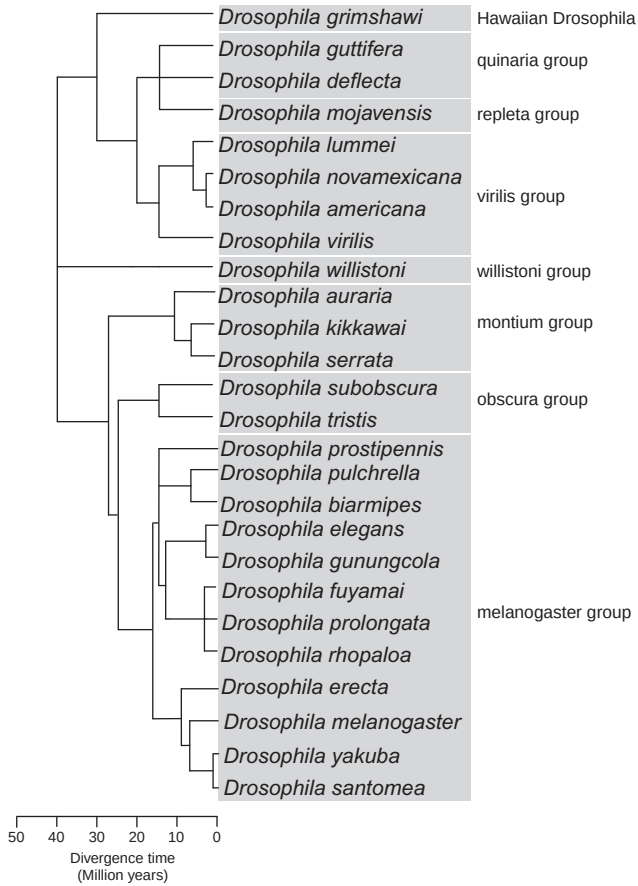

Fig. 3 Phylogeny of *Drosophila* species used to study the genetic basis of pigmentation evolution. Phylogenetic relationships shown were inferred using the online Interactive Tree of Life (iTOL) (Letunic & Bork, 2007, 2011), with branch lengths estimated using data from the online Time Tree website (Hedges, Dudley, & Kumar, 2006).

explained nearly 90% of the species differences. Using a slightly different phenotyping procedure, Carbone et al. (2005) identified four QTL, two located on the X chromosome (one with a much larger effect on pigmentation than the other) and two located on autosomes.

To identify the specific gene(s) that might be responsible for the X-linked QTLs contributing to pigmentation differences between *D. yakuba* and *D. santomea*, Jeong et al. (2008) took a candidate gene approach. Specifically, they examined the pigment synthesis genes *tan* and *yellow*, which were located within the large and small effect X-linked QTLs,

respectively, and found differences in expression of both genes that correlated with differences in abdominal pigmentation between *D. yakuba* and *D. santomea* (Jeong et al., 2008). Analysis of *yellow* and *tan* expression in F1 hybrids from reciprocal crosses showed that only the expression difference in *tan* was caused by *cis*-acting genetic changes on the X chromosome; the difference in *yellow* expression appeared to be caused by one or more *trans*-acting autosomal loci (Jeong et al., 2008). To further localize the genetic changes responsible for divergent *tan* expression and presumably pigmentation, transgenic reporter genes were used to compare enhancer activity of sequences from *D. yakuba* and *D. santomea* in *D. melanogaster*. Three distinct mutations within an MSE located 5′ of *tan* in the genome, each of which reduces *tan* expression, were found to have likely caused, in part, loss of abdominal pigmentation in *D. santomea* (Jeong et al., 2008). This role of *tan* in pigmentation divergence between *D. santomea* and *D. yakuba* was further supported by introgressing the *D. yakuba* allele of *tan* into *D. santomea* and directly demonstrating this gene's contribution to the evolution of abdominal pigmentation differences between these two species (Rebeiz, Ramos-Womack, et al., 2009).

A similar story has emerged for pigmentation differences between the interfertile sister species *D. americana* and *D. novamexicana*, which are also thought to have diverged approximately 400,000 years ago (Morales-Hojas, Vieira, & Vieira, 2008) (Fig. 3). *D. americana* has an overall dark body color typical for a member of the virilis species group, whereas *D. novamexicana* displays a derived light body color with greatly reduced abundance of dark melanins (Wittkopp, Williams, Selegue, & Carroll, 2003). Analysis of F1 hybrids from reciprocal crosses again showed a large contribution of the X chromosome to pigmentation divergence (Wittkopp, Williams, et al., 2003), at least some of which was attributable to loci linked to the *tan* gene (Wittkopp et al., 2009). Fine-scale genetic mapping confirmed that divergence at *tan* was indeed a contributor to pigmentation divergence and localized the functionally divergent sites within *tan* to the first intron (Wittkopp et al., 2009). Subsequent work has shown small, but significant differences in *cis*-regulatory activity of the *D. americana* and *D. novamexicana tan* alleles that presumably contribute to pigmentation differences (Cooley, Shefner, McLaughlin, Stewart, & Wittkopp, 2012). The contribution of *tan* to pigmentation divergence between these two species was further confirmed when the *D. americana tan* allele caused darker pigmentation than the *D. novamexicana tan* allele when each was put into a common *D. melanogaster* genetic background using transgenes

(Wittkopp et al., 2009). Variation linked to the *ebony* gene is also an important source of pigmentation divergence between these two species, with introgression of chromosomal regions containing *tan* and *ebony* from *D. americana* into *D. novamexicana* together explaining 87% of the difference in abdominal pigmentation seen between *D. americana* and *D. novamexicana* (Wittkopp et al., 2009). Effects of *ebony* have yet to be separated from linked loci, however, because *ebony* is located within a region of the genome inverted between these two species, recombination-based mapping is not possible. In all, genetic mapping between *D. americana* and *D. novamexicana* has identified five regions of the genome that contribute to the difference in abdominal pigmentation (Wittkopp et al., 2009; Wittkopp, Williams, et al., 2003).

Variation at *ebony* also appears to be important for abdominal pigmentation differences between the montium subgroup species *D. auraria* and *D. serrata* in the melanogaster group (Johnson et al., 2015), which last shared a common ancestor approximately as long ago as *D. melanogaster* and *D. simulans* (Nikolaidis & Scouras, 1996), that is ~1.5 million years ago (Cutter, 2008) (Fig. 3). In *D. auraria*, males have a stripe of pigment in each abdominal segment similar to *D. melanogaster*, but the more complete pigmentation of male abdominal segments is seen only on A6 rather than in A5 and A6 (Johnson et al., 2015). By contrast, males of *D. serrata* have an abdomen that is more yellow in color overall and lacks dark melanins almost completely in both A5 and A6 (Johnson et al., 2015). Using in situ hybridization, expression of *ebony* was found to be higher in the A5 and A6 segments of *D. serrata* than *D. auraria*, consistent with the role of *ebony* in the formation of yellow-tan sclerotins at the expense of dark melanins (Wittkopp, True, et al., 2002). This evolutionary change in expression appears to have resulted from changes in a *cis*-regulatory element located upstream of *ebony* that controls its expression in the A5 and A6 abdominal segments of males (Johnson et al., 2015).

Another montium subgroup species, *D. kikkawai*, which is estimated to have diverged from *D. melanogaster* ~20 million years ago (Prud'homme et al., 2006) (Fig. 3), has also lost the dark male-specific pigmentation in A5 and A6, but in this case, changes in a MSE of *yellow* that reduce its expression in these segments seem to have played a role (Jeong et al., 2006). Changes in *yellow* expression caused by *cis*-regulatory divergence have also been implicated in an expansion of male-specific abdominal pigmentation to include segments A3 and A4 in *D. prostipennis* relative to *D. takahashi*, two members of the oriental lineage in the melanogaster subgroup (Ordway et al., 2014) (Fig. 3). Interestingly, *D. prostipennis* also showed changes in

ebony and *tan* expression that correlated with the expanded male-specific pigmentation (decrease in *ebony* expression and increase in *tan* expression), but these changes in gene expression were found to be caused by divergence of *trans*-acting loci rather than *cis*-regulatory changes at *ebony* and *tan* (Ordway et al., 2014). Differences in the activity of *yellow cis*-regulatory sequences from *D. melanogaster*, *D. subobscura*, *D. willistoni*, *D. mojavensis*, *D. virilis*, and *D. grimshawi*, much more distantly related species (Fig. 3), that correlate with species-specific pigmentation were also observed when these *cis*-regulatory sequences were assayed in *D. melanogaster* (Kalay & Wittkopp, 2010; Wittkopp, Vaccaro, & Carroll, 2002) (Fig. 3). Observing these changes in *cis*-regulation and gene expression that correlate with divergent abdominal pigmentation for pigment synthesis genes *yellow*, *tan*, and *ebony* strongly suggests that these changes have contributed to pigmentation divergence, although their relative contributions in any individual case remain unknown.

Pigment synthesis genes are not the only source of abdominal pigmentation divergence between species; divergence in a transcription factor regulating expression of pigmentation genes, *bab1*, also plays a role in interspecific differences. In *D. melanogaster*, Bab1 expression represses development of dark pigmentation in segments A5 and A6 of males (Kopp et al., 2000). By contrast, in *D. willistoni*, a species without sexually dimorphic pigmentation in which males and females both have only a stripe of dark melanin near the posterior edge of each tergite, *bab1* is expressed in segments A2–A6 in both sexes (Kopp et al., 2000; Williams et al., 2008). Sex-specific differences in abdominal *bab1* expression seen in *D. melanogaster* were found to be controlled by a dimorphic *cis*-regulatory element containing binding sites for the transcription factors Abd-B and Dsx (Williams et al., 2008). Changes in the binding sites for these transcription factors as well as other changes in the *cis*-regulatory sequence were found to be responsible for the differences in *bab1 cis*-regulatory activity between *D. melanogaster* and *D. willistoni* (Williams et al., 2008). Divergence in this sexually dimorphic *cis*-regulatory element was also found to contribute to interspecific differences in *bab* expression that correlate with differences in female abdominal pigmentation among *D. melanogaster*, *D. yakuba*, *D. fuyamai*, and *D. auraria* (Rogers et al., 2013).

5. THORAX PIGMENTATION

Like abdominal pigmentation, thorax pigmentation varies widely in intensity and patterning within and among *Drosophila* species. Species like

D. guttifera, for example, possess distinctive stripes of black melanin along their thorax that *D. melanogaster* and most other *Drosophila* species lack (Koshikawa et al., 2015). In *D. melanogaster* populations, individuals often vary in the intensity of black and brown melanins that fill a "trident" pattern on the thorax, and variation in this pattern tends to follow altitudinal or latitudinal clines around the world (David & Capy, 1988; Parkash & Munjal, 1999; Telonis-Scott et al., 2011). Intensity of UV radiation was also recently shown to be a good predictor of thorax pigmentation in *D. melanogaster* for clinal variation in Africa, with more darkly pigmented flies found to inhabit regions with higher levels of UV radiation (Bastide et al., 2014). This finding suggests that increased levels of melanin in the thorax may play a protective role for *D. melanogaster* in the wild; however, *D. yakuba* shows the opposite relationship between the intensity of UV radiation and abdominal pigmentation (which is often correlated with thorax pigmentation; Matute & Harris, 2013; Rajpurohit & Gibbs, 2012), indicating that this is not a general relationship for all *Drosophila*. Regardless of the selective forces driving diversity of thorax pigmentation in *Drosophila*, the variety of pigment patterns seen within and among species provides the raw material needed to further investigate the genetic basis of phenotypic evolution.

5.1 Genetic Basis of Thorax Pigmentation Differences Within a Species

In natural populations of *D. melanogaster* and *D. simulans*, variation in a pigmented thorax trident pattern is often seen in which individuals differ in the intensity of darkness in trident shape and size (Capy et al., 1988; David & Capy, 1988). A similar darkening of this trident pattern is also readily observed in *D. melanogaster ebony* loss-of-function mutants (Lindsley & Zimm, 1992), suggesting that variation in *ebony* expression and/or activity might underlie this intraspecific diversity. Consistent with this hypothesis, Takahashi et al. (2007) found that a chromosomal region containing the *ebony* locus was most strongly associated with differences in trident pigmentation intensity between inbred lines of *D. melanogaster* isolated from West Africa and Taiwan. Complementation tests combined with differences in *ebony* expression levels between strains further suggested that regulatory changes at *ebony* contributed to these differences in trident pigmentation (Takahashi et al., 2007). Natural variation in trident intensity within a *D. melanogaster* population collected from Japan was also found to be associated with genetic variants in *ebony* enhancer regions located on the cosmopolitan inversion, *In(3R)Payne* (Takahashi & Takano-Shimizu, 2011).

Interestingly, none of the 19 nucleotide sites found to be in complete association with trident pigment intensity in this study overlapped with sites associated with differences in abdominal pigmentation in African populations described earlier (Pool & Aquadro, 2007; Rebeiz, Pool, et al., 2009). Genetic variants associated with thoracic pigmentation in this Japanese population do still appear to affect *cis*-regulation of *ebony*, however, because differences in relative allelic expression were observed for *ebony* in F1 hybrids produced by crossing lightly and darkly pigmented lines of *D. melanogaster* from this population (Takahashi & Takano-Shimizu, 2011). Variable sites located within an enhancer that drives expression in both the thorax and abdomen (Rebeiz, Ramos-Womack, et al., 2009) failed to cause differences in *cis*-regulatory activity when tested in a common genetic background using reporter genes, however (Takahashi & Takano-Shimizu, 2011). *cis*-Regulatory variation affecting *ebony* expression also seems to contribute to variable thoracic pigmentation observed among the DGRP lines of *D. melanogaster* used in the Dembeck, Huang, Magwire, et al. (2015) study of abdominal pigmentation, with the most strongly associated SNPs again unique to this population (Miyagi et al., 2015). Significant associations were also observed between genetic variants in known enhancers of *tan* and allele-specific *tan* expression levels, but not with variation in thoracic pigmentation (Miyagi et al., 2015). Taken together, these studies indicate that *ebony cis*-regulatory sequences are often variable in natural populations of *D. melanogaster*, with different genetic variants contributing to differences in thoracic pigmentation in different populations.

5.2 Genetic Basis of Thorax Pigmentation Differences Between Species

The best-studied difference in thoracic pigmentation between species is that seen between *D. guttifera* and *D. melanogaster*. In *D. guttifera*, a member of the quinaria species group (Fig. 3), males and females possess a distinct pattern of darkly pigmented stripes along their thorax in addition to the "polka-dot" deposits of black melanin seen on their abdomen and wings. To identify genes involved in the evolution of *D. guttifera* thoracic pigmentation, Koshikawa et al. (2015) examined the regulation of *wingless* expression, which was previously shown to be spatially correlated with the black polka-dots in the wings during development (Werner et al., 2010). After testing many noncoding sequences in and around *wingless* for activity in the thorax, an enhancer driving expression in this part of the body was finally located in an intron of the *Wnt10* gene, two genes away from *wingless* (Koshikawa

et al., 2015). This enhancer, called "gutTS" for *D. guttifera* thorax stripes, was sufficient to activate *wingless* expression during pupal stages of *D. guttifera* that mirrors the thoracic pigment stripes seen in adult *D. guttifera* (Koshikawa et al., 2015). In *D. melanogaster*, this *D. guttifera cis*-regulatory element drove weaker thoracic stripes, indicating that some *trans*-acting regulators of this *wingless* enhancer had diverged between species (Koshikawa et al., 2015). The orthologous enhancer from *D. melanogaster* was also tested for activity in both *D. melanogaster* and *D. guttifera* and failed to drive expression in thoracic strips in either species, indicating that *cis*-regulatory divergence had occurred between *D. melanogaster* and *D. guttifera* within the gutTS *wingless* enhancer (Koshikawa et al., 2015). These results suggest that the evolution of a novel *cis*-regulatory element affecting wingless expression contributes to the derived thoracic stripe pigment pattern seen in *D. guttifera*.

6. WING PIGMENTATION

D. melanogaster wings are evenly pigmented throughout the wing blade, but many other species of *Drosophila* (especially Hawaiian and Oriental species) have wing spots of dark melanins that vary in size, shape, and position on the wing (Edwards, Doescher, Kaneshiro, & Yamamoto, 2007; O'Grady & DeSalle, 2000; Prud'homme et al., 2006; Wittkopp, Carroll, et al., 2003). These darkly pigmented wing patterns are often sexually dimorphic and thought to be the result of sexual selection. Males that possess wing spots in the Oriental *melanogaster* species group, for example, perform an elaborate wing display behavior in front of females during courtship, whereas males without wing spots tend to perform courtship from behind the female (Yeh & True, 2006). Developmentally, these complex wing pigment patterns result from a two-step process in which (i) spatial prepatterns of enzymes involved in the pigmentation synthesis pathway are laid down in the developing wing during the *Drosophila* pupal stage and (ii) precursors for melanin such as dopa and dopamine are transported to the wing through the hemolymph and diffuse from the wing veins post-eclosion, polymerizing to form black and/or brown melanins in the shape of the enzymatic prepatterns (True, Edwards, Yamamoto, & Carroll, 1999). The precise size and shape of wing spots often varies within species, but the genetic basis of this variation has yet to be determined. Several studies have, however, elucidated genetic mechanisms underlying interspecific differences in wing spot size and patterning, and these are reviewed below.

6.1 Genetic Basis of Wing Pigmentation Differences Between Species

In the melanogaster group of *Drosophila*, several species possess a darkly pigmented male-specific spot at the distal tip of their wing. Phylogenetic reconstructions suggest that the common ancestor of the melanogaster group lacked a wing spot and that the current distribution of this trait in this species resulted from at least one gain followed by multiple losses in independent lineages (Prud'homme et al., 2006). The best studied of these spotted species is *D. biarmipes*, a member of the Oriental lineage within the melanogaster species group (Fig. 3), that has a single spot of dark pigmentation at the distal tip of the wing in males. This spot has been shown to be prefigured by expression of the Yellow protein and the absence of the Ebony protein during pupal stages (Wittkopp, True, et al., 2002). For *yellow*, the novel pattern of expression is caused by *cis*-regulatory changes in a preexisting wing enhancer of *yellow*, suggesting that *cis*-regulatory evolution at *yellow* contributed to the evolution of the wing spot pattern (Gompel et al., 2005). Further investigation revealed that *cis*-regulatory changes affecting *yellow* expression had arisen independently in multiple lineages, with different preexisting wing enhancers coopted to create the novel patterns of wing spot expression (Prud'homme et al., 2006). In the case of spot divergence between the two sister species *D. elegans* (spotted) and *D. gunungcola* (spotless), which are also members of the Oriental lineage of the melanogaster group (Fig. 3), the spot of *yellow* expression present in *D. elegans* is controlled by sequences orthologous to the spot enhancer in *D. biarmipes* and divergence of only a few nucleotides in this sequence is responsible for the loss of this *yellow* expression pattern (and presumably at least part of the wing spot) in *D. gunungcola* (Prud'homme et al., 2006). In another spotted species, however, *D. tristis*, which is a member of the obscura group, a wing spot prefigured by *yellow* expression has evolved using a novel *cis*-regulatory element that coopted a different preexisting wing enhancer of *yellow* (Prud'homme et al., 2006). Taken together, these studies suggest that the *cis*-regulatory sequences of *yellow* have evolved repeatedly to cause changes in gene expression that contribute to the gain and loss of wing spots in multiple *Drosophila* species (also reviewed in Monteiro & Das Gupta, 2016).

To better understand how *yellow* expression is regulated and evolves, Arnoult et al. (2013) performed an RNAi screen in a strain of *D. melanogaster* that carried a reporter gene reflecting activity of the *D. biarmipes* spot enhancer. Among the ~350 screened transcription factors,

five candidates emerged as potential activators of the *D. biarmipes* spot enhancer. One of these genes was *Distal-less* (*Dll*), which has previously been shown to be important for *Drosophila* wing development (Cohen, Wimmer, & Cohen, 1991). Using RNAi knockdown, overexpression, and electrophoretic mobility shift assays, *Dll* was shown to be both necessary and sufficient for driving activity of the *yellow* spot enhancer in the wings of *D. melanogaster* (Arnoult et al., 2013). Moreover, manipulating Dll expression in *D. biarmipes* itself lead to a gain and loss of wing pigmentation when Dll was over- and underexpressed, respectively (Arnoult et al., 2013). Neither changes in wing pigmentation nor *yellow* expression were observed when Dll expression was modified in *D. ananassae*, a species without a wing spot, indicating that the regulatory connection between Dll and *yellow* had evolved in the lineage leading to *D. biarmipes* since it last shared a common ancestor with *D. ananassae* (Arnoult et al., 2013). This regulatory link does not appear to be restricted to *D. biarmipes*, however, as correlations between Dll expression, *yellow* expression, and wing spots were also observed in *D. pulchrella*, *D. elegans*, *D. rhopaloa*, and *D. prolongata* (Arnoult et al., 2013). These data suggest an evolutionary trajectory in which Dll regulation of *yellow* was gained and then changes in Dll expression evolved to produce a variety of wing spot patterns. While the second step of this model remains to be tested, it is clear from these data that divergent expression patterns of *Dll* (as well as potentially other transcription factors) have contributed to the divergence of wing pigment patterns through the direct (and likely also indirect) modulation of genes in the pigmentation synthesis pathway (Monteiro & Das Gupta, 2016).

In other *Drosophila* species, wing pigmentation is not limited to males and involves more than a single spot. For example, in *D. guttifera*, both males and females develop a polka-dot pattern of 16 dark melanin spots and 4 melanized areas across their wings (Koshikawa et al., 2015; Werner et al., 2010). Yellow expression during pupal stages again mirrors the final adult wing pigment pattern (Werner et al., 2010), as does expression of Ebony expression, which is reduced in regions with wing spots (Gompel et al., 2005). To identify *cis*-regulatory regions of *yellow* responsible for this spotted expression pattern, noncoding regions surrounding *yellow* were tested for *cis*-regulatory activity using a reporter gene introduced into *D. melanogaster*. Unlike in other studies of *yellow cis*-regulatory elements (Arnoult et al., 2013; Gompel et al., 2005; Kalay & Wittkopp, 2010; Prud'homme et al., 2006; Wittkopp, Vaccaro, et al., 2002), the unique expression pattern of *D. guttifera yellow* could not be recapitulated by reporter genes in

D. melanogaster, indicating that changes in *trans*-regulatory factors controlling *yellow* expression in *D. guttifera* had diverged between these two species. Transforming these reporter genes into *D. guttifera* did, however, drive spotted patterns of expression similar to those seen for endogenous *yellow* (Werner et al., 2010). Through careful examination of the reporter constructs assayed in *D. melanogaster*, phenotypes observed in a spontaneous *D. guttifera* mutant, and prior knowledge of wing development, Werner et al. (2010) identified *wingless* as a potential regulator of *D. guttifera yellow*. Ectopic expression of *wingless* in *D. guttifera* resulted in ectopic wing pigmentation, providing evidence that *wingless* does indeed regulate wing spot pigmentation in *D. guttifera* (Werner et al., 2010). Additional reporter gene experiments using an orthologous spot enhancer from a closely related species lacking wing spots, *D. deflecta*, also showed that *D. guttifera* had evolved a novel pattern of *wingless* expression that contributed to the evolution of its polka-dotted wings (Werner et al., 2010).

The novel expression pattern of *wingless* in *D. guttifera* could have evolved through changes in its *cis*-regulatory sequences, changes in one or more *trans*-acting regulators of *wingless*, or both. To determine whether *cis*-regulatory changes were responsible for divergent *wingless* expression, Koshikawa et al. (2015) tested noncoding sequences in and around the *wingless* gene for *cis*-regulatory activity in pupal wings. A *cis*-regulatory element located 3′ of *D. guttifera wingless* was found to drive expression in *D. guttifera*-like spots near the distal tip of the wing, an activity that seems to have evolved by coopting activity of preexisting *cis*-regulatory elements driving expression in the cross-veins and/or wing margin (Koshikawa et al., 2015). Two more *cis*-regulatory elements that appear to drive novel patterns of *wingless* expression in *D. guttifera* were also identified more than 69 kb away from *wingless* in introns of the *Wnt10* gene (Koshikawa et al., 2015). Testing the activity of these *cis*-regulatory regions using transgenes inserted into *D. melanogaster* showed that changes in the *cis*-regulatory elements of *wingless* were largely sufficient to explain divergent *wingless* expression and presumably thus contribute to the evolution of novel wing pigmentation in *D. guttifera* (Koshikawa et al., 2015).

Because of the candidate gene approaches used to study the evolution of wing spots in the species described earlier, the contribution of *cis*-regulatory changes observed in *yellow* and *wingless* relative to changes that likely exist at other loci in the genome remain unknown. Two studies investigating the genetic basis of a difference in wing spot between interfertile species in the Oriental lineage of the melanogaster subgroup, *D. elegans* and

D. gunungcola (Fig. 3), begin to address this issue (Yeh & True, 2006, 2014). *D. elegans* has a male-specific wing spot of dark pigment similar to that seen in *D. biarmipes*, whereas its sister species *D. gunungcola* has no spots of dark pigment on its wing (Prud'homme et al., 2006). The similarity of wing spots seen in *D. biarmipes* and *D. elegans* is consistent with the proposed inheritance from a common ancestor that also had a wing spot (Prud'homme et al., 2006), suggesting that the roles of *yellow* (Prud'homme et al., 2006) and *Dll* (Arnoult et al., 2013) in the development of the *D. biarmipes* wing spot described earlier are likely conserved in *D. elegans*. Genetic mapping of loci contributing to the difference in wing spot between *D. elegans* and *D. gunungcola* identified three QTL affecting the wing spot (Yeh & True, 2006, 2014). Although each of these QTL encompasses many genes, the inclusion of *yellow* in one QTL and *Dll* in another is consistent with prior studies suggesting that divergence at these loci contributes to the loss of the wing spot in *D. gunungcola* (Arnoult et al., 2013; Prud'homme et al., 2006). The QTL overlapping *yellow* provides more circumstantial evidence that the *cis*-regulatory divergence of *yellow* identified between *D. elegans* and *D. gunungcola* using reporter genes (Prud'homme et al., 2006) impacts pigmentation. In addition, the QTL overlapping *Dll* suggests that differences in *Dll* expression might exist between *D. elegans* and *D. gunungcola* and be caused by *cis*-regulatory changes at *Dll* itself, similar to observations for divergent *wingless* expression in *D. guttifera* (Koshikawa et al., 2015). The third QTL does not include any obvious candidate genes.

7. PUPAL PIGMENTATION

In addition to the highly variable pigment patterns of the *Drosophila* abdomen, thorax, and wings, differences in pigmentation are also seen among some species in the pupal cases from which the adult flies emerge. For example, in the virilis group of *Drosophila* (Fig. 3), *D. virilis* has a distinctly darker pupal case color than its closest relatives, *D. americana*, *D. lummei*, and *D. novamexicana* (Stalker, 1942). The *D. virilis* pupal case appears almost completely black, whereas pupal cases in the other species are lighter shades of brown and tan (Ahmed-Braimah & Sweigart, 2015). The virilis species group is amenable to genetic dissection of this trait because *D. americana*, *D. novamexicana*, and *D. virilis* all produce fertile hybrids when crossed with each other (Heikkinen, 1992). Early studies investigating the genetic basis of this difference in pupal color between *D. virilis* and *D. americana* suggested that it was due to a large effect locus on chromosome

5 as well as other loci, possibly linked to chromosomes 2 and 3 (Stalker, 1942). To identify the molecular basis of pupal color divergence between *D. virilis* and *D. americana* more precisely, Ahmed-Braimah and Sweigart (2015) analyzed a backcross population between these two species and scored more than 30,000 recombinant offspring for pupal case color. This experimental design allowed them to identify an ~11-kb sequence on chromosome 5 that contributes to the difference in pupal case color. This region contains the first exon and noncoding regions of the *Dat* gene (Ahmed-Braimah & Sweigart, 2015). *Dat*, as described earlier and in Fig. 1, is required for the conversion of dopamine to NADA, which is then polymerized into a colorless pigment. Expression differences were observed for *Dat* at the onset of pupation between *D. americana* (high expression) and *D. virilis* (low expression; Ahmed-Braimah & Sweigart, 2015) that suggest reduced expression of *Dat* in *D. virilis* creates an excess of dopamine that allows production of more dark melanins and thus a much darker pupal case. Pupal expression of *Dat* in *D. novamexicana*, which has a lighter body color than *D. americana* but a similarly colored pupal case, was similar to that observed for *D. americana* (Ahmed-Braimah & Sweigart, 2015). Genetic variation linked to *Dat* did not explain any of the difference in body color between *D. americana* and *D. novamexicana*, consistent with prior work identifying *ebony* and *tan* as the primary drivers of divergent body color between these two species (Wittkopp et al., 2009).

8. LESSONS LEARNED FROM *DROSOPHILA* PIGMENTATION

With the rapid growth of studies identifying genes and genetic changes contributing to pigmentation differences within and between *Drosophila* species during the last 10 years, the time is ripe to step back and take an integrative look at the findings from these case studies. What have we learned about the genetic basis of pigmentation evolution and hopefully phenotypic evolution more generally? What questions remain unanswered?

First and foremost, we have learned that the same handful of genes have been modified over and over again in different lineages to give rise to polymorphic pigmentation within a species as well as divergent pigmentation between species (Table 1). A similar pattern has also been seen for other types of evolutionary changes (Martin & Orgogozo, 2013; Stern & Orgogozo, 2009), suggesting that evolutionary trajectories are sometimes

predictable. For pigmentation, genes harboring polymorphism and divergence that affects body color include genes that encode developmental regulators (blue in Fig. 4) as well as enzymes required for pigment biosynthesis (red in Fig. 4). The apparent reuse of these genes has likely been biased by the use of candidate gene approaches that limited analysis to these genes in some studies (Gompel et al., 2005; Johnson et al., 2015; Prud'homme et al., 2006; Werner et al., 2010; Wittkopp, Vaccaro, et al., 2002); however, the same conclusion emerges if only studies using unbiased genetic mapping approaches are considered (Bastide et al., 2013; Dembeck, Huang, Carbone, et al., 2015; Dembeck, Huang, Magwire, et al., 2015; Endler et al., 2016; Pool & Aquadro, 2007; Wittkopp et al., 2009). Despite this repeatability, the set of nine genes implicated in pigmentation diversity thus far is clearly not exhaustive; Dembeck, Huang, Carbone, et al. (2015) found SNPs in 84 loci that had significant associations with variable abdominal pigmentation in a single population of *D. melanogaster*.

A second lesson results from the striking consistency seen in the types of functional genetic changes observed in genes contributing to pigmentation diversity: *cis*-regulatory changes in noncoding sequences appear to be responsible for a gene's effects on pigmentation in all cases where the type of mutation is known (Table 1). This observation holds for both developmental regulators and genes in the pigment synthesis pathway (Table 1). *cis*-Regulatory changes have been proposed to be the predominant source of evolutionary change in genes with pleiotropic effects on multiple traits because they allow one function of the gene to be modified without affecting others (Carroll, 2008; Stern & Orgogozo, 2008; Wray et al., 2003). All of the genes implicated in pigmentation diversity thus far are indeed pleiotropic

Genes	Abdominal pigmentation	Puparium pigmentation	Thorax pigmentation	Wing pigmentation
bab1	Within and between species	–	–	–
bab2	within species	–	–	–
ebony	Within and between species	–	Within species	–
Dat	–	Between species	–	–
Dll	–	–	–	Between species
omb	Within species	–	–	–
tan	Within and between species	–	–	–
yellow	between species	–	–	Between species
wg	–	–	Between species	Between species

Fig. 4 The loci of pigmentation evolution. A summary of genes implicated in pigmentation differences within and/or between species is shown. Genes labeled in *blue* (*bab1*, *bab2*, *Dll*, *omb*, and *wg*) are regulators of pigmentation development. Genes labeled in *red* (*ebony*, *Dat*, *tan*, and *yellow*) are involved in the pigment biosynthesis pathway. All genetic changes identified as likely to be contributing to a pigmentation difference either within or between species thus far affect *cis*-regulatory sequences.

and are regulated by multiple *cis*-regulatory elements that subdivide their functions. In addition to pigmentation, *bab1* and *bab2* also affect development of mechanosensory organs (Godt, Couderc, Cramton, & Laski, 1993; Kopp et al., 2000); *ebony*, *tan*, *yellow*, and *Dat* also impact behavior (Drapeau, Radovic, Wittkopp, & Long, 2003; Shaw, Cirelli, Greenspan, & Tononi, 2000; True et al., 2005), and *Dll*, *omb*, and *wg* have widespread effects on development (Drysdale & FlyBase Consortium, 2008). The genetic basis of pigmentation differences in vertebrates reveals a different pattern, however, with changes in pigmentation attributed more equally to *cis*-regulatory changes and changes in amino acid sequence affecting protein function (Hubbard, Uy, Hauber, Hoekstra, & Safran, 2010).

A final message emerging from these studies is that intra- and interspecific sources of pigmentation diversity share some properties but not others. For example, nearly all genes shown to contribute to differences in abdominal pigmentation within a species also contribute to pigmentation differences that exist between species (Fig. 4). One notable exception is *yellow*. Changes in *yellow* expression often accompany changes in pigmentation between *Drosophila* species, but they have yet to be implicated in intraspecific variation. This might be because overexpression of *yellow* has more subtle effects on pigmentation than overexpression of *ebony*, *tan*, or *bab1* (Jeong et al., 2008; Salomone et al., 2013; Wittkopp et al., 2009; Wittkopp, True, et al., 2002), such that changes in *yellow* expression arising alone within a species are insufficient for altering pigmentation in most populations (but see Wittkopp, Vaccaro, et al., 2002). Genetic changes in the same *cis*-regulatory regions have been observed within and between species, but the scope of these changes differs. Within a species, genetic variants typically modulate activity of existing *cis*-regulatory elements, with different variants affecting *cis*-regulatory activity in different populations. By contrast, divergent sites that differ between species are much more likely to have given rise to a novel enhancer that coopts preexisting developmental regulators. Differences between alleles contributing to intra- and interspecifc pigmentation variation are not always apparent, however, as the alleles of *tan* and *ebony* contributing to divergent pigmentation in *D. novamexiana* were found to also contribute to clinal variation in pigmentation within *D. americana* (Wittkopp et al., 2009).

As illustrated in this chapter, detailed studies of pigmentation divergence within and among *Drosophila* species have provided an unprecedented look at the genetic mechanisms underlying phenotypic evolution over various timescales. There is still much more to be learned from studying this system,

however. For example, many QTLs contributing to pigmentation differences within and between species have been identified for which the causative genes remain unknown. Identifying these genes might alter our view of the types of genes most likely to harbor genetic changes affecting pigmentation. Many direct and indirect regulators of genes in the pigment synthesis pathway are also yet to be identified. Knowing the identity of these factors and the sequences they bind to will help us understand why some noncoding changes alter pigmentation while others do not. Important questions also remain about whether the complementary changes in expression of pigmentation genes such as *yellow* and *ebony* that are often observed between species have evolved through independent genetic changes or a single change affecting a shared regulator. Finally, improving our understanding of both the ecological functions of pigmentation in specific taxa and the pleiotropic effects of pigmentation genes will help us better understand the role natural selection might play in shaping the genetic basis of pigmentation evolution. Ultimately, understanding the genetic and molecular mechanisms underlying pigmentation diversity has the potential to answer questions not only about evolution but also about ecology, biochemistry, and neuroscience.

REFERENCES

Ahmed-Braimah, Y. H., & Sweigart, A. L. (2015). A single gene causes an interspecific difference in pigmentation in Drosophila. *Genetics*, *200*, 331–342.

Arnoult, L., Su, K. F. Y., Manoel, D., Minervino, C., Magriña, J., Gompel, N., et al. (2013). Emergence and diversification of fly pigmentation through evolution of a gene regulatory module. *Science*, *339*, 1423–1426.

Bastide, H., Betancourt, A., Nolte, V., Tobler, R., Stöbe, P., Futschik, A., et al. (2013). A genome-wide, fine-scale map of natural pigmentation variation in Drosophila melanogaster. *PLoS Genetics*, *9*, e1003534.

Bastide, H., Yassin, A., Johanning, E. J., & Pool, J. E. (2014). Pigmentation in Drosophila melanogaster reaches its maximum in Ethiopia and correlates most strongly with ultra--violet radiation in sub-Saharan Africa. *BMC Evolutionary Biology*, *14*, 179.

Bickel, R. D., Kopp, A., & Nuzhdin, S. V. (2011). Composite effects of polymorphisms near multiple regulatory elements create a major-effect QTL. *PLoS Genetics*, 7, e1001275.

Bray, M. J., Werner, T., & Dyer, K. A. (2014). Two genomic regions together cause dark abdominal pigmentation in Drosophila tenebrosa. *Heredity*, *112*, 454–462.

Brisson, J. A., De Toni, D. C., Duncan, I., & Templeton, A. R. (2005). Abdominal pigmentation variation in drosophila polymorpha: Geographic variation in the trait, and underlying phylogeography. *Evolution*, *59*, 1046–1059.

Brisson, J. A., Templeton, A. R., & Duncan, I. (2004). Population genetics of the developmental gene optomotor-blind (omb) in Drosophila polymorpha: Evidence for a role in abdominal pigmentation variation. *Genetics*, *168*, 1999–2010.

Capy, P., David, J. R., & Robertson, A. (1988). Thoracic trident pigmentation in natural populations of Drosophila simulans: A comparison with D. melanogaster. *Heredity*, *61*, 263–268.
Carbone, M. A., Llopart, A., deAngelis, M., Coyne, J. A., & Mackay, T. F. C. (2005). Quantitative trait loci affecting the difference in pigmentation between Drosophila yakuba and D. santomea. *Genetics*, *171*, 211–225.
Cariou, M. L., Silvain, J. F., Daubin, V., Da Lage, J. L., & Lachaise, D. (2001). Divergence between Drosophila santomea and allopatric or sympatric populations of D. yakuba using paralogous amylase genes and migration scenarios along the Cameroon volcanic line. *Molecular Ecology*, *10*, 649–660.
Carroll, S. B. (2008). Evo-devo and an expanding evolutionary synthesis: A genetic theory of morphological evolution. *Cell*, *134*, 25–36.
Clusella-Trullas, S., & Terblanche, J. S. (2011). Local adaptation for body color in Drosophila americana: Commentary on Wittkopp et al. *Heredity*, *106*, 904–905.
Cohen, B., Wimmer, E. A., & Cohen, S. M. (1991). Early development of leg and wing primordia in the Drosophila embryo. *Mechanisms of Development*, *33*, 229–240.
Cooley, A. M., Shefner, L., McLaughlin, W. N., Stewart, E. E., & Wittkopp, P. J. (2012). The ontogeny of color: Developmental origins of divergent pigmentation in Drosophila americana and D. novamexicana. *Evolution & Development*, *14*, 317–325.
Coolon, J. D., Mcmanus, C. J., Stevenson, K. R., Graveley, B. R., & Wittkopp, P. J. (2014). Tempo and mode of regulatory evolution in Drosophila. *Genome Research*, *24*, 797–808.
Cutter, A. D. (2008). Divergence times in Caenorhabditis and Drosophila inferred from direct estimates of the neutral mutation rate. *Molecular Biology and Evolution*, *25*, 778–786.
David, J. R., & Capy, P. (1988). Genetic variation of Drosophila melanogaster natural populations. *Trends in Genetics*, *4*, 106–111.
Dembeck, L. M., Huang, W., Carbone, M. A., & Mackay, T. F. C. (2015). Genetic basis of natural variation in body pigmentation in Drosophila melanogaster. *Fly*, *9*, 75–81.
Dembeck, L. M., Huang, W., Magwire, M. M., Lawrence, F., Lyman, R. F., & Mackay, T. F. C. (2015). Genetic architecture of abdominal pigmentation in Drosophila melanogaster. *PLoS Genetics*, *11*, e1005163.
Drapeau, M. D., Radovic, A., Wittkopp, P. J., & Long, A. D. (2003). A gene necessary for normal male courtship, yellow, acts downstream of fruitless in the Drosophila melanogaster larval brain. *Journal of Neurobiology*, *55*, 53–72.
Drysdale, R., & FlyBase Consortium. (2008). FlyBase: A database for the Drosophila research community. *Methods in Molecular Biology*, *420*, 45–59.
Edwards, K. A., Doescher, L. T., Kaneshiro, K. Y., & Yamamoto, D. (2007). A database of wing diversity in the Hawaiian Drosophila. *PloS One*, *2*, e487.
Endler, L., Betancourt, A. J., Nolte, V., & Schlötterer, C. (2016). Reconciling differences in Pool-GWAS between populations: A case study of female abdominal pigmentation in Drosophila melanogaster. *Genetics*, *202*, 843–855.
Godt, D., Couderc, J. L., Cramton, S. E., & Laski, F. A. (1993). Pattern formation in the limbs of Drosophila: Bric a brac is expressed in both a gradient and a wave-like pattern and is required for specification and proper segmentation of the tarsus. *Development*, *119*, 799–812.
Gompel, N., Prud'homme, B., Wittkopp, P. J., Kassner, V. A., & Carroll, S. B. (2005). Chance caught on the wing: Cis-regulatory evolution and the origin of pigment patterns in Drosophila. *Nature*, *433*, 481–487.
Hedges, S. B., Dudley, J., & Kumar, S. (2006). TimeTree: A public knowledge-base of divergence times among organisms. *Bioinformatics*, *22*, 2971–2972.
Heikkinen, E. (1992). Genetic basis of reduced eyes in the hybrids of Drosophila virilis phylad species. *Hereditas*, *117*, 275–285.

Hollocher, H., Hatcher, J. L., & Dyreson, E. G. (2000). Genetic and developmental analysis of abdominal pigmentation differences across species in the Drosophila dunni subgroup. *Evolution*, *54*, 2057–2071.

Hubbard, J. K., Uy, J. A. C., Hauber, M. E., Hoekstra, H. E., & Safran, R. J. (2010). Vertebrate pigmentation: From underlying genes to adaptive function. *Trends in Genetics*, *26*, 231–239.

Jeong, S., Rebeiz, M., Andolfatto, P., Werner, T., True, J., & Carroll, S. B. (2008). The evolution of gene regulation underlies a morphological difference between two Drosophila sister species. *Cell*, *132*, 783–793.

Jeong, S., Rokas, A., & Carroll, S. B. (2006). Regulation of body pigmentation by the Abdominal-B Hox protein and its gain and loss in Drosophila evolution. *Cell*, *125*, 1387–1399.

Johnson, W. C., Ordway, A. J., Watada, M., Pruitt, J. N., Williams, T. M., & Rebeiz, M. (2015). Genetic changes to a transcriptional silencer element confers phenotypic diversity within and between Drosophila species. *PLoS Genetics*, *11*, e1005279.

Kalay, G. (2012). Rapid evolution of cis-regulatory architecture and activity in the Drosophila yellow gene, PhD Thesis, University of Michigan.

Kalay, G., & Wittkopp, P. J. (2010). Nomadic enhancers: Tissue-specific cis-regulatory elements of yellow have divergent genomic positions among Drosophila species. *PLoS Genetics*, *6*, e1001222.

Kopp, A. (2009). Metamodels and phylogenetic replication: A systematic approach to the evolution of developmental pathways. *Evolution*, *63*, 2771–2789.

Kopp, A., Duncan, I., Godt, D., & Carroll, S. B. (2000). Genetic control and evolution of sexually dimorphic characters in Drosophila. *Nature*, *408*, 553–559.

Kopp, A., Graze, R. M., Xu, S., Carroll, S. B., & Nuzhdin, S. V. (2003). Quantitative trait loci responsible for variation in sexually dimorphic traits in Drosophila melanogaster. *Genetics*, *163*, 771–787.

Koshikawa, S., Giorgianni, M. W., Vaccaro, K., Kassner, V. A., Yoder, J. H., Werner, T., et al. (2015). Gain of cis-regulatory activities underlies novel domains of wingless gene expression in Drosophila. *Proceedings of the National academy of Sciences of the United States of America*, *112*, 7524–7529.

Kraminsky, G. P., Clark, W. C., Estelle, M. A., Gietz, R. D., Sage, B. A., O'Connor, J. D., et al. (1980). Induction of translatable mRNA for dopa decarboxylase in Drosophila: An early response to ecdysterone. *Proceedings of the National academy of Sciences of the United States of America*, *77*, 4175–4179.

Kronforst, M. R., Barsh, G. S., Kopp, A., Mallet, J., Monteiro, A., Mullen, S. P., et al. (2012). Unraveling the thread of nature's tapestry: The genetics of diversity and convergence in animal pigmentation. *Pigment Cell & Melanoma Research*, *25*, 411–433.

Letunic, I., & Bork, P. (2007). Interactive Tree of Life (iTOL): An online tool for phylogenetic tree display and annotation. *Bioinformatics*, *23*, 127–128.

Letunic, I., & Bork, P. (2011). Interactive Tree of Life v2: Online annotation and display of phylogenetic trees made easy. *Nucleic Acids Research*, *39*, W475–W478.

Lindsley, D. L., & Zimm, G. G. (1992). *The genome of Drosophila melanogaster*. San Diego, CA: Academic Press.

Llopart, A., Elwyn, S., Lachaise, D., & Coyne, J. A. (2002). Genetics of a difference in pigmentation between Drosophila yakuba and Drosophila santomea. *Evolution*, *56*, 2262–2277.

Mackay, T. F. C., Richards, S., Stone, E. A., Barbadilla, A., Ayroles, J. F., Zhu, D., et al. (2012). The Drosophila melanogaster genetic reference panel. *Nature*, *482*, 173–178.

Martin, A., & Orgogozo, V. (2013). The loci of repeated evolution: A catalog of genetic hotspots of phenotypic variation. *Evolution*, *67*, 1235–1250.

Martinez, M. N., & Cordeiro, A. R. (1970). Modifiers of color pattern genes in DROSOPHILA POLYMORPHA. *Genetics*, *64*, 573–587.
Matute, D. R., & Harris, A. (2013). The influence of abdominal pigmentation on desiccation and ultraviolet resistance in two species of Drosophila. *Evolution*, *67*, 2451–2460.
Miyagi, R., Akiyama, N., Osada, N., & Takahashi, A. (2015). Complex patterns of cis-regulatory polymorphisms in ebony underlie standing pigmentation variation in Drosophila melanogaster. *Molecular Ecology*, *24*, 5829–5841.
Monteiro, A., & Gupta, M. D. (2016). Identifying coopted networks and causative mutations in the origin of novel complex traits. *Current Topics in Developmental Biology*, *119*, 205–226.
Morales-Hojas, R., Vieira, C. P., & Vieira, J. (2008). Inferring the evolutionary history of Drosophila americana and Drosophila novamexicana using a multilocus approach and the influence of chromosomal rearrangements in single gene analyses. *Molecular Ecology*, *17*, 2910–2926.
Ng, C. S., Hamilton, A. M., Frank, A., Barmina, O., & Kopp, A. (2008). Genetic basis of sex-specific color pattern variation in Drosophila malerkotliana. *Genetics*, *180*, 421–429.
Nikolaidis, N., & Scouras, Z. G. (1996). The Drosophila montium subgroup species. Phylogenetic relationships based on mitochondrial DNA analysis. *Genome*, *39*, 874–883.
O'Grady, P. M., & DeSalle, R. (2000). How the fruit fly changed (some of) its spots. *Current Biology*, *10*, R75–R77.
Ohnishi, S., & Watanabe, T. (1985). Genetic analysis of color dimorphism in the *Drosophila montium* subgroup. *Japanese Journal of Genetics*, *60*, 355–358.
Ordway, A. J., Hancuch, K. N., Johnson, W., Wiliams, T. M., & Rebeiz, M. (2014). The expansion of body coloration involves coordinated evolution in cis and trans within the pigmentation regulatory network of Drosophila prostipennis. *Developmental Biology*, *392*, 431–440.
Orr, H. A. (2001). The genetics of species differences. *Trends in Ecology & Evolution*, *16*, 343–350.
Parkash, R., & Munjal, A. K. (1999). Phenotypic variability of thoracic pigmentation in Indian populations of Drosophila melanogaster. *Journal of Zoological Systematics and Evolutionary Research*, *37*, 133–140.
Pool, J. E., & Aquadro, C. F. (2007). The genetic basis of adaptive pigmentation variation in Drosophila melanogaster. *Molecular Ecology*, *16*, 2844–2851.
Prud'homme, B., Gompel, N., Rokas, A., Kassner, V. A., Williams, T. M., Yeh, S.-D., et al. (2006). Repeated morphological evolution through cis-regulatory changes in a pleiotropic gene. *Nature*, *440*, 1050–1053.
Rajpurohit, S., & Gibbs, A. G. (2012). Selection for abdominal tergite pigmentation and correlated responses in the trident: A case study in Drosophila melanogaster. *Biological Journal of the Linnean Society*, *106*, 287–294.
Rebeiz, M., Pool, J. E., Kassner, V. A., Aquadro, C. F., & Carroll, S. B. (2009). Stepwise modification of a modular enhancer underlies adaptation in a Drosophila population. *Science*, *326*, 1663–1667.
Rebeiz, M., Ramos-Womack, M., Jeong, S., Andolfatto, P., Werner, T., True, J., et al. (2009). Evolution of the tan locus contributed to pigment loss in Drosophila santomea: A response to Matute et al. *Cell*, *139*, 1189–1196.
Riedel, F., Vorkel, D., & Eaton, S. (2011). Megalin-dependent yellow endocytosis restricts melanization in the Drosophila cuticle. *Development*, *138*, 149–158.
Rogers, W. A., Grover, S., Stringer, S. J., Parks, J., Rebeiz, M., & Williams, T. M. (2014). A survey of the trans-regulatory landscape for Drosophila melanogaster abdominal pigmentation. *Developmental Biology*, *385*, 417–432.
Rogers, W. A., Salomone, J. R., Tacy, D. J., Camino, E. M., Davis, K. A., Rebeiz, M., et al. (2013). Recurrent modification of a conserved cis-regulatory element underlies fruit fly pigmentation diversity. *PLoS Genetics*, *9*, e1003740.

Salomone, J. R., Rogers, W. A., Rebeiz, M., & Williams, T. M. (2013). The evolution of Bab paralog expression and abdominal pigmentation among Sophophora fruit fly species. *Evolution & Development*, *15*, 442–457.
Shaw, P. J., Cirelli, C., Greenspan, R. J., & Tononi, G. (2000). Correlates of sleep and waking in Drosophila melanogaster. *Science*, *287*, 1834–1837.
Stalker, H. D. (1942). The inheritance of a subspecific character in the Virilis complex of Drosophila. *The American Naturalist*, *76*, 426–431.
Stern, D. L., & Orgogozo, V. (2008). The loci of evolution: How predictable is genetic evolution? *Evolution*, *62*, 2155–2177.
Stern, D. L., & Orgogozo, V. (2009). Is genetic evolution predictable? *Science*, *323*, 746–751.
Streisfeld, M. A., & Rausher, M. D. (2011). Population genetics, pleiotropy, and the preferential fixation of mutations during adaptive evolution. *Evolution*, *65*, 629–642.
Sugumaran, M., Giglio, L., Kundzicz, H., Saul, S., & Semensi, V. (1992). Studies on the enzymes involved in puparial cuticle sclerotization in Drosophila melanogaster. *Archives of Insect Biochemistry and Physiology*, *19*, 271–283.
Takahashi, A. (2013). Pigmentation and behavior: Potential association through pleiotropic genes in *Drosophila*. *Genes & Genetic Systems*, *88*, 165–174.
Takahashi, A., Takahashi, K., Ueda, R., & Takano-Shimizu, T. (2007). Natural variation of ebony gene controlling thoracic pigmentation in Drosophila melanogaster. *Genetics*, *177*, 1233–1237.
Takahashi, A., & Takano-Shimizu, T. (2011). Divergent enhancer haplotype of ebony on inversion In(3R)Payne associated with pigmentation variation in a tropical population of Drosophila melanogaster. *Molecular Ecology*, *20*, 4277–4287.
Telonis-Scott, M., Hoffmann, A. A., & Sgro, C. M. (2011). The molecular genetics of clinal variation: A case study of ebony and thoracic trident pigmentation in Drosophila melanogaster from eastern Australia. *Molecular Ecology*, *20*, 2100–2110.
True, J. R. (2003). Insect melanism: The molecules matter. *Trends in Ecology & Evolution*, *18*, 640–647.
True, J. R., Edwards, K. A., Yamamoto, D., & Carroll, S. B. (1999). Drosophila wing melanin patterns form by vein-dependent elaboration of enzymatic prepatterns. *Current Biology*, *9*, 1382–1391.
True, J. R., Yeh, S.-D., Hovemann, B. T., Kemme, T., Meinertzhagen, I. A., Edwards, T. N., et al. (2005). Drosophila tan encodes a novel hydrolase required in pigmentation and vision. *PLoS Genetics*, *1*, e63.
Walter, M. F., Zeineh, L. L., Black, B. C., McIvor, W. E., Wright, T. R., & Biessmann, H. (1996). Catecholamine metabolism and in vitro induction of premature cuticle melanization in wild type and pigmentation mutants of Drosophila melanogaster. *Archives of Insect Biochemistry and Physiology*, *31*, 219–233.
Werner, T., Koshikawa, S., Williams, T. M., & Carroll, S. B. (2010). Generation of a novel wing colour pattern by the Wingless morphogen. *Nature*, *464*, 1143–1148.
Williams, T. M., Selegue, J. E., Werner, T., Gompel, N., Kopp, A., & Carroll, S. B. (2008). The regulation and evolution of a genetic switch controlling sexually dimorphic traits in Drosophila. *Cell*, *134*, 610–623.
Wittkopp, P. J., & Beldade, P. (2009). Development and evolution of insect pigmentation: Genetic mechanisms and the potential consequences of pleiotropy. *Seminars in Cell & Developmental Biology*, *20*, 65–71.
Wittkopp, P. J., Carroll, S. B., & Kopp, A. (2003). Evolution in black and white: Genetic control of pigment patterns in Drosophila. *Trends in Genetics*, *19*, 495–504.
Wittkopp, P. J., Haerum, B. K., & Clark, A. G. (2008). Regulatory changes underlying expression differences within and between Drosophila species. *Nature Genetics*, *40*, 346–350.

Wittkopp, P. J., Smith-Winberry, G., Arnold, L. L., Thompson, E. M., Cooley, A. M., Yuan, D. C., et al. (2011). Local adaptation for body color in Drosophila americana. *Heredity*, *106*, 592–602.

Wittkopp, P. J., Stewart, E. E., Arnold, L. L., Neidert, A. H., Haerum, B. K., Thompson, E. M., et al. (2009). Intraspecific polymorphism to interspecific divergence: Genetics of pigmentation in Drosophila. *Science*, *326*, 540–544.

Wittkopp, P. J., True, J. R., & Carroll, S. B. (2002). Reciprocal functions of the Drosophila yellow and ebony proteins in the development and evolution of pigment patterns. *Development*, *129*, 1849–1858.

Wittkopp, P. J., Vaccaro, K., & Carroll, S. B. (2002). Evolution of yellow gene regulation and pigmentation in Drosophila. *Current Biology*, *12*, 1547–1556.

Wittkopp, P. J., Williams, B. L., Selegue, J. E., & Carroll, S. B. (2003). Drosophila pigmentation evolution: Divergent genotypes underlying convergent phenotypes. *Proceedings of the National academy of Sciences of the United States of America*, *100*, 1808–1813.

Wray, G. A., Hahn, M. W., Abouheif, E., Balhoff, J. P., Pizer, M., Rockman, M. V., et al. (2003). The evolution of transcriptional regulation in eukaryotes. *Molecular Biology and Evolution*, *20*, 1377–1419.

Wright, T. R. (1987). The genetics of biogenic amine metabolism, sclerotization, and melanization in Drosophila melanogaster. *Advances in Genetics*, *24*, 127–222.

Yassin, A., Bastide, H., Chung, H., Veuille, M., David, J. R., & Pool, J. E. (2016). Ancient balancing selection at tan underlies female colour dimorphism in Drosophila erecta. *Nature Communications*, *7*, 10400.

Yeh, S.-D., & True, J. R. (2006). The genetic architecture of coordinately evolving male wing pigmentation and courtship behavior in Drosophila elegans and D. gunungcola. *Heredity*, *96*, 383–395.

Yeh, S.-D., & True, J. R. (2014). The genetic architecture of coordinately evolving male wing pigmentation and courtship behavior in Drosophila elegans and Drosophila gunungcola. *G3 (Bethesda, Md.)*, *4*, 2079–2093.

Zhan, S., Guo, Q., Li, M., Li, M., Li, J., Miao, X., et al. (2010). Disruption of an N-acetyltransferase gene in the silkworm reveals a novel role in pigmentation. *Development*, *137*, 4083–4090.